THE MECHANISMS OF ARSENIC DETOXIFICATION BY THE GREEN MICROALGAE *CHLORELLA VULGARIS*

Thesis Submitted to Middlesex University in partial fulfilment of the award of Doctor of Philosophy (Ph.D.) degree in Environmental Science

By

Leonardo Pantoja Munoz

Supervisors:

Prof. Hemda Garelick (Director of studies)

Dr. Diane Purchase

Dr. Huw Jones

MIDDLESEX UNIVERSITY, LONDON, UK

March 2014

Abstract

The mechanisms of arsenic interaction with the green microalga *Chlorella vulgaris* (*C. vulgaris*) and the potential for its bio-remediation from water were investigated.

This was made possible by the development of an improved arsenic extraction from *C. vulgaris*, leading to successful glutathione and phytochelatins (GSH/PC) complex speciation analysis with 71.1% efficiency.

The response of *C. vulgaris* when challenged by As(III), As(V) and dimethylarsinic acid (DMA) was assessed through experiments on adsorption, efflux and speciation of arsenic (reduction, oxidation, methylation and chelation with GSH/PC). At high phosphate concentration (1.62 mM of PO_4^{-3}), poor adsorption of As(V) led to low intracellular uptake; at low phosphate concentration (3.2 µM of PO_4^{-3}), an increase in the level of free thiols was observed as well as a moderate decrease in intracellular pH with no evidence for signals of oxidative stress. *Chlorella vulgaris* cells did not produce any As-GS/PC complex when exposed to As(V). This may indicate that a reduction step is needed for As(V) complexation with GSH/PC. *Chlorella vulgaris* cells formed $DMAS^{V}$-GS upon exposure to DMA. The formation of this complex *in vivo* has only been reported once in *Brassica oleracea* plants. This complex is perhaps a fragment of a bigger molecule and thus part of another detoxification mechanism since its formation was not related to the concentration of DMA in media or the exposure time. It was found that As(III) triggers the formation of arsenic complexes with PC and homophytochelatins (hPC) and their compartmentalisation to vacuoles. It is the first time that, as a result of the newly developed extraction method using sonication, such intact complexes have been identified in *C. vulgaris* exposed to arsenic and their hPC complexes have been reported in any organism. The potential of *C. vulgaris* to bio-remediate arsenic from water is highly selective and effective for the more toxic As(III) (for human life) without the potential hazard to reduce As(V) to As(III). This was possible to assess because of the following empirical observations:

- At low phosphate (3.2 µM of PO_4^{-3}) and in the presence of As(V), *C. vulgaris* are not likely to grow and be efficient at bio-remediating arsenic.
- At high phosphate (1.62 mM of PO_4^{-3}) and in the presence of As(V), *C. vulgaris* are highly likely to grow but are not likely to be efficient at bio-remediating arsenic. However the potential to transform As(V) into more toxic As(III) is very low.
- Under any phosphate concentration and in the presence of As(III), *C. vulgaris* has high potential to bio-remediate arsenic, by storing As(III) into the cell biomass while retaining significantly high growth rates.

Acknowledgments

I would like to thank my supervisors; Prof. Hemda Garelick, Dr. Diane Purchase and Dr. Huw Jones for all of the guidance, support and valuable discussion. Thank you for providing the perfect amount of supervision to allow for independent growth while still giving me guidance through the difficult stages.

I would also like to thank, Alan LaGrue, Manika Choudhury, Tomas Denning, James Kershaw and Marcela Gondek for their help and technical support.

I would like to thank the research group in Middlesex University for all of the help and support provided during my project, especially Prof. Lucy Ghali, Dr. Torben Lund and Dr. Song Wen.

I am thankful for allowing me the use of their laboratory facilities, the help and technical assistance provided by Prof. Jörg Feldmann, Dr. Andrea Raab and Dr. Dagmar Urgast at the Trace Element Speciation Laboratory of the University of Aberdeen, College of Physical Science Chemistry.

To all my friends and family, especially my wife, thank you for all of the encouragement, support and patience I have experienced.

I would finally like to acknowledge the funding support I have received. Thanks to Middlesex University, Department of Natural Sciences of the School of Science and Technology for the opportunity to complete my studies and research.

Table of contents

List of Figures

List of Tables

List of Abbreviations

1/n	Freundlich intensity parameter
ABC	ATP binding cassette
ABCC	ATP binding cassette C family
AES	Atomic emission spectrometry
AFS	Atomic fluorescence spectroscopy
Ala	Alanine
ANOVA	Analysis of variance
As	Arsenic
As(III)	Arsenite (+3)
As(V)	Arsenate (+5)
ASV	Anodic stripping voltammetry
ATG	tri(glutamyl-cysteinyl-glycinyl) trithio-arsenite
ATP	Adenosine triphosphate
BCECF	2',7'-bis-(2-carboxyethyl)-5- and-6- carboxyfluorescein
BDSA	Potassium benzene-1,2-disulfonate
C. vulgaris	Chlorella vulgaris
C_0	Initial concentration of adsorbate
Calcein-AM	Calcein acetoxymethyl ester
CCT	Collision cell technology
CE	Capillary electrophoresis
C_e	Equilibrium concentration of adsorbate after adsorption has occurred
CMFDA	5-chloromethylfluorescein diacetate
Cys	Cysteine
DC/RF	Direct current radio frequency
DMA	Dimethylarsinic acid
DMAG	dimethyl-thio-arsinite
DMF	N,N-Dimethyl-formamide
DMSO	Dimethyl sulfoxide
DNA	Deoxyribonucleic acid
EDTA	Ethylenediaminetetraacetic acid
Eh	Redox potential
ESI	Electrospray ionisation
EXAFS	Extended x-ray absorption fine structure
FL1	Fluorescence channel 1 (515-545 nm)
FL2	Fluorescence channel 2 (564-606 nm)
FL3	Fluorescence channel 3 (670 nm)
FL4	Fluorescence channel 1 (653-669 nm)
frt	Retention time specific response factor
FSC	Forward angle light scatter

FTIC	Fluorescein isothiocyanate
GC	Gas chromatography
GFAAS	Graphite furnace atomic absorption
GFP	Green fluorescent protein
GLM	General linear model
Glu	Glutamic acid
Gly	Glycine
GS	Glutathione (complexed form)
GSH	Reduced glutathione (non complexed form)
GSSG	Oxidised glutathione
GST	Glutathione S-transferase
H_2DCFH-DA	2`,7`-dichlorodihydrofluorescein diacetate
HE	Dihydroethidium
HGAAS	Hydride generation atomic absorption spectroscopy
hGSH	Glutathione homologues (Gly substituted by Ala, Ser, Gln, Glu or is absent)
hPC	Phytochelatin homologues (Gly substituted by Ala, Ser, Gln, Glu or is absent)
HPLC	High performance liquid chromatography
ICP	Inductively coupled plasma
IC_p	Inhibition concentration for a specific concentration
ICP-MS	Inductively coupled plasma mass spectrometry
IT	Ion trap
K_f	Freundlich capacity factor
LOEC	Lowest observed effect concentration
LY	Lucifer Yellow
m/z	Mass to charge
MADG	di(glutamyl-cysteinyl-glycinyl) methyl-di(glutamyl-cysteinyl-glycinyl) methyldithio-arsonite
mBBr	Monobromobimane
mBCl	Monochlorobimane
MDL	Method detection limits
MEN	Menadione
MES	2-(N-morpholino)ethanesulfonic acid
MMA	Monomethylarsonic acid
MQL	Method quantification limits
mRNA	Messenger ribonucleic acid
MRP	Multi Drug Resistance-Associated Protein
MS	Mass spectrometry
n	Number of samples
NEM	N-ethyl-maleimide
NOEC	No observed effect concentration

O_2^-	Superoxide
OES	Optical emission spectrometry
PC	Phytochelatin
PC's	Phytochelatins
PCS	Phytochelatin synthase
pKa	Acid dissociation constant
ppm	Parts per million
p-value	Probability value
Q	Quadrupole
Q_0	Maximum adsorption capacity
q_e	Adsorbent concentration after equilibrium
RAs	Arsenic response factor
RF	Radio frequency
Rh123	Rhodamine 123
ROS	Reactive oxygen species
RtAs	Response factor for a (t) arsenic eluting compound
SAM	S-adenosylmethionine
SE	Standard error
Ser	Serine
SH	Free thiol
SSC	Side angle light scatter
TMA	Trimethylarsine
ToF	Time of Flight
UV	Ultraviolet radiation
WHO	World Health Organization
x/m	Mass of adsorbate per unit mass of adsorbent after equilibrium
XANES	X-ray absorption near-edge spectroscopy

1. INTRODUCTION

Arsenic (As) is a metalloid found in group 15 of the periodic table below nitrogen and phosphorus. Only one stable natural isotope of arsenic exists with an atomic mass of 75. Arsenic is found in some soils and natural waters and most soluble arsenic compounds are toxic and carcinogenic. Arsenic can contaminate natural waters via both natural and anthropogenic sources, whilst man-made sources can be monitored and controlled, natural contamination is very difficult to predict, monitor and control.

Arsenic concentrations in soils around the world range between 2 and 5 mg of arsenic per kg of soil, and most of it is found locked up in arsenopyrite minerals. This form of arsenic is considered not toxic as it has low solubility in water. Arsenic contamination of groundwater normally starts with the weathering of this mineral and the release mechanism can be both microbiological and chemical (Henke, 2009).

Arsenic toxicity to humans can be a result of both acute and chronic exposure. Acute toxicity of arsenic is not different from that of some heavy metals at the same concentration (e.g. cadmium, copper or mercury) or even of pesticides. What makes arsenic particularly dangerous is the combination of high environmental presence and high toxicity, thus the presence of arsenic in drinking water is a major global public health issue (Meharg, 2005).

In Bangladesh alone some 10 million tube-wells were drilled in order to seek good quality drinking water free of microbiological contamination. However, many of the tube-wells were unknowingly sunk into arsenic-contaminated aquifers. As a consequence, although microbiologically superior water supplies were obtained, some 40 million people were exposed to toxic levels of arsenic exceeding the World Health Organization (WHO) guideline value (10 $\mu g\ L^{-1}$; WHO, 2006) by a factor of 20 or more. High levels of arsenic in drinking water have also been found elsewhere, including Argentina, Cambodia, Canada, Chile, China, Ghana, Hungary, India, Laos, Mexico, Mongolia, Nepal, Pakistan, Poland, Taiwan, Thailand, UK, United States, and Vietnam (Caussy and Priest, 2008; Ahuja, 2008). There is clearly a need to develop cost effective technologies to remediate arsenic pollution in water.

The primary mode of human exposure is through chronic ingestion of water containing arsenic and crops irrigated with the same water. As arsenic has no taste and no immediate side effects, toxic chronic effects can only be seen when it is too late. There is no risk to human health by skin exposure when hand washing and bathing because dermal adsorption of arsenic is minimal (Meharg, 2005).

Chronic effects produced by the ingestion of inorganic arsenic include skin lesions, disturbances of the peripheral nervous system, anaemia, leucopoenia, liver damage, circulatory disease, and cancer. Arsenic human carcinogenesis has mainly three modes of action: binding, oxidative stress and DNA methylation (Henke, 2009).

In nature arsenic exists in the following oxidation states: -3 (arsine), 0 (semi-elemental arsenic), +3 (arsenite) and +5 (arsenate). The toxic effects of arsenic depend on the speciation and physical form, while redox potential (Eh) and pH strongly control arsenic speciation in solution. Arsines are the most toxic forms of arsenic, followed by inorganic arsenite As(III), organic arsenites, inorganic arsenate As(V) and finally organic arsenates. To put things into context, arsenic trioxide was found to be in excess of 300 times more toxic than arsenobetaine when it was administered orally to mice (Wang and Mulligan, 2006). Therefore methods capable of converting inorganic arsenic to other, less toxic species are also needed (Frankenberg, 2002).

Plants can remove, contain and accumulate arsenic from soils, sediments and contaminated water. Phytoremediation offers a potentially cost effective and environmentally positive alternative to physical and chemical treatments. Phytoremediation of arsenic had a boost from the discovery of arsenic hyper accumulating ferns e.g. *Pteris vittata*, *Pteris cretica*, *Pityrogramma Calomelanos*, *Pinguicula longifolia* and *Pteris umbrosa.* These plants can effortlessly accumulate more than 1000 µg of arsenic per g of plant biomass with low or no toxic effects (Willey, 2007).

Phytoextraction employs floating plants and macrophytes to remediate water. This differs from normal phytoremediation techniques in the way plants bio-adsorb arsenic from water rather than soil. *Spirodela polyrhiza*, *Lemna spp*., *Azolla pinnata*, *Salvinia natans* and *Eichhornia crassipes* are examples of plants used to

phytoextract arsenic. This approach has the advantage of requiring less effort for plant growth (Golubev, 2011).

Microorganisms have also shown good potential to detoxify arsenic (Munoz and Guieysse, 2006). Three major types of arsenic biotransformations have been reported in microorganisms: the reduction or oxidation of inorganic arsenic (Zouboulis and Katsoyiannis, 2005), methylation and demethylation (Stolz et al., 2006) and chelation to intracellular cysteine-rich polypeptides (Levy et al., 2005). The most important classes of metal-chelating polypeptides are glutathione (GSH) and its derivative forms: phytochelatins (PC's) which contain thiol groups that bind readily with As(III) species (Schmidt et al., 2007). These peptides can be found in microalgae, related eukaryotic photosynthetic organisms, fungi and some nematodes (Vatamanuik et al., 2001; Perales-Vela, Pena-Castro and Canizares-Villanueva, 2006) as organo-metallic complexes. These may be partitioned inside vacuoles to facilitate appropriate control of the cytoplasmic concentration of metal(loid) ions (Cobbett and Goldbrough, 2002).

Chlorella vulgaris (*C. vulgaris*) is a freshwater green unicellular microalga that was first identified and characterised in the 1890's. This alga tolerates a number of heavy metals and metalloids including arsenic (Suhendrayatna et al., 1999). The investigation of the tolerance of the green algae *C. vulgaris* to arsenic can be traced back to the 1970's. Before this date several investigations were made mostly in marine organisms due to the large difference in arsenic accumulation. Until that date marine organisms were found to contain up to 100 mg g^{-1} of arsenic (in dry weight basis) whereas terrestrial organisms rarely contained 1 mg g^{-1} of arsenic and therefore did not draw enough attention to the scientific community (Lunde, 1977).

In some experiments, it has been found that growth of *C. vulgaris* increased with an increase of As(V) concentration up to 2,000 mg L^{-1} and cells survived even at 10,000 mg L^{-1}. Bioaccumulation increased with an increase of the arsenic level and maximum accumulation found was 50,000 µg As g^{-1} dry cell, however growth decreased with an increase of As(III) level and cells were found to be cytolysed at 40 mg L^{-1} (Maeda et al., 1985).

C. vulgaris has already shown great promise in arsenic removal during field trials in the contaminated district of Ron Phibun in Thailand, where *C. vulgaris* demonstrated its ability to accumulate and detoxify As(V) (Jones et al., 2008).

However little is known about the detoxification and tolerance mechanism that *C. vulgaris* employs, because only isolated experiments have been performed so far investigating the mechanisms underlying such tolerance.

Compared to other bioremediation methods, such as those using plants, microalgae have much higher growth rates, greater overall biomass yield, and take up less land for cultivation; they grow in highly selective environments (using inorganic carbon from the environment i.e. CO_2) therefore they can grow in open cultures and still remain free of contamination by other organisms; this makes it cost-effective and relatively easy to use (Barsanti and Gualtieri, 2006).

1.1. Aims and Objectives

This study aims to examine the interactions of arsenic with the microalgae *C. vulgaris* and its potential to bio-remediate arsenic from water. This study will provide information about the factors affecting tolerance and toxicity in the interaction of arsenic with *C. vulgaris*.

The objectives are to investigate the following mechanisms for arsenic removal and detoxification in the microalgae *C. vulgaris*:

- Surface adsorption
- As efflux
- Speciation of As
    - As reduction and oxidation
    - As methylation and demethylation
    - The involvement of glutathione and phytochelatins

Because the main difficulty in the investigation of the mechanism of arsenic interactions is extraction from *C. vulgaris* cells, a method development will involve:

- Improvement of arsenic extraction from *C. vulgaris* for GS/PC complex speciation analysis

2. LITERATURE REVIEW

2.1. Arsenic in soil and water

Arsenic is present in some soils and natural waters and most of arsenic's soluble compounds are toxic and carcinogenic. Arsenic has been part of the cultural and social human history, being used as a poison for Kings and aristocrats (Henke, 2009).

Arsenic in nature exists in the following oxidation states: -3 (arsine), 0 (semi-elemental arsenic), +3 (arsenite) and +5 (arsenate). The inorganic forms of arsenic that occur more often in natural waters are: arsenite (As(III), AsO_3^{3-}) and arsenate (As(V), AsO_4^{3-}). Some of the pentavalent ions (+5) found in solution are: AsO_4^{3-}, $HAsO_4^{2-}$ and $H_2AsO_4^-$, while trivalent (+3) arsenites comprise: $As(OH)_3$, $AsO_3H_2^-$, AsO_2OH^{2-} and AsO_3^{3-} (Wang and Mulligan, 2006).

Redox potential (Eh) and pH strongly control arsenic speciation in solution. The species found in nature according to redox potential and pH are shown in Fig 2.1. In the upper right part of the graph, the predominance of arsenate at high Eh and pH can be observed. Trivalent arsenites are present as uncharged molecules throughout a wide range of pH values (0-9) (Wang and Mulligan, 2006).

Although more than 18,800 tonnes/year of arsenic are introduced to the atmosphere (which is then deposited into surface water) by anthropogenic sources, natural sources of arsenic are the main contributors for contamination in terrestrial waters (Nriagu and Pacyna, 1988).

Natural weathering reactions, wind erosion, volcanic emissions, low temperature volatilisation from soil, biological activity and marine aerosols contribute to arsenic's presence in groundwater. Soil erosion and leaching alone contribute 61,200 and 238,000 tonnes/year respectively to the input of arsenic in dissolved and suspended forms into the oceans (Mohan and Pittman, 2007).

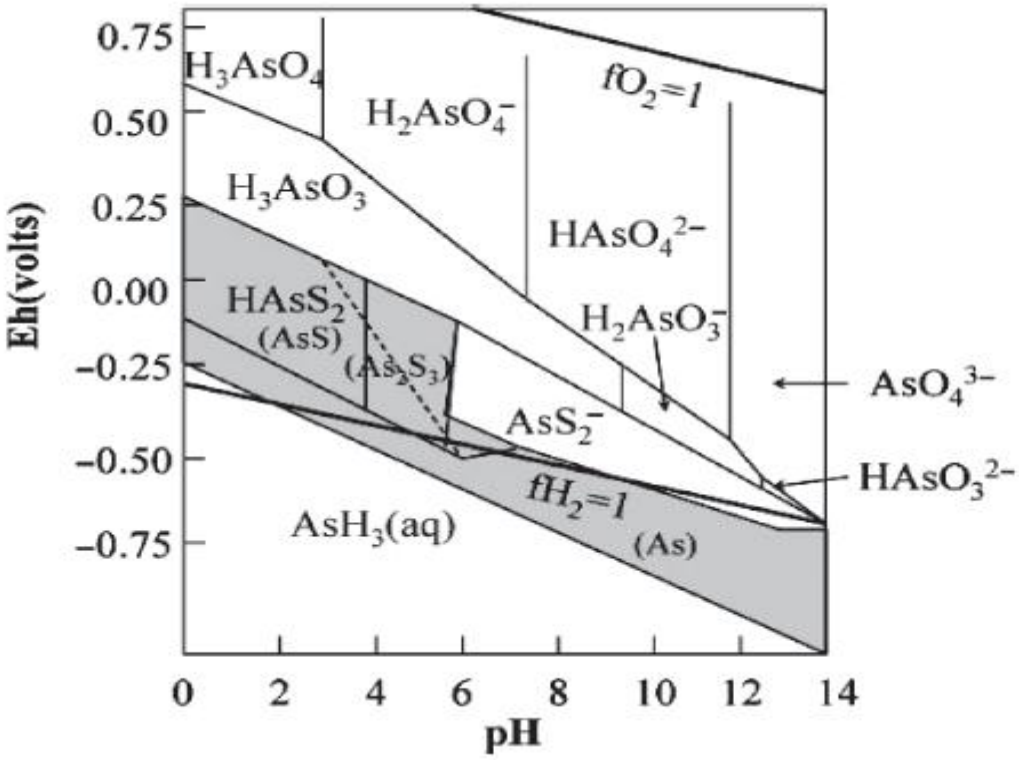

Fig 2. 1 Redox potential-pH (Eh-pH) diagram for arsenic at 25°C, solid species depicted in shaded area, from Garelick et al., (2008).

Mobilisation of arsenic in groundwater is very complex. It can be affected by the chemical properties mentioned before: redox conditions and pH but also by biological activity, solid-phase precipitation and dissolution reactions, adsorption/desorption reactions, salinity, soil/clay content, soil grain size and composition, presence of other metal and non-metal ions such as iron(II), iron(III) sulphate, phosphates and silicates (Pandey et al., 2002).

The level of arsenic in groundwater throughout the world varies from country to country; however, concentrations as high as 3200 µg L^{-1} have been reported in Bangladesh and India. It is estimated that 150 million people in these regions are exposed to arsenic contaminated groundwater (Ahmed et al., 2004).

The World Health Organization has set a provisional guideline value for arsenic in drinking water of 10 µg L^{-1} (WHO, 2006). Following this and due to the increasing groundwater arsenic problems, many countries have lowered their drinking water limits.

Toxicity of arsenic depends on several factors; this is why along with the total concentration of arsenic it is often required to know its speciation. Speciation is defined as follows: “Chemical compounds that differ in isotopic composition, conformation, oxidation or electronic state or in the nature of their complexed or covalently bound substituents” (Templeton et al., 2000).

Toxicity of arsenic for humans has been investigated extensively. Toxicity mechanisms for human cells are very similar to other arsenic sensitive organisms as As(III) and As(V) are readily metabolised following exposure. However trivalent forms of arsenic are more toxic than pentavalent ones. The mechanisms of arsenic toxicity rely mainly on its similarity to essential molecules (e.g. As(V) and phosphate) and its high reactivity (e.g. As(III) affinity to sulphur in proteins and peptides). Thus these mechanisms include: phosphate replacement, enzyme inhibition, oxidative stress, genotoxicity and alteration of: DNA repair, signal transduction, gene transcription, DNA methylation and growth factors (Henke, 2009).

The combination of high toxicity and localised relative environmental abundance is the cause for recent concern regarding the limits and techniques that would allow for better monitoring and control of arsenic in terrestrial waters.

2.2. Phytoremediation of arsenic

In order to apply a well-rounded phytoremediation strategy to decontaminate arsenic from soil or water, firstly it is important to understand the basic biochemistry of arsenic in plants, the extent of the contamination, the bioavailability of arsenic in the contaminated media and finally to understand the interaction between arsenic, media and the plants (Willey, 2007).

The biochemistry of arsenic in plants is explained in detail in section 2.5. The extent of the contamination needs to be assessed in a case-specific basis. Redox potential, pH and the reactive sorbents (clay minerals, Al, Fe and Mn oxides) in soils and sediments are key factors in controlling the partitioning, speciation and bioavailability of arsenic (Lombi and Holm, 2010; Sun, 2011; Lui, Fernandez and Cai, 2011). In the particular case of arsenate, phosphates have shown to impact on bioavailability and therefore on toxicity (Levy et al., 2005). In contrast, as uncharged molecule, arsenite

is very similar in structure to glycerol and other uncharged molecules and consequently, these molecules may also impact on its bioavailability (Thomas and Gerd, 2010).

Results for arsenic phytoremediation from field studies are scarce; one example of such studies was carried out in Chenzhou City, Hunan Province, China (Willey, 2007). The hyper-accumulator fern *Pteris vittata* was used to bioremediate arsenic contaminated soil mainly in the surface layer (0 – 20cm) with arsenic concentration ranging from 24 to 192 mg kg^{-1}. Results showed that the addition of phosphate increased significantly the accumulation of arsenic compared with controls with no addition of phosphate. It was also found that the concentration of arsenic in soil was significantly reduced after 7 months of treatment. The efficiency of arsenic removal ranged from 6 to 13% and the concentrations of arsenic in shoot plants varied from 127 to 3269 mg kg^{-1}.

In other field experiments in the Ron Phibun area in Thailand, a filter made of *C. vulgaris* cells entrapped in alginate beads was shown to reduce arsenic concentration in water from 50 to 5 mg L^{-1}. The system generated low waste since contaminated beads were used to feed Nile tilapia (*Oreochromis nilotica*) produced by local residents. Most of the arsenic inside the algae was in inorganic form. However, arsenic is transformed to the organic form inside fish and this makes toxicity of arsenic negligible (Garelick et al., 2008). *Chlorella vulgaris* cells have also shown potential to bio-remediate a wide range of pollutants among them: Cd, Ag, Cu, Th, Zn, Pb, Ni, Ra, Fe, U and textile wastewater among others (Asku, 1992; Bajguz, 2011; Harris and Ramelow, 1990; Lim, Chu and Phang, 2010).

2.3. The green algae *Chlorella vulgaris* (*C. vulgaris*)

The term algae often refers to photosynthetic organisms which do not show a high degree of differentiation, as opposed to plants that do differentiate forming roots, leaves, stems and xylem/phloem vascular networks. While plants and algae share characteristics in common (e.g. both produce the same storage compounds, use similar defence strategies, and share morphological functions) there are more differences than similarities between plants and algae (e.g. the reproductive organs of plants are surrounded by sterile cells, they have a multi-cellular diploid embryo

that remains dependent on the parental gametophyte for a long period and they produce tissues that differentiate in several shapes) (Barsanti and Gualtieri, 2006).

Taxonomical classification of algae has changed vastly over the years (the most recent classification rely on 18S-rDNA sequencing); nevertheless previous classifications are still useful today. One of several classifications describes *C. vulgaris* belonging to Kingdom: *Eukaryota*, Phylum: *Chlorophyta,* Class: *Chlorophyceae*, Order: *Chlorellales*. This classification is based on morphology and physiological properties (Friedl and O'Kelly, 2002).

According to this classification *C. vulgaris* is a freshwater green unicellular microalgae, autospore forming, spherical in shape (cells 2-10 μm in diameter), with a single pariental cup-shaped chloroplast which nearly fills the cell, having a single pyrenoid present, producing chlorophyll a and b with absent *phycobilins*. The main carotenoid produced by *C. vulgaris* is lutein and produces little cellulose in the cell wall, instead the cell wall contains hemicelluloses which accounts for the stability and rigidity of the cells. One mature cell divides into four new ones every 16-20 h. The photosynthetic rate exceeds the respiration rate of *C. vulgaris* cells by 10-100 times (Lee, 2008).

C. vulgaris is a mixotrophic algae; this means that as well as using sunlight as the source of energy and CO_2 as the carbon source, all the attainment of its metabolic necessities and the production of carbohydrates and ATP (adenosine triphosphate) can also be obtained from organic carbon in the external environment without using their photosynthetic apparatus (Barsanti and Gualtieri, 2006).

2.3.1. Culture conditions

Conditions for *C. vulgaris* growth have been optimised and reviewed since the 1950's. The two most frequently used conditions for optimal growth of *C. vulgaris* that can be found in the literature are: Bold basal medium (Bold, 1949) and modified-Detmer's medium (Maeda et al., 1983). The main difference between these media is pH (Bold's pH = 6, Detmer's pH = 8) and Bold's use of KH_2PO_4 plus K_2HPO_4 while Detmer's only use K_2HPO_4, which is more soluble and renders the medium less acidic. Many researchers prefer the use of Bold's medium for freshwater algae in

different dilutions because natural water is more likely to contain a combination of the two soluble forms of phosphate and also because of its more acidic pH.

Many freshwater microalgae cultures can be maintained efficiently at temperatures between 17-27 °C and some species can grow even at 40 °C. Cells of *C. vulgaris* grow optimally between 20-25 °C (Barsanti and Gualtieri, 2006; Sayed and El-Shahed, 2000).

The photosynthetic reactions carried out by algae to produce energy and metabolites are dependent on light. Optimal conditions for this source of energy rely on intensity, quality and periods of illumination. These conditions vary greatly among algae species. The light intensities most often employed range between 100 and 200 µmol m^{-2} s^{-1} which corresponds to about 5-10% of full daylight (for fluorescent lamps 1 mol m^{-2} s^{-1} = 74 Lux). Higher light intensities may cause photo-inhibition and also, if not controlled, can cause a rise in the culture temperature (Barsanti and Gualtieri, 2006) .

Sedimentation is a common characteristic of non-motile unicellular algae cultures. This happens when the population is not homogeneously exposed to light and nutrients and gas exchange (e.g. CO_2) between air and the medium is poor. Bubbling CO_2 supplemented-air into the media can provide sufficient inorganic carbon and mixing. However this can lead to contamination of the cultures, some species of algae do not grow under turbulent conditions and also excessive CO_2 concentrations may inhibit metal-dependent enzyme systems. When growing algae in batch cultures (e.g. conical flasks), some authors recommend occasional shaking several times a day maintaining the sample to flask volume ratio of about 0.2 in order to minimise sedimentation and improve light and nutrient exposure and gas exchange. However, under these conditions uniform mixing between experiments is very difficult to achieve (Barsanti and Gualtieri, 2006; Stevenson, Bothwell and Lowe, 1996).

Conditions for supplementation of algae with organic carbon have been explored for the production of bio-fuels. Algae can take up carbon in the form of acetate, glucose and glycerol without stopping their photosynthetic activities. It has been found that optimal growth can be obtained at 1% glucose or glycerol (Liang, Sarkany and Cui, 2009). Therefore, instead of supplementation with CO_2, sufficient carbon and mixing

can be provided to algae cultures by providing 1% glucose or glycerol and daily manual shaking to avoid the problems mentioned above.

2.4. Application of *C. vulgaris* to bioremediate pollutants

The potential of the microalgae *C. vulgaris* to bioremediate a wide variety of pollutants has been particularly well documented. Living *C. vulgaris* cells, immobilised biomass and dry cells have been used for bioabsorption and bioadsorption of several pollutants.

Reports for the potential to decontaminate heavy metals from water such as cadmium, cobalt, copper, chromium, lead, mercury, silver and zinc have shown promising results (Maeda et al., 1990; Afkar, Ababna and Fathi, 2010; Regaldo, Gagneten and Troiani, 2009; Harris and Ramelow, 1990; Inthorn, Sidititoon and Silapanuntakul, 2011).

Examples for remediation of organic pollutants such as bisphenol A (Gulnaz and Dincer, 2009), textile wastewater (Lim, Chu and Phang, 2010), naphthalene (Kong, Zhu and Shen, 2010) and tributyl tin (Luan et al., 2006) have also been reported.

Nutrients removal such as carbon, nitrogen and phosphorus mainly from wastewater has also shown good potential (Lau, Tam and Wong, 1996; Andersen, 2005; Yan et al., 2013).

2.5. Toxicity and tolerance of *C. vulgaris* to arsenic

In the 1970's Jeanjean et al. (1970) investigated the absorption of arsenate by a strain of the freshwater algae *Chlorella pyrenoidosa*. This group started investigating the effect of the presence of arsenate in the absorption of phosphate, then focused on the absorption of arsenate alone using radioactively tagged arsenic and drew very interesting and useful conclusions which were somehow neglected by many authors (Jeanjean and Blasco, 1970; Jeanjean, Blasco and Gaudin, 1971; Blasco, Gaudin and Jeanjean, 1971). Some of their conclusions include:

- Arsenate competitively inhibits phosphate uptake and that inhibition is reversible

- There is no complete recovery of phosphate absorption when there is a previous exposure with arsenate
- When arsenate is accumulated inside the cell the internal concentration becomes superior to the external concentration
- As opposite to phosphate, after a certain time there is a decrease in absorption rate that corresponds to an equilibrium between absorption and desorption.
- There are two mechanism for arsenate absorption, similar to the high affininty and low affinity for phosphate.
- A fraction of the arsenate absorbed is promptly effluxed.
- There is a little reduction of arsenate to arsenite that is not transported out of the cells

These conclusions did not differentiate between adsorption and absorption and the speciation methodologies were indirectly determined.

The investigations carried out by Maeda et al. starting in 1983 (Maeda et al., 1983) drew attention to the tolerance of freshwater green algae to arsenic. First they screened several freshwater organisms from sites contaminated with high concentrations of arsenic, then they grew them into medium containing up to 2,000 mg L^{-1} of arsenate, this mixture contained blue-green algae, green algae, diatoms and also minor populations of protozoa, rotifera and bacteria. They concluded that the organism that had the highest resistance and accumulated arsenic in the most efficient way was the microalga *C. vulgaris*.

The same group also investigated tolerance of *C. vulgaris* to arsenic under different conditions of exposure, among these conditions: arsenic concentrations, arsenic species, temperature, illumination, phosphate levels, and metabolic inhibitors (respiratory and photosynthetic) (Maeda et al., 1985). Conclusions included:

- Growth of *C. vulgaris* increased with an increase of As(V) concentration up to 2,000 mg L^{-1} and cells survived even at 10,000 mg L^{-1}
- Bioaccumulation increased with an increase of the arsenic level and maximum accumulation was 50,000 µg As g^{-1} dry cell,

- Growth decreased with an increase of As(III) level and cells were cytolysed at 40 mg L^{-1}
- A respiratory inhibitor (dinitrophenol) stopped bioaccumulation, and a photosynthesis inhibitor (sodium azide) did not affect bioaccumulation.

Other experiments investigated by the same group included: transformations in the freshwater food chain starting with *C. vulgaris* as autotrophic organism, bio-methylation, the formation of metallothionein proteins, efflux of radioactively labelled As(V) after bioaccumulation and formation of arsenic molecules after exposure to As(III) (Maeda et al., 1990; Maeda et al., 1992; Maeda et al., 1992; Maeda et al., 1992; Suhendrayatna et al., 1999).

The tolerance of *C. vulgaris* cells to arsenic was also investigated by: surface adsorption experiments using living cells, heat-dried cells and freeze-dried cells as well as experiments on the fluidization of the cell membranes. The following transformations of arsenic have been investigated: arsenosugar formation and identification and quantification of glutathione and phytochelatins (Levy et al., 2005; Simmons et al., 2009; Jiang et al., 2011).

Early toxicity tests using *C. vulgaris* used media containing high amounts of phosphate, emulating conditions for maximal algae growth. These experiments found that the alga was more sensitive to As(III) than As(V), similar to marine organisms, plants, insects, mammalian and cancer cells (Maeda et al., 1985; Knauer, Behra and Hemond, 1999; Pawlik-Skowronska et al., 2004). However these nutrient conditions greatly exceed those found in most surface waters and may over or under estimate the effects of some toxicants. More recent experiments have demonstrated that at low concentrations of phosphate, *Chlorella sp.* cells are more sensitive to As(V) than As(III), because phosphate releases some of the toxicity of the analogue arsenate, and probably because there is no equivalent for As(III) that control growth rate as phosphate does. This is a clear example that the conclusions made by Jeanjean et al. (Jeanjean and Blasco, 1970; Jeanjean, Blasco and Gaudin, 1971; Blasco, Gaudin and Jeanjean, 1971) were not taken into consideration when early toxicity test were carried out by other researchers (Levy et al., 2005; Pawlik-Skowronska et al., 2004; Stolz et al., 2006).

There are also considerations regarding the initial concentrations of cells to be used in toxicological experiments. For a long time high initial concentrations of cells have been used mainly because of technical reasons (as later explained in section 2.3.1.1). However, it has been shown that the use of high initial concentrations of cells can decrease the toxic load that the tested chemical exerts (Franklin et al., 2002; Levy et al., 2005).

Humic acids, organic matter and specially EDTA (Ethylenedieminetetraacetic acid) can bind to metals and metalloids and thus their toxicity in the media can be under estimated if EDTA is used. EDTA is a chelating agent commonly added to culture media to minimise trace metals precipitation and acts as an ion buffer (Stevenson, Bothwell and Lowe, 1996). Therefore the use of EDTA should be avoided and the amount of humic acids and organic matter should be kept at minimum concentration in toxicity tests.

2.5.1. Toxicity tests

2.5.1.1. Toxicity tests for freshwater microalgae

Several toxicity tests and other assessments related to the tolerance of stressors to freshwater organisms have been published and reviewed extensively. However gathering all the information for the specific conditions to be tested for a particular organism under a particular stress to be able to offer reliable and reproducible results is not always straightforward. This is the reason why some standard methodologies allow for modifications in their scope (Blaise and Ferard, 2005; ASTM, 2004).

Toxicity tests are designed to determine the adverse effects that chemicals have on biological systems or individual organisms. In the particular case of arsenic, it can help to rank the toxicity of the different arsenic species, the toxic conditions, test for the mechanisms of detoxification, the development of the conditions under which the test is performed as well as the development of treatment technologies among others (Blaise and Ferard, 2005).

Toxicity test for freshwater microalgae in batch systems can be undertaken in 96-well micro-plates or conical flasks. Micro-plate tests have the advantage of using low

sample volumes, less space in an incubator and disposable plasticware. However, mixing is complicated, accurate measurement of volume is difficult and the risk of contamination of the sample is high as the sole method to prevent contamination is by using plastic lids. On the other hand, more space intense flasks use more media but mixing and contamination are not issues. Mixing can be done via manual shaking and contamination is prevented through use of stoppers that allow gas exchange (Blaise and Ferard, 2005).

Normally, after the algae is inoculated, cells follow a series of phases in which the exponential phase can be maintained for a long period of time, avoiding long lag phases, ensuring optimal metabolic conditions and growth rate. To do this in *C. vulgaris*, cells that have been sub-cultured every 5-7 days can be used to inoculate test experiments (Blaise and Ferard, 2005; Janssen and Heijerick, 2003).

A control and at least five test concentrations of the toxicant are required with a minimum of three replicates (the control with concentration that have no effect, a concentration that will have 90-100% inhibition, two concentrations below 50% inhibition and two concentrations above 50% inhibition) (Janssen and Heijerick, 2003; ASTM, 2004).

Tests are usually conducted in terms of 72 or 96 h because at longer exposure periods, the medium may become nutrient limited and changes in bioavailability and arsenic species may occur. Results are reported in terms of IC_p (the inhibition concentration for a specified percentage), NOEC (no observed effect concentration), and LOEC (lowest observed effect concentration) among others.

Tests should be conducted under controlled temperature, light, and initial pH. Because arsenic can adhere to glass surfaces, all glassware should be cleaned following an appropriate procedure (e.g. 12 h in an acid bath followed by rinsing 3 times with deionised water).

Low initial cell concentration (e.g. $5x10^3$ cells mL^{-1}) is recommended to avoid a decrease in toxic load; also a better pH control can be achieved by reducing the initial inoculums size (Andersen, 2005).

Data on population growth is used to determine the effects of the toxicant on microalgae and this should be estimated at several intervals. Population growth or biomass production can be measured in several ways using indicator parameters. Some of the parameters that have been used to measure biomass are: dry weight, cell counts, carbon 14 assimilation, optical density, chlorophyll a and b, adenosine triphosphate (ATP) and deoxyribonucleic acid (DNA) content. All these parameters are surrogates of population growth and some advantages and disadvantages exist (Appendix 1). Their use depends on the type of toxicant to be employed. The analytical capabilities, cost and analysis time are also to be considered (Janssen and Heijerick, 2003).

Regardless of the method used to quantify cells, direct observations using a microscope and a counting chamber should be used for quality assurance and for the creation of calibration curves. The most common counting chamber is the improved Neubauer haemocytometer and is used to count cells in the range 10^4-10^7.

Measuring optical density (absorbance at 670 nm) is one of the most common methods to indirectly estimate the number of cells in a given population. The technique is not expensive but also not very sensitive, only useful for highly concentrated cultures and any suspended particles will account for an increase in optical density. Toxicity tests are increasingly requiring low concentrations of cells to avoid under/over estimation of toxicity and to reproduce environmental natural conditions.

Chlorophyll a, b and other pigments are produced by autotrophic organisms as part of their photosynthetic machinery. Measurements of these pigments *in vivo* and *in vitro* have been used over the years.

Measurements of chlorophyll fluorescence *in vivo* are hampered because the amount of pigment that is re-emitted as fluorescence in intact cells is only about 1% of the total amount of the pigment inside the cells. Also the signal varies depending on the light regime that the cells are in and the presence of some chemicals such as herbicides. Nevertheless the sensitivity of this technique compared with optical density is greater (Kirk, 1994).

Measurements of chlorophyll fluorescence *in vitro* normally require filtration or centrifugation, and extraction with an organic solvent. This technique is highly sensitive and allows counting of cells as low as 500 cells mL^{-1}. However, the technique is very time consuming (Phinney and Yentsch, 1985).

Recently a whole water extract technique has been described to overcome many of the drawbacks of previous techniques. It is based on a direct extraction in the media with a mixture of acetone and dimethyl sulfoxide (DMSO) (1:1, v/v). In contrast to traditional techniques that aim to extract chlorophyll a or b only, the whole water extraction aims to extract all the pigments that produce fluorescence with an excitation of 430 nm and emission at 671 nm, consequently eliminating some of the acidification steps designed to distinguish chlorophyll a from other pigments. In this way the fluorescence signal is maximised to increase the precision of the correlation with the cell numbers and not the total content of chlorophyll a (Mayer, Cuhel and Nyholm, 1997).

2.5.1.2. Flow cytometry based methods

Automated cell counting techniques are faster than traditional methods and reduce the counting error by increasing the amount of cells counted per sample. Furthermore they allow other cellular parameters to be determined such as cell volume, DNA content, glutathione (GSH) and related thiols, pH, the free radical H_2O_2, superoxide O_2^- and cell viability. Also a differentiation between populations based on size can be performed, allowing the isolation of cells from debris or counting specific populations within a mixture (Andersen, 2005; Peperzak and Brussaard, 2010).

In a flow cytometer, the suspension containing the cells is passed through a small aperture onto which one or several light sources are focused. The scattered light that is produced each time a particle passes the light beam is used to measure size and shape of the particle. If the particle emits a fluorescent signal which corresponds to the excitation wavelength of the light source, then the signal emitted can be detected and is proportional to the concentration of the fluorescent molecule in the particle. Microalgae cells naturally contain fluorescent pigments such as chlorophyll a, b and phycoerythrin. Moreover cells can be fluorescently labelled with other chemicals that react with specific molecules within the cell and thus helping the determination of

such molecules (Andersen, 2005). Among these chemicals, monochlorobimane, monobromobimane, Calcein-AM, SYTOX Green, HE dihydroethidium, CMFDA, BCECF and H_2DCFH-DA have been used to dye molecules using flow cytometry. Special care should be taken when analysing algae cells, because auto-fluorescence caused by photosynthetic pigments may interfere with other molecules (Andersen, 2005; Cossarizza et al., 2009; Blaise and Ferard, 2005). This can be observed in Table 2.1.

Table 2. 1 Fluorescent molecules for use in flow cytometry along with their properties

Molecular probes	Excitation (nm)	Emission (nm)	Determination	Notes
Chlorophyll a	488	690	Auto fluorescence	Algae cells produce it naturally
Phycoerythrin	488	570	Auto fluorescence	Algae cells produce it naturally
SYTOX green™	504	523	Viability /Dead Cell Stain	
H_2DCFH-DA	492-495	517-527	H_2O_2 Free radical sensor	
HE dihydroethidium	355, 488	See notes	O_2 Super oxide indicator	Dihydroethidium has blue fluorescence (Em ~420 nm) until oxidized to ethidium (Em ~605 nm). The reduced dye does not bind to nucleic acids
Monobromobimane mBBr	394-405	490	Glutathione (GSH reduced)	Low molecular weight thiols, including glutathione, N-acetylcysteine, mercaptopurine, peptides and plasma thiols
Cell Tracker™ Green CMFDA	492	517	Glutathione (GSH reduced)	This is a useful alternative to the UV light–excitable monochlorobimane for determining levels of intracellular glutathione
BCECF	490	535	Radiometric pH indicator	Measures changes in the cytosolic pH of most cells. pH (~6.8–7.4).

SYTOX Green™ can be used for the analysis of cell viability because it can penetrate cells that have lost membrane integrity, having great affinity for nucleic acid, thus only dead cells will emit a fluorescent signal (Andersen, 2005).

Reactive oxygen species (ROS), which are produced as a result of oxidative stress in cells, can be detected using the H_2DCFH-DA probe. This molecule is non-

fluorescent and can diffuse into the cell membrane freely. The molecule is sensitive to redox changes inside the cell. It is cleaved by esterases and in the presence of H_2O_2 is oxidised by peroxidases into a fluorescent molecule with good specificity (Langsrud and Sundheim, 1996; Cossarizza et al., 2009).

CMFDA (5-chloromethyl fluorescein diacetate) is hydrolysed by intracellular estereases to yield highly fluorescent molecules capable of binding GSH under the action of glutathione S-transferase (Hedley and Chow, 1994).

Intracellular super oxide O_2^- is detected by using HE dihydroethidium. This molecule is oxidised to the fluorescent molecule ethidium bromide by O_2^-. This oxidation occurs faster than oxidation in the presence of O_2, H_2O_2, HOCl or $ONOO^-$.

BCECF (bis-carboxyethyl-carboxyfluorescein) is incorporated into intact cells and is subsequently hydrolysed forming a less permeable compound which can be used as a reporter molecule for normal cytoplasmic pH. This molecule is capable of emitting different fluorescence intensities at different pH. The acid dissociation constant (pKa) of 7.0 is suitable to measure the normal range of cytoplasmic pH in most cells (~6.8-7.4) (Rink, Tsien and Pozzan, 1982).

2.5.2. Detoxification mechanisms

Isolated studies have been performed so far investigating the mechanisms underlying *C. vulgaris* tolerance and toxicity to arsenic. Some of the mechanisms are assumptions of behaviour observed in other species of freshwater green algae, marine algae, higher plants or even bacteria.

More detailed studies have only been performed on total bioaccumulation, surface adsorption and arsenosugar formation but so far, arsenic efflux, reduction/oxidation, methylation/demethylation and glutathione/phytochelatin (GS/PC) complexation in *C. vulgaris* cells lack deep investigation. A graphic model of these transformations is shown in Fig 2.2.

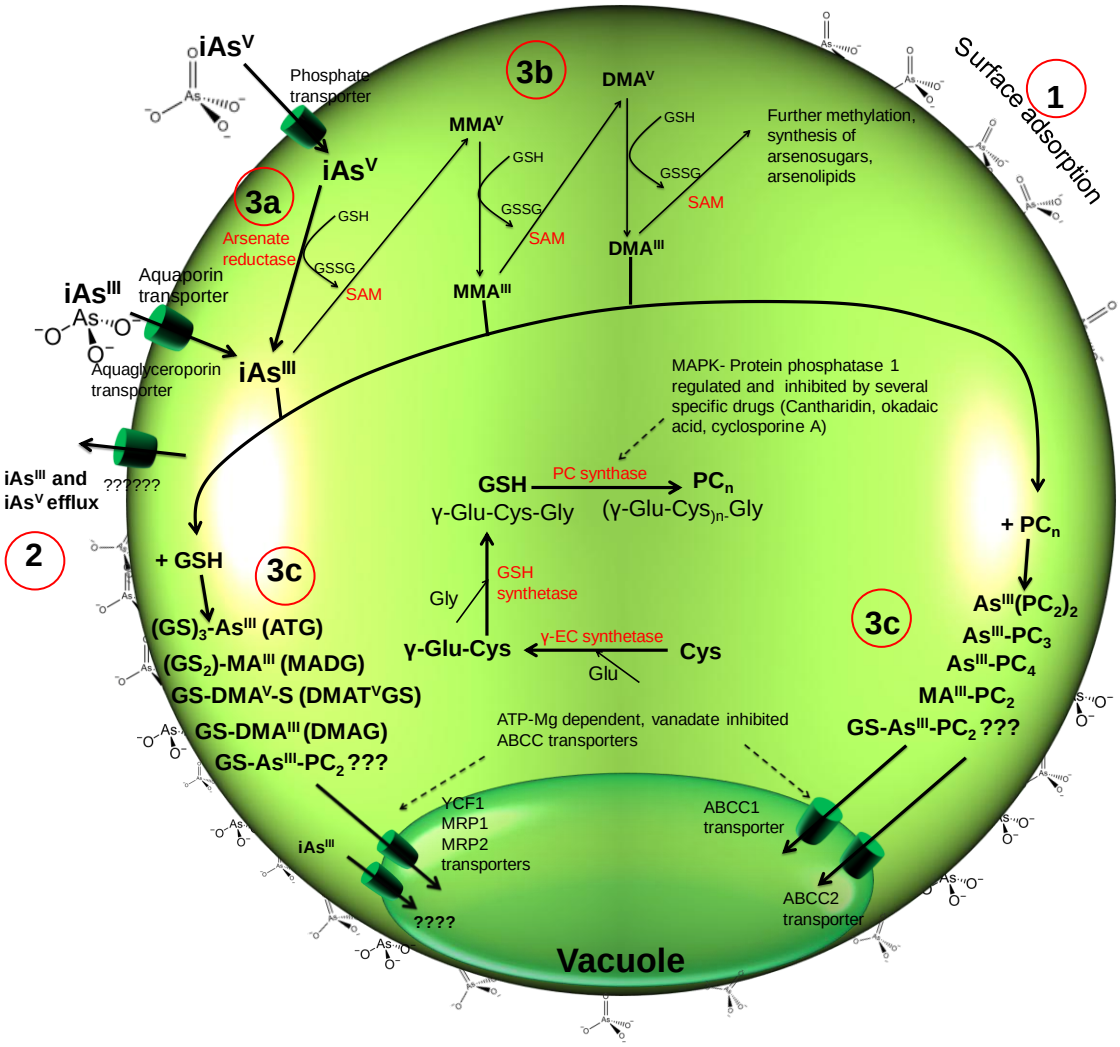

Fig 2. 2 Representation of the theoretical arsenic tolerance/toxicity mechanisms in *C. vulgaris* cells (1: surface adsorption, 2: efflux, 3a: reduction/oxidation, 3b methylation/demethylation, 3c: GS/PC complexation)

2.5.2.1. Surface adsorption

Passive surface adsorption can be driven by electrostatic attraction, ion exchange, coordination, complexation, chelation and micro-precipitation (Donmez et al., 1999). Thus the mechanism of arsenic adsorption in *C. vulgaris* depends on the surface properties of the algae cell wall.

The characteristics of the cell wall differ among freshwater algae and also between algae species, some of these properties are: cell surface hydrophobicity (hydrophobicity is linked to the polysaccharide content in the cell wall which is correlated to nitrogen and carbon content in the hydrocarbon and inversely correlated to the concentration of oxygen), zeta potential, the presence of anionic or

cationic groups (charged carboxyl, phosphate, or amine groups), shape and cell size (Hadjoudja, Deluchat and Baudu, 2010).

These properties have been investigated in *C. vulgaris* cells. The cell surface of this alga is a strong electron donator and weak electron acceptor; this combined with the hydrophobicity of the cell can be linked to its low concentration of polysaccharides. The iso-electric point in the cell wall is 2.9 (measured as the zeta potential). This indicates that at neutral pH the cell surface is negatively charged therefore attracting positively charged molecules such as metal ions. The main functional groups (determined by potentiometric titrations) were found to be carboxyl, phosphoryl, amine and hydroxyl; the total buffering capacity was $0.22x10^{-3}$ mol g^{-1} which is an indication of the total concentration of functional binding groups (Hadjoudja, Deluchat and Baudu, 2010).

Since the studies carried out by Jeanjean et al. (1970) and based on their conclusions, an adsorption mechanism of arsenic that differs considerably from absorption in *C. vulgaris* cells could be devised due to the following facts: equilibrium for arsenate uptake was achieved, the recovery of phosphate uptake was not complete after exposure to arsenate and there was competition between arsenate and phosphate. Without having the means to differentiate between adsorption and absorption, the conclusions made in these investigations were put in place only partially (Jeanjean and Blasco, 1970).

Another group of researchers found that neither dinitrophenol treated, heat-killed nor ethanol-killed *C. vulgaris* cells adsorbed any arsenate. The protocol involved measuring arsenic adsorption by its depletion from the media (8 mg L^{-1}) after 4 and 6 h. Unfortunately, the authors did not attempt to desorb arsenic from the surface of the cells (Maeda et al., 1985). The same group investigated the adsorption of arsenate using the residue of *C. vulgaris* cells extracted with chloroform/methanol (2:1) and cultured in an arsenic-free medium. This time cells adsorbed arsenic in column experiments and the adsorption capacity was found to be 1100 µg g^{-1} and only 24% of this adsorption was reversible (desorbed with 1 M HCl) (Maeda et al., 1992).

In a more comprehensive investigation, it was found that *C. vulgaris* cells cultured for 7 days adsorbed up to 50% of isotopically labelled arsenate in solution. However the protocol included washing the cells only with deionised water three to nine times until no arsenic was detected in the washings; the washings were pooled and analyzed for arsenic but clearly this can under estimate the amount of arsenic adhered to the cell wall (Maeda et al., 1992).

Several mechanisms have been attributed to arsenate toxicity to living cells but few of them have been explored in detail. The effect of arsenate to algae cell membranes has been studied. Artificial membranes and *C. vulgaris* cells were exposed to arsenate at different concentrations. It was found that Calcein-AM accumulation into living cells was increased by arsenate exposure. Moreover, Calcein-AM entrapped into artificial membranes was released after incubation with arsenate in contrast with no release for control experiments. The results in this study gave indication that fluidisation of the membrane happened due to arsenic substitution of phosphate or the choline group of membranes (Tuan et al., 2008).

Arsenite adsorption using dry *C. vulgaris* cells has also been investigated. Arsenite was selectively adsorbed from As(V), MMA (monomethylarsonic acid), and DMA (dimethylarsinic acid) under strong basic conditions (pH>10) at room temperature in batch experiments with 15 min contact time. No significant changes were observed in arsenic adsorption when algae were taken from different growth phase. Again arsenic adsorption was measured by its depletion from the media without any attempt to desorb arsenic form the surface of the cells (Taboada de la Calzada et al., 1999).

Because reversible adsorption is strongly controlled by pH, desorption is also a pH dependent process. Several desorption solutions have been previously used, some consist on raising the pH above 10 for inorganic adsorbents, however this may cause undesirable changes in cell biomass. Other washing solutions are based on EDTA and ice-cold phosphate buffer. One desorption solution that has been used recently in arsenic experiments consist of 1 mM K_2HPO_4, 5 mM 2-(N-morpholino)ethanesulfonic acid (MES), 0.5 mM $Ca(NO_3)_2$ at pH 6 for 10 min (Sandau, Pulz and Zimmermann, 1996; Abedin, Feldmann and Meharg, 2002).

a) Adsorption Models

A way to interpret and fit specific observations into general adsorption data is the use of adsorption models or adsorption isotherms. These models can predict very accurately the behaviour of arsenic adsorption; however, the models do not provide information on the adsorption mechanism (Everett, 1998; Asano et al., 2007).

An initial review of the kinetics and rates of adsorption must be performed. In a kinetic study the initial concentration of adsorbent is held constant and the fraction of adsorbate remaining is measured as a function of time under appropriate mixing. Mixing is critical as adsorption rates may be limited by diffusion in the bulk solution, as random molecular motion only allows ions to be transported in the absence of bulk flow in the direction of a concentration gradient. Film diffusion is considered to be a rapid process and pore diffusion varies depending on the characteristics of the adsorbent (Jang et al., 2006; Guo, Stuben and Berner, 2007).

Pseudo-equilibrium is reached when the rate of change is at minimum in the concentration of the adsorbate remaining in the solution over time (Everett, 1998).

Freundlich and Langmuir equations have been the most used and best explained models. Nevertheless all adsorption equations are variants of the mass action law. Adsorption isotherms are developed experimentally by stimulating contact between a given amount of adsorbate and a fixed volume of liquid while altering the amount of adsorbent (Everett, 1998).

Adsorption capacity is a function of the characteristics and concentration of the adsorbate and temperature. These characteristics include: solubility, molecular structure, molecular weight, polarity, hydrocarbon saturation, particle size and pore size. The pH of the solution is also a characteristic to take into account particularly in physical adsorption (Asano et al., 2007).

The Freundlich model is defined as follows (Everett, 1998):

$$x/m = q_e = K_f C_e^{1/n}$$

Where:

x/m= mass of adsorbate adsorbed per unit mass of adsorbent after equilibrium, mg adsorbate/g adsorbent.

K_f= Freundlich capacity factor (mg adsorbate/g adsorbent)X (L water/mg adsorbate)$^{1/n}$

1/n= Freundlich intensity parameter

q_e= $(C_0-C_e)V/m$

q_e= adsorbent concentration after equilibrium, mg adsorbate/g adsorbent

C_0= initial concentration of adsorbate mg.L^{-1}

C_e= equilibrium concentration of adsorbate after adsorption has occurred, mg.L^{-1}

V= volume of liquid, L

m= mass of the adsorbent, g

The constants of the Freundlich isotherm can be determined by plotting log(x/m) vs. log C_e and using the following linearised expression:

$$\log(x/m)=(\log K_f) + (1/n) \log C_e$$

Langmuir derived a model using the activity of the predominant aqueous species and mole fraction of the adsorbed metal. Assumptions for this model are: the number of available accessible sites on the adsorbent surface does not change, all sites have the same energy, and adsorption is reversible (Aragon and Thompson, 2005). The Langmuir isotherm is defined as:

$$x/m= q_e = (Q_0 K C_e)/ (1+ KC_e)$$

Where:

Q_0 is the maximum adsorption capacity (mg arsenic /g of D-Fe media) and K is the Langmuir empirical constant, other terms as previously defined.

Freundlich and Langmuir models differ from each other with respect to how the free adsorption energy is assumed to vary with q_e and the existence of a finite adsorption capacity. The success of Freundlich versus Langmuir equations or vice-versa, depends on the concentration range of the adsorbent and the capacity of the adsorbent (Everett, 1998).

2.5.2.2. Arsenic efflux

There is no metabolic or nutritional function for arsenic within the cells. Thus there is no known dedicated transport uptake system for arsenic. Instead, arsenic crosses

the cell membrane by using existing transporter systems that share similar molecular structure. Arsenate gets inside *E. coli* cells by using specific phosphate transporters thanks to its similarity to phosphate (Rosemberg, Gerdes and Chegwidden, 1977). In plants arsenate and phosphate also share the same transport system having more affinity for phosphate (Meharg, Nylor and Macnair, 1994).

Arsenite has been found to be transported inside the cells by aqua-glycerolporin channels and glucose permeases in *E. coli*, yeast and mammalian cells (Meng, Liu and Rosen, 2004; Liu et al., 2004). However there is evidence that in some plants, arsenite is transported by aquaporin channels, which selectively transports water inside cells. This is of particular importance in rice and other plants growing in anaerobic flooded environments, where arsenite is predominant (Zhao et al., 2009).

Efflux of the two most common soluble inorganic forms (As(III) and As(V)) has been investigated in some detail using radio-labelled arsenic inside *C. vulgaris* cells. Great insight was obtained from the conclusions drawn by Maeda et al., (1992). First, arsenate (10 mg L^{-1}) accumulation was higher at the beginning of the lag phase which was maintained through the log phase and decreased in the stationary phase. Arsenite (1 mg L^{-1}) accumulation reached its maximum at the beginning of the log phase and up to 48 h and then decreased dramatically. Arsenite was transformed to As(V), MMA, DMA and trimethyl arsine (TMA). Both arsenate and arsenite metabolites (As(V), MMA, DMA and TMA) were readily excreted under conditions undesirable for the growth of the algae such as low nutrients and darkness (Maeda et al., 1992; Suhendrayatna et al., 1999). Cells were only washed three times with deionised water before transferring them to an arsenic free media for the efflux experiments. This cannot differentiate between adsorbed arsenic being desorbed and any efflux of absorbed arsenic.

Arsenate efflux in plants is thought to be via anion channels (Zhao et al., 2009). Arsenite and arsenate efflux has also been observed in experiments in roots of tomato plants. Up to 16% of the arsenic uptake was released by this plant. In this experiment all the arsenic previously adsorbed was desorbed with ice-cold phosphate buffer. The inhibitor of oxidative phosphorylation, carbonyl cyanide, significantly enhanced arsenate efflux and decreased arsenite efflux; this gave an

indication that arsenite efflux is an energy-dependent active process. An inhibitor of ATP did not produce any change in efflux (Xu, McGrath and Zhao, 2007).

In other experiments using bacteria, efflux of radioactive arsenate was tested with inhibitors of ATPase, respiration, glycolysis and proton gradient. Efflux was correlated with the ATP content in the cell but not with the membrane potential (Broer et al., 1993).

As-GS complexes have been observed to be excreted from mammalian cells mediated by Multi Drug Resistance-Associated Proteins (MRP1-9). These are ATP dependent transporters, known to confer resistance to several xenobiotic and toxic drugs in bile, hepatocytes and breast cancer cells among others. Even when plant cells express MRP transporters, these are more likely localised in vacuoles therefore they do not mediate transport outside the cells but inside the vacuoles (Leslie, 2012; Guoa, Xua and Ma, 2012; Mendoza-Cozatl et al., 2011).

With respect to methylated forms of arsenic, MMA and DMA can readily cross biological membranes; this is suggested to be a passive diffusion process (Cullen, McBride and Picke, 1990).

2.5.2.3. Arsenic biotransformations

a) Reduction/oxidation

Reduction of arsenate inside cells has been found to occur by two main mechanisms: the first one where As(V) is used as a terminal electron acceptor during anaerobic respiration to obtain energy, and a detoxification process dependent on enzymatic reactions with arsenate reductases (thioredoxin and glutaredoxin families) followed by arsenite excretion (Frankenberg, 2002). Although chemical reduction of arsenate can occur via glutathione, this reaction is negligible compared to the reaction speed of the enzymatic transformations (Zhao et al., 2009).

Many algae species can reduce arsenate to arsenite. The freshwater alga *Chlamydomonas reinhardtii* has been found to be able to reduce 18-24% of the total arsenic inside the cells (Yin et al., 2011). The marine alga *Chlorella salina* can reduce up to 32% of the arsenic inside the cells when exposed only to arsenate for

72 h (Karajova, Slaveykova and Tsalev, 2008). The hyper-accumulators *Pteris vittata*, *Pteris cretica* and *Boehmeria nivea* are also able to reduce up to 88% of the intracellular arsenic (Huang et al., 2008). Roots and shoots of *Brassica juncea* contained 96-100% arsenite after arsenate exposure. However, arsenite was thought to be complexed with either glutathione or phytochelatins but this was not investigated further (Pickering et al., 2000).

In contrast little reduction of arsenate has been found in the marine alga *Hizika fusiforme*, *Laminaria* and *Dunaliella terciolecta* (Kohlmeyer, Kuballa and Jantzen, 2002; Duncan, Foster and Maher, 2010). Arsenate is only reduced between 1-6% inside *C. vulgaris* cells, observed in 7 days incubation experiments with 12/12 h illumination cycles (Murray et al., 2003).

Arsenite is hardly oxidised chemically at neutral pH only in the presence of O_2. This however is different in basic conditions (pH > 9), where arsenite is readily oxidised. Under oxidative stress, where H_2O_2, OH^- radicals and super oxide O^{2-} are present, oxidation can occur chemically very fast. Oxidation in natural waters is also significant under UV light, this occurs via free-radical generating reactions (Frankenberg, 2002).

Biological oxidation of arsenite has been characterized in *Alcaligenes faecalis*. This organism can be induced to produce arsenite oxidase which is found on the outer surface of the cytoplasmic membrane (Anderson, Williams and Hille, 1992). Some microorganisms excrete fatty acids that give oxidative capabilities to the surrounding media, and arsenite can be oxidised, but not selectively (Frankenberg, 2002).

Oxidation of arsenite was observed in dry and living *C. vulgaris* cells exposed to 50 μg L^{-1} of arsenite under basic conditions (pH > 10) for 10 min with mixing. This alga was able to transform around 50% of arsenite to arsenate. The authors stated that arsenic bio-oxidation occurred in dead and living cells. Their conclusion were slim due to the fact that the protocol did not included controls for speciation in the solutions with a change in pH, where in basic conditions and under illumination arsenite is readily oxidised (Beceiro Gonzalez et al., 2000; Taboada de la Calzada et al., 1999; Frankenberg, 2002).

b) Methylation/demethylation and arsenosugar formation

The most common stable forms of organic arsenic found inside freshwater algae are methylated species: monomethylarsonic acid MMA(V), dimethylarsinic acid DMA(V) and some trimethylated forms (Murray et al., 2003).

Pentavalent methylated arsenic species are less toxic than As(V) and As(III). Therefore methylation is believed to form part of a detoxification mechanism were chemical methylation is considered negligible (Frankenberg, 2002; Henke, 2009).

The "Challenger" mechanism is the most accepted rationalization for arsenic methylation in living organisms. Inorganic arsenic is transformed to organic methylated arsenic in a series of reiterative reductive/oxidative additions of methyl groups giving place to the formation of monomethyl arsenic, dimethyl arsenic and to a lesser extent trimethyl arsenic. In the reduction step, GSH and lipoic acid (6, 8-dithiooctanoic acid) have been found to act as reducing agents while the reaction is enzymatically catalysed. In the oxidative methylation, S-adenosylmethionine (SAM) acts as a methyl donor and is converted to S-adenosylhomocysteine (Bentley and Chasteen, 2002). The mechanism can be observed in Fig 2.3.

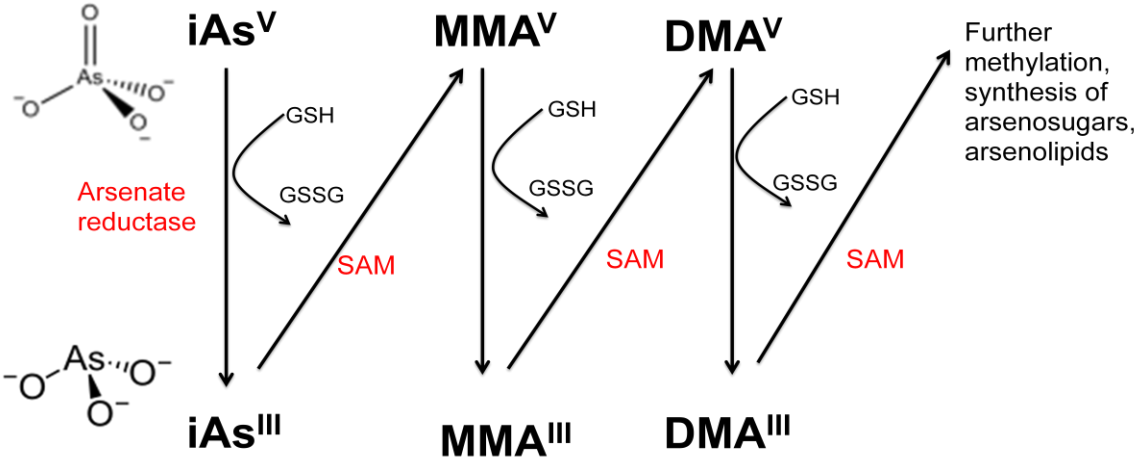

Fig 2. 3 "Challenger" mechanism for arsenic methylation, S-adenosyl methionine (SAM), GSH reduced glutathione, GSSG oxidised glutathione, MMA monomethylarsonic, DMA dimethylarsinic acid (Bentley and Chasteen, 2002).

Further transformations of methylated arsenic compounds are believed to form arsenosugars, arsenolipids and arsenobetaine (Phillips, 1990). Arsenosugars are a

range of arsenic containing carbohydrates discovered in 1981 (Edmonds and Francesconi, 1981). Arsenosugars have three general structures where the functional group of arsenic contains either DMA(V) (with oxygen or sulphur), DMA(III) or TMA. This is illustrated in Fig 2.4 (Meier et al., 2005; Regmi, Milne and Feldmann, 2007).

Few studies dealing with lipid soluble arsenicals have been done so far, and the reason for this is not for lack of interest but because of technical difficulties. The use of High Performance Liquid Chromatography (HPLC) coupled with Inductively Coupled Plasma Mass Spectrometry (ICP-MS) boosted research on water soluble arsenicals due to its nature: soluble mobile phases are compatible with the plasma ionisation source, where organic solvents in the mobile phase, needed for non-polar species, are not compatible at all (Schmeisser, Goessler and Kienzl, 2005; Amayo et al., 2011). This is discussed in more detail in section 2.4.1.

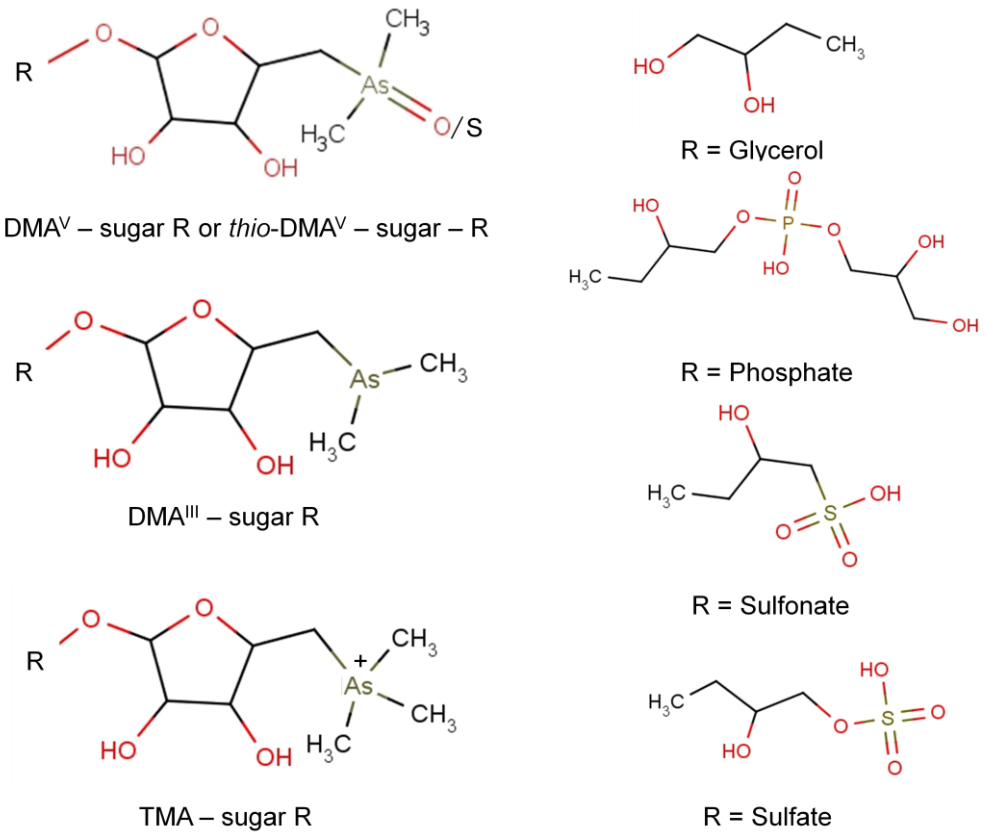

Fig 2. 4 Arsenosugar general structures form and nomenclature modified from Feldmann and Krupp, (2011)

C. vulgaris cells exposed to As(V) cultured with antiseptic and antimycotic compounds have been found to produce As(III), DMA(V), DMAAsSugarGlycol, DMAAsSugarphosphate and DMAAsSugarsulfonate. Interestingly, the most abundant species, after As(V) inside the cells, was DMAAsSugarphosphate. MMA(V) was absent which indicates that the metabolic pathway starting with the addition of the first methyl group takes place very fast or this species is somehow excreted (Murray et al., 2003). Sadly however, they also found that when extracting with 1:1 (v/v) methanol/water followed by 10 min in a sonication bath, the extraction efficiency was between 11 to 27%, a surprisingly low figure compared to other algae. This led to the conclusion that the arsenic species found were not representative of the species present in the algae cells and therefore a better extraction method was needed. This is discussed in more detail in section 2.4.3.

In other experiments with As(III) exposure to *C. vulgaris* cells, it was found that the predominant transformation was to As(V) followed by MMA(V), DMA(V) and TMA(V). However the method for arsenic speciation involved treatment with hot sodium hydroxide that could have converted arsenobetaine to TMA(V) and arsenosugars to DMA(V) and therefore some uncertainty was expected (Suhendrayatna et al., 1999).

c) GS/PC complexation

Glutathione (L-γ-glutamyl-L-cysteinyl-glycine, GSH) was discovered in 1922 by Frederick Gowland Hopkins (Masella and Mazza, 2009). GSH and its homologues hGSH (where the C-terminal Gly is substituted by Ala, Ser, Gln or Glu or is absent) encompass a group of tripeptide thiols that are present in high concentrations in most eukaryotic cells (Hedley and Chow, 1994).

GSH is directly synthesised by cells using the constituent amino acids rather than by translation of messenger ribonucleic acid (mRNA). GSH is characterised by a functional N-terminal (γ–Glu), a central cysteine residue (Cys) and a variable C-terminal amino acid, as can be observed in Fig 2.5 (Grill, Tausz and De Kok, 2002).

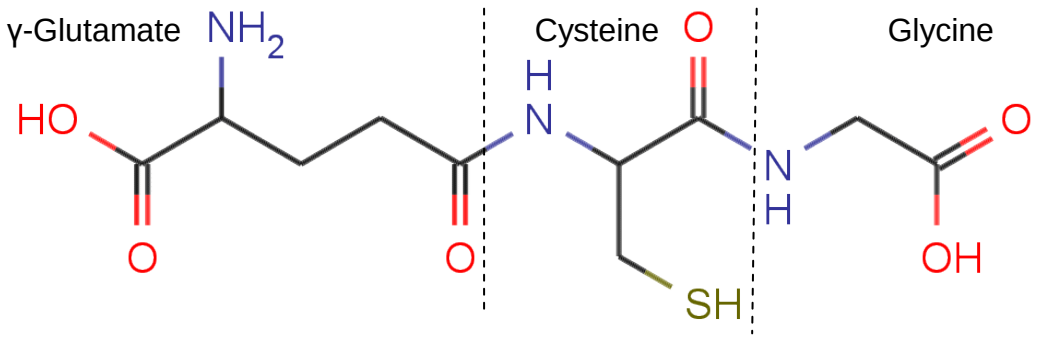

Fig 2. 5 Basic structure of Glutathione (GSH), the general formula is γ-Glu-Cys-Gly, where: Glu, Glutamate; Cys, Cysteine; and, Gly, Glycine (in homoglutathione Gly is substituted by Ala, Ser or Glu or is absent). Modified from (Kawakami, Gledhill and Achterberg, 2006)

The cysteine residue in glutathione and its homologues has been linked with several functions and they all rely on the unique chemistry of sulphur. The most characteristic property of cysteine is the ability to form a disulfide linkage (Fig 2.6) with another cysteine residue, thus providing a readily reversible covalent bond *in vivo* (GSSG: Glutathione oxidised form; GSH glutathione reduced form) (Masella and Mazza, 2009; Karp, 2010).

GSH and its oxidised or disulfide form GSSG are major intracellular reducing agents involved in a wide range of cellular functions. These include: storage and transport of reduced sulphur, regulation of sulphur nutrition, compensation of oxidative stress, chemical anti-oxidant and co-substrate in enzymatic reactions, redox regulation and buffering, regulation of enzyme activity, mRNA translation and gene transcription, modification and transport of hormones and detoxification and transport of xenobiotics or heavy metals (Deneke, 2001).

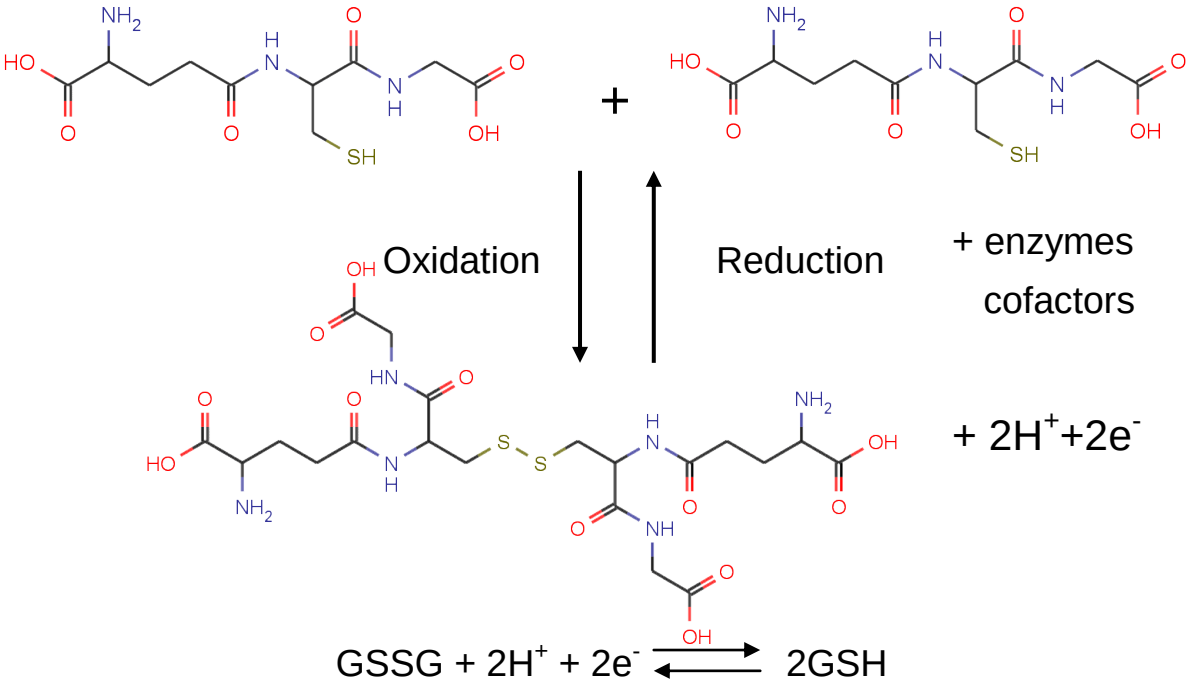

Fig 2. 6 Disulfide bonds between two cysteine residues, GSSG: Glutathione oxidised form; GSH glutathione reduced form

There is a particular importance of GSH in oncology because of its role in resistance to cytotoxic agents that damage DNA through the generation of free radicals or oxidising species; GSH protects cells by hunting free radicals and by reducing hydrogen peroxide catalytically (Hedley and Chow, 1994). This is the reason why the study of GSH in mammalian biochemistry and medical sciences rapidly evolved, but in plant sciences glutathione was overlooked for a long time (Grill, Tausz and De Kok, 2002).

Glutathione interest in plants grew after 1957 (Price, 1957), when the isolation of L-γ-Glutamyl-L-Cysteinyl-β-alanine from legumes was possible and it was renamed as homoglutathione. But the real boost in research on glutathione with applications for agriculture was developed after the discovery of glutathione S-transferase (GST) enzymes in plants in 1970 and subsequent identification of the role of GSH in ascorbate metabolism, compensation of oxidative stress and as a long distance transporter of reduced sulphur (Grill, Tausz and De Kok, 2002) .

Phytochelatins (PC's) are GSH derivatives identified in 1985 and also contributors of heavy metal homeostasis. PC's, (γ-glutamyl-L-cysteinyl)$_n$-glycine, where n = 2-11) (Fig 2.7), are produced enzymatically via phytochelatin synthase (PCS) by plants taking GSH as substrate. PC's are able to chelate/complex heavy metal(loids) and therefore lower their toxicity (Wood et al., 2011).

PC's can be found in microalgae, related eukaryotic photosynthetic organisms, some nematodes and fungi as organo-metallic complexes (Perales-Vela, Pena-Castro and Canizares-Villanueva, 2006). These complexes are stable only in acidic conditions and thus may be partitioned inside vacuoles to facilitate appropriate control of the cytoplasmic concentration of heavy metal ions.

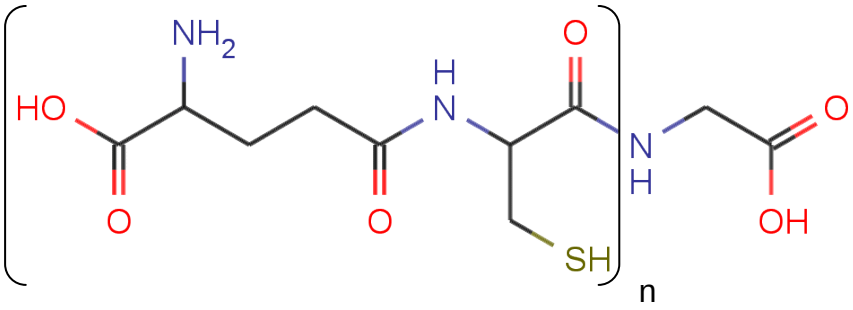

Fig 2. 7 Phytochelatin (PC) structure (n = 2-11)

PC synthesis is triggered/enhanced by several metal salts in the following order: Cd^{2+}, Hg^{2+}, As^{3+}, AsO_2^-, Cu^{2+}, Zn^{2+}, Pb^+, AsO_4^{3-}, Mg^{2+}, Ni^{2+} and SeO_4^{2-} (Vatamaniuk et al., 2000; Simmons and Emery, 2011). Whereas stress with heat, cold, ultraviolet radiation (UV), hormones, fungal cell wall metabolites or anoxia do not seem to induce PC synthesis (Perales-Vela, Pena-Castro and Canizares-Villanueva, 2006).

Nowadays it is well established that GSH and PC's are a central components of the plant defence system against various forms of natural and man-made stresses. They are able to bind heavy metals and can contribute to heavy metal homeostasis in plants living in contaminated environments (Grill, Tausz and De Kok, 2002; Klapheck, 1988).

PC synthase is believed to be constitutively expressed by plant cells. Therefore a signalling mechanism of PC synthase activation is suggested to exist. Some

evidence of a possible regulation by protein phosphatases has been obtained (Gusmao-Lima, Da-Cruz-eSilva and Almeida-Figueira, 2012; Wang et al., 2009).

Phosphorylation of proteins is a control mechanism in several plants and animals. This control is reversible thanks to the opposing activities of protein kinases (phosphorylation) and protein phosphatases (dephosphorylation). Because of similarities in animal and plant evolution, some well characterised mammalian phosphatases are analogous in plants. The PPP-Family of Ser/Thr protein phosphatases is one example. This family includes PP1, PP2A, PP2B, PP4 PP5 and PP7 protein phosphatases. This family of phosphatases has been linked with glycogen accumulation, mitosis, translational controls, sucrose synthesis, nitrate reductase and recently with PC synthesis (Smith and Walker, 1996; Gusmao-Lima, Da-Cruz-eSilva and Almeida-Figueira, 2012; Wang et al., 2009).

The analysis of different protein phosphatase activities has been possible due to their selective inhibition of several natural toxins. Table 2.2 shows some of these toxins with their specific inhibition concentration.

Table 2. 2 Natural toxins which inhibit selectively the PPP-Family Ser/Thr protein phosphatases, from (Moorhead, 2007).

	IC_{50} nanomolar					
Compound	PP1	PP2A	PP2B	PP4	PP5	PP7
Okadaic acid	15-50	0.1-0.3	~4000	0.1	3.5	>1000
Microsystin-LR	0.3-1	<0.1-1	~1000	0.15	1	>1000
Nodularin	2.4	0.3	>1000	ND	~4	>1000
Calyculin A	0.4	0.25	>1000	0.4	3	>1000
Tautomycin	0.23	0.94-32	>1000	0.2	10	ND
Cantharidin	1,100	194	>10,000	50	600	ND
Fostriecin	45,000-58,000	1.5-5.5	>100,000	3	50,000-70,000	ND

ND= not determined

Okadaic acid, tautomycin and cantharidin show good selectivity between the different protein phosphatases families and readily enter cell membranes. This makes them attractive for investigation of PC regulation in living cells.

Intact arsenic complexes with GSH/PC have been studied in *Brassica oleracea, Arabidopsis thaliana*, *Helianthus annuus*, *Thunberia alata*, *Pteris cretica* and *Holcus*

lanatus. The identification of these complexes remained elusive for many years due to analytical difficulties. So far the following complexes have been identified: tri(glutamyl-cysteinyl-glycinyl) trithio-arsenite (ATG), di(glutamyl-cysteinyl-glycinyl) methyl-di(glutamyl-cysteinyl-glycinyl) methyldithio-arsonite (MADG), dimethyl-thio-arsinite (DMAG) , $DMAS^{V}$-GS, GS-As(III)-PC_2, As(III)-PC_3, As(III)-PC_2, GS-As(III)-PC_2, As(III)-PC_4, MMA(III)-PC_2 and As(III)-$(PC_2)_2$ and the presence of unbound reduced PC_2, oxidised PC_2, reduced PC_3, oxidised PC_3, reduced PC_4, oxidised PC_4 and several PC homologues (hPC) (where Gly is substituted by Ala, Ser, Glu or is absent) (Liu et al., 2010; Bluemlein et al., 2008; Raab et al., 2007; Raab et al., 2007; Raab, Feldmann and Meharg, 2004). The structure of arsenic complexes with GSH and PC's is shown in Fig 2.8 and 2.9 respectively.

Production of phytochelatins by *C. vulgaris* has been investigated by many groups but has only been found in experiments with cells challenged with cadmium and selenate (Simmons and Emery, 2011; Simmons et al., 2009). In one of the studies cells were cultured in 100 µg L^{-1} $CdCl_2$ and the extraction was performed under oxygen-free conditions to reduce auto-oxidation. Radio-labelled GSH was used as internal standard and tandem mass spectrometry was used to detect the molecules. However, only the presence of GSH, PC_2 and PC_3 were reported and no Cd-GS/PC intact complex was found. When cells were challenged with selenate and extracted in the same oxygen-free conditions again only the presence of GSH, PC_2, PC_3 were reported. Even when Cd-GS/PC complexes are reported to be more stable (there is no information reported for selenate) than their arsenic analogues, all the attempts so far to identify intact metal(loid)-GS/PC complexes in *C. vulgaris* cells have failed. In these studies, protocols did not include conditions described for stability of the complexes (discussed in more detail in section 2.4.3), and that might have been the cause for failure (Simmons et al., 2009).

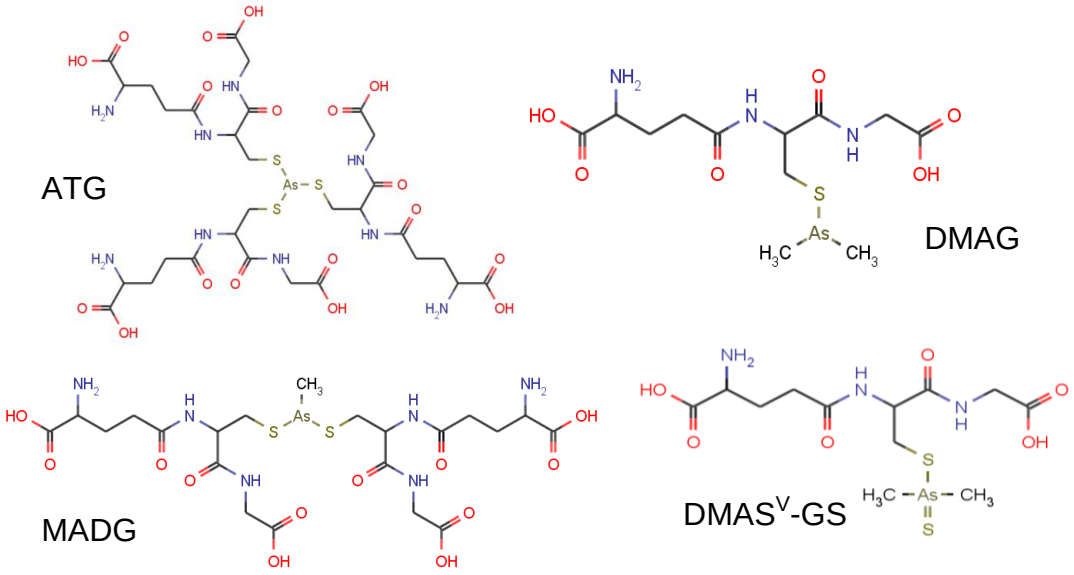

Fig 2. 8 Arsenic-GS complex structures

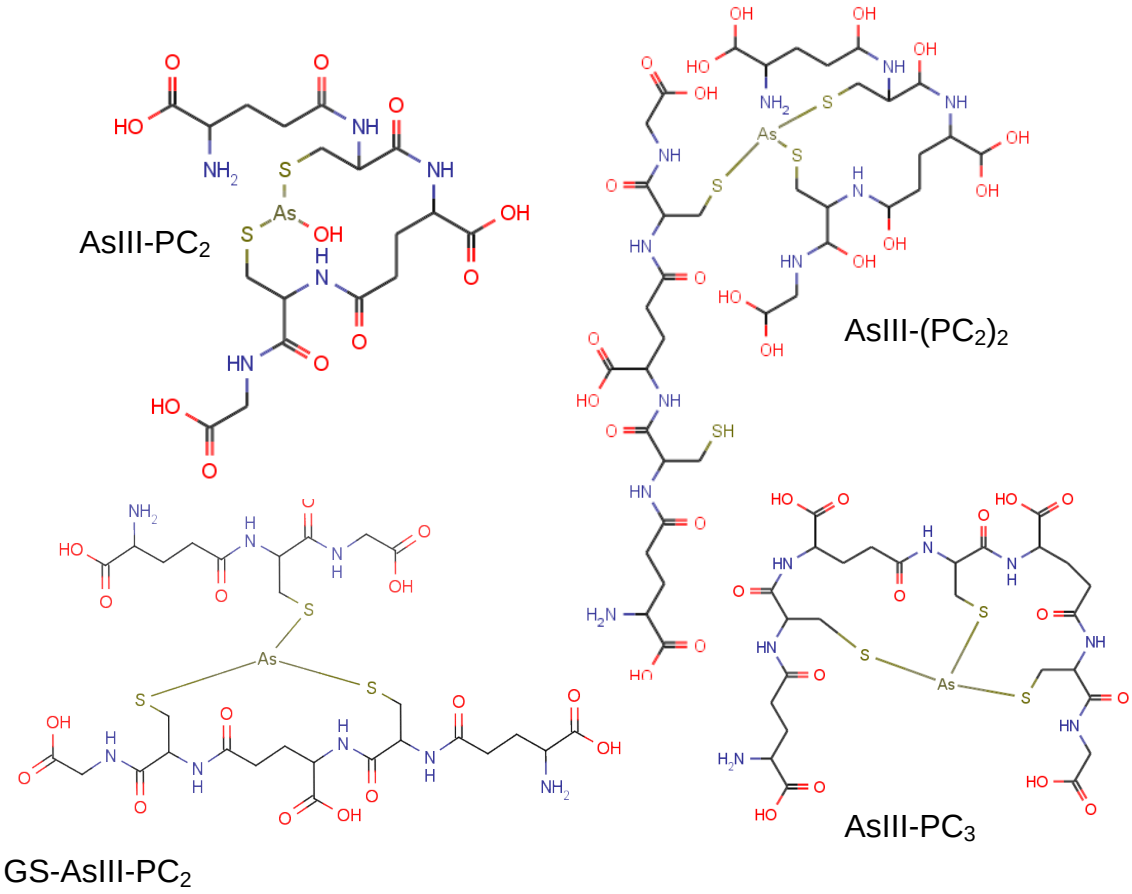

Fig 2. 9 Arsenic-GS/PC complex structures

Stimulation of glutathione transport has been investigated in tumour cells. These cells transport several drugs as glutathione conjugates outside the plasma membrane using MRP1 (ABCC1) transport molecules. It has been observed that several flavonoids cause stimulation of MRP1 mediated transport. Examples of these chemicals are the flavonoid apigenin and the calcium channel blocker verapamil with maximum stimulation at 30 µM (Leslie, Deeley and Cole, 2003; Trompier et al., 2004).

The investigation of these chemicals on arsenic tolerance in algae has not been explored. One way to investigate these effects is the direct measurement of GSH and PC with and without the treatment with those chemicals.

d) Vacuole compartmentalisation

As mentioned before, PC's are synthesised in the cytosol and their complexes with metal(loids) are believed to be compartmentalised into vacuoles. The transport mechanism for As-PC complexes to the vacuole has been recently discovered in *Arabidopsis* cells. This transport is mediated by two independent and redundant transport molecules: AtABCC1 and AtABCC2 (Song et al., 2010). The identification of this transport mechanism took a long time because early investigations were hampered by the following facts: tolerance to arsenic is mediated not only by PC production (PC synthase) but the two transport molecules are needed for complex transport to the vacuole, where PC's may be recycled (Zenk, 1996); expression of only one ABCC transporter along with PC production does not confer arsenic tolerance, and; these two transporters are not efficient in As-GS transport because expression of these molecules in mutant yeast that do not produce PC's, does not confer resistance to arsenic (Mendoza-Cozatl et al., 2011). As-GS transport is mediated by MRP2, an analogue of ABCC2 in mammalian and plant cells (Kala et al., 2000; Lu et al., 1998).

ABCC (ATP Binding Cassette C family) transporters also identified as MRP (Multidrug Resistance-associated Proteins) are Mg-ATP hydrolysis driven pumps which are situated in cell membranes and vacuoles. These transporters are sensitive to vanadate at milimolar concentration (5 mM).

Three functions have been attributed to ABCC2 transport molecules: GSH conjugate transport, bile acid transport and excretion of tetrapyrroles derived during the catabolism of chlorophyll. Taurocholate (a bile acid) inhibits MRP2 transport by competition (Lu et al., 1998). MK571 is an efficient Cysteinyl leukotriene receptor type 1 (leukotriene CysLT1 receptor) antagonist and ABCC1 (MRP1) inhibitor (Wong, Zhu and Liao, 2007). Probenecid is also an inhibitor of ABCC2 transport (Long et al., 2011). Together these chemicals can help in the investigation of arsenic resistance in algae by measuring sensitivity of cells with and without the addition of inhibitors.

In addition to anticancer drugs, herbicides, pesticides and heavy metals, a number of fluorescent molecules may act as substrates for ABCC/MRP transport proteins, among them: Calcein-AM acetoxymethyl ester (Calcein-AM) (Gayet et al., 2006), 5-chloromethylfluorescein diacetate (CMFDA) (Lebedeva, Pande and Patton, 2011), Rhodamine 123 (Rh123), Lucifer Yellow CH (LY) (Cole et al., 1991; Oparka et al., 1991), 2',7'-bis-(2-carboxyethyl)-5- and-6- carboxyfluorescein (BCECF) (Swanson, Bethke and Jones, 1998), Fura 2 (Steinberg et al., 1987), Monochlorobimane (mBCI), Monobromobimane (mBBr) and Fluorescein isothiocyanate (FITC) (Cole et al., 1990).

Several types of cells have been used to study ABCC/MRP activity using fluorescent molecules as substrates including: a number of human cancer cells (HepG2, THP-1, K562, HGC-27, SKOV3, PANC-1, SW480, Hela, A549, MDA-MB-453, U937, HHT90, HHT100, HHT150, HL60/S, HL60/130 and HL60P-gp) (Zhu et al., 2012; Dogan et al., 2004), hamster ovary cells (CHO-K1) (Lebedeva, Pande and Patton, 2011), Madin-Darby canine kidney II cells (MDCKII-MRP1/2/3) (Weiss et al., 2007), mouse fibroblasts cells (3T3), murine erythroleukemia cells (PC4) (Draper, Martell and Levy, 1997), macrophages (mouse macrophage-like J774) (Steinberg et al., 1987), zebrafish cells (*Danio rerio*) (Long et al., 2011), sea urchin embryos (Strongylocentrotus purpuratus) (Bosnjak et al., 2009), diatoms (*Thalassiosira rotul*) (Scherer, Wiltshire and Bickmeyer, 2008), plant cells (*Arabidopsis thaliana, Hordeum vulgare, Allium cepa, Daucus carota, Zea mays*) (Gayet et al., 2006; Forestier et al., 2003; Cole et al., 1991) and yeast (*Saccharomyces cerevisiae*) (Ortiz et al., 1995).

There are, however, differences in the way investigations on ABCC/MRP activity using fluorescent molecules are conducted. Because ABCC/MRP proteins have been found to be expressed in plasma and vacuole membranes, the fate of this

substrates is either outside of the cells or inside the vacuoles. Several techniques have been used to test this transport; the most common rely on the use of specific inhibitors (e.g. probenecid, MK571, taurocholate) or gene silencing. When cells are exposed to fluorescent molecules with/without the inhibitor or on/off gene silenced cells, the fate of the fluorescent molecules is observed. Specific fluorescence is then measured *in vivo*, using flow cytometry or *in vitro*, by measuring fluorescence in cell extracts.

To date most of the ABCC/MRP transporters characterized in plants have been localized in the vacuolar membrane and are considered to be involved in the intracellular sequestration of xenobiotics (Song et al., 2010; Forestier et al., 2003; Swanson, Bethke and Jones, 1998). Only certain ABC/MRP transporters might be involved in defence metabolite secretion, expressed in the plasma membrane and thus their expression regulated by the concentration of these metabolites. One example of such behaviour was found in *Nicotiana plumbaginifolia*, where NpABC1, a member of ABC proteins was identified and was found to be expressed in the plasma membrane (Jasinski et al., 2001).

Some studies have reported low or even negligible capacity to stain microalgae cells using Calcein-AM. This is because the response ratio of Calcein-AM fluorescence of live cells compared to dead controls is significantly low compared to other fluorescent molecules (Peperzak and Brussaard, 2011). The ability to stain such cells may have been compromised if the cells express plasma membrane ABCC/MRP transporters, thus being able to excrete the fluorescent molecule; however this has not been properly investigated.

BCECF (2',7'-bis-(2-carboxyethyl) 5 and 6-carboxyfluorescein) is among the fluorescent molecules used to study ABCC/MRP transport. BCECF is an uncharged molecule that can cross cell membranes; once inside cells, the lipophilic blocking groups are cleaved by non-specific esterases, resulting in a charged form that leak out of the cell far more slowly than its parent compound. BCECF exhibits a pH dependent spectral shift, being less intense at lower pH and having more intense signals at higher pH (Rink, Tsien and Pozzan, 1982; Boyer and Hedley, 1994).

Another fluorescent molecule used to study ABCC/MRP transport is CMFDA (5-chloromethylfluorescein diacetate). CMDFA passes freely through cell membranes, but once inside the cell, is transformed into a cell-impermeant reaction product. CMDFA contains a chloromethyl or bromomethyl group that reacts with thiols, probably in a glutathione S-transferase-mediated reaction, since this has been shown to occur *in vitro*. In most cells, glutathione levels are high (up to 10 mM) and glutathione transferase is ubiquitous. The reagent is transformed into a cell-impermeant fluorescent dye-thioether adduct. Excess unconjugated reagent passively diffuses to the extracellular medium (Barhoumi et al., 1993).

2.6. Experimental methods for the analysis of arsenic

Total arsenic analysis of environmental samples normally requires complete mineralization of the matrix in order to mobilise arsenic's organic and inorganic insoluble forms into soluble inorganic ones. This has to be done as efficient and effective as possible while preventing any loss. Some of the methods to achieve this goal are: dry ashing, wet ashing with mixtures of acids and solvents and microwave-assisted digestion. Sometimes a pre-treatment is necessary to conserve, homogenise or ensure representativeness of the sample; this depends on the specific conditions of the sampling method (Frankenberg, 2002; Rubio, Ruiz Chancho and Lopez Sanchez, 2010).

Fixed laboratory techniques are generally required to measure total arsenic in an environmental sample to μg L^{-1} for water and μg kg^{-1} for solids. These laboratory techniques can be classified as (UNACCSWR, 2012):

- Single analyte methods: Only one element can be measured per run e.g. atomic fluorescence spectroscopy (AFS), graphite furnace atomic absorption spectroscopy (GFAA), hydride generation atomic absorption spectroscopy (HGAAS) and Anodic Stripping Voltammetry (ASV).
- Multiple analyte methods: Several elements other than arsenic can be measured per run e.g. inductively coupled plasma optical emission spectrometry (ICP-OES) and inductively coupled plasma mass spectroscopy (ICP-MS).

Because toxicity, mobilisation, bioavailability, risk and environmental impacts of arsenic depend on its speciation, analytical techniques to measure arsenic species rather than total arsenic are needed (Frankenberg, 2002).

As opposite to maximum mineralization for total arsenic analysis where all the species are converted into soluble inorganic forms, the mobilisation in speciation analysis has to avoid or minimise species transformation. In this way, because there is always a compromise between extraction efficiency and minimal transformation, it is recognised that the method for extraction has to be tailored to the species that are to be investigated e.g. water soluble or ionic forms will need a polar solvent and lipid based forms will need a non-polar solvent (Francesconi, 2003).

Several extraction methods for arsenic speciation have been reported: extraction with a solvent such as water, variable ratios of water/methanol and other solvents (e.g. orthophosphoric acid, trifluoroacetic acid, formic acid), enzymatic extraction, any of the methods assisted by ultrasonication (in a bath or with probes), shaking, freeze-thawing, microwaving, grinding in liquid nitrogen, vortex mixing or accelerated solvent extraction (Rubio, Ruiz Chancho and Lopez Sanchez, 2010; Francesconi and Kuehnelt, 2004; McSheehy et al., 2003).

Methods available for arsenic speciation commonly require a separation step before a detection system is coupled, although some methods do not require a separation step e.g. XANES (X-ray absorption near-edge spectroscopy) and EXAFS (extended X-ray absorption fine structure (Bluemlein et al., 2008). Separation methods include HPLC, GC (Gas Chromatography) and CE (Capillary Electrophoresis) (Francesconi and Kuehnelt, 2004).

After separation is achieved, a highly sensitive method for detection is needed, some of these methods are also used in total arsenic analysis, including: HPLC-HGAAS, HPLC-ICP-MS, GC-ICP-MS, and CE-ICP-MS. Some detectors are suited only for organo-arsenical species such as HPLC-ESI-MS (Electrospray Ionisation Mass spectrometry), CE-UV (Ultraviolet detection), and GC-MS. The principal methods used for arsenic analysis are summarized in Table 2.3.

Table 2. 3 Summary of analytical methods for arsenic measurement modified from (UNACCSWR, 2012)

Technique	LoD ($\mu g.L^{-1}$)	Sample size (mL)	Major equipment cost (US$)	Analytical throughput	Comments	Method
HGAAS	0.05	50	20-100,000	30-60	Single element	ISO 11969 SM 3114
GFAAS	1-5	1-2	40-100,000	50-100	Single element	ISO/CD 15586 SM 3120
ICP-OES	35-50	10-20	60-100,000	50-100	Multiple element	ISO/CD 11885 SM 3120
ICP-MS	0.02-1	10-20	150-400,000	20-100	Multiple element	SM 3125 USEPA 1638
HGAFS	0.01	40-50	20-25,000	30-60	Single element	CEN/TC/230/WG1/TG 12N3
ASV	0.1	25-50	10-20,000	25-50	Only free dissolved arsenic	USEPA 7063
SDDC	1-10	100	2-10,000	20-30	Limited to water samples	SM 3500 ISO 6595

Note: LoD: Limit of detection; HGAAS: hydride generation atomic absorption spectroscopy; GFAAS: graphite furnace atomic absorption spectroscopy; ICP-OES: inductively coupled plasma optical emission spectrometry; ICP-MS: inductively coupled plasma mass spectroscopy; HGAFS atomic fluorescence spectrometry with hydride system; ASV: anodic stripping voltammetry; SDDC: silver diethyldithiocarbamate spectrometry.

High Performance Liquid Chromatography (HPLC) coupled with either ICP-MS or ESI-MS are the methods most often chosen by analytical chemist for arsenic speciation analysis. This is supported by an ever increasing trend in publication and citation articles since 1988, as shown in Fig 2.10. This is most likely because of the combination of high sensitivity, specificity and the complementary information that the combination of the two techniques offers (Feldmann, 2008).

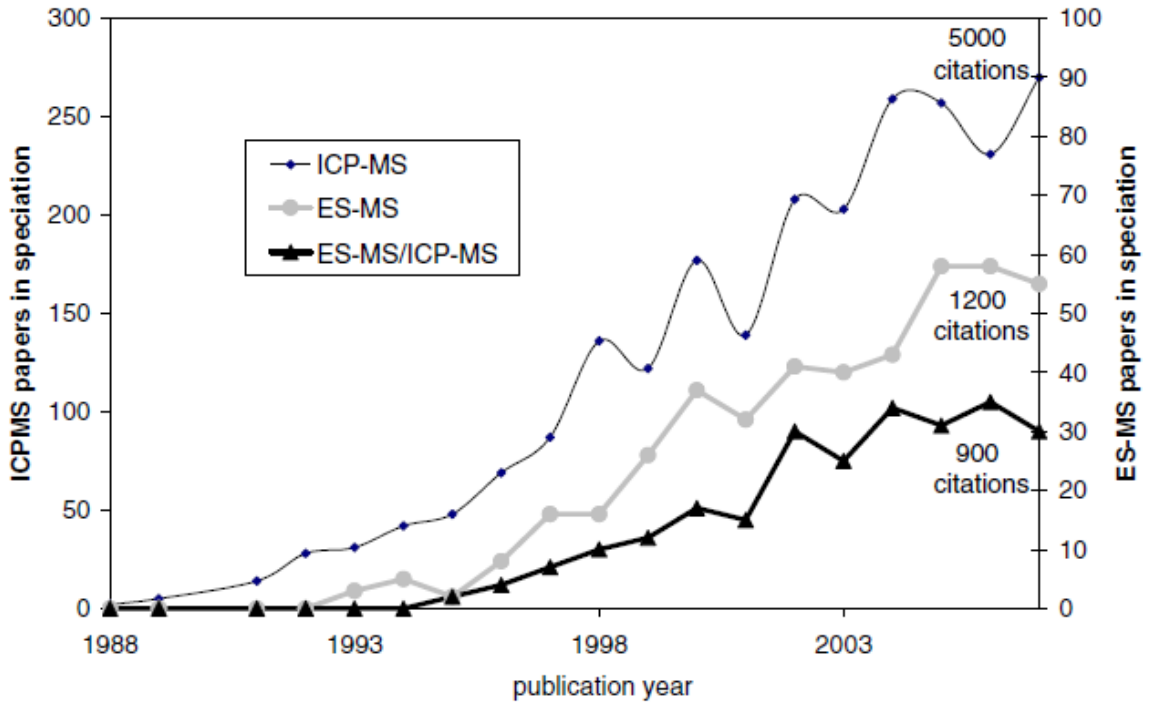

Fig 2. 10 ICP-MS/ ESI-MS and combination of publications by year since 1988 (Feldmann, 2008)

Separation of arsenic species in a HPLC occurs in the column. The sample, generally dissolved in the mobile phase, is injected into the flowing mobile phase on the column. The sample is attached to the column because of its selective affinity. Specific separation occurs (dependent on the type of column), and the separated molecules elute causing a signal to be later analysed (Becker, 2007).

Several combinations of stationary and mobile phases can be used, these combinations, as many of the steps in speciation analysis, have to be tailored to the species to be analysed and also depend on the detection method. The most common stationary phases include ion exchange (anion and cation exchange resins), normal phase (hydrophilic substrate), reversed phase (hydrophobic substrate) and size exclusion. Sometimes separation is aided with an ion-pairing reagent or a combination of columns is used to give a multidimensional separation (McSheehy et al., 2003). Mobile phases are predominantly aqueous dissolutions of phosphate, carbonate and bicarbonate buffers, nitric acid, phosphoric acid, formic acid, methanol, trifluoroacetic acid and acetonitrile. Generally ICP-MS based buffers should be low in organic solvents and ESI-MS low in phosphate buffers.

2.6.1. HPLC-ICP-MS

Inductively Coupled Plasma (ICP) as a ionisation source has developed extensively in the last two decades to become the source for both atomic emission spectroscopy and mass spectrometry, capable of detection of multiple elements below parts per billion (μg L^{-1}) with good accuracy and precision (Dean, 2005).

An ICP-MS consist of a sample introduction system, an ionisation source, a focalisation zone, a separation zone and a detection zone. An example of this system is shown in Fig 2.11.

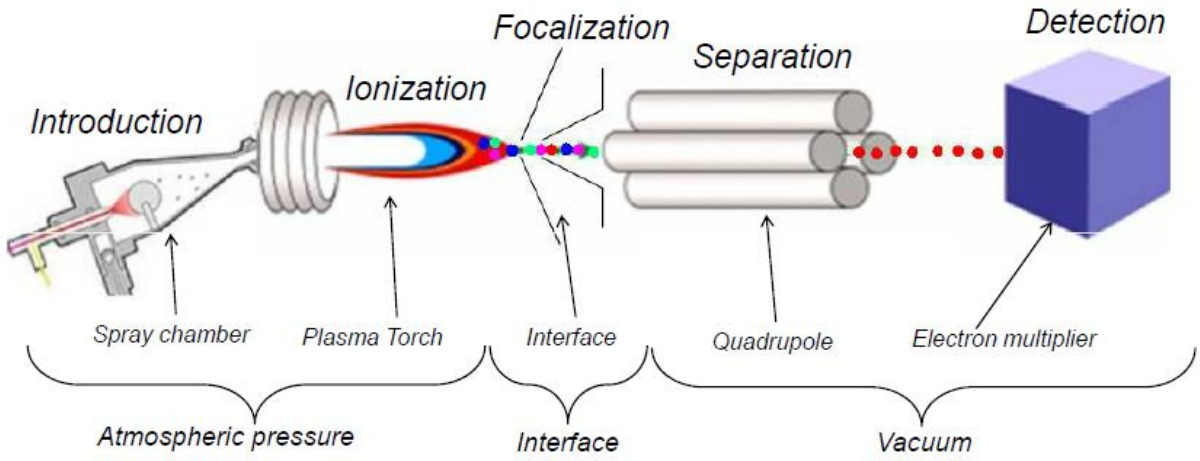

Fig 2. 11 ICP-MS schematic parts

The introduction system is of high importance and has been extensively investigated, being the combination of a nebuliser and spray chamber the most common and cost effective approach, however only a small portion (often < 2%) of the sample reaches the ICP source using this combination (Dean, 2005).

The most commonly used nebuliser is the pneumatic concentric glass nebuliser. The spray chamber is located immediately after the nebuliser and its purpose is to remove droplets that are < 10 μm and thus avoiding the plasma source extinguishing due to cooling, leading to severe matrix interferences (Dean, 2005).

The heart of the ionisation source is the plasma torch (Fig 2.12). The torch is formed of three concentric glass tubes through which the sample, a coolant and plasma gas are transported. An induction coil is placed at the end of the torch to which a Radio Frequency (RF) power between 750 and 1700 W is applied to generate the plasma.

Since the sample is introduced as an aerosol, four main processes will occur in the plasma: desolvation, vaporisation, atomisation and ionisation. Because of the high temperature in the plasma (6,000 and 10,000 ^{o}K), desolvation, vaporisation and atomisation are straightforward, while ionisation will depend on the element to be analysed. The most commonly used plasma gas is argon (Nelms, 2005).

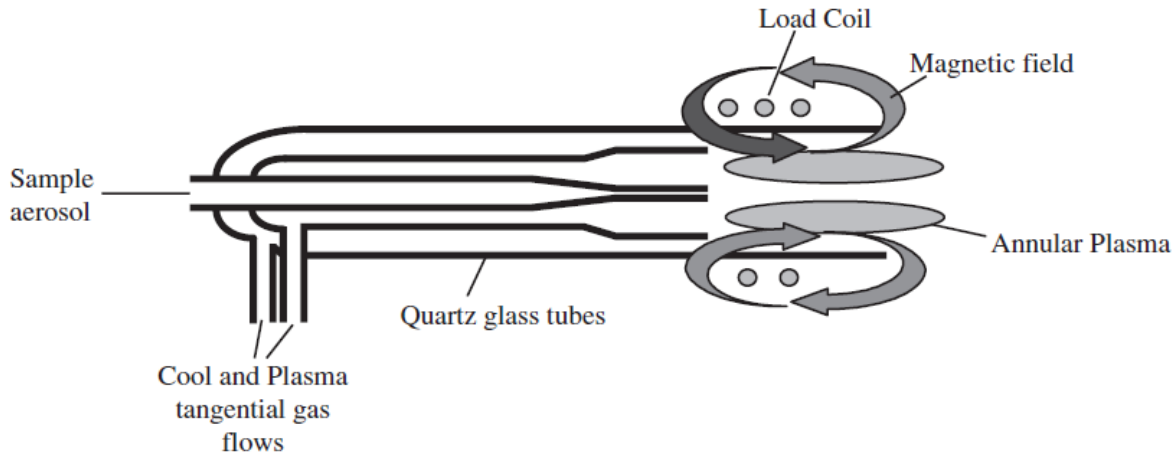

Fig 2. 12 Conventional glass Torch for ICP-MS (Nelms, 2005)

Ionisation is primarily a function of the first ionisation potential (the energy required to remove the most loosely held electron from a molecule) of the element relative to that of the plasma gas (for argon 15.76 eV). In argon plasmas, under hot plasma conditions, most of the elements in the periodic table produce predominantly singly charged ions with high efficiency (5% to 100%). Regardless of their high first ionisation potential, important metalloids and non-metals such as As, Se, S or Cl are still sufficiently ionised to allow sensitive determination (Nelms, 2005; Cornelis et al., 2003).

Focalisation is carried out in the interface of the introduction system and detection system; its role is to extract analyte ions from the plasma, as efficiently as possible so they can be detected in the mass spectrometer side of the instrument where the mass analysis takes place (Nelms, 2005).

The mass analyser sorts the ions extracted from the ICP source according to their mass to charge ratio (m/z); this is done ideally under vacuum (Hill, 2007). There are several types of mass analysers, but the most robust, practical and cost effective is

the quadrupole mass analyser. The quadrupole allows transmitting certain ions and rejecting others depending on the stability of their path and thus the complete mass range from Be to U can be scanned in approximately 0.1 s. One drawback of quadrupole analysers is that they show only unit mass resolution. Hence, there is spectral overlap of signals from ions showing the same nominal mass (Cornelis et al., 2003).

The electron multiplier is the most common type of detector. After the ion beam exits the separation zone, the beam is directed to a conversion plate. This plate converts ions into electrons which are accelerated by the voltage applied to the plate and the signal is finally detected (Hill, 2007).

2.6.1.1. ICP-MS Interferences

Spectral interferences coming from overlapping signals of ions showing the same nominal mass is one disadvantage of quadrupole based ICP-MS. This has been the subject for intensive investigation for possible solutions to those interferences. Table 2.4 shows the major spectral interferences for elements of environmental interest (Cornelis et al., 2003).

The remedies for spectral interference problems presented here are focused on arsenic, sulphur and phosphorus for obvious reasons, but some of those solutions have also helped eliminate interferences generated from other elements.

First of all, the conditions for sample preparation and species separation should be selected to avoid the occurrence of spectral interferences. For total arsenic determinations, the selection of the digestion acids is crucial. HCl should be avoided as it causes interference (Table 2.4). External standards for calibration should also avoid the use of HCl for sample stability. The use of blank correction, using a matrix-matched blank, has been shown to be helpful. Mathematical correction has also been used successfully (Nelms, 2005) .

Table 2. 4 Spectral interferences from elements of environmental interest from (Cornelis et al., 2003)

Element	Major isotope and isotopic abundance (%)	Molecular ions (potentially) causing spectral overlap at low mass resolution
Al	^{27}Al, 100%	$^{12}C^{14}NH+$, $^{13}C^{14}N+$
Si	^{28}Si, 92.2%	$^{14}N_2+$, $^{12}C^{16}O+$
P	^{31}P, 100%	$^{14}N^{16}OH+$
S	^{32}S, 95.0%	$^{16}O_2+$
K	^{39}K, 100%	$^{38}ArH+$
Ca	^{40}Ca, 96.9%	$^{40}Ar+$
Cs	^{45}Sc, 100%	$^{12}C^{16}O_2H+$, $^{28}Si^{16}OH+$, $^{29}Si^{16}O+$
Ti	^{48}Ti, 73.8%	$^{32}S^{16}O+$, $^{31}P^{16}OH+$
V	^{51}V, 99.8%	$^{35}Cl^{16}O+$, $^{37}Cl^{14}N+$
Cr	^{52}Cr, 83.8%	$^{40}Ar^{12}C+$, $^{35}Cl^{16}OH+$
Fe	^{56}Fe, 91.7%	$^{40}Ar^{16}O+$, $^{40}Ca^{16}O+$
Cu	^{63}Cu, 69.2%	$^{40}Ar^{23}Na+$, $^{31}P^{16}O_2+$
Zn	^{64}Zn, 48.6%	$^{32}S^{16}O_2+$, $^{31}P^{16}O_2H+$
As	^{75}As, 100%	$^{40}Ar^{35}Cl+$
Se	^{80}Se, 49.6%	$^{40}Ar_2+$

Most of the commercial ICP-MS instruments are equipped with a multipole collision cell. The collision cell consists of six (hexapole) or eight (octopole) rods to which a RF voltage is applied. When a gas is added to the cell (e.g. H_2 or He/H_2), selective ion-molecule reactions occur (e.g., charge, atom and proton transfer) and the signal intensities of Ar^+ and of Ar^- containing molecular ions such as ArC^+, ArO^+, $ArCl^+$ and Ar_2^+ are suppressed by three or more orders of magnitude. In this way trace levels of Ca, Cr, Fe, As and Se can be accurately determined (Cornelis et al., 2003; Kadar et al., 2011).

Reaction and collision gases such as O_2 and Xe have been used to remove polyatomic interferences in the determination of sulphur caused by $^{16}O_2^+$ (Table 2.4). By using oxygen in the collision cell, sulphur can be converted to sulphur oxide with quantification performed at m/z 48 ($[^{32}S^{16}O^+]$) while molecular oxygen is removed by collision-induced dissociation. Moreover arsenic can be quantified in the same way

at m/z 91 ([$^{75}As^{16}O^{+}$]) with method quantification limits of 0.9 µg L^{-1} for arsenic and 86 µg L^{-1} for sulphur (Wang et al., 2007; Bluemlein et al., 2008).

Non-spectral interferences (matrix-induced signal suppression or enhancement, signal instability and/or drift) can often be corrected for by using a carefully selected internal reference. To all blank, sample and standard solutions, an equal amount of an internal reference element (with a mass number close to that of the analyte element) is added. It is assumed that this element undergoes the same suppression or enhancement as the analyte element(s). It is to be noted that some matrices (e.g. methanol and organic solvents) selectively enhance the signal intensity of specific elements such as As, Sb and Se (Nelms, 2005; Cornelis et al., 2003).

Finally matrix separation of interfering species can be done in the chromatographic systems.

2.6.1.2. Methanol effect

Methanol is commonly used to elute arsenic from the stationary phase in a HPLC system. This causes a selectively increase of the arsenic signal when detected by ICP-MS. Thus a correction for quantification has to be made. One approach uses a blank injected using the same chromatographic conditions with a post column addition of a solution containing a constant amount of arsenic (generally DMA) and an internal standard (indium or gallium). The blank is then analysed by ICP-MS (Amayo et al., 2011). The corrections are performed by calculating the relative intensity for every eluting peak. The relative intensity is calculated using the following equation:

$$RtAs(t)=(RAs)x(frt)$$

Where:
RtAs is the response factor for a (t) arsenic eluting compound
RAs is the arsenic response factor, and.
frt is the retention time specific arsenic response factor.

The factor frt can be determined for every retention time by taking the intensity data over the anticipated peak width of the unknown arsenic compound, as illustrated in Fig 2.13.

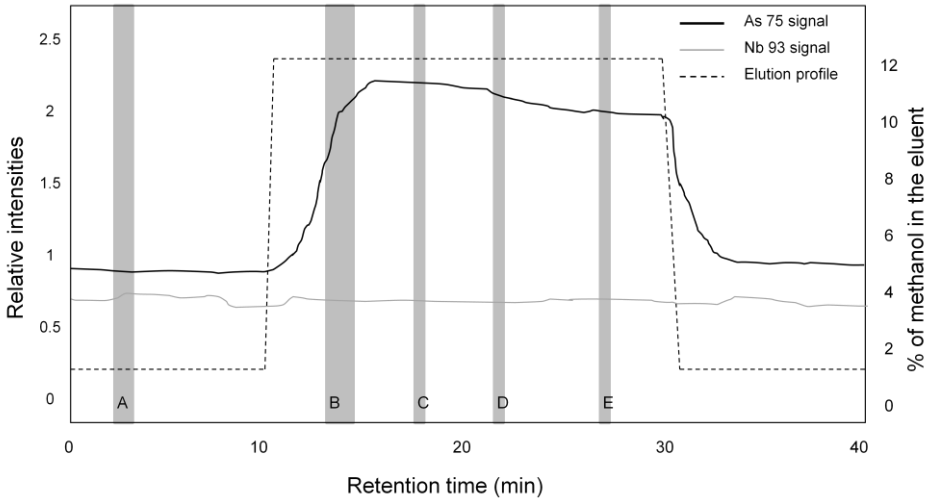

Fig 2. 13 Correction of arsenic intensity due to methanol in the mobile phase with post column addition of DMA and internal standard. Mobile phase: 0.1% formic acid (eluent A) and 99.9% HPLC grade methanol (eluent B). Elution profile: 0-20 min linear increase 0-20% B, 20-30 min 20%B, 30-32 min 20-0% B 32-40 min 0%B. The vertical areas indicate eluting species A, B, C, D and E at specific retention times and relative intensity

2.6.2. HPLC-ESI-MS

Electrospray Ionisation Mass Spectrometry (ESI-MS) has caused a big impact on speciation analysis, in particular on arsenic and selenium, because it is a very soft ionisation technique that results in little fragmentation of the molecules to be analysed. The technique can be used to identify unknown organic species based on their mass without the need for standards. But because of the serious limitations for quantification, the use of the technique has been limited to the online or offline paired used with ICP-MS in order to allow qualitative and quantitative analysis. These limitations include: lack of element specificity, some species are difficult to ionise using ESI ionisation and ionisation efficiency is severely suppressed by the co-existing matrix (Hoffmann and Stroobant, 2007; Mcmaster, 2005; Feldmann, 2005).

ESI is produced when a strong electric field is applied, under atmospheric pressure, to a liquid passing through a capillary tube under a weak flow rate (normally 1-10 µL min^{-1}). A gas is injected to disperse the spray into droplets. These droplets then pass

either through a curtain of heated inert gas, commonly nitrogen, or through a heated capillary to remove the last solvent molecules. Small molecules (> 1000 Daltons) will produce mainly mono-charged ions. ESI can also be used to identify molecules by the formation of sodium, potassium, ammonium, chloride, acetate or other adducts (Hoffmann and Stroobant, 2007).

For detection of positively charged ions, electrons have to be provided by the solution, and thus an oxidation occurs. For negatively charged ions, electrons have to be consumed, and thus a reduction occurs. The ions are separated according to their m/z ratio and are detected in proportion to their abundance. Several types of detectors/separators exist, among them: Quadrupole (Q), Ion Trap (IT), Time of Flight (ToF), Fourier Transform (FT), magnetic sector and orbitrap (Hoffmann and Stroobant, 2007).

An IT analyser uses a three-dimensional spherical segment stable orbit between electrodes with a trapping voltage from a Direct Current Radio Frequency (DC/RF) source. Ions are then extracted in an increasing mass (m/z) order by raising the DC/RF voltage (Mcmaster, 2005).

In a ToF analyser ions are separated, after their initial acceleration by an electric field, according to their velocities when they drift in a free-field region that is called a flight tube (Hoffmann and Stroobant, 2007).

Generally, ESI ionization methods yield relatively little information on the structure of the ions and fragments. This is because the presence of other compounds or other ions in the mixture may hide such fragments, thus another method is required. MS/MS analysis usually combines two mass spectrometer analyzers with a collision cell. The target ion is selected from the first analyzer and allowed to collide with an inert gas to induce fragmentation. The fragmented ions are then passed into the second MS analyzer for separation and detection, giving structural information (Hoffmann and Stroobant, 2007).

An IT-ToF hybrid mass analyser has an IT that accumulates and focuses selected ions before ejection to the ToF measurements. An IT-ToF is capable of high resolution (R = 10,000) full scanning and also can perform sequential MS/MS (MS^n) analysis of selected ions. The accuracy of measurement of molecular ions and their

fragments is generally < 5 parts per million (ppm) (Zhang and Surapaneni, 2012). The schematic of an IT-ToF can be seen in Fig 2.14.

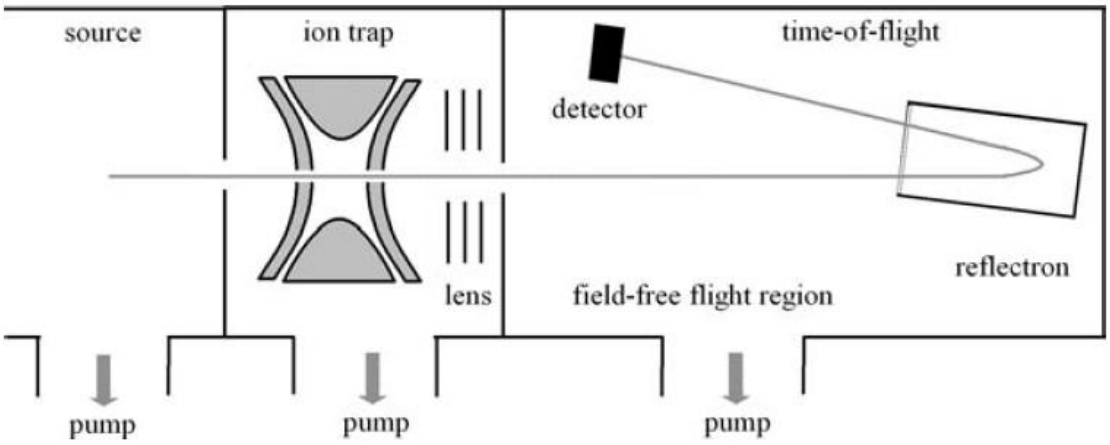

Fig 2. 14 Schematic of an Ion Trap-Time of Flight (IT-ToF) mass analyser form Zhang and Surapaneni, (2012)

By using MS/MS analysis, more detailed structural information can be obtained on particular ionic species. First the molecule to be studied have to be selected to undergo fragmentation and the energy induced to produce dissociation has to be optimised for that molecule. The resulting fragments are analysed by the second analyser. The mass difference between consecutive fragment ions within a series allows the identification of the sequence of amino acids within the molecule. However several incomplete series of fragments can make the mass spectrum difficult to interpret (Hoffmann and Stroobant, 2007).

Examples of mass spectra obtained experimentally for GSH, PC's and As-GS/PC complexes can help in the identification and interpretation of such molecules. Some examples are shown in Appendix 2.

2.6.3. Sample preparation and speciation for As-GS/PC complexes

The identification and quantification of metal complexes with GSH and PC's has been shown to be elusive due to their instability, especially As-GS/PC complexes. As such this presents a challenge for modern speciation techniques (Bluemlein, Raab and Feldmann, 2009).

The most challenging steps in the analysis of these complexes are their extraction from the biological material and the maintenance of their stability during HPLC separation (Bluemlein et al., 2008). Despite this, the conditions for stability of the complexes in a mobile phase and HPLC column have been documented and achieved (Bluemlein, Raab and Feldmann, 2009; Raab et al., 2004; Kanaki and Pergantis, 2008). In contrast, relatively little progress has been made in ensuring the integrity and representativeness of the complexes when extracted from solid samples or cells such as the green microalgae *C. vulgaris*.

Murray et al. (2003) studied the biotransformations of arsenate in *C. vulgaris*, and found surprisingly low extraction efficiency when extracting with 1:1 (v/v) methanol/water followed by 10 min in a sonication bath (11 to 27%). This led to the conclusion that the arsenic species found were not representative of the species present in the algae cells. Another group investigated the blue green-algae *Nostoc commune var. flagelliforme* and found extraction efficiency of only 34% when using the same extraction conditions (Lai et al., 1997).

Conditions for the stability of As-GS/PC during extraction and analysis rely on:

i) pH of the solution: acidic and compatible with both ICP-MS and ESI (e.g. 0.5-1% formic acid);
ii) choice of separation column: a strong anion exchange and size exclusion column can break As-S bonds, the only suitable conditions so far have been found in a reversed phase C_{18} column (Raab et al., 2004);
iii) temperature of the solution: it has been found that during freeze-drying more than 90% of As-PC_3 and other small peptides such as PC_2 and PC_3 can be lost and temperatures above 4ºC do not favour integrity and;
iv) time of analysis: integrity of the complexes is only guaranteed for 4h, even at optimal conditions (Bluemlein, Raab and Feldmann, 2009; Raab et al., 2004).

Currently, the only method used routinely to extract As-GS/PC complexes consists of extraction with 0.5-1% (v/v) formic acid for 1 h at 4 ºC. This method requires grinding the samples in liquid nitrogen, a process which may compromise the integrity of the complexes (Raab et al., 2005; Liu et al., 2010; Wood et al., 2011; Bluemlein, Raab and Feldmann, 2009; Raab et al., 2007). The extraction efficiencies reported for this

method are 87 ± 6% (n = 28), 77 ± 19% (n = 28) (Raab et al., 2005) and 92 ± 9% (n = 42) (Raab et al., 2007) in plants (roots, stems and leaves) and seaweed tissues.

When using focused sonication, a probe is directly put in contact with the sample and ultrasound energy is applied to create cavitation bubbles to break and disrupt intermolecular interactions. This conveys 100 times more energy than an ultrasonic bath and if used correctly can provide conditions conducive for complex stability while avoiding the necessity to freeze and grind the cells in liquid nitrogen. Extraction can be performed in 1% formic acid, at low temperature (4 ˚C, when using an ice bath) with a fast extraction time (30 s) (Raab et al., 2004).

A detailed study into arsenic extraction efficiency from *C. vulgaris* cells using focused sonication has been published. Magnetic stirring, ultrasonic bath and focused sonication were compared. Different focused sonication times were used (from 30 to 300 s). Optimal extraction was achieved with 5 mL of deionised water per 200 mg of dry algae and 30 s of focused sonication. The best efficiency was found at 64 ± 3%. The study also included speciation of arsenic but the stability of those species was not further investigated (Garcia, Quijano and Bonilla, 2006).

2.7. Genetic markers for arsenic resistance

As a result of common evolutionary history, genes from different organisms that have similar functions have also similar sequences (Brown, 2010). This fact helps in hypothesis-driven experimental gene discovery and in phylogenetic analysis to find the taxonomic range of sequences. To do this, once a gene has been identified, the desired sequence in the gene is compared with genes in a database. This comparison is usually done by translating the nucleotide sequence into the respective amino acid sequence. This is because only 4 nucleotides encode for 20 different amino acids and the probability of 2 sequences appearing to be similar purely by chance is less for amino acids than for nucleotides. One of the most widely used tool to perform this comparison is the Basic Local Alignment Search Tool (BLAST) algorithm (Altschul et al., 1997; Dereeper et al., 2010).

The output for a BLAST search (for amino acids) is a list of database entries ordered according to their alignment scores and E-value (statistical measure) together with

their position in the query sequence. This output gives a measure of the sequences similarity and identity (the occurrence of exactly the same amino acid in the same position in aligned sequences) (Krauthammer et al., 2000).

Genes involved in arsenic resistance based on phytochelatin production and compartmentalisation span across many kingdoms, e.g. Animalia, Plantae and Fungi (Perales-Vela, Pena-Castro and Canizares Villanueva, 2006; Vatamanuik et al., 2001). Therefore a BLAST search could help to compare two sequences directly, map the query sequence, determine the genomic structure, identify novel genes, find homologs and other data mining applications such as phylogenetic tree construction (Altschul et al., 1997; Dereeper et al., 2010).

3. MATERIALS AND METHODS

3.1. Overview

In order to examine the interactions of arsenic with the microalgae *C. vulgaris* and its potential to bio-remediate arsenic from water, an experimental approach was designed which included the determination of the toxic concentrations of inorganic forms of arsenic and DMA and the role of oxidative stress, intracellular pH and GSH in such toxicity. It also included the characterisation and quantification of arsenic adsorption to the cell membrane, absorption inside the cells and the biotransformations of absorbed arsenic.

Among the biotransformations of arsenic inside *C. vulgaris* cells special attention was given to the complexation of arsenic with rich free thiol (SH) molecules (GS/PC). Because intact As-GS/PC molecules have never been observed inside *C. vulgaris* cells, such investigation required the optimisation of the extraction method, the validation and characterisation of the extracted molecules as well as their quantification. The experimental approach also included the analysis of the genetic markers for arsenic resistance.

Microwave assisted digestion was used to extract total arsenic from samples. For speciation extraction, focused sonication and grinding with liquid nitrogen were used. Anion exchange and reversed phase liquid chromatography were used to separate arsenic species. ICP-MS (with H_2/He as collision gas CCT) and ICP-MS (with O_2 as CCT) were used for arsenic and sulphur quantification, this is illustrated in Fig 3.1.

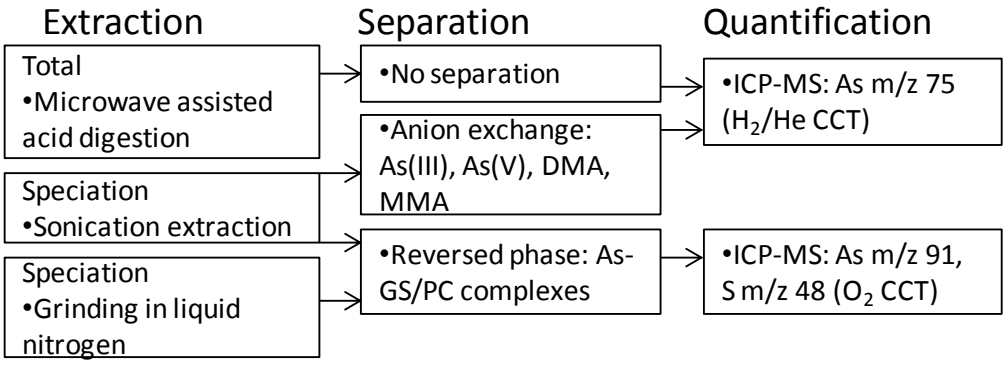

Fig 3. 1 Experimental approach for extraction, separation and quantification of arsenic

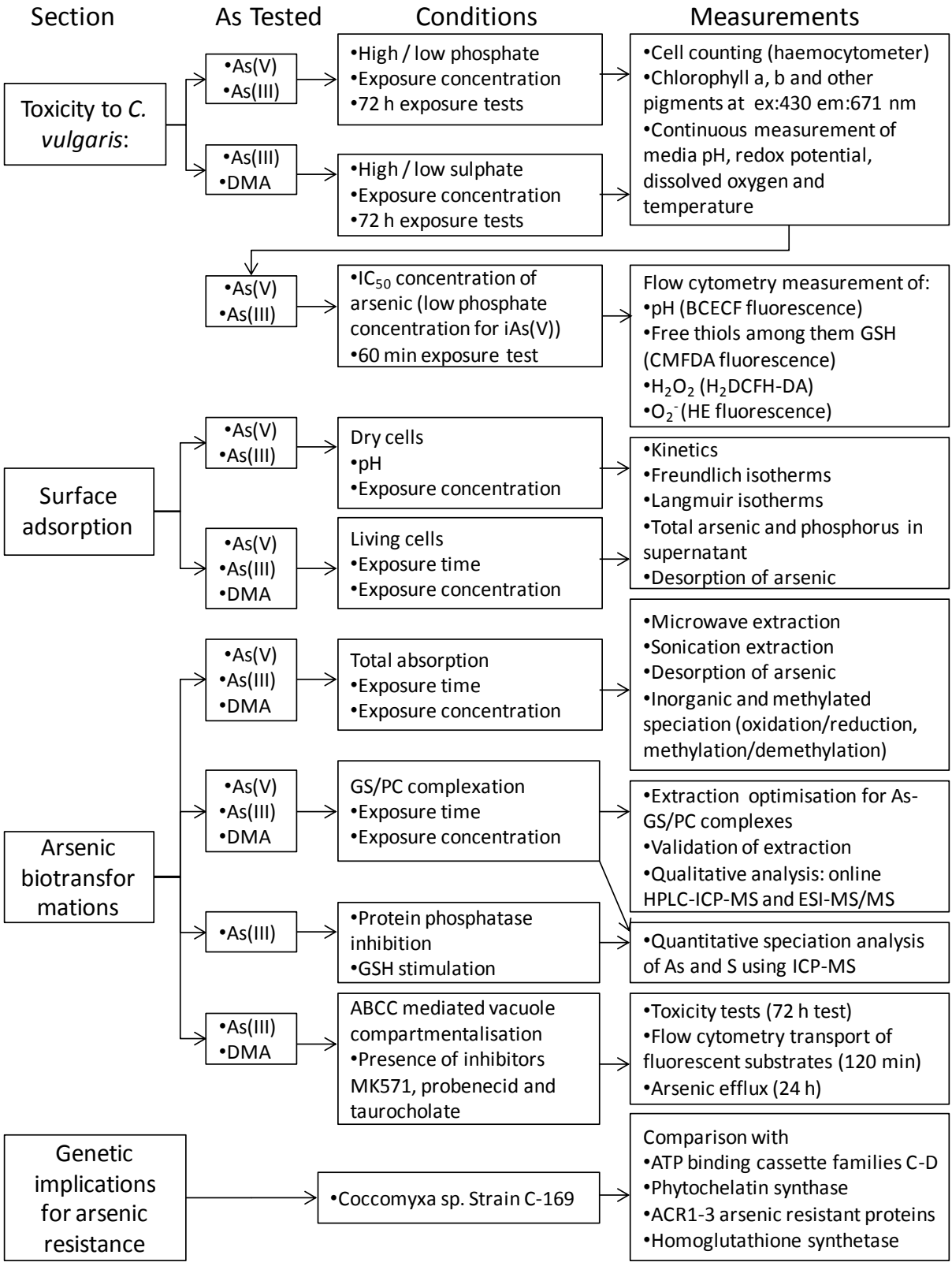

Fig 3. 2 Overview of the experimental approach used in the present study to examine the interactions of arsenic with the microalgae *C. vulgaris.*

This chapter is divided into four main experimental sections: Arsenic toxicity to *C. vulgaris*, surface adsorption, arsenic biotransformations inside *C. vulgaris* cells and the genetic markers for arsenic resistance. An overview of the overall experimental approach is presented in Fig 3.2. All materials used in the experiments are described in the procedure for individual experiments.

3.2. Culture conditions

All reagents, growth media and eluents were made with 18.2 MΩ deionised water (Purite). Sodium arsenite (As(III)), gallium, indium, arsenic solutions for quantification (ICP, 1 g L^{-1} in 2% HNO_3), L-cysteine and nitric acid (trace metal analysis) were purchased from Fisher Scientific (Loughborough, UK). Sodium arsenate dibasic heptahydrate (As(V)), dimethylarsinic acid (DMA), L-glutathione reduced, cerium standard (ICP, 1 g L^{-1} in 5% HNO_3), uranium standard (973 mg L^{-1}), potassium benzene-1,2-disulfonate (BDSA), HPLC grade formic acid and HPLC grade methanol were purchased from Sigma Aldrich (Poole, UK). Cobalt standard (1 g L^{-1}) was purchased from Hopkin & Williams Ltd (London). Lithium nitrate (1 g L^{-1}) was purchased from BDH Chemicals (Poole, UK). Phytochelatin PC_2 standard was purchased from Cambridge Biosciences (Cambridge, UK).

All glassware was washed with alkaline laboratory detergent (Fisher Scientific), allowed to soak overnight in 10% HNO_3 solution, triple rinsed with deionised water and allowed to air dry.

C. vulgaris cells were obtained from “Algae and Protozoa”, SAMS Research Services Ltd, Dunstaffnage Marine Laboratory, UK (CCAP 211/11B). Cells were grown in conical flasks (500 mL, 250 mL and 100 mL) capped with foam stoppers (Fisher Scientific) containing Bold’s medium ($NaNO_3$ 25 mg L^{-1}, $CaCl_2.2H_2O$ 2.5 mg L^{-1}, $MgSO_4.7H_2O$ 7.5 mg L^{-1}, $K_2HPO_4.3H_2O$ 7.5 mg L^{-1}, KH_2PO_4 17.5 mg L^{-1}, NaCl 2.5 mg L^{-1}, $FeCl_3.6H_2O$ 0.058 mg L^{-1}, $MnCl_2.4H_2O$ 0.024 mg L^{-1}, $ZnCl_2$ 0.003 mg L^{-1}, $CoCl_2.6H_2O$ 0.001 mg L^{-1}, $Na_2MoO_4.2H_2O$ 0.0024 mg L^{-1}) without EDTA (Perales-Vela, Pena-Castro and Canizares-Villanueva, 2006). In some experiments cells were supplemented with 0.05% w/v dextrose (Oxoid, bacteriological grade). Cells were grown under continuous illumination at 2,646 lux (n = 33, SE = 154) and 25 ± 0.5 ºC

(LMS Cooled Incubator, Model 300WA). Cells were shaken by hand once a day to avoid sedimentation. All the nutrients were reagent grade unless stated otherwise.

3.3. Toxicity Tests

3.3.1. Determination of cell concentration (cell enumeration)

Cells were counted using an improved Neubauer haemocytometer. Cells were counted using the 40x objective. The amount of cells in 16 small squares (0.0024 mm^2) was recorded, as illustrated in Fig 3.3. Cells falling on the bordering triple lines were only counted if they were on either the top or on the left lines, those cells touching the bottom and the right hand side lines were excluded. The concentration of cells was calculated by the following formula:

No cells/mL of suspension= $[(25)(A)(1X10^4)]/n$

Where: A = number of cells and n = number of squares counted

.

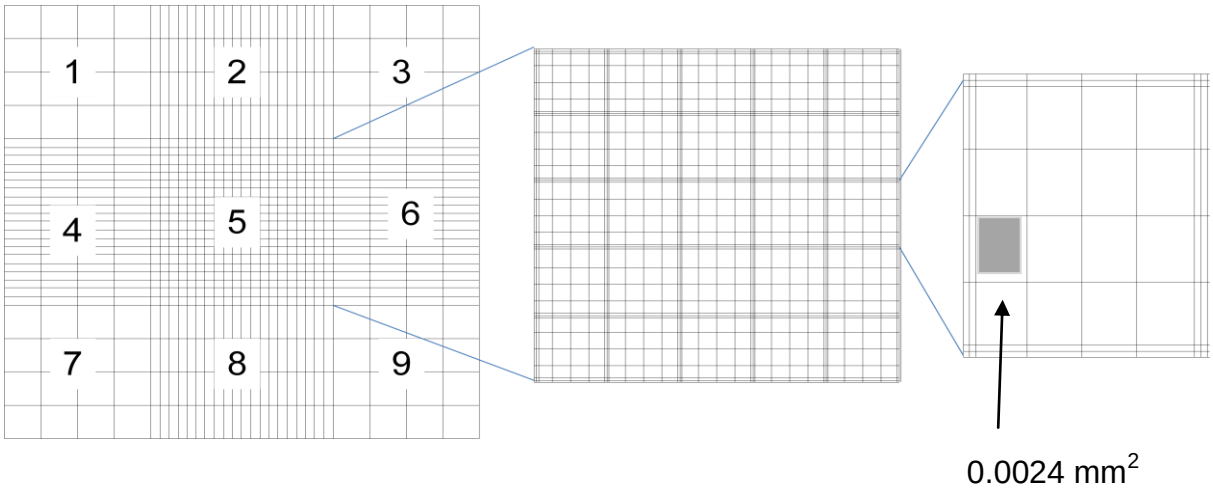

Fig 3. 3 Haemocytomer configuration grids and small squares area

The counting accuracy depends on the number of cells counted and the number of squares used. When the sample adequately represents the culture population, accuracy is defined as the ratio of the standard error to the mean for replicated counts and assumes a Poisson distribution of counting units in the counting chamber. The accuracy is increased as the square root of the number of items counted, thus the counting error can be calculated from the following formula for a 95% confidence interval (Andersen, 2005):

Counting error (± %) = $(100)(2/n)^{1/2}$

The associated errors and cells counts can be observed in Table 3.1. Thus a minimum of 500 cells were counted per sample to obtain less than a 6.32% error. Samples for calibration curves were counted in triplicates.

Table 3. 1 Counting error in percentage for cell counts with 95% CI

No of organisms counted	Percentage error
50	20
100	14.14
400	7.07
500	6.32
1000	4.47
2000	3.16

3.3.2. Arsenic toxicity to *C. vulgaris* cells

Toxicity of As(III), As(V) and DMA to *C. vulgaris* cells was investigated using 72 h tests following the "Standard guide for conducting static toxicity tests with microalgae" with minor modifications regarding phosphate and sulphur concentrations as well as initial cell numbers (ASTM, 2004).

The data from cells counted using the haemocytometer was used to create a calibration curve between number of cells and pigment fluorescence. Fluorescent extractions for calibration curves were performed in triplicates.

Chlorophyll a, b and other pigments were extracted using a whole water extraction technique (Mayer, Cuhel and Nyholm, 1997). Firstly, 0.6 mL of culture media containing *C. vulgaris cells* were added to a 20 mL glass vials, covered with aluminium foil to avoid photo-oxidation. Then 2.4 mL of a mixture of acetone/DMSO (1:1, v/v) were added to extract the pigments. The content of the vials were then mixed with a vortex mixer for 1 min and incubated for 20 min. A blank for all experiments and calibration curves were prepared to correct background fluorescence by adding the same amount of media and extractant without cells. Fluorescence intensity (unitless) was measured at 430 nm excitation and 671 nm

emission wavelengths on a spectroflourometer (RF-1501, Shimadzu) using standard 12 mm cuvettes (Fisher Scientific).

Toxicity tests were performed using 100 ml borosilicate conical flasks containing 40 mL of media. A set of experiments was performed with high (13 mg L^{-1}) and low (0.3 mg L^{-1}) phosphate concentrations as well as different concentrations of As(III) and As(V) ranging from 2.5 to 130 mg L^{-1}, prepared from 1000 mg L^{-1} stock solutions of the corresponding salts. Another set of experiments was performed with high (29.23 mg L^{-1}) and low (0.1 mg L^{-1}) concentrations of SO_4 and different concentrations of As(III) and DMA ranging from 10 to 100 mg L^{-1}.

Cells were supplemented with 0.05% w/v dextrose and buffered with 0.2 M MOPS (Fisher Scientific) solution (pH 7) for the low phosphate experiments. In low sulphur experiments, sulphate salts were replaced by their corresponding chloride salts. Six control experiments (with no added arsenic) and triplicate experiments for arsenic concentrations were used. Redox potential/dissolve oxygen or pH/dissolved oxygen and temperature were monitored continuously in a control containing an intermediate concentration of arsenic; cells were not counted for this control.

Cells at the exponential growth phase (5-6 days old, cultured in 500 mL conical flasks without dextrose) were used to inoculate controls and arsenic experiments to an initial concentration of $5x10^3$ cells mL^{-1} and the flasks were placed randomly in an incubator under continuous illumination at 2,646 lux (n = 33, SE = 154) and 25 ± 0.5 ºC. Cells were shaken by hand once a day to avoid sedimentation. Each day, the flasks were transferred to a class II biological safety cabinet and then a sample was taken (0.6 mL) from each flask in order to measure chlorophyll a, b and other pigments.

3.3.3. Oxidative stress, GSH and pH measurements by flow cytometry

Flow cytometry was used to investigate the toxicity of As(III) and As(V) to *C. vulgaris* and the influence of intracellular H_2O_2, O_2^-, GSH (low molecular thiols) and pH on such toxicity (Cossarizza et al., 2009).

The inhibition concentrations to fifty percent of the population (IC_{50}) obtained in section 3.3.2 for As(III) and As(V) were used as the exposure concentration for flow cytometry experiments.

For the flow cytometry analysis, plastic tubes (BD, 3.5 mL, 55X12 mm^2) and a FACSCalibur (Becton Dickson) flow cytometer equipped with a blue (excitation, 488 nm) and red laser (excitation, 635 nm) were used. Channel detection included: forward angle light scatter (FSC), side angle light scatter (SSC), fluorescence channel 1 (FL1, 515-545 nm), fluorescence channel 2 (FL2, 564-606 nm), fluorescence channel 3 (FL3, 670 nm) and fluorescence channel 4 (FL4, 653-669 nm).

The following reagents were used: Bold's media (section 3.2), N,N-Dimethyl-formamide (DMF, Sigma-Aldrich D4551), dimethyl sulfoxide (DMSO, Sigma-Aldrich D5879), ethanol, H_2DCF-DA (2',7'-dichlorodihydrofluorescein diacetate, Invitrogen D-399), HE (Dihydroethidium, Invitrogen D-1168), SYTOX Green (Nucleic acid stain, Invitrogen S34860), BCECF (2',7'-Bis-(2-Carboxyethyl)-5- and-6 -Carboxyfluorescein, Acetoxymethyl Ester, Invitrogen B-1170), Menadione (MEN Sigma-Aldrich M57405), H_2O_2 (AnalaR, 30%, 100 volumes), N-ethyl-maleimide (NEM Sigma-Aldrich E3876) and CMFDA (5-chloromethylfluorescein diacetate, Invitrogen C-7070) .

The reagents were set up in the following way:

H_2DCF-DA was dissolved in DMSO (50 mg in 4 mL) at a concentration of 25.65 mM to obtain a stock solution. Stock solution was diluted at an intermediate concentration of 1 mM in culture media. Final concentration was 2 µM.

HE was dissolved in DMF (25 mg in 1.585 mL) at a concentration of 50 mM to obtain a stock solution. Stock solution was diluted at an intermediate concentration of 500 µM in culture media. Final concentration was 2.5 µM.

SYTOX Green was thawed at room temperature before used; the stock solution concentration was 30 µM. Final concentration was 90 nM.

BCECF was dissolved in DMSO (50 µg in 0.230 mL) at a concentration of 350 µM to obtain a stock solution. Final concentration was 3.5 µM.

CMFDA was dissolved in DMSO (50 µg in 0.430 mL) at a concentration of 250 µM to obtain a stock solution. Final concentration was 2.5 µM.

MEN was dissolved in culture media (172.2 mg in 1 mL) at a concentration of 1 M to obtain a stock solution. Stock solution was diluted at an intermediate concentration of 10 mM in culture media. This solution was stored at 4 °C and protected from light. Final concentration was 20 µM.

H_2O_2 was prepared from a stock solution of 8.82 M. Stock was diluted to an intermediate concentration and it was used at a final concentration of 50 µM.

H_2DCF-DA, HE, SYTOX Green, and NEM were stored in small aliquots at -20 °C for up to 6 months.

Three controls were used: stained negative controls (heat-killed cells, 20 min at 80˚C), stained cell blanks (no treatment added, only labelled with dye), cell blanks (no treatment, no dye) and the following specific controls:

- MEN as positive control for HE: Cells were incubated in 1mL of medium containing 10 µM of MEN for 1 hour at room temperature, then washed and HE was added.
- H_2O_2 as positive control for H_2DCF-DA: Cells were incubated with H_2DCF-DA, then washed and 1 mL of PBS and 50 µM of H_2O_2 were added and finally incubated for 15 min in the dark at room temperature.

All probes were excited by the argon-ion laser at 450-490 nm. The fluorescence emission of H_2DCF-DA, CMFDA and SYTOX Green were detected through the FL1 filter, HE and BCECF were detected through the FL1 and FL2 filters whereas chlorophyll fluorescence was detected at emission 670 nm, filter FL3.

To calibrate the flow cytometer, a blank sample was taken (no treatment, no dye) to set the scatter signals and auto-fluorescence FL3 and FL4. Then the stained samples were run and the signal voltage was optimised.

Chlorophyll fluorescence (FL3) was used to gate healthy viable cells. The same gated population was then used to measure changes in fluorescence at excitation 530 ± 15 nm (FL1) and 585 ± 20 nm (FL2).

Samples and controls were incubated for 120 min for all the fluorescent probes and were run by triplicates on the flow cytometer, collecting at least 20,000 events for each sample.

Kolmogorov-Smirnov statistics were used; this generates a D-value ranging between 0 and 1.0. D values obtained in this form, were categorised in the following way: Strong ($D > 0.30$), moderate ($0.20 < D < 0.30$), weak ($0.15 < D < 0.20$) and negligible ($D < 0.15$) difference (Lebedeva, Pande and Patton, 2011).

3.4. Surface adsorption

3.4.1. Kinetic experiments using dry *C. vulgaris* cells

To establish pseudo-equilibrium time, 0.2 g of dry *C. vulgaris* cells (obtained from Sevenhills Organics, Cork, UK) were transferred to 50 mL screw top polyethylene tubes with a solution containing 15 mL of 1 mg L^{-1} of As(V) or As(III). The mixture was shaken in an orbital shaker (IKA KS 130 Basic) for 2, 4, 6, and 8 h. Then, samples were centrifuged for 10 min at 4,500 *g*. The supernatant was analysed for total arsenic and phosphorus concentration.

The experiments were performed at pH 4 and 7. The pH was adjusted with MOPS buffer (pH 7) and potassium hydrogen phthalate (pH 4). Experiments were performed in triplicates, and a set of control experiments was performed for each condition with no arsenic added.

3.4.2. Freundlich and Langmuir isotherms using dry *C. vulgaris* cells

Pseudo equilibrium time determined in the kinetic studies was used as shaking time in isotherm experiments.

Freundlich and Langmuir isotherms were calculated by the following method: 50 mL screw top polyethylene centrifuge tubes were filled with 15 mL of 1 mg L^{-1} arsenic solution (As(V) or As(III) in deionised water), containing varying amounts of dry *C. vulgaris* cells (0.2, 0.3, 0.4, 0.5 and 0.6 g). The tubes were shaken for 6 h. After equilibrium was reached, the tubes were centrifuged for 10 min at 4,500 *g*. The supernatant was taken to 15 mL polyethylene vials to measure arsenic and

phosphorus content. Experiments were performed in triplicates and a set of control experiments was performed for each condition with no arsenic added.

The results were fitted into the following isotherm equations:

- Freundlich: $x/m = q_e = K_f C_e^{1/n}$ using a logarithmic scale and a power type regression line
- Langmuir: $x/m = q_e = a\ b\ C_e / 1 + bC_e$. The constants in the Langmuir isotherm can be determined by plotting $C_e/(x/m)$ vs. C_e and using the linearised form of the following expression: $C_e/(x/m) = (1/Q_0K) + (C_e/Q_0)$, applying $y = a+bx$, where: $a = 1/Q_0K$ and $b = 1/Q_0$

To determined if arsenic replaces phosphate or the choline head of phospholipids in the cell membrane an analysis of relationship was carried out, by analysing the correlation between the concentrations of phosphorus and arsenic in the isotherm experiments.

3.4.3. Living *C. vulgaris* cells, kinetics and concentration effects

Living *C. vulgaris* cells were studied for arsenic adsorption. Cells were grown in Bold's medium supplemented with 0.05% w/v dextrose and free of arsenic for 3-5 days.

Cells were then exposed to arsenic (As(III), As(V) or DMA) by adding 50 mg L^{-1} (from 10 g L^{-1} stock solutions) at several time intervals (4, 24, 48 and 72 h). Adsorption was also investigated at different arsenic concentrations (10, 50, 100 and 200 mg L^{-1}) for a fixed period of 48 h.

After the exposure period, cells were counted using a whole water extraction technique (section 3.3.2), harvested by centrifugation (5 min 3,000 *g*) and washed 3 times with deionised water. Then the pellet was washed for 10 min with 10 mL of ice-cold desorption solution (1 mM K_2HPO_4, 0.5 mM $Ca(NO_3)_2$ and 5 mM MES) (Sandau, Pulz and Zimmermann, 1996). The supernatant was analysed for arsenic. The residue was washed one more time with deionised water, freeze-dried and digested according to section 3.5.1.1.a. for total arsenic analysis. The procedure is illustrated in schematic way in Fig 3.4. The experiments were performed in triplicates.

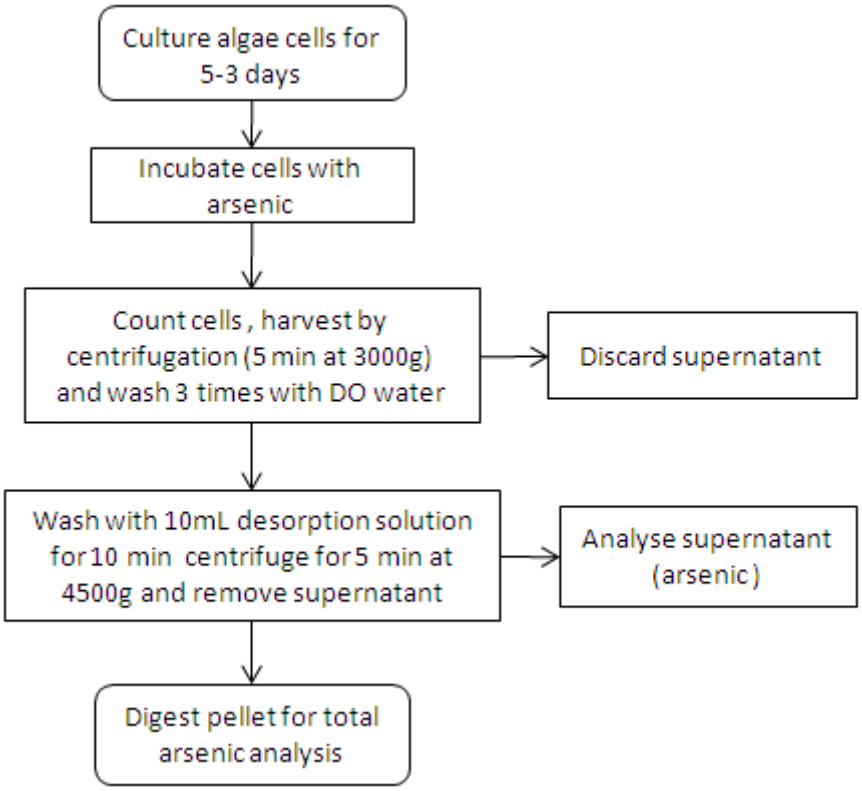

Fig 3. 4 Surface adsorption for *C. vulgaris* living cells exposed to As(V), As(III) and DMA

3.5. Arsenic biotransformation experiments

3.5.1. Reduction/oxidation, methylation/demethylation and arsenosugar formation

3.5.1.1. Arsenic extraction

The extraction method was different for total extraction and speciation analysis. For total or speciation extraction, cells were counted, harvested by centrifugation (5 min, 3,000 *g*) washed with desorption solution (1 mM K_2HPO_4, 0.5 mM $Ca(NO_3)_2$ and 5 mM MES) and finally with deionised water. Wet cells were then ready for arsenic extraction.

a) Total arsenic extraction

For total extraction (acid microwave-assisted extraction), wet cells or dry cells were transferred to teflon tubes, 3 mL of concentrated nitric acid, 3 mL of deionised water were added and the mixture was digested in a MARS XPRESS microwave digestion

system (Method EPA 3051A 2007). Briefly, the temperature of each sample should rise to 175 ± 5 ºC in approximately 5.5 ± 0.25 min and remain at 175 ± 5 ºC for 4.5 min, or for the remainder of the 10 min digestion period. The digested sample was transferred to 15 mL centrifuge tubes and the volume was determined gravimetrically. Then the sample was analysed accordingly.

b) Arsenic speciation extraction

For speciation analysis wet or dry cells were subject to sonication extraction as described in section 3.5.2.2.

3.5.1.2. Arsenic quantification

Quantification conditions for inorganic and methylated arsenic species were are as follows. Separation was achieved in a Hamilton PRP-X100 (10 µm, 250x4.1 mm) column. An isocratic elution was used with 6.6 mM $NH_4H_2PO_4$ (Sigma 17842) and 6.6 mM NH_4NO_3 (Sigma 256064). The pH was adjusted to 6.3 with NH_4OH. The flow rate was 1 $mL.min^{-1}$ (Liu et al., 2010).

Total arsenic and arsenic species were quantified using an ICP-MS (X series II, Thermo Scientific) in CCT mode with He/H as collision cell gas using 20 µg L^{-1} gallium as internal standard. The instrument was tuned daily using a 10 µg L^{-1} In, Ce, Co, U and Li solution and the software provided from the manufacturer (Plasmalab).

3.5.2. As-GS/PC complexation

3.5.2.1. Focused sonication extraction for GS/PC complexes validation

To validate the extraction procedure for As-GS/PC complexes proposed in this study, cells were cultured for 3-5 days in Bold's media free of arsenic and were used to inoculate experiments.

For total extraction validation two sets of samples were used: *C. vulgaris* cells that were exposed to 100 mg L^{-1} As(V) for 5 days (supplemented with 0.05% w/v dextrose) and commercially available Kelp Powder (Galloway's, Richmond, BC, Canada), which has been used for determination of arsenosugars (total arsenic: 27.7

± 0.08 µg g^{-1}) (Lai et al., 1997; Koch et al., 2000; Miguens-Rodriguez, Pickford and Thomas-Oates, 2002).

C. vulgaris cells were harvested by centrifugation (5 min, 3,000 *g*, Rotina 420R), washed three times with deionised water and immediately freeze-dried (Scanvac Coolsafe 55-4). Approximately 0.02 g of dried *C. vulgaris* cells and 0.3 g of dried Kelp powder were taken and total extraction was carried out as described in section 3.5.1.1.a.

For the sonication extraction, dried *C. vulgaris* cells and Kelp powder were transferred to 15 mL centrifuge tubes and extraction was performed as described in section 3.5.2.2.

The certified reference material SRM 2669 (National Institute of Standards and Technology, total and arsenic species in human frozen urine) was used for quality control.

3.5.2.2. Sonication extraction for GS/PC complexes

For the sonication extraction, wet or dried cells were transferred to 15 mL centrifuge tubes; 5 mL of 1% formic acid was added, the volume was determined gravimetrically (assuming a density of 1 g mL^{-1}) and the mixture was sonicated for 30 s using a Minidelta 8935 generator (FFR ultrasonics, 500 W, 35 kHz) fitted with a 3 mm titanium microtip. The microtip was rinsed with methanol then sonicated in 1% formic acid for 10 s between each extraction to avoid cross-contamination. The resulting extracts were centrifuged further to 16,000 *g* for 3 min at 4 ºC (Eppendorf 5415R) and filtered through 0.45 µm syringe filters (Supelco).

3.5.2.3. Comparison of extraction methods: grinding in liquid Nitrogen and focused sonication

The effect on the stability of the of the As-GS/PC bonds caused by high energy sonication was investigated by comparing the traditional method (grinding in liquid nitrogen) and focused sonication. Cells were exposed to 50 mg L^{-1} As(III), As(V) and DMA for 48 h then washed three times with deionised water and harvested by centrifugation (5 min 3,000 *g*) at 4 ºC without freeze-drying.

For one set of samples, cells were extracted using the conventional method: pellets were grinded in liquid nitrogen, then 5 mL 1% formic acid was added and samples were kept at 4 ºC; extracts were centrifuged at 16,000 *g* for 3 min at 4 ºC (Raab et al., 2004).

For the second set of samples, cells were extracted by addition of 5 mL 1% formic acid, and focused sonication was applied for 30 s in an ice bath. The resulting extracts were centrifuged at 16,000 *g* for 3 min at 4 ºC (Eppendorf 5415R) and filtered through 0.45 µm syringe filters (Supelco).

3.5.2.4. Qualitative analysis using on-line HPLC-ESI-MS and HPLC-ICP-MS

For the qualitative analysis, samples were run immediately after extraction by using on-line (one chromatographic system simultaneously analysed by two methods) high resolution HR-ICPMS and ESI-MS/MS. The chromatographic conditions were as follows. Separation was achieved in a Discovery C_{18} (15x2.1 mm, 5 µm) column. A gradient elution was used with 0.1% formic acid (eluent A) and 99.9% HPLC grade methanol (eluent B). The detailed elution profile was as follows: 0-20 min linear increase 0-20% B, 20-30 min 20%B, 30-32 min 20-0% B 32-40 min 0%B. The flow rate was 0.75 $mL.min^{-1}$ (Kanaki and Pergantis, 2008).

The injection volume was 75 µL. The flow from the HPLC was divided ¼ parts to the HR-ICP-MS and ¾ to the ESI-MS/MS. The oven temperature was 30 ºC and auto sampler temperature 4 ºC.

The HR-ICP-MS (Element II, Thermo Scientific) was tuned daily and post column make up flow was achieved with a tee connector and 20 µg L^{-1} gallium in 1% HNO_3

as internal standard. The monitored masses were: As 75, Ga 69 and S 34 in medium resolution. The ESI-MS/MS (Orbitrap Discovery LTQ-XL, Thermo Scientific) was a set up with spray voltage 4.5 V, capillary temperature 320 °C and tube lens 120 V. The ESI-MS/MS was set up in positive scan mode from m/z 50 to 2000.

a) MS/MS analysis using Orbitrap

For quality control, the following synthetic As-GS complexes were prepared and analysed. The synthesis of tri(glutamyl-cysteinyl-glycinyl)trithio-arsenite (ATG), di(glutamyl-cysteinyl-glycinyl)methyl-di(glutamyl-cysteinyl-glycinyl)methyldithio-arsonite (MADG) and dimethyl-thio-arsinite (DMAG) was carried out according to previous procedures (Liu et al., 2010; Kanaki and Pergantis, 2008). The preparation procedure is summarised in Fig 3.5.

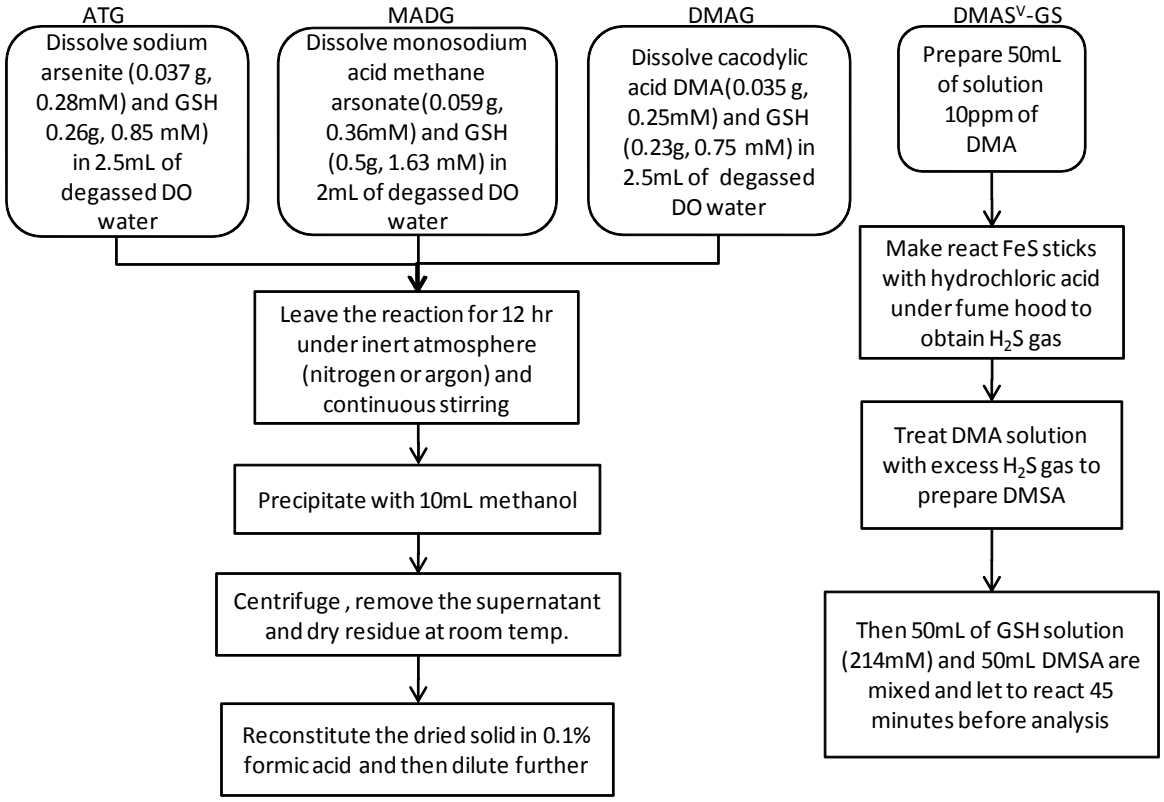

Fig 3. 5 Preparation of synthetic As-GS standards, (ATG, MADG, DMAG, DMAS^{V}-GS)

Table 3.2 shows the theoretical masses that were monitored in all experiments. The masses and fragments obtained were compared to fragmentation pathways already reported in the literature (Appendix 2).

Table 3. 2 Molecule identification and monitored masses for As-GS/PC complexes for mass spectrometry qualitative analysis

Molecule	Formula (M)	Monoisotopic mass ($M+H^+$ or $M+2H^+$)
GSH/PC		
GSH	$C_{10}H_{17}N_3O_6S$	308.0916
GSSG	$C_{20}H_{32}N_6O_{12}S_2$	613.1598
Reduced PC_2	$C_{18}H_{29}N_5O_{10}S_2$	540.1434
Oxidised PC_2	$C_{18}H_{27}N_5O_{10}S_2$	538.1278
Reduced PC_3	$C_{26}H_{41}N_7O_{14}S_3$	772.1952
Oxidised PC_3	$C_{26}H_{39}N_7O_{14}S_3$	770.1795
Reduced PC_4	$C_{34}H_{53}N_9O_{18}S_4$	1004.2470
As(III)-PC_2	$C_{18}H_{28}N_5O_{11}S_2As$	630.0443
As(III)-PC_3	$C_{26}H_{38}N_7O_{14}S_3As$	844.0933
GS-As(III)-PC_2	$C_{28}H_{43}N_8O_{16}S_3As$	460.0666
		919.1253
As(III)-$(PC_2)_2$	$C_{36}H_{54}N_{10}O_{20}S_4As$	576.0925
As(III)-PC_4	$C_{34}H_{50}N_9O_{18}S_4As$	1076.1451
MMA(III)-PC_2	$C_{19}H_{30}N_5O_{10}S_2As$	628.0728
$DMAS^V$-GS	$C_{12}H_{23}N_3O_6S_2As$	444.0244
hGSH/PC		
γ-(Glu-Cys)-Ala	$C_{11}H_{19}N_3O_6S$	322.1073
γ-$(Glu\text{-}Cys)_2$-Ala	$C_{19}H_{31}N_5O_{10}S_2$	554.1591
As(III)-γ-$(Glu\text{-}Cys)_3$-Ala	$C_{27}H_{40}N_7O_{14}S_3As$	858.1090
GS-As(III)-γ-$(Glu\text{-}Cys)_2$-Ala	$C_{29}H_{45}N_8O_{16}S_3As$	467.0744
As(III)-γ-$((Glu\text{-}Cys)_2)_2$-Ala	$C_{37}H_{57}N_{10}O_{20}S_4As$	583.1003
MMA(III)-γ-$(Glu\text{-}Cys)_2$-Ala	$C_{20}H_{32}N_5O_{10}S_2As$	642.0885
desGly-GSH/PC		
γ-(Glu-Cys)	$C_8H_{14}N_2O_5S$	251.0702
γ-$(Glu\text{-}Cys)_2$	$C_{16}H_{26}N_4O_9S_2$	483.1219
γ-$(Glu\text{-}Cys)_3$	$C_{24}H_{38}N_6O_{13}S_3$	715.1737
As(III)-γ-$(Glu\text{-}Cys)_2$	$C_{16}H_{25}N_4O_{10}S_2As$	573.0306
GS-As(III)-γ-$(Glu\text{-}Cys)_2$	$C_{26}H_{40}N_7O_{15}S_3As$	431.5558

3.5.2.5. Quantitative analysis, kinetics and concentration effect experiments

C. vulgaris cells were cultured for 3-5 days in Bold's media free of arsenic. The cells were then exposed to different concentrations (0-200 mg L^{-1}) of As(III) (sodium arsenite) and As(V) (sodium arsenate) for 48 h. In other experiments cells were

exposed to 50 mg L^{-1} of As(III) or As(V) at different exposure times (1, 4, 24, 48 and 72 h). The experiments were performed in triplicates. Cells were supplemented with 0.05% dextrose and were harvested and extracted according to the protocol described in section 3.5.2.2.

The same chromatographic conditions were used as in the qualitative analysis (section 3.5.2.4) with the following exceptions. The flow rate was 0.2 mL min^{-1}. A post column make up flow was achieved with a tee connector and 0.9 mL min^{-1} 20 µg L^{-1} indium in 2% HNO_3 as internal standard. The injection volume was 50 µL.

The ICP-MS (X series II, Thermo Scientific) was tuned daily with a solution containing 10 µg L^{-1} of In, Ce, Co, U, Li and Ce. Then the following parameters were adjusted for O_2 CCT (collision cell technology) according to the manufacturer's instructions: O_2 cell gas flow 1.45 mL min^{-1}, hexapole bias -9 V, quadrupole bias -14 V, focus voltage -2 V, D2 voltage -100 V. The following masses were monitored: As, m/z 91 ($[^{75}As^{16}O+]$), S, m/z 48 ($[^{32}S^{16}O+]$) and In, m/z 115. Fresh external standards were prepared for quantification. For arsenic, different solutions of DMA were used and L-cysteine for the quantification of sulphur.

Method quantification limits (MQL) were calculated by multiplying 10 times the standard deviation signal (at the retention time of the quantification species) of 7 consecutive blank samples. Method detection limits (MDL) were calculated by 3.14 times the standard deviation signal of 7 consecutive blank samples (at the retention time of the quantification species).

The chromatographic recovery was calculated by injecting a sample containing As-GS/PC complexes using the same conditions and the eluent was collected entirely (Fraction I). A second sample was injected, without column, and the eluent collected (Fraction II). Blank fractions consisting of mobile phase were collected and used to correct arsenic background.

All fractions were measured with ICP-MS for total arsenic (section 3.5.1.2). The percentage of chromatographic recovery was calculated using the following formula:

$$\% \text{ recovery} = \left(\frac{\text{(blank corrected arsenic intensity of fraction I)}}{\text{(blank corrected arsenic intensity of fraction II}} \right) \text{ X } 100$$

A correction for methanol content in the mobile phase was performed as follows (Amayo et al., 2011): A blank was injected through the same chromatographic conditions. A post column addition of a solution containing 100 µg L^{-1} DMA and 20 µg L^{-1} In as internal standard was made. The blank was analysed by ICP-MS for arsenic, sulphur and indium at m/z 91 ([$^{75}As^{16}O+$]), S, m/z 48 ([$^{32}S^{16}O+$]) and In, m/z 115.

Because the quantification of sulphur was be made with L-cysteine, a correction for GSSG was made. L-cysteine contains one molecule of sulphur whereas GSSG contains 2 sulphur molecules. Thus a factor of 0.5 for GSSG was used for correction.

3.5.2.6. Vacuole compartmentalisation

For the investigation of vacuole transport mediated by ABCC proteins, two methods were used. In the first method, toxicity to As(III) was tested in the presence and absence of specific inhibitors. In the second method, the fate of substrates to ABCC proteins was investigated (BCECF and CMFDA) in the presence and absence of specific inhibitors using flow cytometry.

Probenecid (Sigma, P8761), sodium taurocholate (Sigma, 86339) and MK571 (Sigma, M7571) were used as specific inhibitors of ABCC transport.

Probenecid was dissolved in 1 M NaOH and then diluted with MOPS buffer solution (pH7) (1% w/v) at a concentration of 10 g L^{-1} (35.04 mM) to obtain a stock solution. The final concentration was 500 µM.

Taurocholate was dissolved in deionised water (50 mg in 10 mL) at a concentration of 5 g L^{-1} (9.3 mM) to obtain a stock solution. The final concentration was 50 µM.

The inhibitor MK571 was dissolved in deionised water (25 mg in 10 mL) at a concentration of 2.5 g L^{-1} (4.65 mM) to obtain a stock solution. The final concentration was 25 µM.

A 72 h As(III) toxicity test was carried out (section 3.3.2) in the presence and absence of the inhibitors.

Flow cytometry was used to investigate the fate of fluorescent substrates, BCECF and CMFDA. The transport was evaluated in the presence of the inhibitors probenecid and MK571.

A FACSCalibur (Becton Dickson) flow cytometer was used. BCECF was used at 3.5 µM and CMFDA was used at 2.5 µM.

Three controls were used: stained negative controls (heat-killed, 20 min at 80 ˚C), background controls (no treatment, only labelled with dye) and blanks (no treatment, no dye).

To calibrate the flow cytometer, a blank sample was taken to set the scatter signals and auto-fluorescence FL3 and FL4. Then the stained samples were run and the signal voltage was optimised.

Samples were run by triplicates on the flow cytometer, collecting at least 20,000 events for each sample.

Chlorophyll fluorescence (FL3) was used to gate healthy viable cells. The same gated population was then used to measure changes in fluorescence at excitation 530 ± 15 nm (FL1) and 585 ± 20 nm (FL2).

Kolmogorov-Smirnov statistics were used to measure the difference between two distributions. D values obtained in this form, were categorised in the following way: Strong ($D > 0.30$), moderate ($0.20 < D < 0.30$), weak ($0.15 < D < 0.20$) and negative ($D < 0.15$) difference.

3.5.2.7. Arsenic efflux

The fate of As-GS/PC complexes inside cells of *C. vulgaris* after exposure to 150 mg L^{-1} As(III) for 24 h, using the two inhibitors probenecid (500 µM) and MK571 (25 µM) was investigated. Inhibitors were added one hour before arsenic exposure.

After arsenic exposure cells were harvested by centrifugation (10 min at 3,000 *g*), washed three times with deionised water and with desorption solution (1 mM K_2HPO_4, 0.5 mM $Ca(NO_3)_2$ and 5 mM MES). Then the pellet was extracted and analysed for total arsenic as described in section 3.5.1.1.a.

3.5.2.8. Protein phosphatase inhibition experiments

Cantharidin (Sigma, C7632), tautomycin (Sigma, 86305) and okadaic acid (Sigma, O7760) were used for protein phosphatase inhibition experiments.

Cantharidin was dissolved in DMSO at a concentration of 1 g L^{-1} (5.097 mM) to obtain a stock solution. The stock solution was further diluted to 50.97 µM with DMSO. The final concentration was 100 nM, diluted in culture media.

Tautomycin was dissolved in DMSO at a concentration of 500 µg.L^{-1} (0.652 µM) to obtain a stock solution. The final concentration was 0.3 nM, diluted in culture media.

Okadaic acid was dissolved in DMSO at a concentration of 250 µg.L^{-1} (0.302 µM) to obtain a stock solution. The final concentration was 1 nM, diluted in culture media.

C. vulgaris cells were cultured for 3-5 days in Bold's media free of arsenic. In one set of experiments, controls were exposed to 50 mg L^{-1} of As(III) for 48 h without the addition of the inhibitors (cantharidin/tautomycin/okadaic acid). In the other set of experiments, cells were exposed to the inhibitors (cantharidin/tautomycin/okadaic acid) with and without exposure to 50 mg L^{-1} As(III) for 48 h. The experiments were performed in triplicates.

Cell were harvested and extracted according to the protocol described in section 3.5.2.2. GSH, GSSG and As-GS/PC complexes were determined according to the protocol described in section 3.5.2.5. The final concentration of DMSO in the treatments did not exceed 0.37%.

3.5.2.9. GSH transport stimulation experiments

Stimulation of ABCC mediated transport was investigated by using the flavonoid apigenin (Sigma, A3145) and the calcium channel blocker verapamil (Sigma, PHR1131).

Verapamil was dissolved in deionised water at a concentration of 10 g L^{-1} (20.36 mM) to obtain a stock solution. The final concentration was 30 µM, diluted in culture media.

Apigenin was dissolved in DMSO at a concentration of 2.5 g L^{-1} (9.25 mM) to obtain a stock solution. The final concentration was 15 µM, diluted in culture media.

C. vulgaris cells were cultured for 3-5 days in Bold's media free of arsenic. In one set of experiments, controls were exposed to 50 mg L^{-1} of As(III) for 48 h without the addition of the chemicals (apigenin/verapamil). In the other set of experiments, cells exposed to the chemicals (apigenin/verapamil) with and without exposure to 50 mg L^{-1} As(III) for 48 h. The experiments were performed in triplicates

Cell were harvested and extracted according to the protocol described in section 3.5.2.2. GSH, GSSG and As-GS/PC complexes were determined according to the protocol described in section 3.5.2.5. The final concentration of DMSO in the treatments did not exceed 0.2%.

3.6. Genetic markers for arsenic resistance in *C. vulgaris*

Genes involved in arsenic resistance based on phytochelatin production and compartmentalisation span across many kingdoms, e.g. Animalia, Plantae and Fungi (Perales-Vela, Pena-Castro and Canizares Villanueva, 2006; Vatamanuik et al., 2001). Therefore a BLAST search could help to answer the following question: Could arsenic resistance observed in *C. vulgaris* cells based on PC production and compartmentalisation be a possible mechanism by which other organisms help to detoxify arsenic?

The full genome of a different strain of *C. vulgaris* (*Coccomyxa* sp. strain C-169) has been sequenced and reported (Higashiva and Yamada, 1991). Although the strain C-169 is not the same as the one used in the present study (CCAP 211/11B), the genome of C-169 was used to compare similarities with key proteins in arsenic resistance from model organisms.

Genes encoding for ATP binding cassette families C-D (atABC/MRP) and phytochelatin synthase (atPCS1) from *Arabidopsis thaliana* (Song et al., 2010; Vatamaniuk et al., 1999) as well as the genes ACR1-3 arsenic resistant proteins (As(V) reductases and As(III) efflux pumps) from *Saccharomyces cerevisiae* (Bobrowicz et al., 1997) and homoglutathione synthetase (gshs2, addition of Ala instead of Gly in GSH) from *Medicago truncatula* (Frendo et al., 2005) were compared with those of *C. vulgaris* C-169 in a sequence similarity search BLASTP using the Uniprot (BLASTP 2.2.28+ software) database (Uniprot, 2009). Identity is

defined in the database as the percentage of identical amino acids, between the query and the search.

The search generated a list of organisms that shared similarities with genes implicated in arsenic resistance. These organisms were order by similarity to the proteins ABCC1/2 followed by phytochelatin synthase, Ala GSH synthetase, ABCD1/2 and finally arsenic reductase. Finally the table was summarised showing organisms that only express simultaneous similarity to the main genes implicated in arsenic resistance.

3.7. Statistical analysis

Statistical analyses were undertaken using MINITAB v15. Correlation coefficients were calculated using a simple regression, least squares method. Analyses of difference were obtained using two-sample t-tests and one-way analysis of variance (ANOVA). Normality and equal variance assumptions were tested in all experiments. The General Linear Model (GLM) was used to perform univariate analysis of variance with balanced and unbalanced designs, analysis of covariance, and regression, for each response variable. A "full rank " design matrix is formed from the factors and covariates and each response variable is regressed on the columns of the design matrix. The method for comparisons used was the Tukey-Kramer method.

For the flow cytometry analysis, Kolmogorov-Smirnov statistics were used to measure the difference between two distributions and were calculated using BD CellQuest software; this generates a D-value ranging between 0 and 1.0, with higher values indicating a greater difference between the distributions. Then a p-value is assigned which is a function of a prefixed confidence level and the total counts of the two histograms. The null hypothesis states that the samples come from the same distribution. Thus for $p <= 0.001$ there is 99.9% confidence level that the two histograms are not samples from the same probability density function. D values obtained in this form, were categorised in the following way: Strong ($D > 0.30$), moderate ($0.20 < D < 0.30$), weak ($0.15 < D < 0.20$) and negligible ($D < 0.15$) difference (Lebedeva, Pande and Patton, 2011). All D-values obtained in this study were calculated using Kolmogorov-Smirnov statistics with a sample size n = 20,000.

4. RESULTS

4.1. Toxicity tests

C. vulgaris cells were counted using an improved Neubauer haemocytometer. After this, consecutive dilutions of the original sample were done and two calibrations curves were created and plotted for cell counts using a whole water fluorescent extraction method in the following ranges: from $7.94x10^2$ to $7.94x10^3$ cells mL^{-1} and from $7.94x10^2$ to $2.27x10^5$ cells mL^{-1}. The results are shown in Fig 4.1 and 4.2.

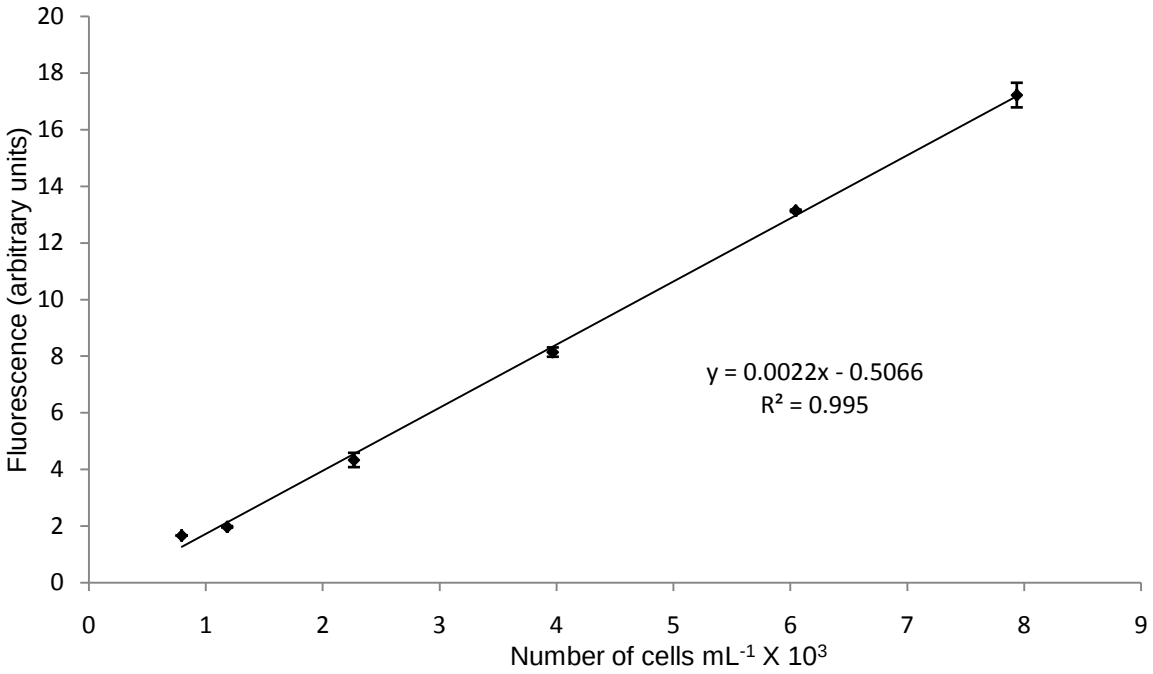

Fig 4. 1 Estimation of the relationship between number of cells and fluorescence (excitation 430 nm, emission 671 nm) for *C. vulgaris* cells using a whole water extraction method in the following range: $7.94x10^2$ to $7.94x10^3$ cells mL^{-1}. Horizontal bars denote ± 1 standard error, n = 3.

It can be observed from Fig 4.1 and 4.2 that there was a very strong correlation (simple linear least squares, R^2 = 0.995 and R^2 = 0.999, n =3) between the number of cells counted using a settling chamber and fluorescence extracted using a whole water extraction technique. Also concentrations as low as 1000 cells mL^{-1} had good correlation and a very narrow standard error. Unless stated otherwise, this methodology for estimating the number of cells in *C. vulgaris* cell populations was used throughout all the experiments.

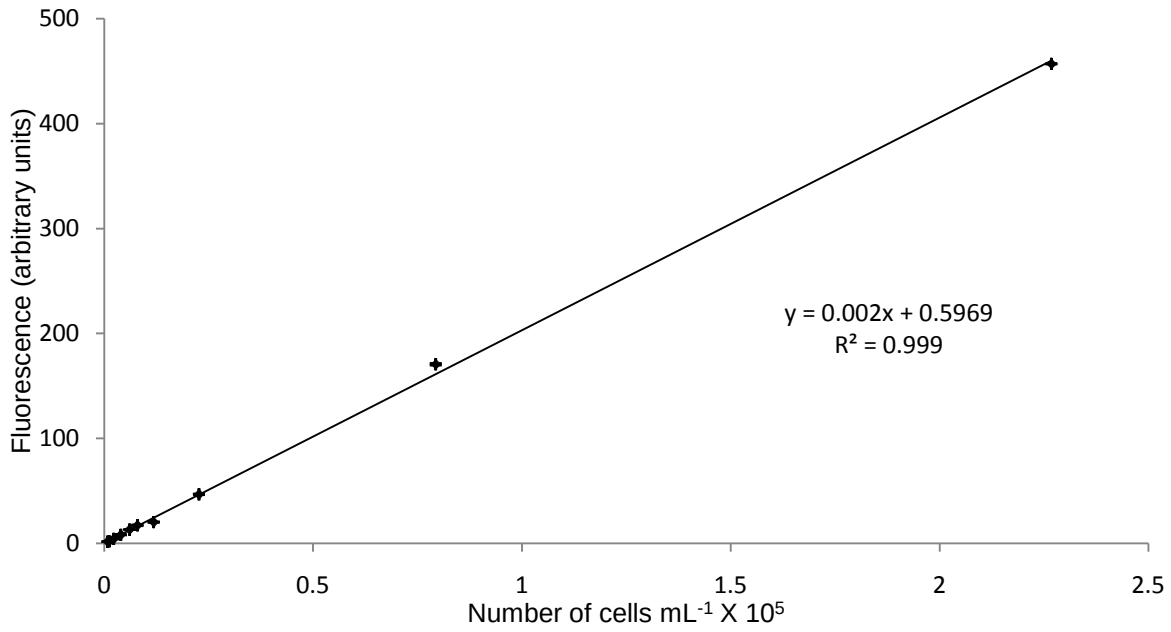

Fig 4. 2 Estimation of the relationship between number of cells and fluorescence (excitation 430 nm, emission 671 nm) for *C. vulgaris* cells using a whole water extraction method in the following range: $7.94x10^2$ to $2.27x10^5$ cells mL^{-1}. Horizontal bars denote ± 1 standard error, n = 3.

4.1.1. Arsenic toxicity to *C. vulgaris*

a) As(III)

Toxicity of As(III) to *C. vulgaris* was investigated at different concentrations of phosphate. For the first experiments the media contained 13 mg L^{-1} of phosphate and test concentrations of arsenic were: 30, 60, 100, 130 and 160 mg L^{-1}. The results for this test can be seen in Fig 4.3.

Cells remained in lag phase for about one day and then started growing logarithmically. Even when growth was markedly affected by an increase in the As(III) concentration, such concentrations were extremely high for freshwater algae.

Growth inhibition with reference to the controls was investigated. A graph for the percentage of growth inhibition versus test concentration was plotted for three replicates in order to determine the inhibition concentration for 50% of the cells (IC_{50}). This can be seen in Fig 4.4. The results were: IC_{50} = 55.33 mg L^{-1} for 95% CI (48.95-61.42). The calculations were performed by linear interpolation (5 points) from

Conc = (1.19) X (% inhibition) – (4.16), for 95% CI (simple linear least squares, R^2 = 0.952, n = 3) (Fig 4.5).

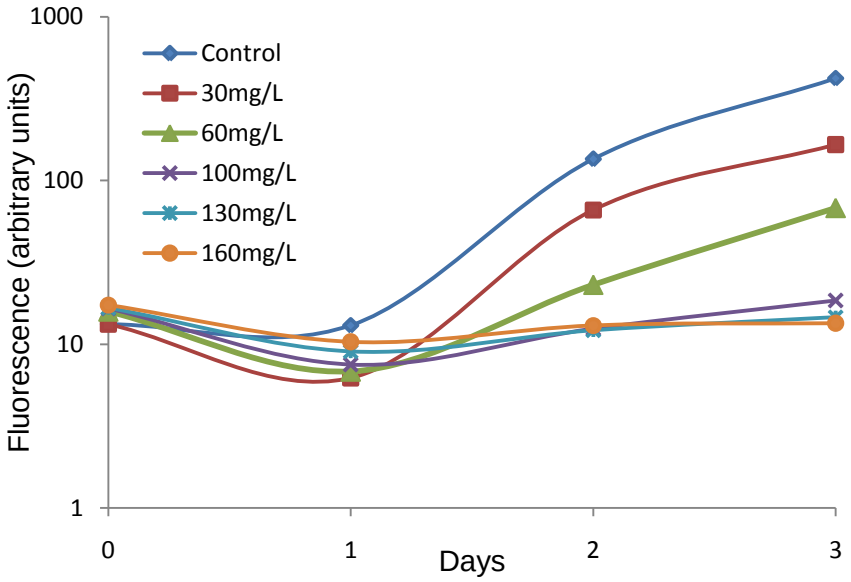

Fig 4. 3 Toxicity of As(III) to *C. vulgaris* (0,30,60,100,130 and 160 mg L^{-1}) in media containing 13 mg L^{-1} of phosphate; fluorescent pigments were extracted using a whole water extraction procedure at 430 nm excitation and 671 nm emission wavelengths. n = 3, controls = 5

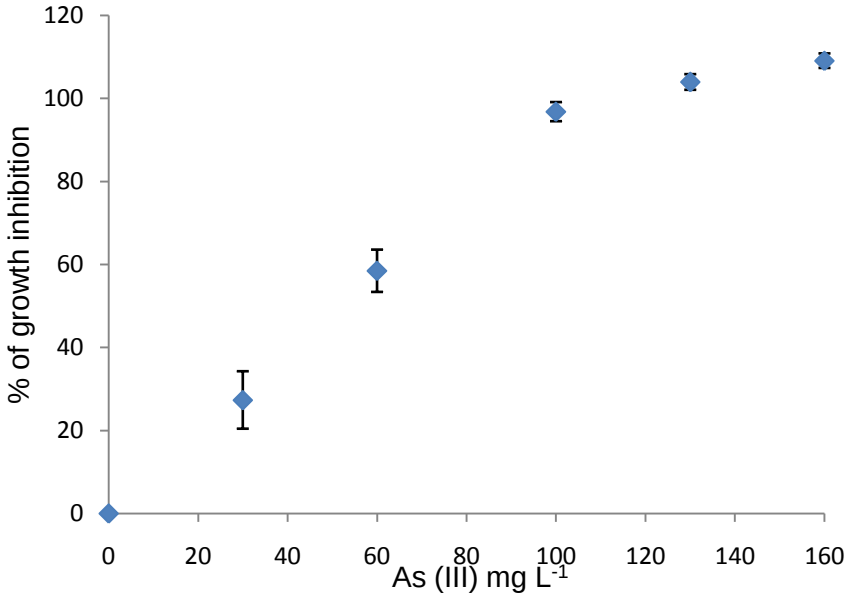

Fig 4. 4 Percentage of growth inhibition versus test concentration, As(III) tested (0, 30, 60, 100, 130 and 160 mg L^{-1}), 13 mg L^{-1} of phosphate, 72 h. Vertical bars denote ± 1 standard error, n = 3, controls = 5

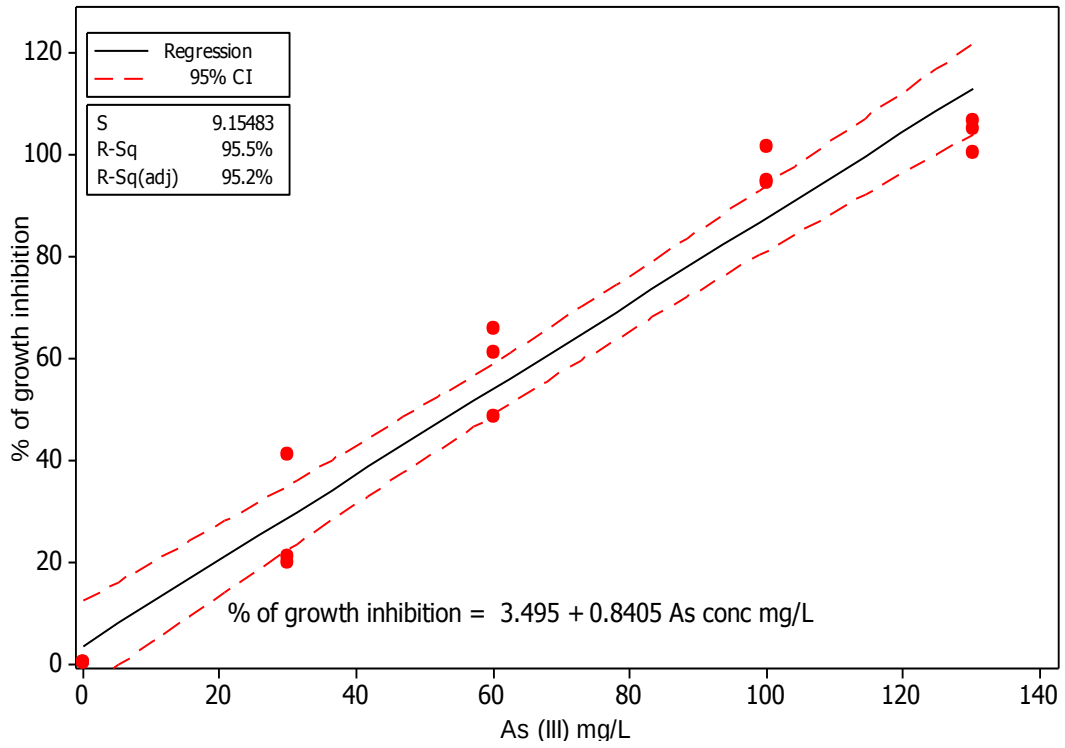

Fig 4. 5 Calculation of IC_{50} by linear interpolation. IC_{50} = 55.33 mg L^{-1} for 95% CI (48.95-61.42), calculated from Conc = (1.1898) X (% inhibition) – (4.1582). As(III) tested (0, 30, 60, 100, 130 and 160 mg L^{-1}), 13 mg L^{-1} of phosphate, 72 h, n = 3, controls = 5

Dissolved oxygen, pH, redox potential and temperature were monitored for one control experiment at an intermediate concentration of As(III) (45 mg L^{-1}), this is shown in Fig 4.6. Temperature in the media matched the temperature set up for the incubator with a variation of 0.5 ˚C, pH was slightly basic at 7.5 throughout all the experiment. Dissolved oxygen varied between 6.5 to 8.2 mg L^{-1} and was observed to decrease during the daily stirring which is a normal behaviour.

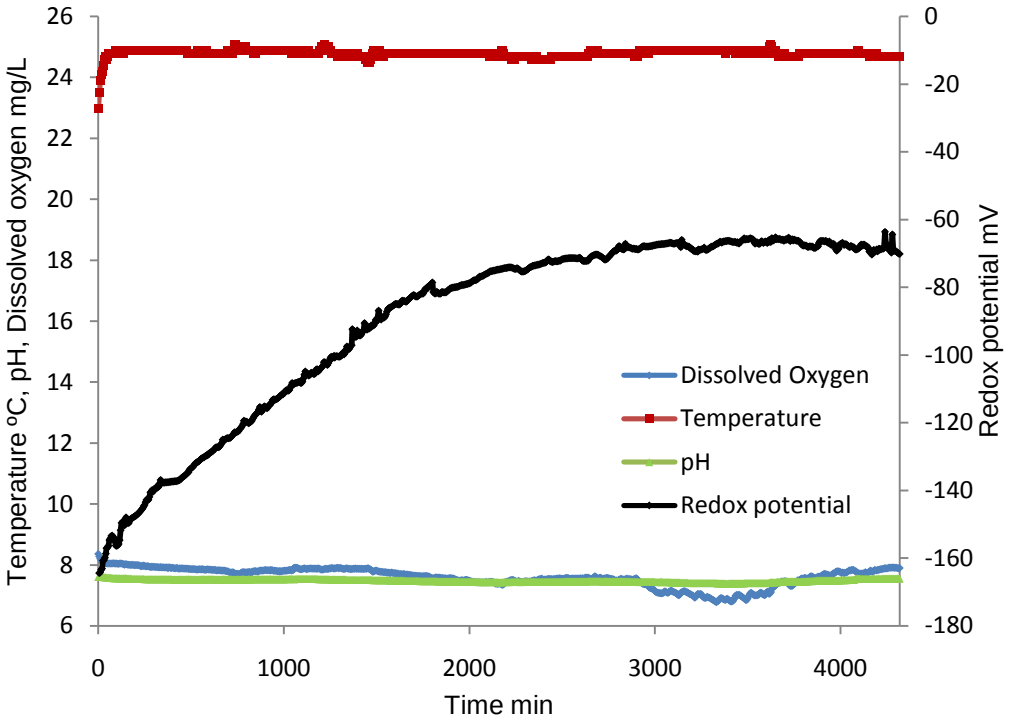

Fig 4. 6 Continuous (5 min) monitoring of dissolved oxygen, pH and temperature for a control experiment, 45 mg L^{-1} As(III) and 13 mg L^{-1} PO_4^{3-}

Toxicity of As(III) to *C. vulgaris* was investigated at low phosphate concentration. The media contained 0.15 mg L^{-1} of phosphate and the test concentrations for arsenic were: 15, 30, 45, 60 and 75 mg L^{-1}. The results for this test can be seen in Fig 4.7.

Cells growing at low phosphate concentration started growing slightly earlier than cells growing in high phosphate concentration. Control cells grew logarithmically until day 2 and then reached stationary phase. In this case growth was not so markedly affected by an increase in As(III) concentration, but this was most likely due to such low concentration of phosphate and slower growth in the controls compared to the treatment experiments.

A graph for the percentage of growth inhibition versus test concentration was plotted as shown in Fig 4.8. Toxicity did not reach 50% but the IC_{50} could be extrapolated to 106.79 mg L^{-1}. In this case the apparent greater resistance to arsenic could be attributed to lower growth in the controls with a mean growth rate of 0.92 day^{-1} compared to 1.17 day^{-1} in the high phosphate environment.

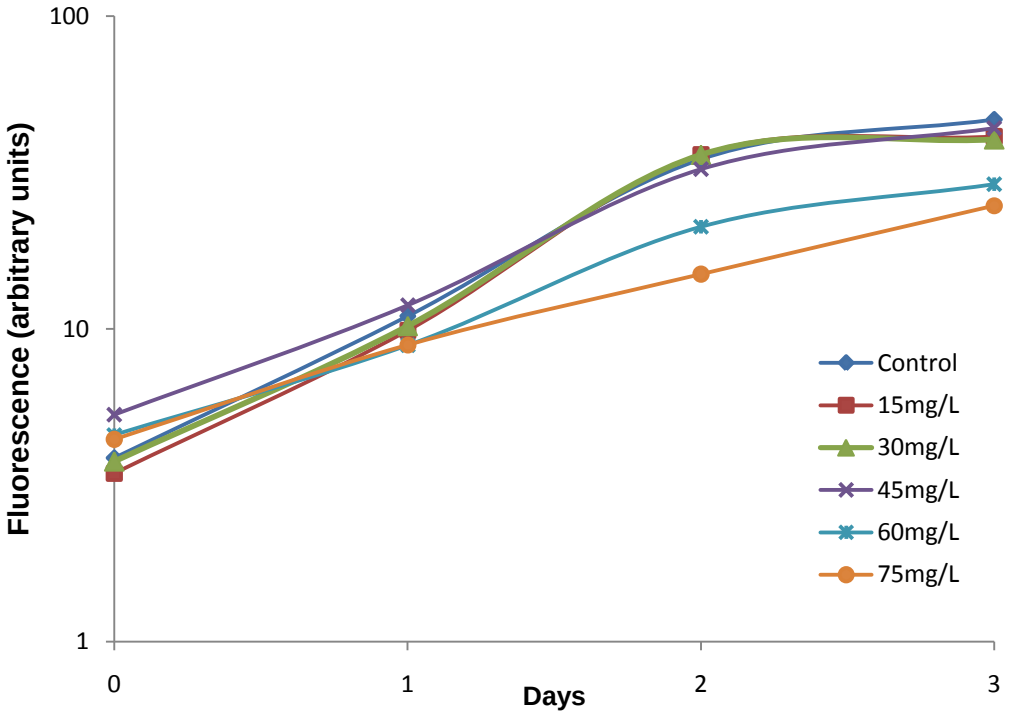

Fig 4. 7 Toxicity of As(III) to *C. vulgaris* (0, 15, 30, 45, 60 and 75 mg L^{-1}) in media containing 0.15 mg L^{-1} of phosphate; fluorescent pigments were extracted using a whole water extraction procedure at 430 nm excitation and 671 nm emission wavelengths, n = 3, controls = 5

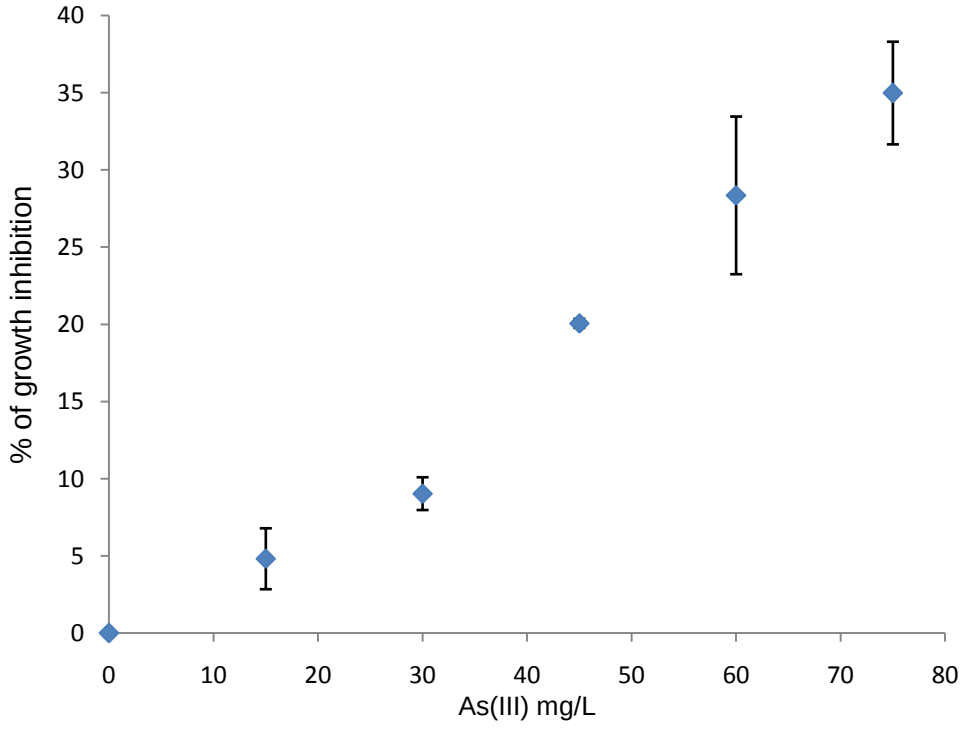

Fig 4. 8 Percentage of growth inhibition versus test concentration, As(III) tested (0, 15, 30, 45, 60 and 75 mg L^{-1}), 0.15 mg L^{-1} phosphate, 72 h. Vertical bars denote ± 1 standard error, n = 3, controls = 5

Toxicity of As(III) to *C. vulgaris* was investigated at intermediate concentration of phosphate. The media contained 0.3 mg L^{-1} of phosphate and the test concentrations for arsenic were: 30, 60, 100, 130 and 160 mg L^{-1}. The results for this test can be seen in Fig 4.9.

In this case growth was linearly affected by an increase in As(III) concentration, even at 160 mg L^{-1}. The graph for growth inhibition with reference to the controls can be seen in Fig 4.10. The results were: IC_{50} = 64.23 mg L^{-1} for 95% CI (58.52-69.65). The calculations were performed by linear interpolation from Conc = (1.1612) X (% inhibition) + (6.1716), for 95% CI (R^2 = 0.976, simple linear least squares) (Fig 4.11).

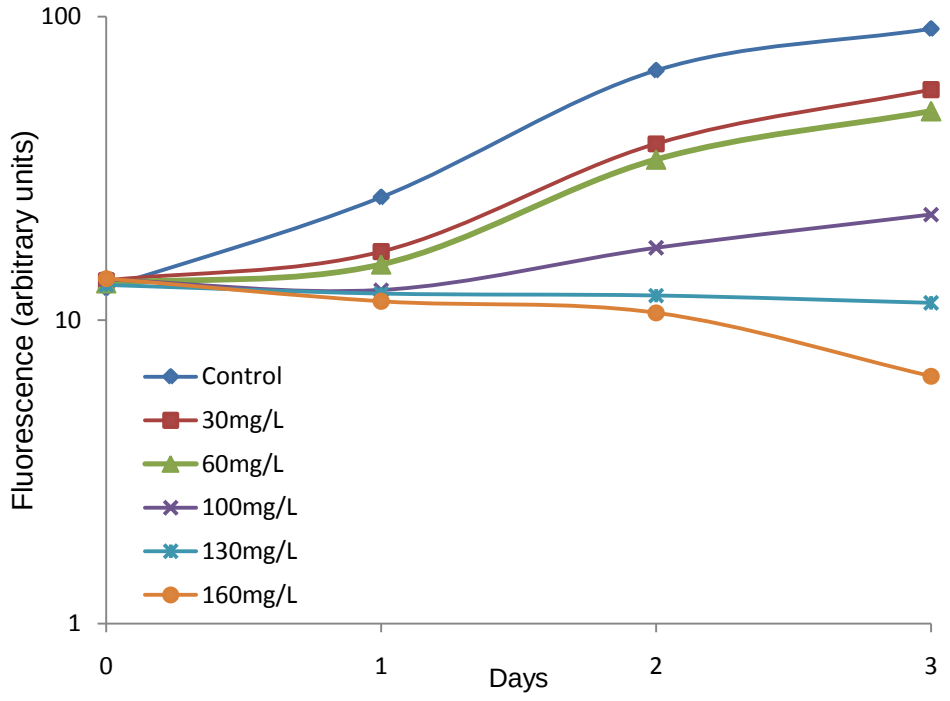

Fig 4. 9 Toxicity of As(III) to *C. vulgaris* (0, 30, 60, 100, 130 and 160 mg L^{-1}) in media containing 0.3 mg L^{-1} of phosphate; fluorescent pigments were extracted using a whole water extraction procedure at 430 nm excitation and 671 nm emission wavelengths, n = 3, controls = 5

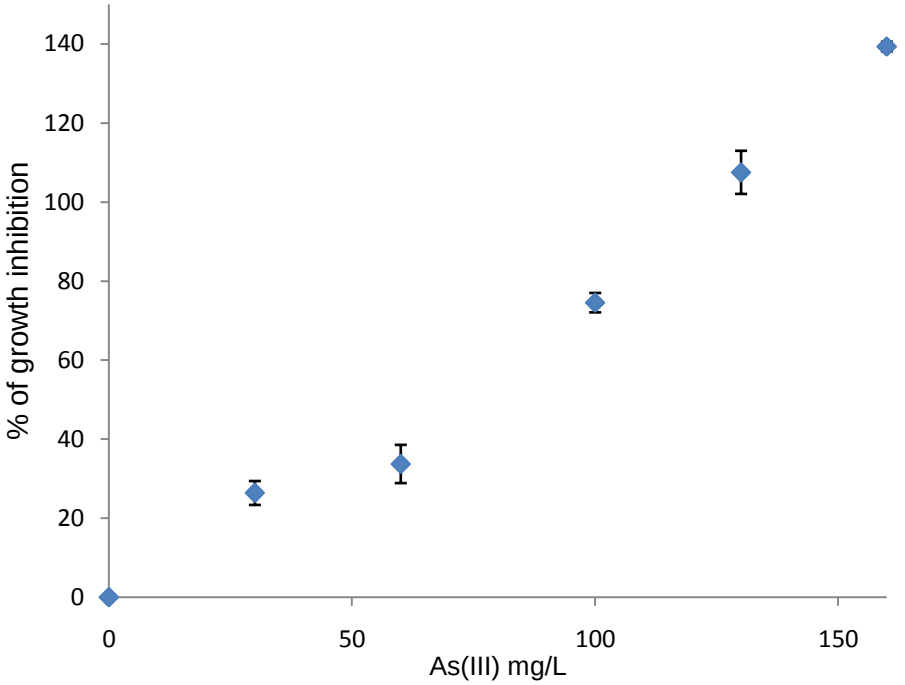

Fig 4. 10 Percentage of growth inhibition versus test concentration, As(III) tested (0, 30, 60, 100, 130 and 160 mg L^{-1}), 0.3 mg L^{-1} of phosphate, 72 h. Vertical bars denote ± 1 standard error, n = 3, control = 5

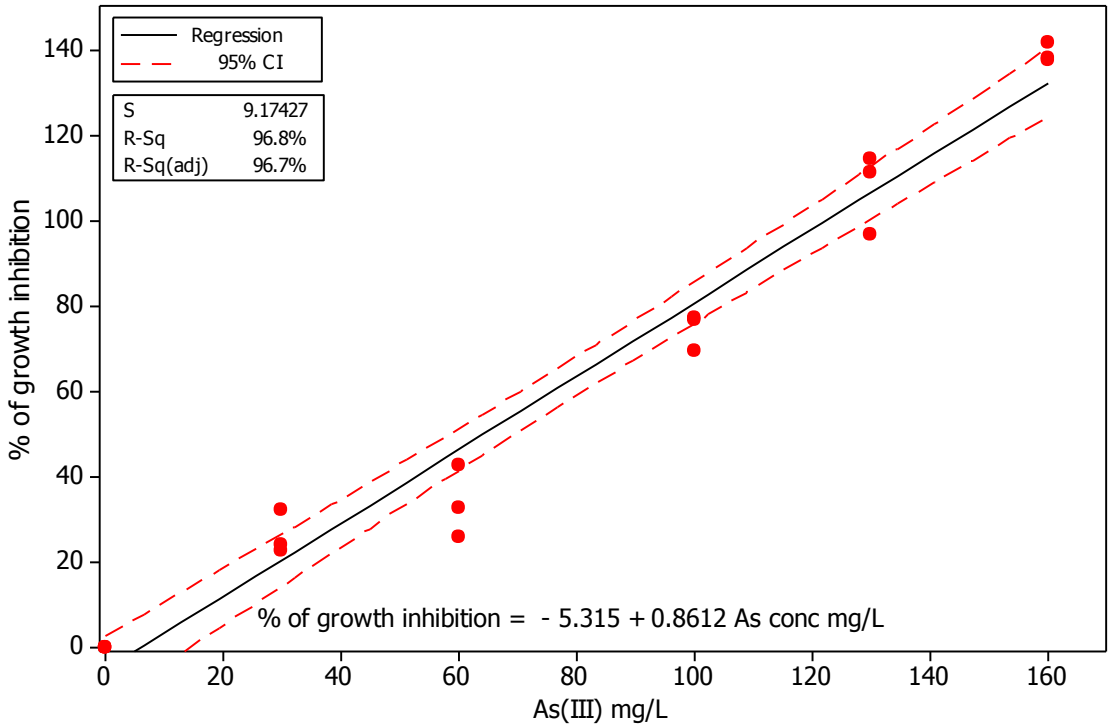

Fig 4. 11 Calculation of IC_{50} by linear interpolation. 64.23 mg L^{-1} for 95% CI (58.52-69.65), calculated from Conc = (1.1612) X (% inhibition) + (6.1716). As(III) tested (0, 30, 60, 100, 130 and 160 mg L^{-1}), 0.3 mg L^{-1} of phosphate, 72 h, n = 3, controls = 5

b) As(V)

Toxicity of As(V) to *C. vulgaris* cells was investigated at high concentration of phosphate. The media contained 13 mg L^{-1} of phosphate and the test concentrations for arsenic were: 2.5, 4.5, 6.5, 8.5 and 10.5 mg L^{-1}. The results for this test can be seen in Fig 4.12.

Cells were also in lag phase for about one day and started growing logarithmically from then on. Growth of *C. vulgaris* under these conditions was slightly increased with an increase in the concentration of arsenic in the media therefore no inhibition was envisaged nor calculated.

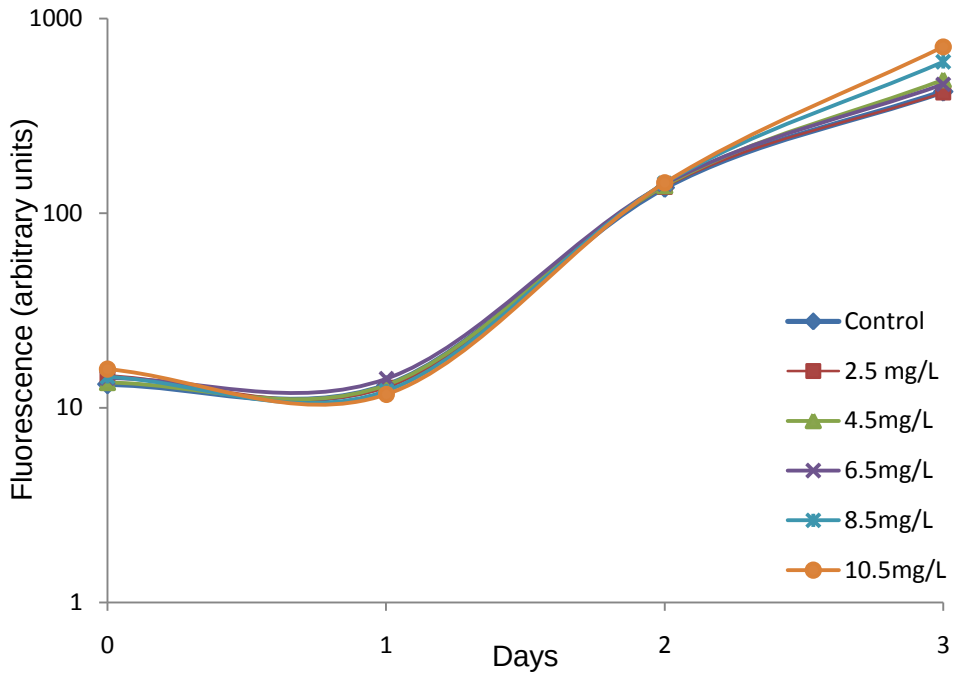

Fig 4. 12 Toxicity of As(V) to *C. vulgaris* (0, 2.5, 4.5, 6.5, 8.5 and 10.5 mg L^{-1}) in media containing 13 mg L^{-1} of phosphate; fluorescent pigments were extracted using a whole water extraction procedure at 430 nm excitation and 671 nm emission wavelengths, n = 3, controls = 5

Toxicity of As(V) to *C. vulgaris* was investigated at intermediate phosphate concentration. The media contained 0.3 mg L^{-1} of phosphate (previous experiments

using 0.15 mg L^{-1} resulted in reduced growth) and test concentrations for arsenic were: 0, 0.1, 0.2, 0.3, 0.4 and 0.5 mg L^{-1}.

The results for toxicity can be seen in Fig 4.13. Cells growing at intermediate phosphate concentration started growing slightly before than cells growing at high phosphate concentration. Again, control cells grew logarithmically until day 2 and then reached stationary phase. In this case cells growing in media with arsenic had a longer lag phase that lasted for one day and then started to grow logarithmically for one day to reach stationary phase after day 2.

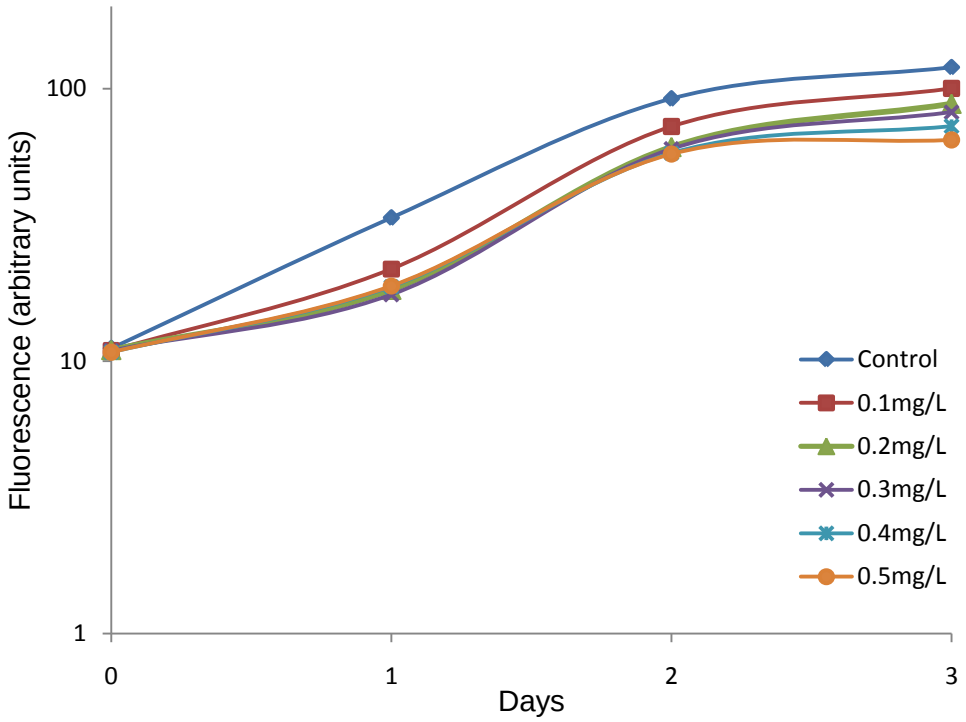

Fig 4. 13 Toxicity of As(V) to *C. vulgaris* (0, 0.1, 0.2, 0.3, 0.4 and 0.5 mg L^{-1}) in media containing 0.3 mg L^{-1} of phosphate; fluorescent pigments were extracted using a whole water extraction procedure at 430 nm excitation and 671 nm emission wavelengths, n = 3, controls = 5

A graph for the percentage of growth inhibition versus test concentration was plotted (Fig 4.14). Toxicity did not reach 50% but IC_{50} could be extrapolated to 1.07 mg L^{-1}. The mean growth rate for the controls was 0.80 day^{-1}.

Dissolved oxygen, pH and temperature were monitored for a control experiment at an intermediate concentration of As(V) (0.1 mg L^{-1}) and 0.3 mg L^{-1} PO_4^{3-}; the results for this experiment can be seen in Fig 4.15.

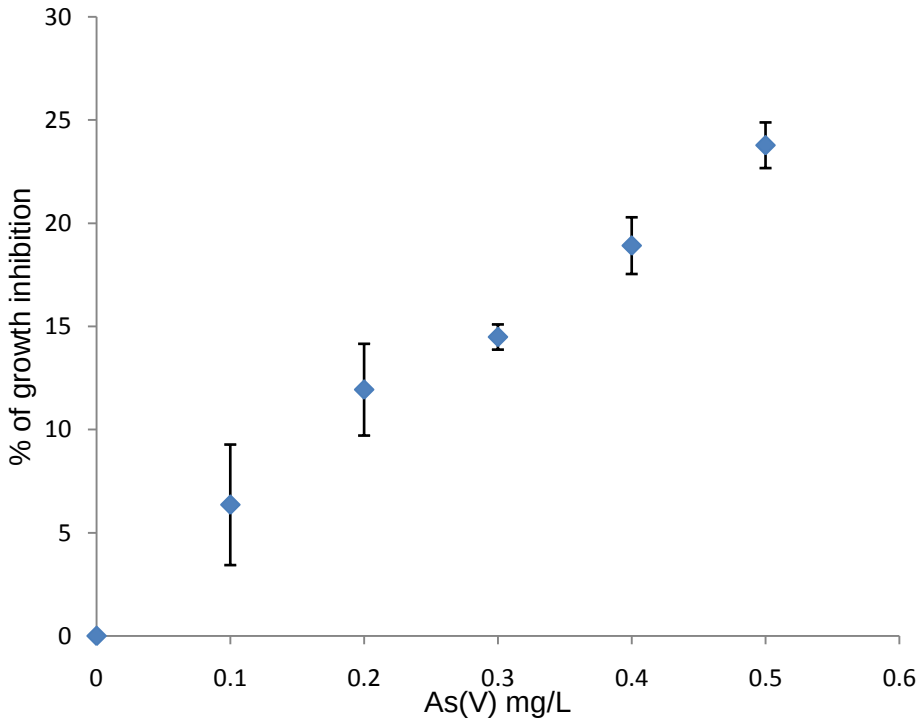

Fig 4. 14 Percentage of growth inhibition versus test concentration, As(V) tested (0, 0.1, 0.2, 0.3, 0.4 and 0.5 mg L^{-1}), 0.3 mg L^{-1} of phosphate, 72 h. Vertical bars denote ± 1 standard error, n = 3, controls = 5

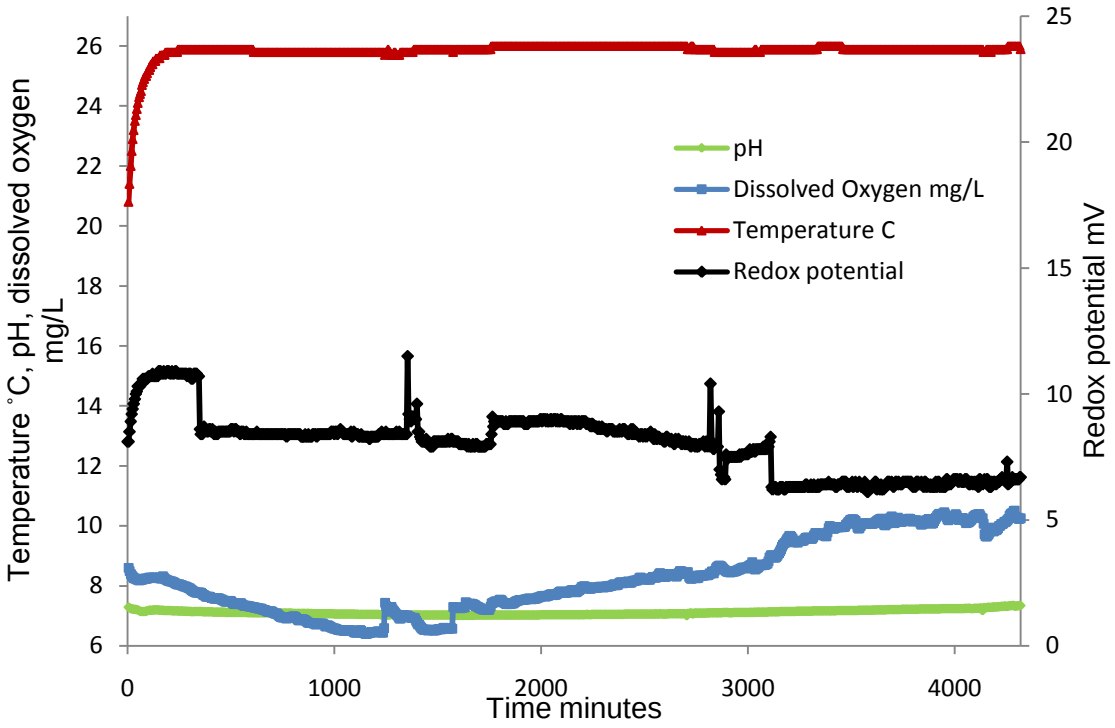

Fig 4. 15 Continuous (5 min) monitoring of dissolved oxygen, pH and temperature for a control experiment at 0.1 mg L^{-1} As(V) and 0.3 mg L^{-1} PO_4^{3-}, 72 h

c) DMA and As(III) at different sulphur concentrations

Toxicity of DMA and As(III) to *C. vulgaris* cells was investigated at different concentration of sulphur.

Firstly, toxicity of DMA was tested at 29.23 mg L^{-1} SO_4^{2-} and the test concentrations for arsenic were: 20, 40, 60, 80 and 100 mg L^{-1}. The results for this experiment can be seen in Fig 4.16 and 4.17. Cells started growing logarithmically until day 2 and then reached stationary phase. Growth inhibition was only about 25% at the highest concentrations of arsenic therefore no IC_{50} was calculated.

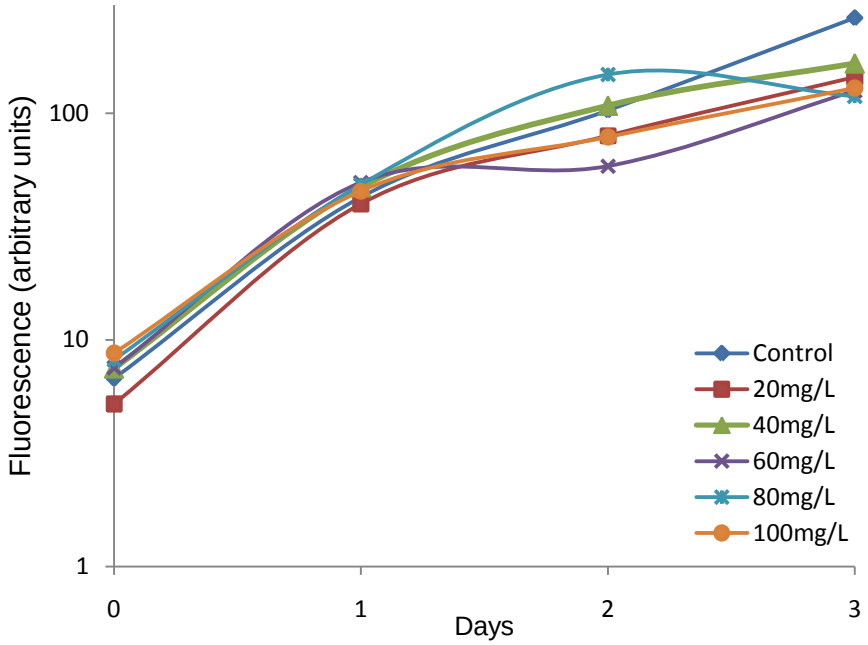

Fig 4. 16 Toxicity of DMA to *C. vulgaris* (0, 20, 40, 60, 80 and 100 mg L^{-1}) in media containing 29.23 mg L^{-1} SO_4^{2-}, fluorescent pigments were extracted using a whole water extraction procedure at 430 nm excitation and 671 nm emission wavelengths n = 3, controls = 5

When the concentration of SO_4^{2-} was lowered to 0.1 mg L^{-1} (0.34% the concentration used in high sulphur experiments), cells treated with As(III) and DMA did not grow significantly different from control cells, this can be observed in Fig 4.18. Therefore no IC_{50} was calculated. Importantly, this may indicate that the amount of sulphur in the media does not play an important role in As(III) and DMA resistance.

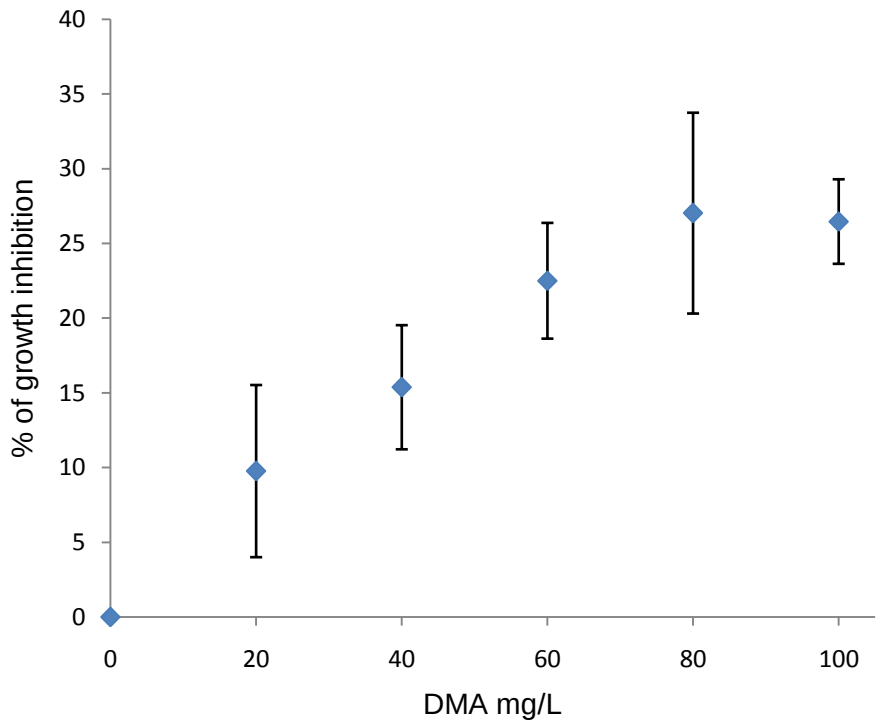

Fig 4. 17 Percentage of growth inhibition versus test concentration, DMA tested (0, 20, 40, 60, 80 and 100 mg L^{-1}) in media containing 29.23 mg L^{-1} SO_4^{2-}, 72 h. Vertical bars denote ± 1 standard error, n = 3, controls = 5

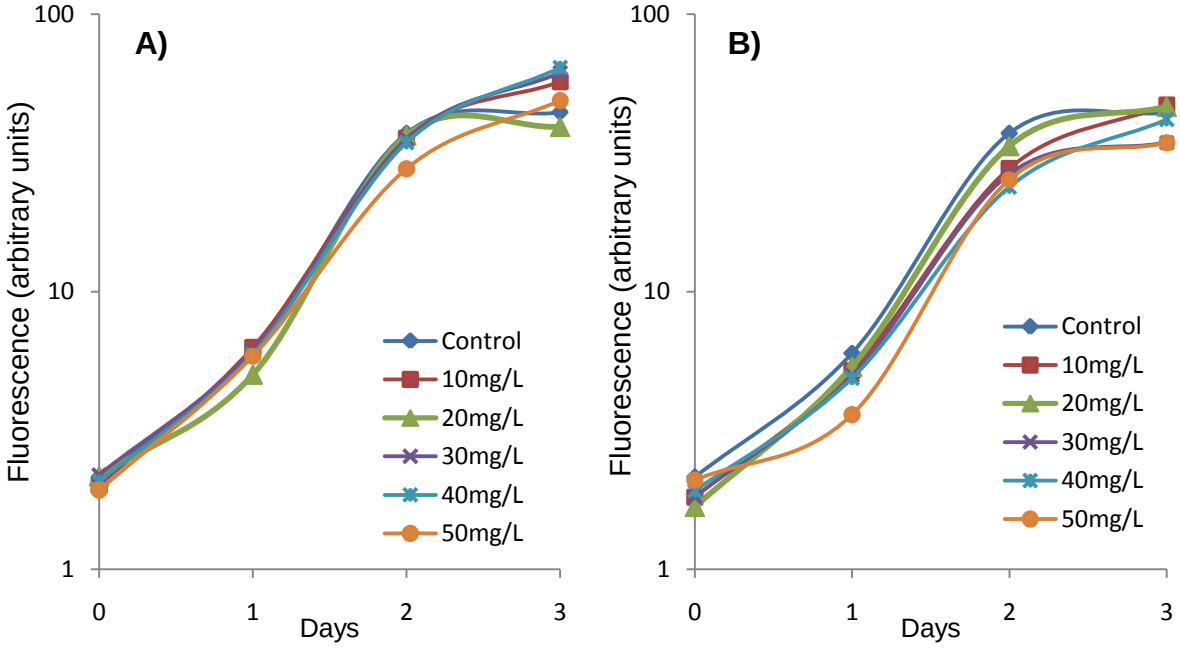

Fig 4. 18 Toxicity of arsenic to *C. vulgaris* (0, 10, 20, 30, 40 and 50 mg L^{-1}) in media containing 0.1 mg L^{-1} SO_4^{2-}, fluorescent pigments were extracted using a whole water extraction procedure at 430 nm excitation and 671 nm emission wavelengths, n = 3, controls = 5, A) DMA, B) As(III)

4.1.2. Oxidative stress, GSH and pH measurements by flow cytometry

Flow cytometry was used to investigate the role of oxidative stress, GSH and pH inside arsenic-treated *C. vulgaris* cells. All fluorescent signals were excited by the argon-ion laser at 488 nm wavelength. Chlorophyll fluorescence was measured at emission 670 nm (FL3) and was used to gate healthy viable cells, the same gated population was then used to measure changes in fluorescence at excitation 530 ± 15 nm (FL1) and 585 ± 20 nm (FL2). It is important to note that given the extremely large number of individual observations generated during flow cytometry experiments, any small difference in distribution will generate a significant p-value and so it is the effect size as indicated by the D-value that should be the focus of interpretation of distribution differences. Therefore D-values obtained from Kolmogorov-Smirnov statistics, were categorised in the following way: Strong (D > 0.30), moderate (0.20 < D <= 0.30), weak (0.15 < D <= 0.20) and negligible (D <= 0.15) difference (Lebedeva, Pande and Patton, 2011).

4.1.2.1. Determination of intracellular pH, As(III) and As(V)

Histogram distributions of negative control cells (heat-killed), As(III) (50 mg L^{-1} at 153.3 mg L^{-1} PO_4^{-3}) and As(V) (1 mg L^{-1} at 0.3 mg L^{-1} PO_4^{-3}) treated cells stained with BCECF can be seen in Fig 4.19.

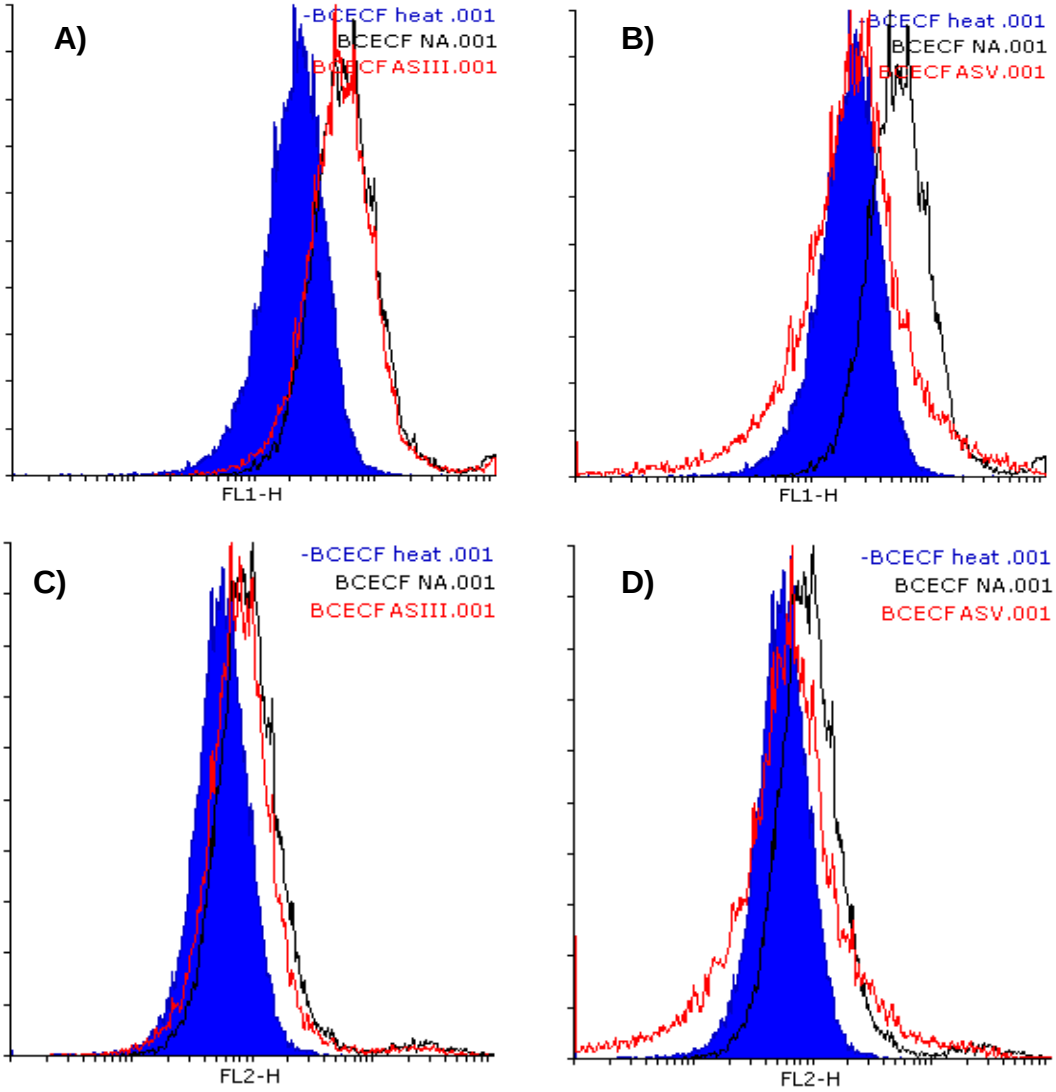

Fig 4. 19 Flow cytometry histogram distributions of negative control cells (heat-killed, blue), non-treated cells (black) as well as As(III) and As(V) treated cells (red). Stained used, treatment, Channel: A) BCECF, As(III), FL1; B) BCECF, As(V), FL1; C) BCECF, As(III), FL2; D) BCECF, As(V), FL2. Measured at 530 ± 15 nm (FL1) and 585 ± 20 nm (FL2). Treatment time 120 min

Treatment with As(III) had negligible effect (D = 0.06) in BCECF fluorescence intensity signal, whereas treatment with As(V) had a moderate decrease (D = 0.30) in BCECF fluorescence intensity signal and therefore a decrease in intracellular pH, this can be observed in Fig 4.19 and Table 4.1.

Table 4. 1 Kolmogorov-Smirnov statistics calculated using BD CellQuest software for negative control cells (heat-killed, -C), As(III), As(V) treated and non-treated (No As) cells, stained with BCECF measured at 530 ± 15 nm (FL1) and 585 ± 20 nm (FL2). * denotes p<=0.001, + denotes 0.001 < p <= 0.005, ** denotes p > 0.1, n = 20,000.

BCECF FL1

D-value	-C1	-C2	-C3	AsIII1	AsIII2	AsIII3	AsV1	AsV2	AsV3
NoAs1	0.62*	0.50*	0.51*	0.06*	0.09*	0.04*	0.51*	0.21*	0.28*
NoAs2	0.63*	0.51*	0.52*	0.07*	0.10*	0.05*	0.51*	0.21*	0.28*
NoAs3	0.60*	0.48*	0.48*	0.03*	0.06*	0.02+	0.48*	0.18*	0.25*

BCECF FL2

D-value	-C1	-C2	-C3	AsIII1	AsIII2	AsIII3	AsV1	AsV2	AsV3
NoAs1	0.38*	0.24*	0.25*	0.11*	0.14*	0.09*	0.27*	0.26*	0.32*
NoAs2	0.39*	0.25*	0.26*	0.12*	0.15*	0.10*	0.28*	0.27*	0.33*
NoAs3	0.35*	0.21*	0.22*	0.08*	0.11*	0.06*	0.25*	0.23*	0.29*

Strong (D > 0.30)
Moderate (0.20 < D <= 0.30)
Weak (0.15 < D < =0.20)
Negligible (D <= 0.15)

4.1.2.2. Determination of intracellular GSH, As(III) and As(V)

Histogram distributions of negative control cells (heat-killed), As(III) (50 mg L^{-1} at 153.3 mg L^{-1} PO_4^{-3}) and As(V) (1 mg L^{-1} at 0.3 mg L^{-1} PO_4^{-3}) treated cells stained with CMFDA can be seen in Fig 4.20.

Treatment with As(III) had negligible effect (D = 0.03) in CMFDA fluorescence intensity signal. In contrast, treatment with As(V) had a strong increase (D = 0.56) in CMFDA fluorescence intensity signal and therefore an increase in intracellular GSH (as free thiols), this can be observed in Fig 4.20 and Table 4.2.

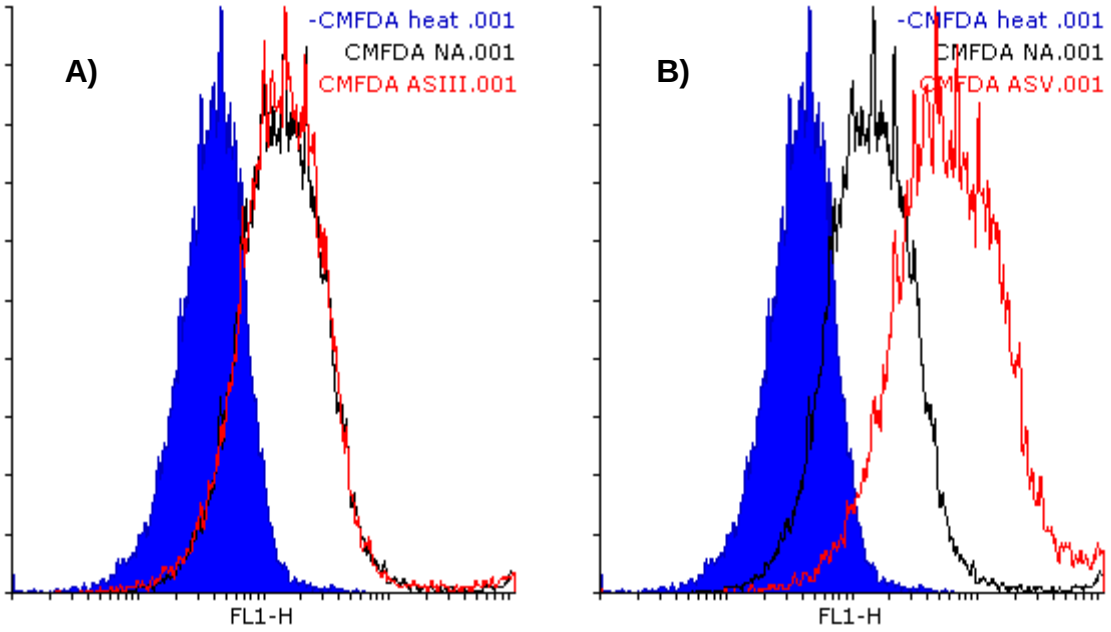

Fig 4. 20 Flow cytometry histogram distributions of negative control cells (heat-killed, blue), non-treated cells (black) as well as As(III) and As(V) treated cells (red). Stained used, treatment, Channel: A) CMFDA, As(III), FL1; B) CMFDA, As(V), FL1. Measured at 530 ± 15 nm. Treatment time 120 min

Table 4. 2 Kolmogorov-Smirnov statistics calculated using BD CellQuest software for negative control cells (heat-killed, -C), As(III), As(V) treated and non-treated (No As) cells, stained with CMFDA measured at 530 ± 15 nm (FL1). * denotes p <= 0.001, + denotes 0.001 < p <= 0.005, ** denotes p > 0.1, n = 20,000.

CMFDA FL1

D-value	-C1	-C2	-C3	AsIII1	AsIII2	AsIII3	AsV1	AsV2	AsV3
NoAs1	0.68*	0.70*	0.71*	0.01**	0.02+	0.04*	0.59*	0.56*	0.57*
NoAs2	0.71*	0.72*	0.74*	0.03*	0.05*	0.02+	0.56*	0.53*	0.55*
NoAs3	0.69*	0.70*	0.72*	0.01**	0.02*	0.04*	0.59*	0.55*	0.57*

Strong (D > 0.30)
Moderate (0.20 < D <= 0.30)
Weak (0.15 < D < =0.20)
Negligible (D <= 0.15)

4.1.2.3. Determination of H_2O_2 free radical, As(III) and As(V)

Histogram distributions of negative control cells (heat-killed), As(III) (50 mg L^{-1} at 153.3 mg L^{-1} PO_4^{-3}), As(V) (1 mg L^{-1} at 0.3 mg L^{-1} PO_4^{-3}) and positive control (50 µM H_2O_2) cells stained with H_2DCFH-DA can be seen in Fig 4.21.

Neither treatment with As(III) (D = 0.02) nor treatment with As(V) (D = 0.07) had a significant effect on H_2DCFH-DA fluorescence intensity signal. This was corroborated by the use of a positive control which had a strong stimulatory effect (D = 0.89). This indicates that at the conditions used in this experiment no H_2O_2 free radical formation was observed upon exposure to inorganic arsenic (III and V). This is shown in Fig 21 and Table 4.3.

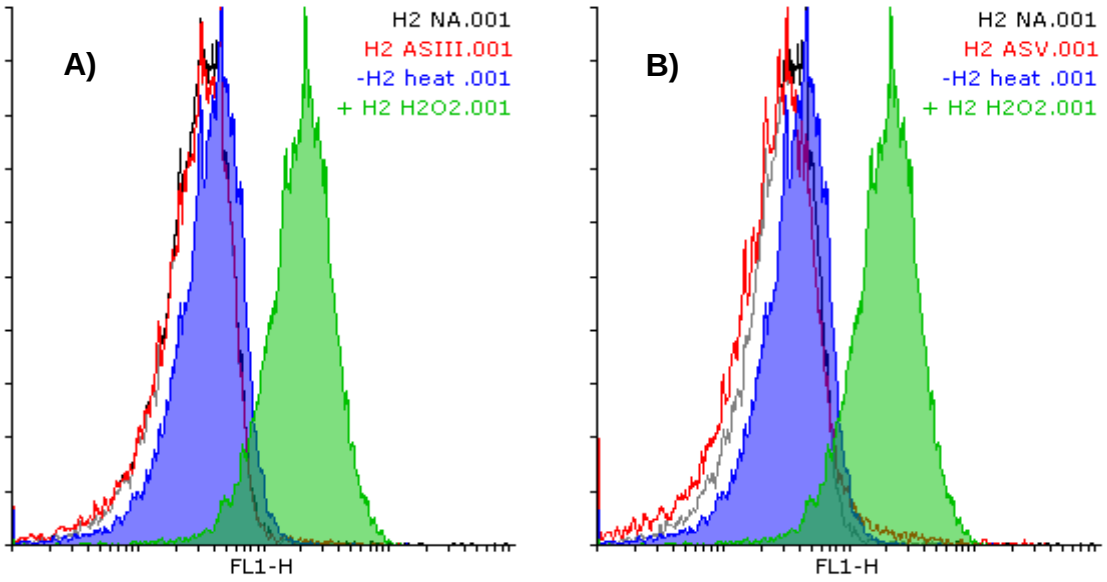

Fig 4. 21 Flow cytometry histogram distributions of negative control cells (heat-killed, blue), positive control (50 µM H_2O_2, green), non-treated cells (black) as well as As(III) and As(V) treated cells (red). Stained used, treatment, Channel: A) H2DCFH-DA, As(III), FL1; B) H2DCFH-DA, As(V), FL1. Measured at 530 ± 15 nm. Treatment time 120 min

Table 4. 3 Kolmogorov-Smirnov statistics calculated using BD CellQuest software for negative control cells (heat-killed, -C), As(III) and As(V) treated cells, positive controls (+H_2O_2) and non-treated cells (No As), stained with H2DCFH-DA measured at 530 ± 15 nm (FL1). * denotes p <= 0.001, + denotes 0.001 < p <= 0.005, ** denotes p > 0.1, n = 20,000.

H2DCFH-DA FL1

D-value	-C1	-C2	-C3	AsIII1	AsIII2	AsIII3	AsV1	AsV2	AsV3	+H2O2-1	+H2O2-2	+H2O2-3
NoAs1	0.17*	0.17*	0.16*	0.02*	0.03*	0.03*	0.08*	0.07*	0.05*	0.90*	0.89*	0.87*
NoAs2	0.17*	0.17*	0.16*	0.02+	0.02*	0.02*	0.08*	0.06*	0.05*	0.90*	0.89*	0.87*
NoAs3	0.17*	0.17*	0.16*	0.02*	0.03*	0.03*	0.08*	0.07*	0.05*	0.90*	0.89*	0.87*

Strong (D > 0.30)
Moderate (0.20 < D <= 0.30)
Weak (0.15 < D < =0.20)
Negligible (D <= 0.15)

4.1.2.4. Determination of O_2^- super oxide ion, As(III) and As(V)

Histogram distributions of negative control cells (heat-killed), As(III) (50 mg L^{-1} at 153.3 mg L^{-1} PO_4^{-3}), As(V) (1 mg L^{-1} at 0.3 mg L^{-1} PO_4^{-3}) and positive control (20 µM Menadione) cells stained with HE can be seen in Fig 4.22.

Neither treatment with As(III) (D = 0.03) nor treatment with As(V) (D = 0.10) had effect on HE dihydroethidium fluorescence intensity signal. This was corroborated by the use of a positive control (menadione) which had a strong stimulatory effect (D = 0.30). This also indicates that at the conditions used in this experiment no O_2^- super oxide radical formation was observed. This is shown in Fig 4.22 and Table 4.4.

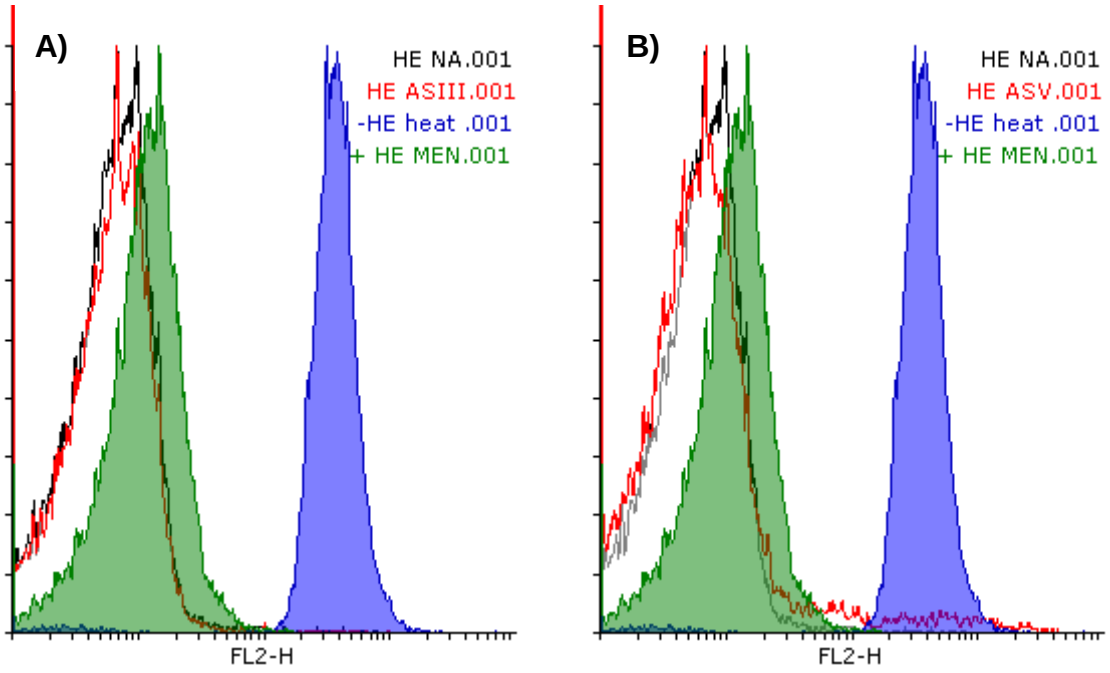

Fig 4. 22 Flow cytometry histogram distributions of negative control cells (heat-killed, blue), positive control (20 µM Menadione, green), non-treated cells (black) as well as As(III) and As(V) treated cells (red).. Stained used, treatment, Channel: A) HE dihydroethidium, As(III), FL2; B) HE dihydroethidium, As(V), FL2. Measured at 585 ± 20 nm (FL2). Treatment time 120 min

Table 4. 4 Kolmogorov-Smirnov statistics calculated using BD CellQuest software for control cells (heat-killed, -C), As(III), As(V) treated and non-treated (No As) cells, stained with HE dihydroethidium measured at 585 ± 20 nm.. * denotes p <= 0.001, + denotes 0.001 < p <= 0.005, ** denotes p > 0.1, n = 20,000.

HE	**FL2**								
D-value	-C1	-C2	-C3	AsIII1	AsIII2	AsIII3	AsV1	AsV2	AsV3
NoAs1	0.97*	0.98*	0.98*	0.02+	0.05*	0.02+	0.05*	0.05*	0.06*
NoAs2	0.97*	0.98*	0.98*	0.03*	0.04*	0.02*	0.06*	0.05*	0.07
NoAs3	0.97*	0.98*	0.98*	0.03*	0.04*	0.03*	0.06*	0.05*	0.07*

Strong (D > 0.30)
Moderate (0.20 < D <= 0.30)
Weak (0.15 < D < =0.20)
Negligible (D <= 0.15)

4.2. Surface adsorption

4.2.1. Kinetic experiments using dry *C. vulgaris* cells

a) Arsenic (III)

Kinetics studies on the adsorption of As(III) onto dry *C. vulgaris* cells were performed at initial concentration of 1 mg L^{-1} and 0.2 g of dry algae, pH was adjusted with MOPS (pH 7) and potassium hydrogen phthalate (pH 4). Arsenic and phosphorus were measured using ICP-MS. Phosphate release was simultaneously measured and compared along with a control experiment with no addition of arsenic. As shown in Fig 4.23A, pseudo-equilibrium was achieved after 4 h. The release of phosphate was dependent on pH but not related to arsenic adsorption. Correlation coefficients for arsenic adsorbed vs. phosphate released were found for pH 4, R^2 = 0.196 (simple linear least squares, n = 9) and pH 7, R^2 = 0.867 (simple linear least squares, n = 9) (Fig 4.23B). There was also insufficient evidence to establish a difference in the levels of phosphate release from experiments with addition of arsenic and no addition of arsenic (two-sample t-test, p = 0.5, n=9).

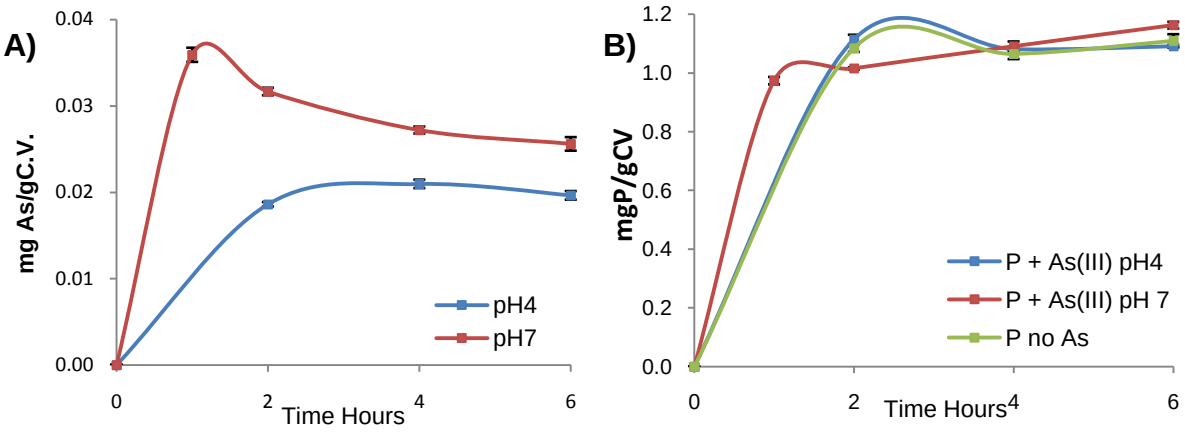

Fig 4. 23 Kinetics study on the adsorption of As(III) onto dry *C. vulgaris* cells, initial concentration 1 mg L^{-1} and 0.2 mg of dry algae, pH adjusted with MOPS (pH 7) and potassium hydrogen phthalate (pH 4). Measured using ICP-MS A) As(III) adsorption B) Phosphate released, n = 3, vertical bars denote ± 1 standard error

b) Arsenic (V)

Kinetics studies on the adsorption of As(V) onto dry *C. vulgaris* cells were performed at the same conditions as in As(III) experiments. Pseudo-equilibrium was also achieved after 4 h. There was a very small but consistent negative adsorption of arsenic which indicates a negligible adsorption or even a very small release of arsenic from the adsorbent. The release of phosphate was also dependent on pH but not related to arsenic adsorption (as such adsorption did not occur, Fig 4.24).

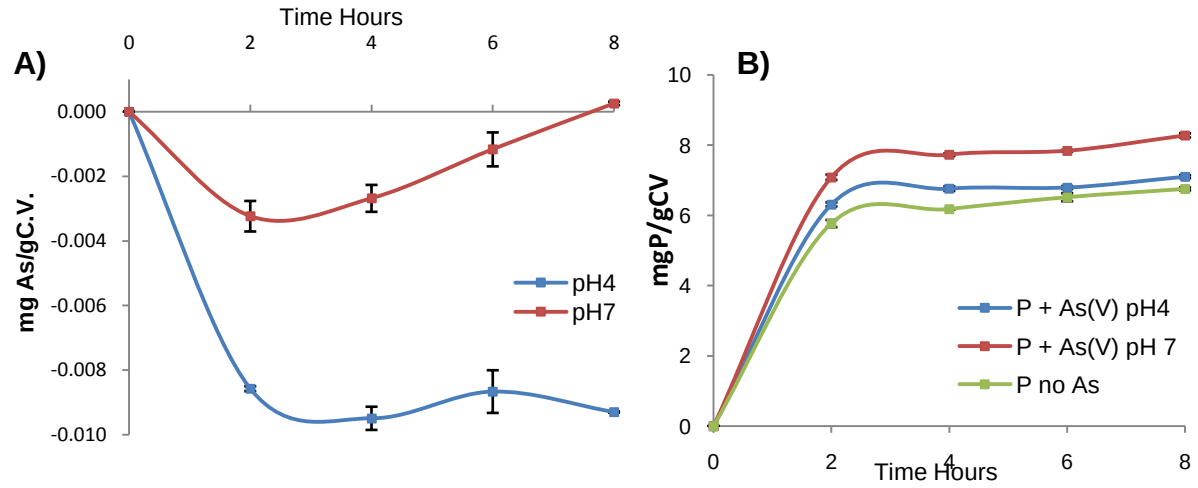

Fig 4. 24 Kinetics study on the adsorption of As(V) onto dry *C. vulgaris* cells, initial concentration 1 mg L^{-1} and 0.2 mg of dry algae, pH adjusted with MOPS (pH 7) and potassium hydrogen phthalate (pH 4). Measured using ICP-MS A) Arsenic adsorption B) Phosphate released, n = 3. Vertical bars denote ± 1 standard error

4.2.2. Freundlich and Langmuir isotherms using dry *C. vulgaris* cells

Because only As(III) kinetics show positive adsorption, this was further investigated by isotherm studies. Langmuir and Freundlich isotherms were calculated using a fixed amount of adsorbate (1 mg L^{-1}) and different amounts of adsorbent (0.2, 0.3, 0.4 and 0.5 mg of dry algae), pH was adjusted with MOPS (pH 7) and potassium hydrogen phthalate (pH 4). Although Freundlich (simple least squares; pH 4, R^2 = 0.97; pH 7, R^2 = 0.99; n = 3) and Langmuir (simple least squares; pH 4, R^2 = 0.89; pH 7, R^2 = 0.96; n = 3) isotherms were strongly correlated, the adsorption capacity (taken from Langmuir constants, Table 4.5), had negative values, which indicate poor adsorption. This capacity was not different between the different pH values studied (pH 4, Q_0 = -0.01; pH 7, Q_0 = -0.01) (Fig 4.25 and Table 4.5).

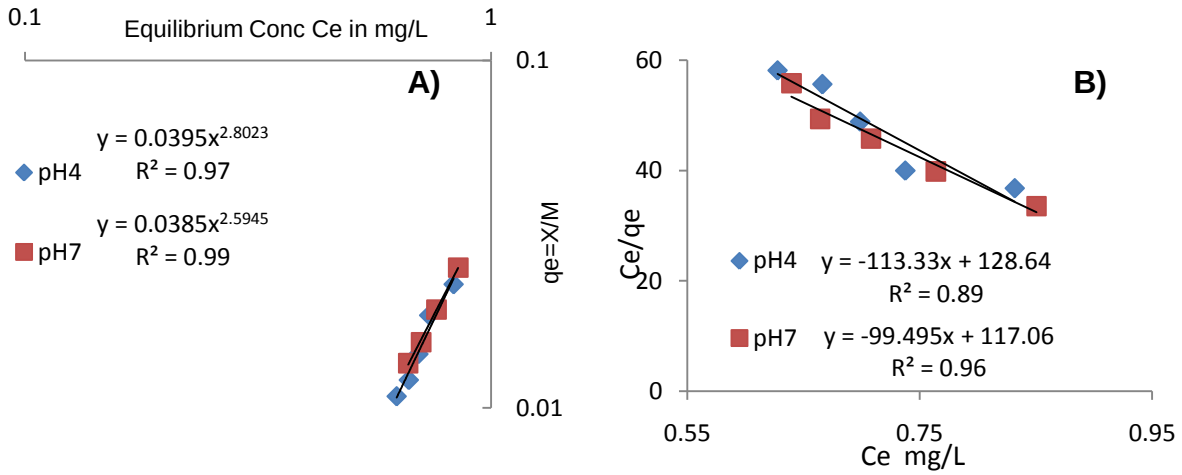

Fig 4. 25 Isotherms for the adsorption of As(III) onto dry *C. vulgaris* cells, fixed adsorbate (1 mg L^{-1}) and varying the amount of adsorbent (0.2, 0.3, 0.4 and 0.5 mg of dry algae), pH adjusted with MOPS (pH 7) and potassium hydrogen phthalate (pH 4). Measured using ICP-MS. A) Freundlich and B) Langmuir isotherm

Table 4. 5 Freundlich and Langmuir constants for the adsorption of As(III) onto dry *C. vulgaris* cells, fixed adsorbate (1 mg L^{-1}) and varying the amount of adsorbent (0.2, 0.3, 0.4 and 0.5 mg of dry algae), pH adjusted with MOPS (pH 7) and potassium hydrogen phthalate (pH 4).

	Freundlich Isotherm equation $q_e=K_FC^{1/n}$			Langmuir equation $C_e/q_e=1/Q_oK + C_e/Q_o$		
	KF	1/n	R^2	Qo	K	R2
pH4	0.04	2.63	0.86	-0.01	-0.85	0.68
pH7	0.04	2.61	0.94	-0.01	-1.21	0.80

4.2.3. Living *C. vulgaris* cells, kinetics and concentration effects

Adsorption studies after exposure of As(III), As(V) and DMA to living *C. vulgaris* cells were performed by adding 50 mg L^{-1} of arsenic for several time intervals (4, 24, 48 and 72 h). Adsorption was also investigated at different arsenic concentrations (10, 50, 100 and 200 mg L^{-1}) for a period of 48 h.

As shown in Fig 4.26, As(III) did not show a normal saturation curve. In contrast, adsorption of As(V) and DMA showed saturation after 48 h and adsorption was considerably lower than that of As(III) being 15 times lower.

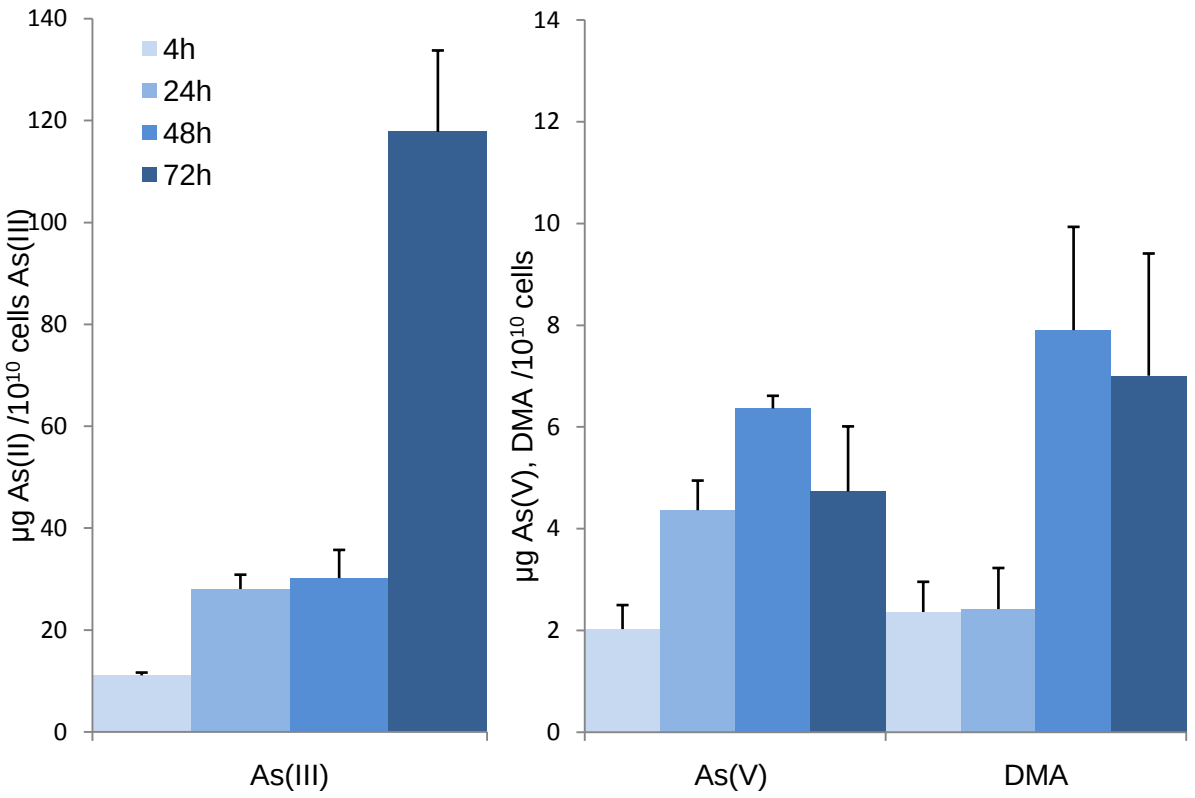

Fig 4. 26 Surface adsorption of *C. vulgaris* cells exposed to 50 mg L^{-1} of As(III), As(V) and DMA, at different time intervals (4, 24, 48 and 72 h), vertical bars indicate 1 standard error, n = 3

When cells were exposed to different concentrations of As(III), As(V) and DMA (10, 50, 100 and 200 mg L^{-1}) for 48 h (Fig 4.27), adsorption increased with an increase in the arsenic concentration in the media for all the arsenic forms. However adsorption of As(III) was 17 times higher than that of As(V) and DMA. Adsorption of As(III) followed a second order polynomial curve with high correlation coefficient (simple least squares, $R^2 = 0.99$, n = 3). As(V) (R^2=0.99) and DMA (R^2=0.92) followed simple linear adsorption curves (Fig 4.28).

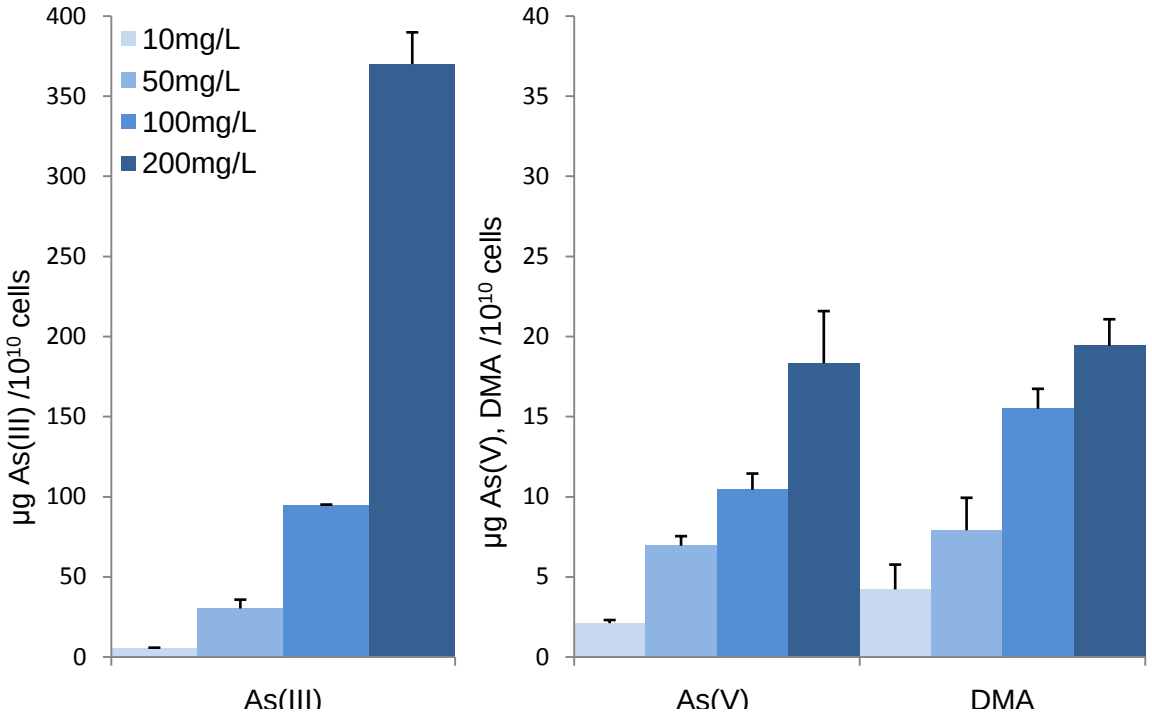

Fig 4. 27 Surface adsorption of *C. vulgaris* cells exposed to different concentrations of As(III), As(V) and DMA (10, 50, 100 and 200 mg L^{-1}) for 48 h, vertical bars indicate 1 standard error, n = 3

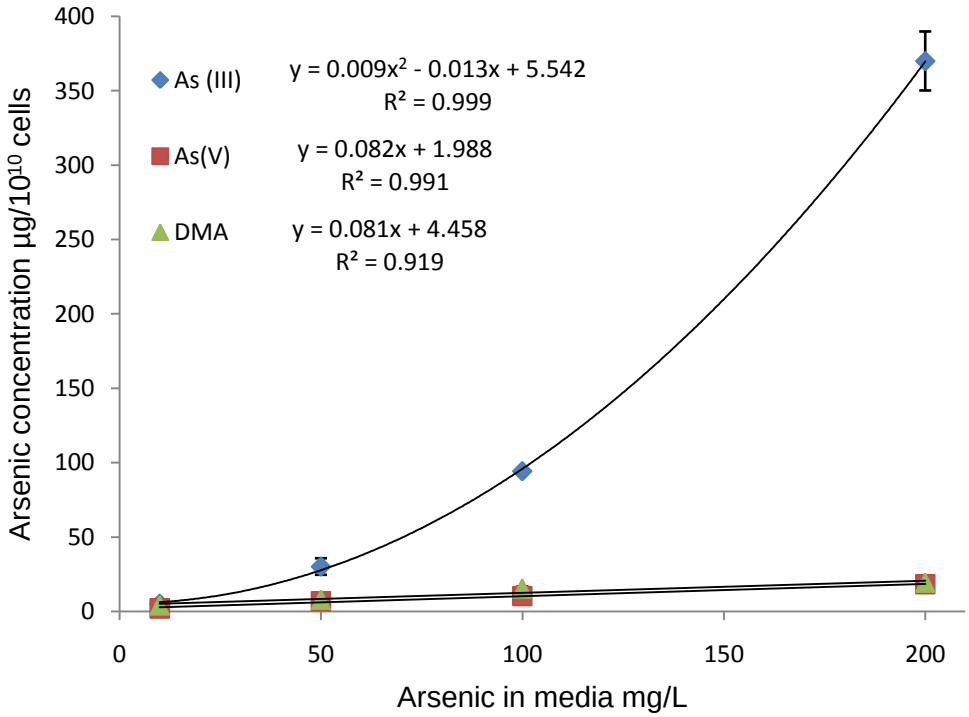

Fig 4. 28 Adsorption curves and correlation coefficients for *C. vulgaris* cells exposed to different concentrations of As(III), As(V) and DMA, for 48 h, vertical bars indicate 1 standard error, n = 3

4.3. Arsenic biotransformation experiments

4.3.1. Reduction/oxidation, methylation/demethylation and arsenosugar formation

4.3.1.1. Total absorption

In order to investigate the biotransformations of arsenic occurring inside *C. vulgaris* cells, the total amount of arsenic inside cells was calculated upon exposure to As(III), As(V) and DMA at different concentrations and exposure times. Arsenic was calculated after arsenic was desorbed for 10 min using 1 mM K_2HPO_4, 5 mM MES and 0.5 mM $Ca(NO_3)_2$. The results for this experiment can be seen in Fig 4.29 and 4.30. Interestingly total arsenic inside cells exposed to 50 mg L^{-1} did not change significantly with time (from 4 to 72 h). However, cells absorbed 8 times more As(III) than As(V) or DMA. Cells showed an increase in the amount of arsenic absorbed with an increase of the concentration of arsenic in the media for all forms of arsenic tested (Fig 4.30).

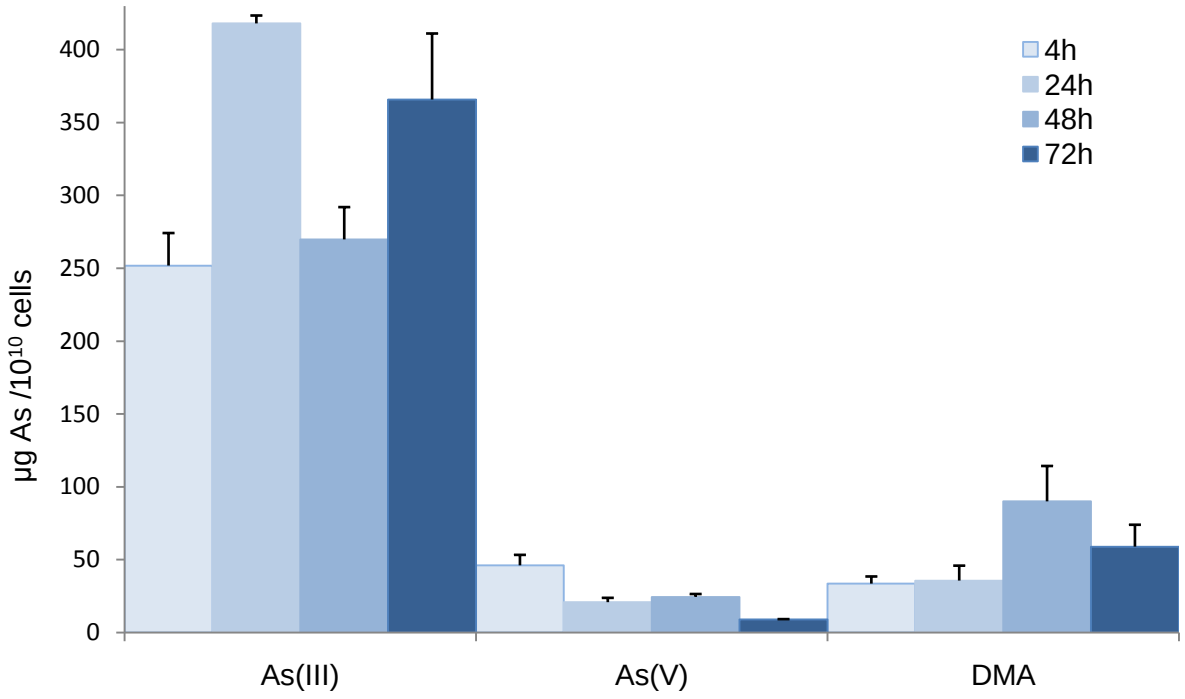

Fig 4. 29 Total arsenic inside of *C. vulgaris* cells exposed to 50 mg L^{-1} of As(III), As(V) and DMA, over different time intervals, vertical bars indicate 1 standard error, n = 3

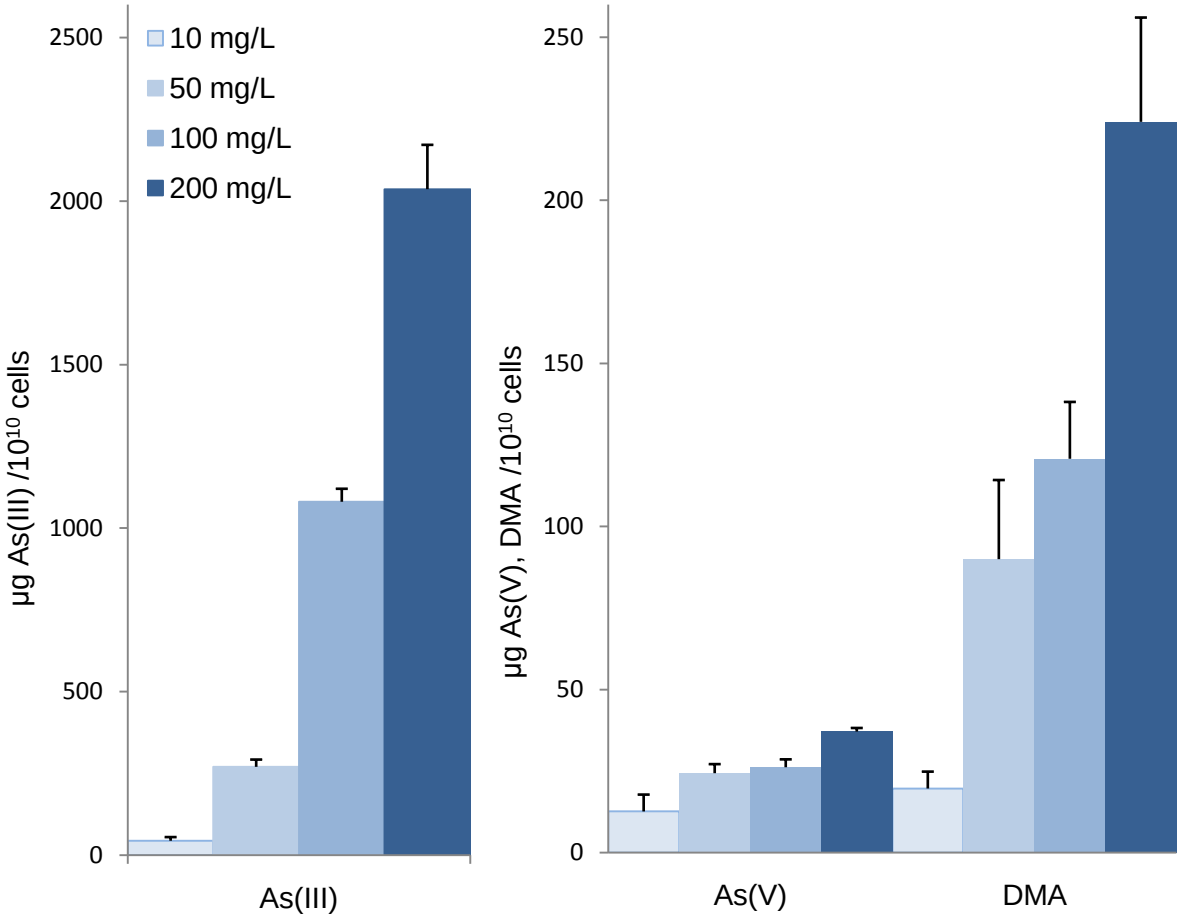

Fig 4. 30 Total arsenic inside of *C. vulgaris* cells exposed to different concentrations of As(III), As(V) and DMA, for 48 h, vertical bars indicate 1 standard error, n = 3

It can also be observed from Fig 4.29 and 4.30 that absorption of As(III) was higher than that of As(V) and DMA being 55 times higher than As(V) and 9 times higher than that of cells exposed to DMA.

All absorption curves followed simple linear adsorption curves with high correlation coefficients: As(III), R^2 = 0.98; As(V), R^2 = 0.91; DMA, R^2 = 0.98 (simple least squares, n = 3) (Fig 4.31).

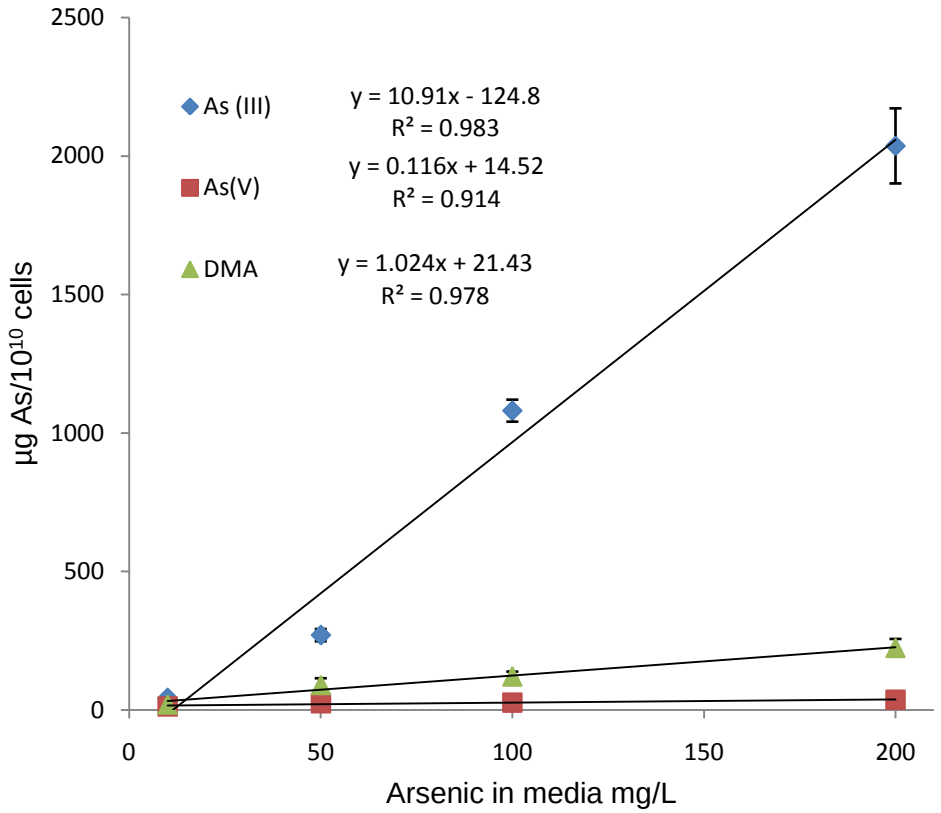

Fig 4. 31 Absorption curves and correlation coefficients for total arsenic inside of *C. vulgaris* cells exposed to different concentrations of As(III), As(V) and DMA, for 48 h, vertical bars indicate 1 standard error, n = 3

4.3.1.2. Inorganic arsenic speciation, exposure to DMA, As(V) and As(III)

When cells were exposed to different concentrations of DMA for 48 h and to 50 mg L^{-1} over different exposure times, only DMA and As(V) were detected using inorganic speciation of arsenic (PRP-X100 column and 6.6 mM $NH_4H_2PO_4$ / 6.6 mM NH_4NO_3, section 3.5.1.2). This can be observed in Fig 4.32A and 4.32B. Most of the arsenic was still in DMA form and only up to 7% was converted to As(V).

When cells were exposed to different concentrations of As(V) for 48 h and to 50 mg L^{-1} over different exposure times, As(III), DMA and As(V) were detected. This can be observed in Fig 4.32C and 4.32D. On average 41% was still in As(V) form, followed by 30% of DMA and there was a 29% reduction to As(III).

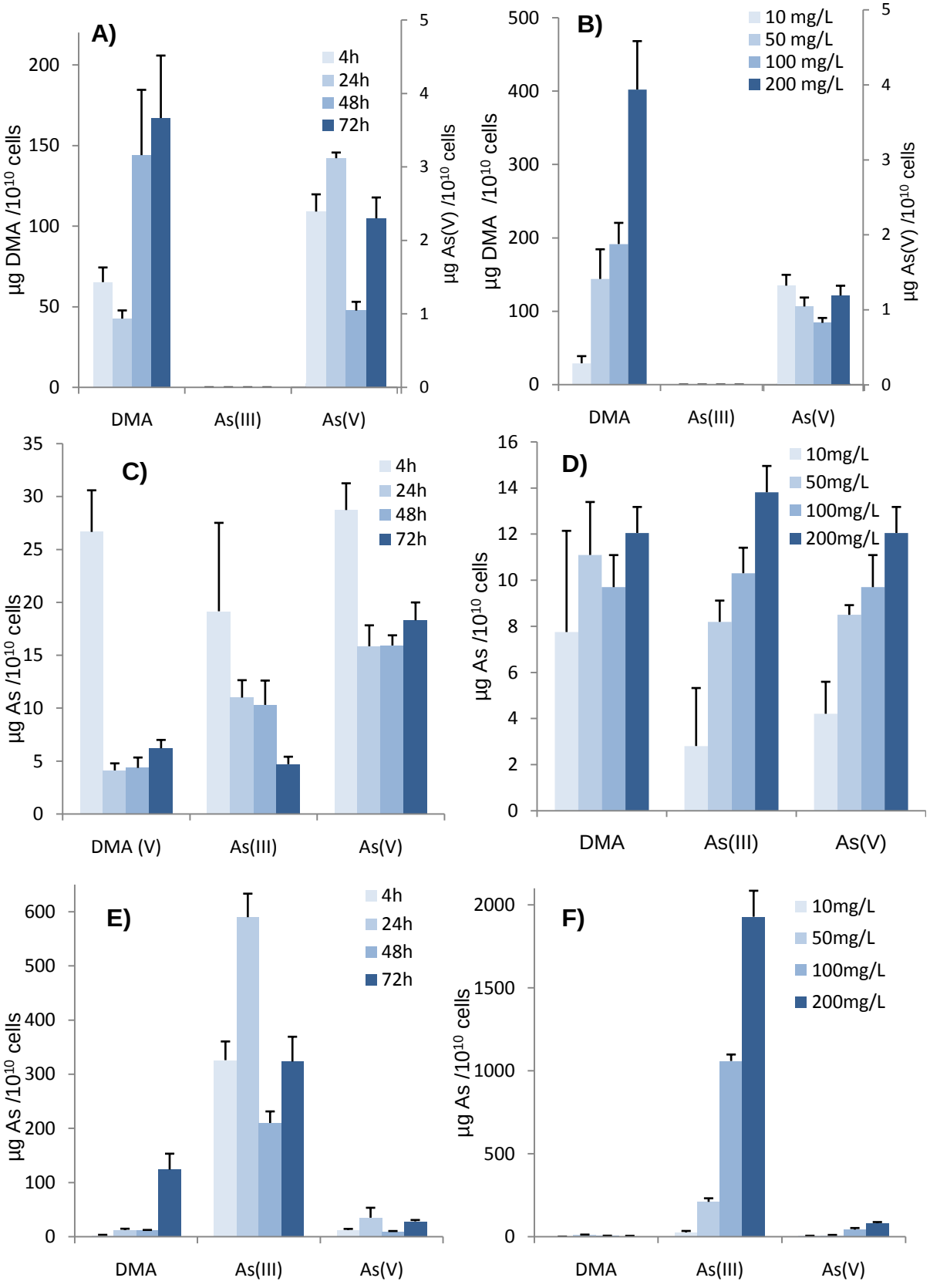

Fig 4. 32 Inorganic speciation of arsenic for cells exposed to 50 mg L^{-1} at different exposure times A) DMA, C) As(V) and E) As(III) and at different concentrations for 48 h of B) DMA, D) As(V) and F) As(III), n=3. Vertical bars denote 1 standard error

When cells were exposed to different concentrations of As(III) for 48 h and to 50 mg L^{-1} over different exposure times, As(III), DMA and As(V) were detected. This is shown in Fig 4.32E and 4.32F. Only trace amounts of As(V) and DMA were observed with the exemption for treatments with 50 mg L^{-1} for 72 h where 38% of DMA was found. Again, no free MMA was detected. On average 90% of the arsenic was still in As(III) form, and only 5% was oxidised or methylated to DMA.

4.3.2. GS/PC complexation

4.3.2.1. Focused sonication extraction for GS/PC complexes validation

Total extraction was performed to validate the specific (As-GS/PC) extraction proposed in this study. Cells of *C. vulgaris* exposed to arsenic and Kelp Powder were analysed for total arsenic.

The extraction method using focused sonication was able to achieve 94.7% and 71.1% recovery in Kelp powder and *C. vulgaris* cells respectively compared with acid microwave-assisted extraction. The results for comparisons can be observed in Fig 4.33.

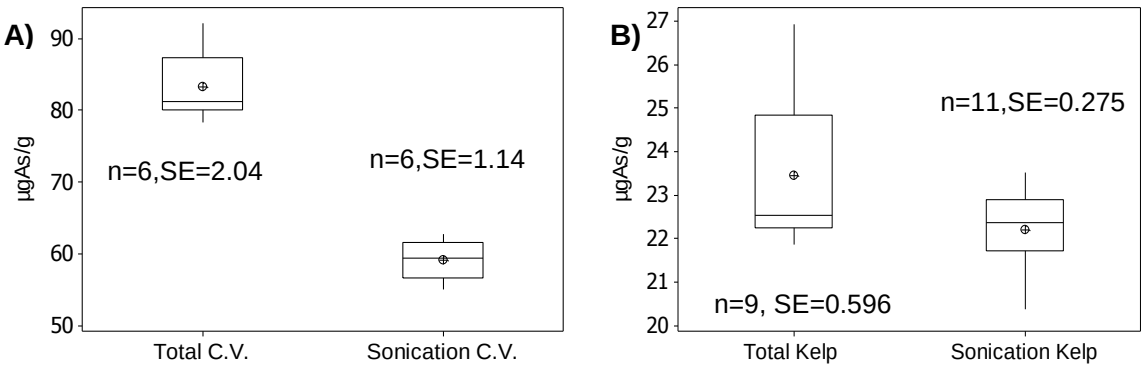

Fig 4. 33 Box plot (circles, mean value) for the comparison of total extraction (acid microwave-assisted digestion) and focused sonication (30 s, 500 W, 35 kHz) in *C. vulgaris* and commercially available Kelp powder.

An arsenic concentration of 48.06 µg L^{-1} with %RSD 2.16 was found in the certified material SRM2669 (certified value is 50.7 µg/L ± 6.3, 95% C.I.). This result indicates

that the method for total arsenic quantification used in this study is within the confidence range of the certified standard.

4.3.2.2. Qualitative analysis using online HPLC-ESI and HPLC-ICP-MS

a) Mass calculations and molecule identification

Qualitative analysis for identification of the eluting molecules was performed at the Trace Element Speciation Laboratory (TESLA) at the University of Aberdeen. Because the quantification experiments were made off-line, peak identification using on-line (ICP-MS and ESI-MS) analysis was essential to give accurate information in the quantification analysis.

Exposure of cells to As(V) resulted in signals for GSH, GSSG and oxidised PC_2 but no signals for As bound to GS/PC at any of the concentrations used (1-200 mg L^{-1}) or the exposure times (1, 4, 24, 48, 72 and 96 h) (section 4.3.2.3 Fig 4.41, 4.42 and 4.43).

Cells exposed to DMA formed one complex of arsenic bound to GSH. Only signals for GSH, reduced PC_2, oxidised PC_2 and $DMAS^V$-GS were observed. The ESI-MS and ICP-MS chromatograms are shown in Fig 4.34. Reduced PC_2 co-eluted with $DMAS^V$-GS and signals for S and As were observed, however the signal for arsenic can only come from $DMAS^V$-GS since PC_2 is not complexed with arsenic.

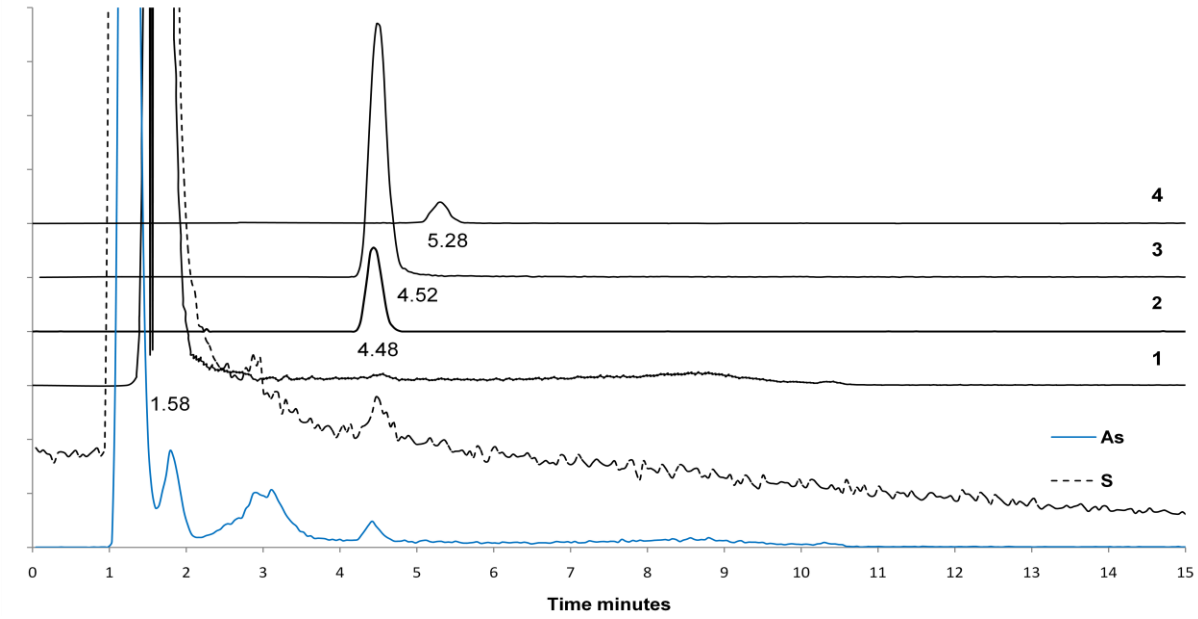

Fig 4. 34 GSH/PC and bound As-GS/PC, ESI-MS and HR-ICP-MS chromatograms of *C. vulgaris* cells exposed to 50 mg L^{-1} DMA for 48 h, extracted in 1% formic acid 30 s focused sonication. Peak identification (m/z) (scale): **1** GSH (308) (1), **2** $DMAS^{V}$-GS (444) (1), **3** Reduced PC_2 (540) (1) and **4** Oxidised PC_2 (538) (1), As and S signals from HR-ICP-MS

Table 4. 6 Molecule identification and mass difference for GS/PC complexes found in *C. vulgaris* cells exposed to 50 mg L^{-1} DMA, analysed using ESI-MS/MS (Orbitrap Discovery LTQ-XL)

Molecule	**Formula (M)**	**Monoisotopic mass ($M+H^+$)**	**Experimental mass**	**Difference ppm**
GSH	$C_{10}H_{17}N_3O_6S$	308.0916	308.0918	0.65
Red PC_2	$C_{18}H_{29}N_5O_{10}S_2$	540.1434	540.1433	-0.16
Ox PC_2	$C_{18}H_{28}N_5O_{10}S_2$	538.1278	538.1288	1.86
$DMAS^{V}$-GS	$C_{12}H_{23}N_3O_6S_2As$	444.0244	444.0247	0.56

The difference between the experimental and exact mass did not exceed 1.86 ppm for any of the molecules. These results can be observed in Table 4.6.

In sharp contrast, cells exposed to As(III) shown to form complexes of arsenic bound to GS/PC. Signals for GSH, GSSG, oxidised PC_2, reduced PC_2, oxidised PC_3, reduced PC_3, γ-(Glu-Cys), γ-(Glu-Cys)-Ala, γ-$(Glu-Cys)_2$, γ-$(Glu-Cys)_2$-Ala and γ-$(Glu-Cys)_3$-Ala as well as their respective arsenic bound complexes were observed.

Because of their complexity, the ESI-MS and ICP-MS chromatograms are shown in two separate graphs: unbound and bound peptides, Fig 4.35 and 4.36 respectively.

Two signals of unbound GSH/PC molecules co-eluted with bound As-GS/PC signals (Oxidised PC_3 / GS-As(III)-PC_2 [9.99 / 10.07 min] and γ-(Glu-Cys)$_3$-Ala/As(III)-PC_3 / MMA(III)-PC_2 [11.25 / 11.42 min], Fig 4.35 and 4.36).

Peaks for γ-(Glu-Cys)$_2$ and reduced PC_2 also co-eluted very close together at 4.80 and 4.65 min respectively (Fig 4.35).

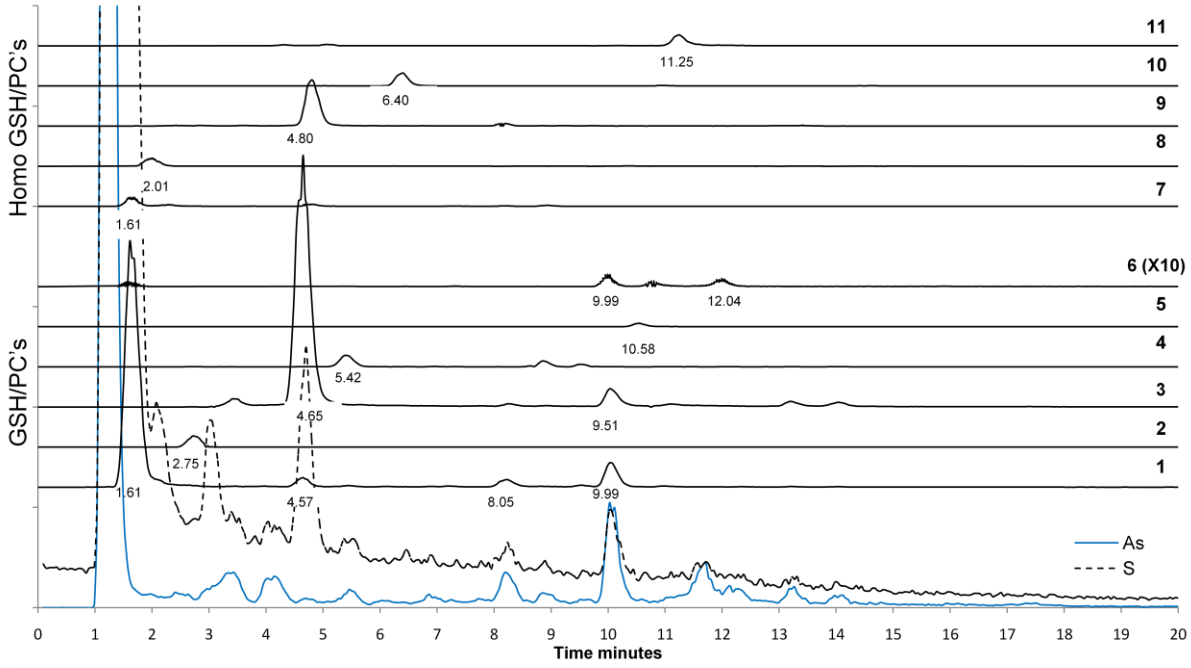

Fig 4. 35 ESI-MS (positive mode) and HR-CP-MS chromatograms of unbound GSH/PC and hGSH/PC of *C. vulgaris* cells exposed to 50 mg L^{-1} for 48 h, extracted in 1% formic acid 30 s focused sonication. Peak identification (m/z) (scale): **1** GSH (308), **2** GSSG (613) (1), **3** Reduced PC_2 (540)(1), **4** Oxidised PC_2(538)(1), **5** Reduced PC_3 (772)(1), **6** Oxidised PC_3 (770)(10), **7** γ-(Glu-Cys) (251)(1), **8** γ-(Glu-Cys)-Ala (322)(1), **9** γ-(Glu-Cys)$_2$ (483)(1), **10** γ-(Glu-Cys)$_2$-Ala (554)(1), **11** γ-(Glu-Cys)$_3$-Ala (715)(1), As and S signals from HR-ICP-MS

It was also noted that peaks for GS-As(III)-PC_2 (9.31 / 10.07 min), As(III)-(PC_2)$_2$ (13.23 / 14.12 min), As(III)-PC_4 (15.18 / 16.22 min), MMA(III)-PC_2 (11.42 / 12.17) and GS-As(III)-(Glu-Cys)$_2$ (8.14 / 8.89 min) showed two isomers, already reported (Simmons and Emery, 2011) eluting at different times.

The following bound complexes also showed elution at very similar retention times: GS-As(III)-PC_2 / GS-As(III)-(Glu-Cys)$_2$ (8.31 / 8.14 min), As(III)-PC_3 / MMA(III)-PC_2

(11.42 / 11.42 min), As(III)-PC_3 / As(III)-$(PC_2)_2$ (13.23 / 13.23 min) and As(III)-$(PC_2)_2$ / As(III)-$(Glu\text{-}Cys)_3$-Ala / As(III)-$((Glu\text{-}Cys)_2)_2$-Ala / MMA(III)-$(Glu\text{-}Cys)_2$-Ala (14.12 / 14.35 / 14.39 / 14.78 min). These facts increased the difficulty of the interpretation of the results.

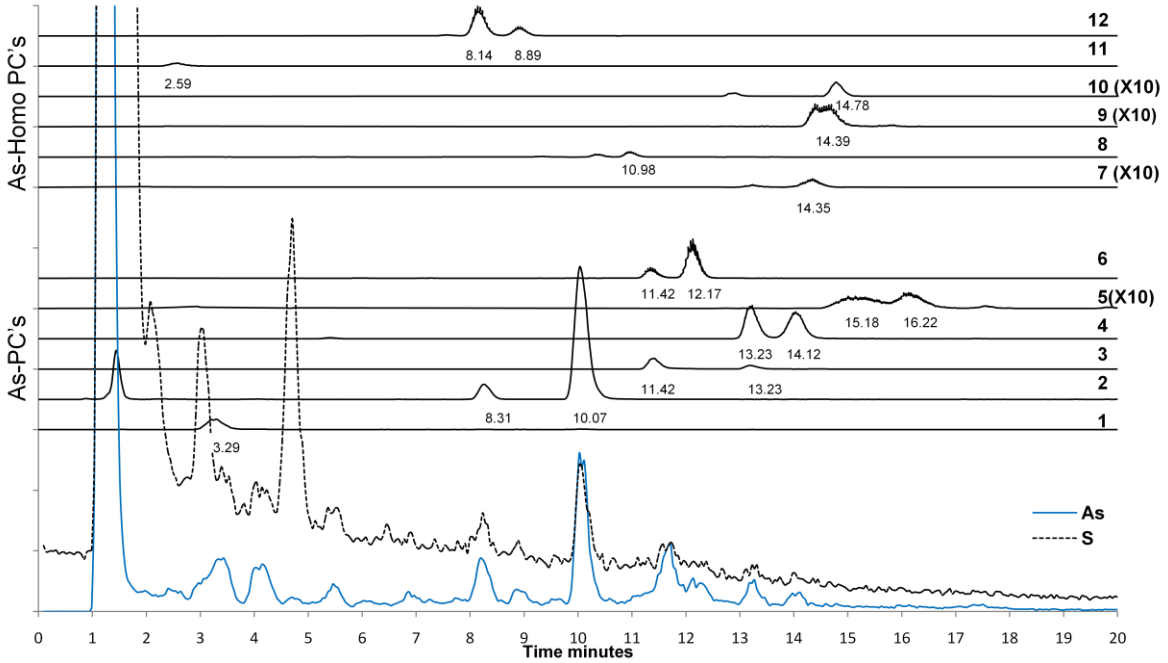

Fig 4. 36 ESI-MS (positive mode) and HR-CP-MS chromatograms of bound GS/PC and hGS/PC of *C. vulgaris* cells exposed to 50 mg L^{-1} for 48 h, extracted in 1% formic acid 30 s focused sonication. Peak identification (m/z) (scale): **1** As(III)-PC_2 (630), **2** GS-As(III)-PC_2 (460) (1), **3** As(III)-PC_3 (844)(1), **4** As(III)-$(PC_2)_2$ (576)(1), **5** As(III)-PC_4 (1076)(1), **6** MMA(III)-PC_2 (628)(1), **7** As(III)-$(Glu\text{-}Cys)_3$-Ala (858)(10), **8** GS-As(III)-$(Glu\text{-}Cys)_2$-Ala (467)(1), **9** As(III)-$((Glu\text{-}Cys)_2)_2$-Ala (583)(10), **10** MMA(III)-$(Glu\text{-}Cys)_2$-Ala (642)(10), **11** As(III)-$(Glu\text{-}Cys)_2$ (573)(1), **12** GS-As(III)-$(Glu\text{-}Cys)_2$ (431)(1), As and S signals from HR-ICP-MS.

The difference between the experimental and exact mass did not exceed 2.04 ppm for any of the As-GS/PC complexes and 2.20 for As-hGS/PC. These results can be observed in Table 4.7, along with their respective molecular formula.

The signals for GS-As(III)-PC_2 (m/z 460 and 919) MMA(III)-PC_2, As(III)-PC_3, As(III)-$(PC_2)_2$, As(III)-PC_4, $DMAS^V$-GS , γ-$(Glu\text{-}Cys)_2$-Ala (m/z 554), As(III)-$(Glu\text{-}Cys)_3$-Ala (m/z 858), As(III)-$((Glu\text{-}Cys)_2)_2$-Ala (m/z 583), MMA(III)-$(Glu\text{-}Cys)_2$-Ala (m/z 642), γ-$(Glu\text{-}Cys)_2$ (m/z 483) and GS-As(III)-$(Glu\text{-}Cys)_2$ (m/z 431) were strong enough to isolate and perform MS/MS analysis. The complete dissociation pathways are sown in Fig 1A4-13A4 and Table 1A4 (Appendix 4). The fragmentation pathways agree

with previously published data (Bluemlein, Raab and Feldmann, 2009; Bluemlein et al., 2008; Raab et al., 2007; Kanaki and Pergantis, 2008). However MS/MS information has not been previously reported for As(III)-(Glu-Cys)$_3$-Ala, As(III)-((Glu-Cys)$_2$)$_2$-Ala, MMA(III)-(Glu-Cys)$_2$-Ala and GS-As(III)-(Glu-Cys)$_2$.

Table 4. 7 Molecule identification and mass difference for GSH/PC, hGSH/PC and desGly complexes found in *C. vulgaris* cells exposed to 50 mg L^{-1} As(III), for 48 h analysed using ESI-MS/MS (Orbitrap Discovery LTQ-XL)

Molecule	Formula (M)	Monoisotopic mass ($M+H^+$ or $M+2H^+$)	Experimental mass	Difference ppm
GSH/PC				
GSH	$C_{10}H_{17}N_3O_6S$	308.0916	308.0912	-1.34
GSSG	$C_{20}H_{32}N_6O_{12}S_2$	613.1598	613.1598	0.00
Reduced PC_2	$C_{18}H_{29}N_5O_{10}S_2$	540.1434	540.1433	-0.16
Oxidised PC_2	$C_{18}H_{27}N_5O_{10}S_2$	538.1278	538.1289	2.04
Reduced PC_3	$C_{26}H_{41}N_7O_{14}S_3$	772.1952	772.1952	-0.01
Oxidised PC_3	$C_{26}H_{39}N_7O_{14}S_3$	770.1795	770.1795	0.00
Reduced PC_4	$C_{34}H_{53}N_9O_{18}S_4$	1004.2470	Not Found	
As(III)-PC_2	$C_{18}H_{28}N_5O_{11}S_2As$	630.0443	630.0437	-0.88
As(III)-PC_3	$C_{26}H_{38}N_7O_{14}S_3As$	844.0933	844.0931	-0.19
GS-As(III)-PC_2	$C_{28}H_{43}N_8O_{16}S_3As$	460.0666	460.0663	-0.06
		919.1253	919.1247	-0.69
As(III)-$(PC_2)_2$	$C_{36}H_{54}N_{10}O_{20}S_4As$	576.0925	576.0923	-0.37
As(III)-PC_4	$C_{34}H_{50}N_9O_{18}S_4As$	1076.1451	1076.1455	0.37
MMA(III)-PC_2	$C_{19}H_{30}N_5O_{10}S_2As$	628.0728	628.0729	0.12
hGSH/PC				
γ-(Glu-Cys)-Ala	$C_{11}H_{19}N_3O_6S$	322.1073	322.1072	-0.21
γ-(Glu-Cys)$_2$-Ala	$C_{19}H_{31}N_5O_{10}S_2$	554.1591	554.1578	-2.20
As(III)-γ-(Glu-Cys)$_3$-Ala	$C_{27}H_{40}N_7O_{14}S_3As$	858.1090	858.1082	-0.87
GS-As(III)-γ-(Glu-Cys)$_2$-Ala	$C_{29}H_{45}N_8O_{16}S_3As$	467.0744	467.0744	0.09
As(III)-γ-((Glu-Cys)$_2$)$_2$-Ala	$C_{37}H_{57}N_{10}O_{20}S_4As$	583.1003	583.1010	1.19
MMA(III)-γ-(Glu-Cys)$_2$-Ala	$C_{20}H_{32}N_5O_{10}S_2As$	642.0885	642.0889	0.66
desGly-GSH/PC				
γ-(Glu-Cys)	$C_8H_{14}N_2O_5S$	251.0702	251.0706	1.55
γ-(Glu-Cys)$_2$	$C_{16}H_{26}N_4O_9S_2$	483.1219	483.1217	-0.58
γ-(Glu-Cys)$_3$	$C_{24}H_{38}N_6O_{13}S_3$	715.1737	715.1747	1.41
As(III)-γ-(Glu-Cys)$_2$	$C_{16}H_{25}N_4O_{10}S_2As$	573.0306	573.0318	2.11
GS-As(III)-γ-(Glu-Cys)$_2$	$C_{26}H_{40}N_7O_{15}S_3As$	431.5558	431.5558	-0.17

b) Elemental peak identification (ICP-MS)

High resolution signals for arsenic, sulphur as well as exact molecular masses and structural information from the MS/MS analyses allowed the unequivocal identification of the eluting molecules for quantification purposes using low resolution ICP-MS (simple quadruple with O_2 as collision cell gas).

Low resolution HPLC-ICP-MS was used under the same conditions employed in the online analysis with the exemption in flow rate (from 0.9 to 0.2mL min^{-1}) and injection (from 75µL to 50µL) as well as the different monitored signals for arsenic at m/z 91 and for sulphur at m/z 48 (this are necessary using O_2 as collision cell gas CCT). The results for this experiment are shown in Fig 4.37.

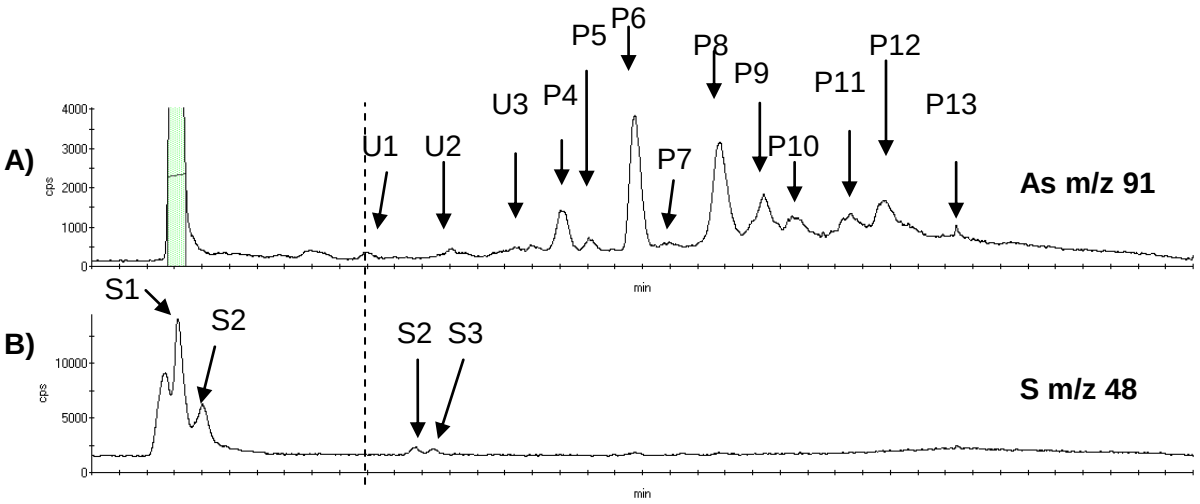

Fig 4. 37 Chromatogram of *C. vulgaris* cells exposed to 50 mg L^{-1} As(III) for 48 h, extracted in 1% formic acid 30 s focused sonication. A) signal for arsenic at m/z 91 B) signal for sulphur at m/z 48. Peak identification: **U1-3** Unknowns, **P4** GS-As(III)-PC_2 / GS-As(III)-γ-$(Glu\text{-}Cys)_2$, **P5** As(III)-γ-$(Glu\text{-}Cys)_2$, **P6** GS-As(III)-PC_2, **P7** GS-As(III)-γ-$(Glu\text{-}Cys)_2$-Ala, **P8** As(III)-PC_3 / MMA(III)-PC_2, **P9** MMA(III)-PC_2, **P10** As(III)-PC_3 / As(III)-$(PC_2)_2$, **P11** As(III)-$(PC_2)_2$ / As(III)-γ-$(Glu\text{-}Cys)_3$-Ala / As(III)-γ-$((Glu\text{-}Cys)_2)_2$-Ala / MMA(III)-γ-$(Glu\text{-}Cys)_2$-Ala, **P12** As(III)-PC_4 and **P13** As(III)-PC_4.

As mentioned before, some of the molecules showed peaks at two different retention times, these correspond to iso-forms of the different peptides. Also there was co-elution of different molecules at the same retention time. However all the arsenic signals observed after 10 min correspond to As-GS/PC related complexes and were subject to quantification.

Fig 4.37A shows the peak identification for arsenic signal at m/z 91: U1-3 Unknowns, P4 GS-As(III)-PC_2 / GS-As(III)-γ-$(Glu\text{-}Cys)_2$, P5 As(III)-γ-$(Glu\text{-}Cys)_2$, P6 GS-As(III)-PC_2, P7 GS-As(III)-γ-$(Glu\text{-}Cys)_2$-Ala, P8 As(III)-PC_3 / MMA(III)-PC_2, P9 MMA(III)-PC_2, P10 As(III)-PC_3 / As(III)-$(PC_2)_2$, P11 As(III)-$(PC_2)_2$ / As(III)-γ-$(Glu\text{-}Cys)_3$-Ala / As(III)-γ-$((Glu\text{-}Cys)_2)_2$-Ala / MMA(III)-γ-$(Glu\text{-}Cys)_2$-Ala, P12 As(III)-PC_4 and P13 As(III)-PC_4.

Fig 4.37B shows the signal for sulphur at m/z 48. Peaks S1, S2, S3 and S4 were confirmed to be GSH, GSSG, reduced PC_2 and oxidised PC_2 by injection of the corresponding standards.

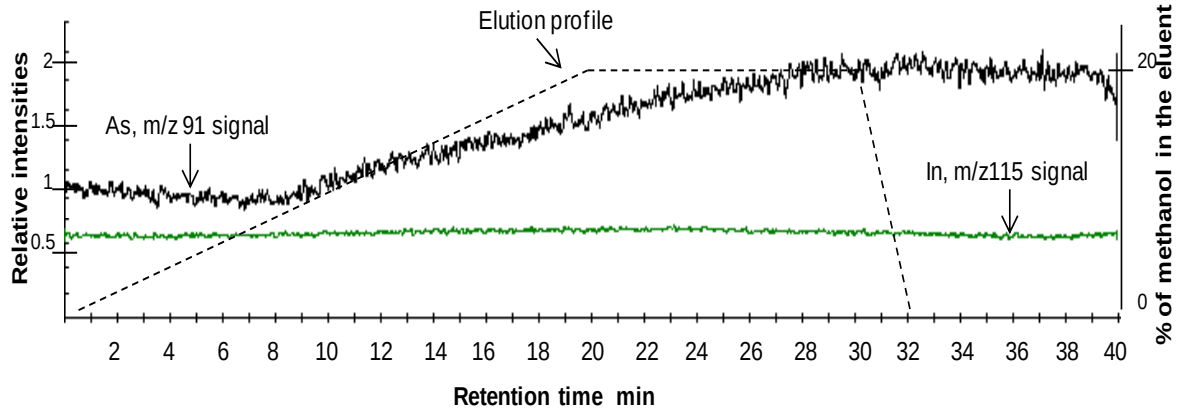

Fig 4. 38 Methanol correction effect; a blank was injected using the same chromatographic conditions with a post column addition of a solution containing 100 µg L^{-1} DMA and 20 µg L^{-1} In (as internal standard).

Before quantification could be made, a consideration for the effect of methanol in the mobile phase using ICP-MS had to be made. The approach chosen here was by injecting a blank using the same chromatographic conditions with a post column addition of a solution containing 100 µg L^{-1} DMA and 20 µg L^{-1} In (as internal standard). It can be observed from Fig 4.38 that there is a delay from the moment the addition of methanol is started and the increase in arsenic response, this delay was about 8 min long.

The response for arsenic increased twice given an increase of 20% methanol in the mobile phase. The signal for indium and sulphur did not change due to the increase in methanol, as expected (Fig 4.38). All signals considered for this study eluted after

10 min and until 32 min. Thus a modification factor was applied for all peaks as follows: U1(0.95), U2(0.83), U3(0.74), P4(0.71), P5(0.69), P6(0.66), P7(0.63), P8(0.61), P9(0.57), P10(0.56), P11(0.53), P12(0.51) and P13(0.50).

Extraction recovery from the Discovery C_{18} (15x2.1 mm) column and supelguard pre-column Discovery C_{18} was measured giving 94.27% (SE = 0.12, n = 4) and 98.24% (SE = 1.52, n = 4) for arsenic and sulphur respectively.

4.3.2.3. Comparison of extraction methods: grinding in liquid nitrogen and focused sonication

Focused sonication extraction was compared with extraction by grinding using liquid nitrogen for cells exposed to 50 mg L^{-1} of As(III). Chromatograms of the two samples are shown in Fig 4.39. The chromatograms showed that for the same sample there was comparable arsenic signal intensity in the complex eluting at 10 min for the two extraction procedures. However, the integrity of some of the peaks eluting after 12 min (arsenic signal) appears to have been compromised by grinding in liquid nitrogen. There is also a much stronger sulphur signal for the sonication extraction for the peak eluting at 4.65 min (this corresponds to reduced PC_2).

The quantitative results for the comparison are shown in Fig 4.40. The results show that there is comparable total complex extraction. However, individual peak stability was favoured for peaks 5, 11, 12 and 13 for samples extracted using focused sonication, whereas integrity was better for peaks 4, 6, 8, 9 and 10 for the conventional extraction method.

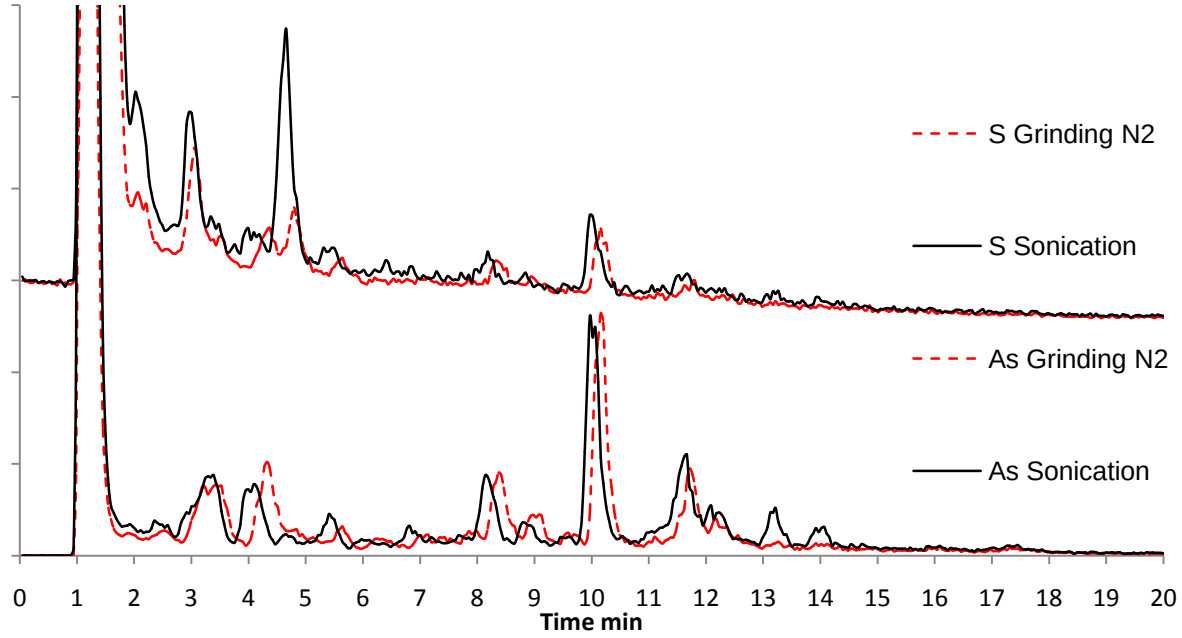

Fig 4. 39 ESI-MS and HR-ICP-MS chromatograms of *C. vulgaris* cells exposed to 50 mg L^{-1} As(III) for 48 h, extracted in 1% formic acid with 30 s focused sonication or grinding with liquid nitrogen, As and S signals from HR-ICP-MS

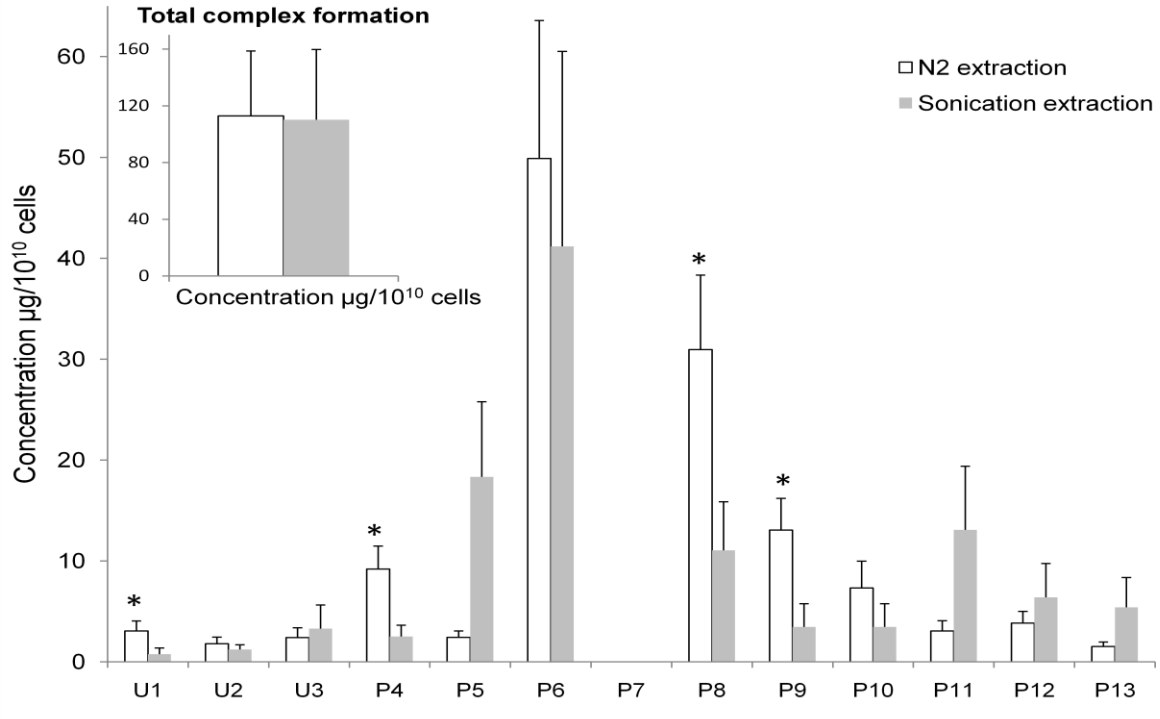

Fig 4. 40 Comparative arsenic speciation analysis, extraction by grinding with N_2 and focused sonication (30 s, 500 W, 35 kHz) in *C. vulgaris* cells exposed to 50 mg L^{-1}As(III) for 48 h, inset total complex formation, vertical bars indicate +1 SE, n = 5, * denotes statistical difference (two-sample t-test, p <= 0.05),

4.3.2.4. Quantitative analysis, kinetics and concentration effect experiments

a) As(V)

Exposure of cells to As(V) resulted in signals for GSH, GSSG, oxidised PC_2 but no signals for As bound to GS/PC at any of the concentrations used (1-200 mg L^{-1}) or the exposure times (1, 4, 24, 48, 72 and 96 h).

The chromatograms for experiments using 50 mg L^{-1} of As(V) exposed to different periods of time can be seen in Fig 4.41. None of the treatments produced peaks for arsenic signal after 10 min.

The chromatograms for experiments using different As(V) exposure concentrations can be seen in Fig 4.42. Again, none of the treatments produced peaks for arsenic signal after 10 min which indicates arsenic bound to sulphur in an organic molecule.

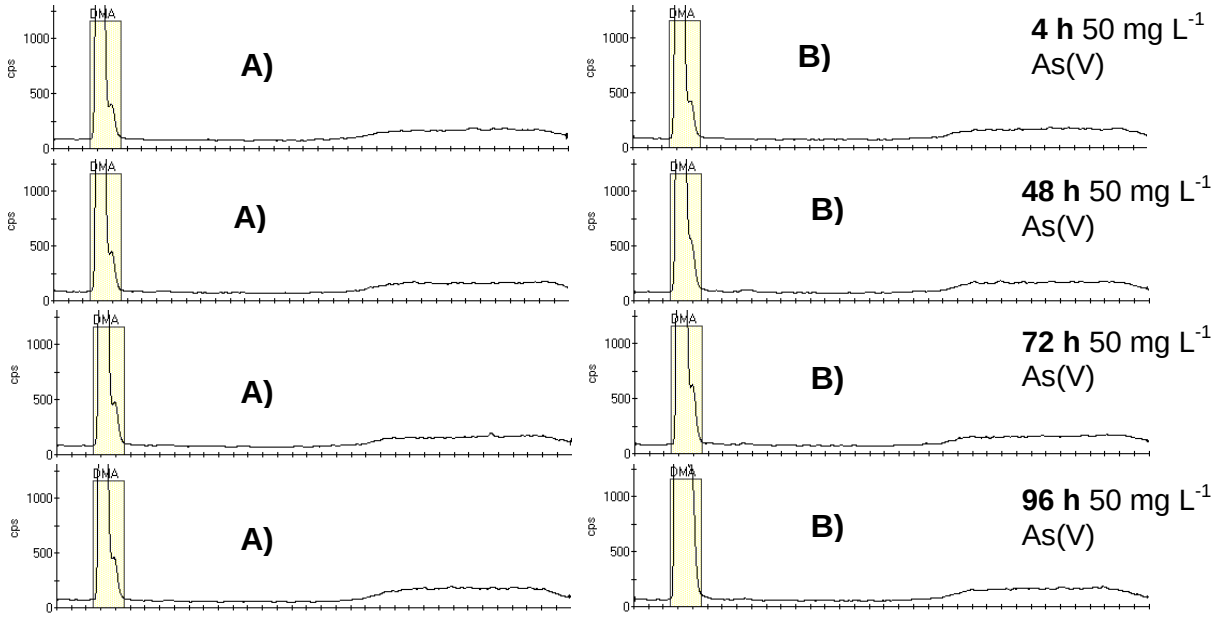

Fig 4. 41 *C. vulgaris* cells exposed to 50 mg L^{-1} of As(V) for 4, 48, 72 and 96 h, analysed by HPLC-ICP-MS, two replicates (A and B)

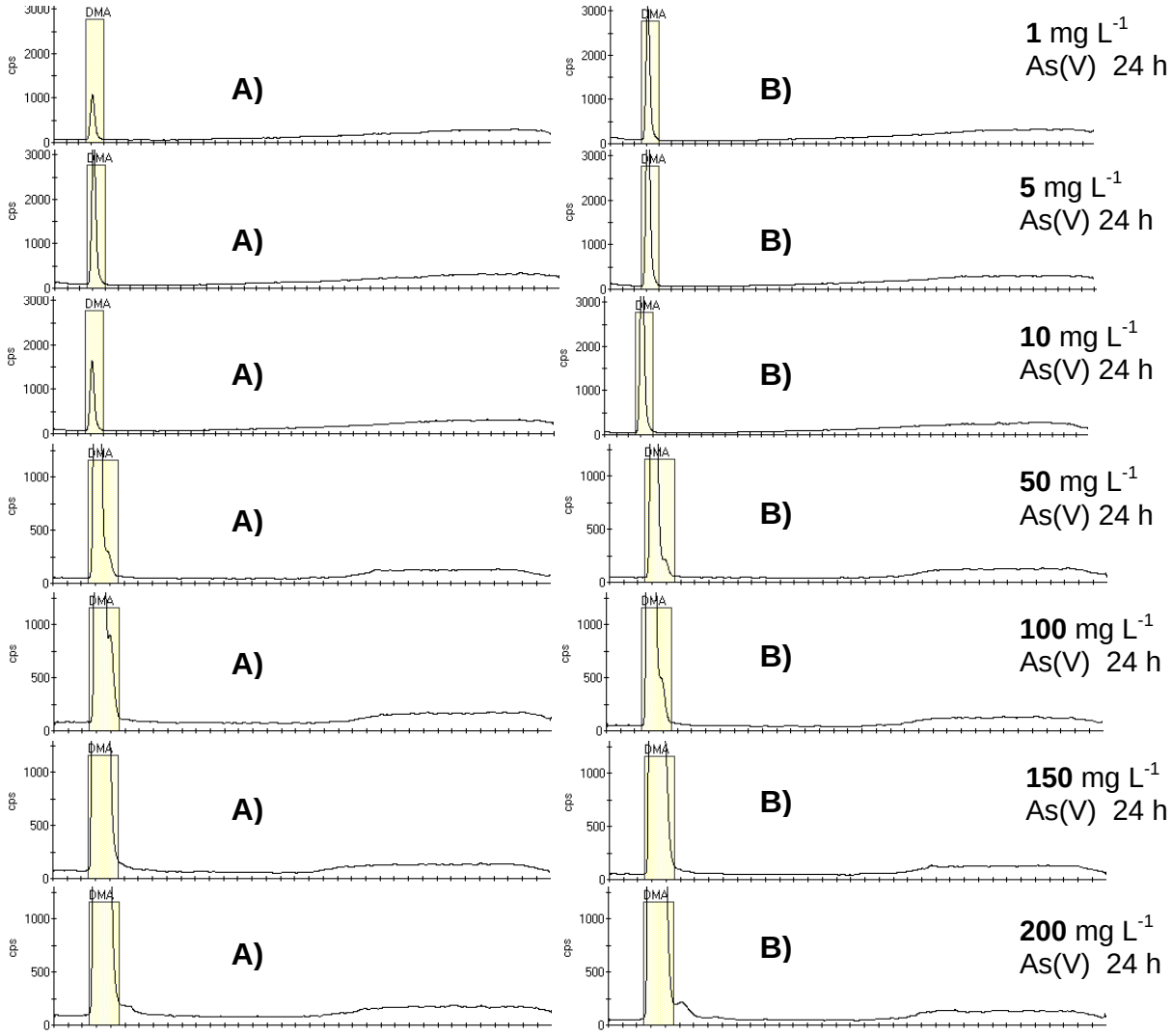

Fig 4. 42 *C. vulgaris* cells exposed to 1, 5, 10, 50, 100, 150 and 200 mg L^{-1} of As(V) for 24 h, analysed by HPLC-ICP-MS, two replicates (A and B)

Fig 4.43 shows the results for the quantification of sulphur in experiments using different As(V) exposure concentrations and exposure periods. The signals for GSH and GSSG were strong enough to allow quantification of sulphur using ICP-MS at m/z 48 (O_2, CCT). The bars indicate the concentration of unbound GSH (bottom) and GSSG (top). Percentages indicate the ratio of GSH/(GSH+GSG). The MQL for this experiment was 20.20 µg L^{-1} (SE = 2.28, n = 13).

Insufficient evidence for a difference was found in the levels of GSH for the different exposure times or exposure concentrations (ANOVA-GLM, $p > 0.05$, n=3) (Fig 4.43, Table 4.8).

There was very strong statistical evidence for a difference (Fig 4.43A, Table 4.8) in the level of GSSG for the first 4 hours after exposure to 50 mg L^{-1} of As(V). However there seemed to be a recovery in the level of GSSG after 24 h and was continued up to 48 h. This new level was not statistically different from the levels observed in the control experiments.

A moderate positive correlation was found for an increase in the level of total GSH (GSH+GSSG) with respect to treatment time (simple linear least squares, R^2 = 0.562, n = 3) and a weak positive correlation with respect to the concentration of arsenic in the media (simple linear least squares, R^2 = 0.144, n = 3).

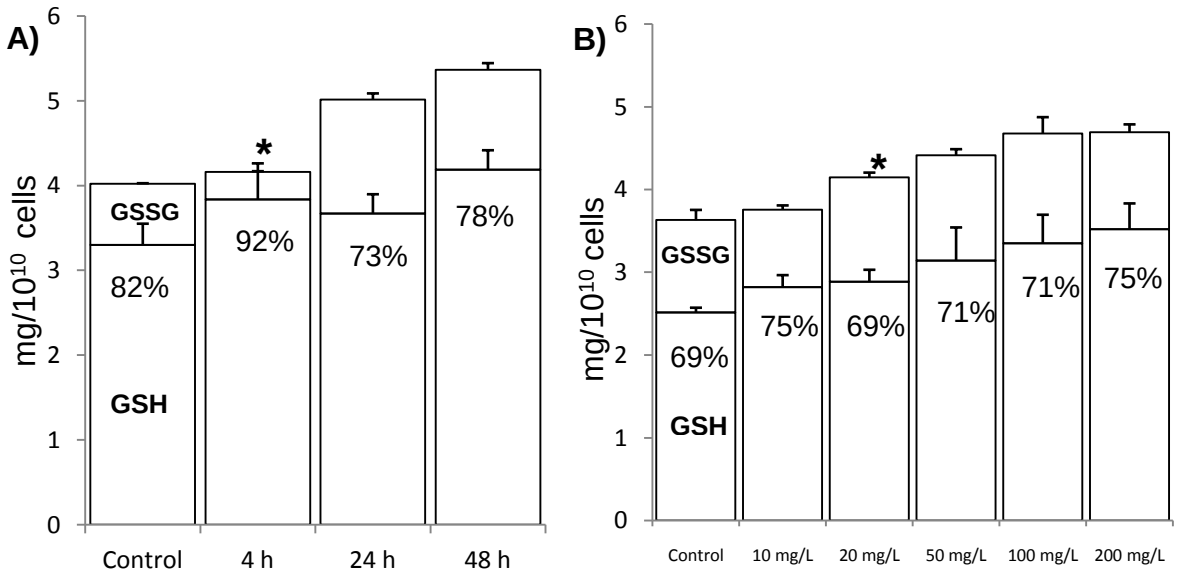

Fig 4. 43 Concentration of GSH (bottom bars) and GSSG (top bars) for *C. vulgaris* exposed to A) 50 mg L^{-1} of As(V) at different exposure times and B) different concentrations for 48 h. Analysed by HPLC-ICP-MS (O_2, CCT) m/z 48. Percentages indicate the ratio of GSH/(GSH+GSG). * denotes statistical difference using ANOVA-GLM (p <= 0.05). Vertical bars denote + 1 standard error, n = 3

Table 4. 8 ANOVA General Linear Model (GLM) for univariate analysis of variance, analysis of covariance, and regression, for each response variable (Tukey-Kramer). For analysis of GSH and GSSG in *C. vulgaris* cells exposed to As(V) at different concentrations and periods of time, analysed by HPLC-ICP-MS

GSH

	Control	4 h	24 h
4 h	NS		
24 h	NS	NS	
48 h	NS	NS	NS

GSSG

	Control	4 h	24 h
4 h	0.0084		
24 h	NS	0.0013	
48 h	NS	0.0004	NS

NS: Not significant,
$p > 0.05$

GSH

	Control	10 mg L^{-1}	20 mg L^{-1}	50 mg L^{-1}	100 mg L^{-1}
10 mg L^{-1}	NS				
20 mg L^{-1}	NS	NS			
50 mg L^{-1}	NS	NS	NS		
100 mg L^{-1}	NS	NS	NS	NS	
200 mg L^{-1}	NS	NS	NS	NS	NS

GSSG

	Control	10 mg L^{-1}	20 mg L^{-1}	50 mg L^{-1}	100 mg L^{-1}
10 mg L^{-1}	NS				
20 mg L^{-1}	NS	NS			
50 mg L^{-1}	NS	NS	NS		
100 mg L^{-1}	NS	NS	0.0121	NS	
200 mg L^{-1}	0.0172	NS	0.0041	NS	NS

b) As(III)

The results for the quantification of sulphur in experiments with cells exposed to 50 mg L^{-1} of As(III) for different periods of time (1, 4, 24, 48 and 72h) can be seen in Fig 4.44A. The results for cells exposed for 48 h to As(III) at different concentrations (10, 20, 50, 100 and 200 mg L^{-1}) can be seen in Fig 4.44B.

Insufficient evidence for a difference was found in the levels of reduced GSH due to exposure time (Fig 4.44A and Table 4.9). There was, however, strong statistical evidence for a reduction in the level of oxidised glutathione with time compared to the controls as well as in the ratio of GSH/(GSH+GSG) (Fig 4.44A and Table 4.9).

Insufficient evidence was found for a difference in the concentration of reduced GSH with an increase of As(III) concentration in the media (Fig 4.44B and Table 4.9) with the exemption of the levels of GSH and GSSG in the treatments exposed to 100 mg L^{-1} compared to treatments with 200 mg L^{-1} As(III) (Fig 4.44B and Table 4.9).

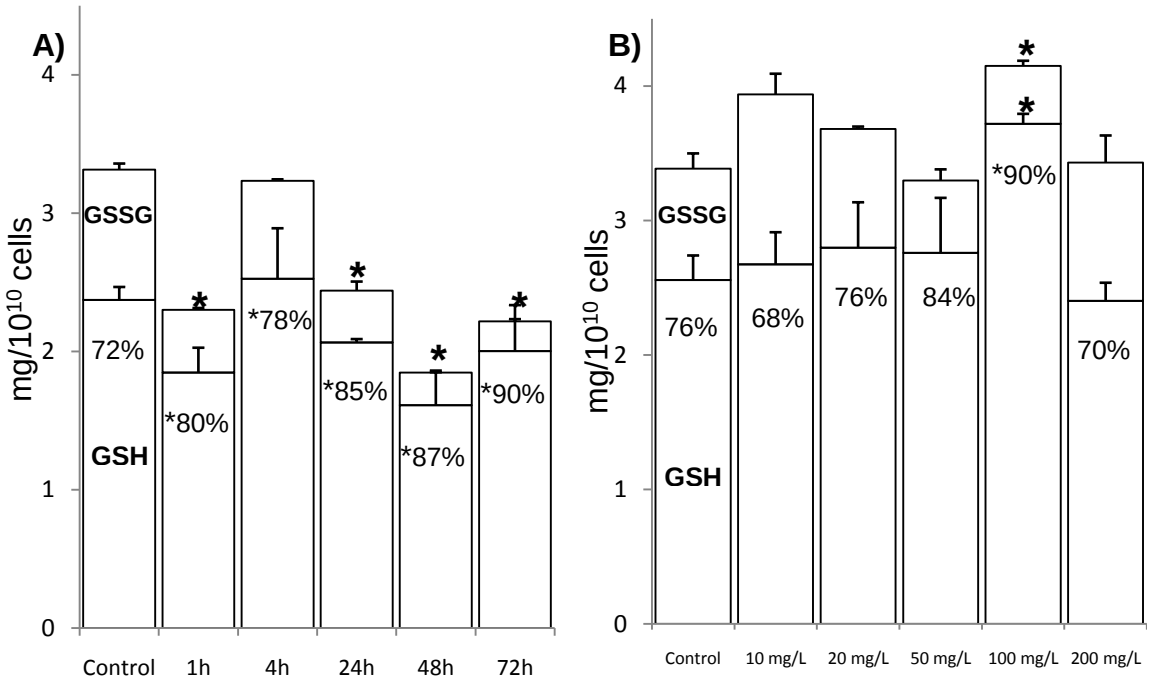

Fig 4. 44 Concentration of GSH (bottom bars) and GSSG (top bars) for *C. vulgaris* exposed to A) 50 mg L^{-1} of As(III) at different exposure times and B) different concentrations for 48 h. Analysed by HPLC-ICP-MS (O_2, CCT) m/z 48. Percentages indicate the ratio of GSH/(GSH+GSG). * denotes statistical difference using ANOVA-GLM ($p <= 0.05$). Vertical bars denote + 1 standard error, n = 3

Table 4. 9 ANOVA General Linear Model (GLM) for univariate analysis of variance, analysis of covariance, and regression, for each response variable (Tukey-Kramer). For analysis of GSH and GSSG in *C. vulgaris* cells exposed to As(III) at different concentrations and periods of time, analysed by HPLC-ICP-MS.

GSH

	Control	1h	4h	24h	48h
1h	NS				
4h	NS	NS			
24h	NS	NS	NS		
48h	NS	NS	NS	NS	
72h	NS	NS	NS	NS	NS

GSSG

	Control	1h	4h	24h	48h
1h	0.0126				
4h	NS	NS			
24h	0.0047	NS	NS		
48h	0.0013	NS	0.0446	NS	
72h	0.0017	NS	NS	NS	NS

GSH

	Control	10 mg L^{-1}	20 mg L^{-1}	50 mg L^{-1}	100 mg L^{-1}
10 mg L^{-1}	NS				
20 mg L^{-1}	NS	NS			
50 mg L^{-1}	NS	NS	NS		
100 mg L^{-1}	NS	NS	NS	NS	
200 mg L^{-1}	NS	NS	NS	NS	0.0319

GSSG

	Control	10 mg L^{-1}	20 mg L^{-1}	50 mg L^{-1}	100 mg L^{-1}
10 mg L^{-1}	NS				
20 mg L^{-1}	NS	NS			
50 mg L^{-1}	NS	0.0104	NS		
100 mg L^{-1}	NS	0.0037	NS	NS	
200 mg L^{-1}	NS	NS	NS	NS	0.0373

NS: Not significant, $p > 0.05$

Cells exposed to As(III) shown to form complexes of arsenic bound to GS/PC (Section 4.3.2.2). The results for the quantification of bound As-GS/PC complexes for experiments with cells exposed to 50 mg L^{-1} of As(III) for different periods of time analysed using ICP-MS at m/z 91 (O_2, CCT) are shown in Fig 4.45. The MQL for this experiment were 0.5516 μgL^{-1} (SE = 0.067, n = 10).

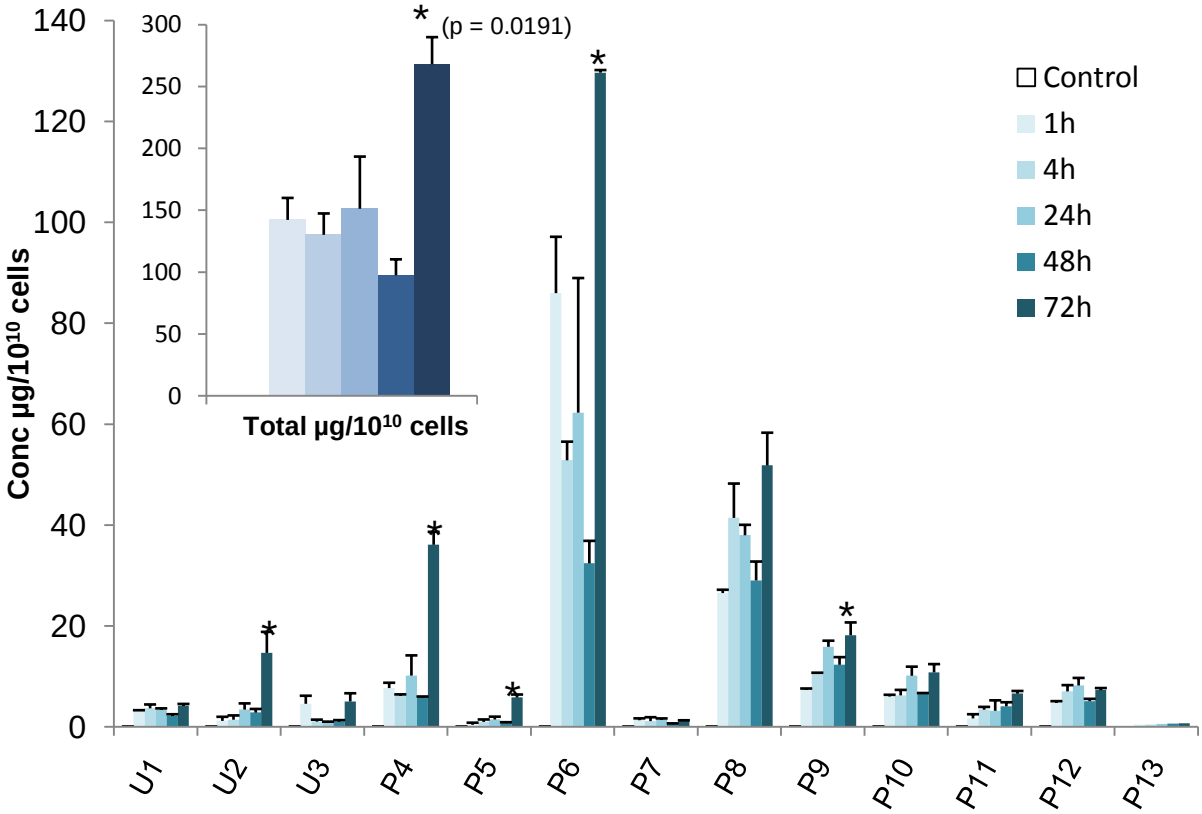

Fig 4. 45 Concentration of As-GS/PC complexes for *C. vulgaris* exposed to 50 mg L^{-1} of As(III) for different periods of time, analysed by HPLC-ICP-MS (O_2, CCT) m/z 91. * denotes statistical difference using ANOVA- GLM ($p <= 0.05$). Vertical bars denote +1 standard error. Peak identification: **U1-3** Unknowns, **P4** GS-As(III)-PC_2/GS-As(III)-γ-$(Glu\text{-}Cys)_2$, **P5** As(III)-γ-$(Glu\text{-}Cys)_2$, **P6** GS-As(III)-PC_2, **P7** GS-As(III)-γ-$(Glu\text{-}Cys)_2$-Ala, **P8** As(III)-PC_3/ MMA(III)-PC_2, **P9** MMA(III)-PC_2, **P10** As(III)-PC_3/ As(III)-$(PC_2)_2$, **P11** As(III)-$(PC_2)_2$/ As(III)-γ-$(Glu\text{-}Cys)_3$-Ala/ As(III)-γ-$((Glu\text{-}Cys)_2)_2$-Ala/ MMA(III)-γ-$(Glu\text{-}Cys)_2$-Ala, **P12** As(III)-PC_4 and **P13** As(III)-PC_4.

Some statistical evidence was found (Fig 4.45 and Table 4.10) for an increase in the amount of As-GS/PC complexes with time.

It can be observed from Table 4.10 that the increase in bound As-GS/PC complexes was statistically significant only after 72 h of treatment for the following peaks: U2, P4, P5, P6 and P9. It should also be noted that controls did not produce any arsenic peaks therefore were not compared.

Table 4. 10 ANOVA General Linear Model (GLM) for univariate analysis of variance, analysis of covariance, and regression, for each response variable (Tukey-Kramer). For concentration of As-GS/PC complexes for *C. vulgaris* exposed to different concentrations of As(III) for 48 h analysed by HPLC-ICP-MS.

U2

	1h	4h	24h	48h
4h	NS			
24h	NS	NS		
48h	NS	NS	NS	
72h	0.0274	0.0294	NS	0.0455

P6

	1h	4h	24h	48h
4h	NS			
24h	NS	NS		
48h	NS	NS	NS	
72h	NS	0.0453	NS	0.0177

P4

	1h	4h	24h	48h
4h	NS			
24h	NS	NS		
48h	NS	NS	NS	
72h	0.0014	0.0011	0.0021	0.001

P9

	1h	4h	24h	48h
4h	NS			
24h	0.0434	NS		
48h	NS	NS	NS	
72h	0.0165	NS	NS	NS

P5

	1h	4h	24h	48h
4h	NS			
24h	NS	NS		
48h	NS	NS	NS	
72h	NS	0.0069	0.0101	0.0063

NS: Not significant, $p > 0.05$

Fig 4.46 shows the results for the quantification of bound As-GS/PC complexes for experiments using different exposure concentrations of As(III).

Strong statistical evidence was found (Fig 4.46 and Table 4.11) for an increase in the formation of the As-GS/PC complexes with an increase in As(III) concentration in the media.

It should be noted that the concentration of unbound GSH/GSSG is in mg of arsenic per 10^{10} $cells^{-1}$ and the concentration for the As-GS/PC complexes is in µg of arsenic per 10^{10} $cells^{-1}$.

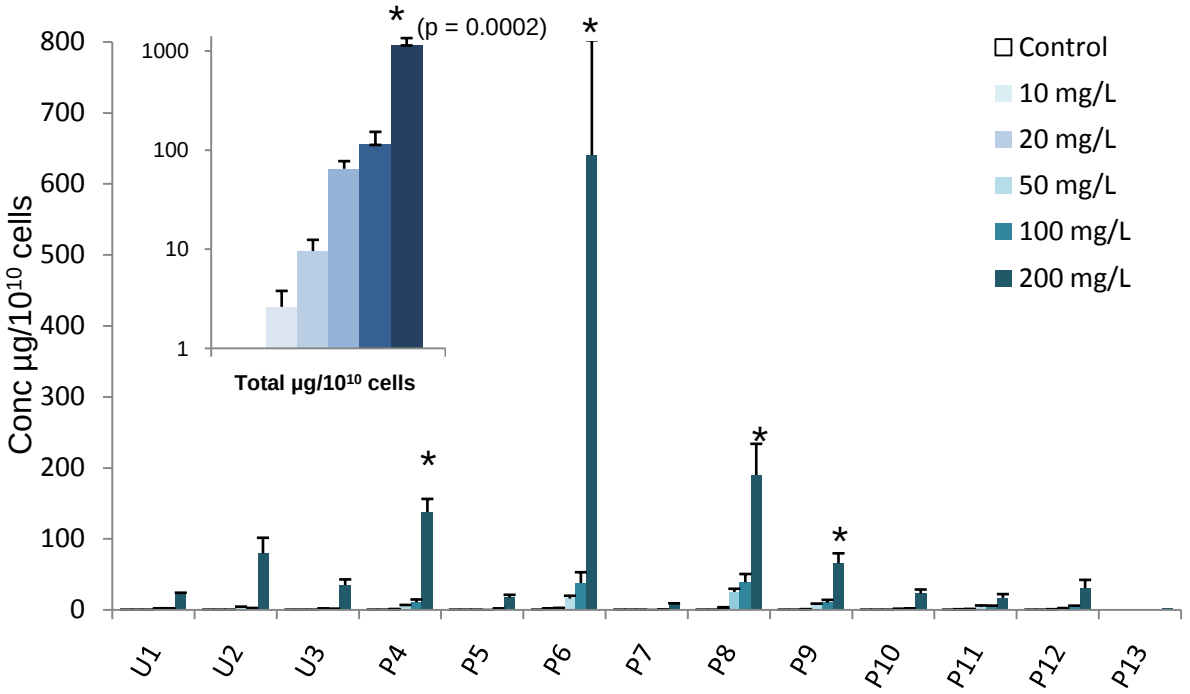

Fig 4. 46 Concentration of As-GS/PC complexes in *C. vulgaris* cells exposed to different concentrations of As(III) for 48 h, (inset, total As-GS/PC concentration), analysed by HPLC-ICP-MS (O_2, CCT) m/z 91. * denotes statistical difference using ANOVA-GLM ($p <= 0.05$). Vertical bars denote +1 standard error. Peak identification: **U1-3** Unknowns, **P4** GS-As(III)-PC_2/GS-As(III)-γ-$(Glu\text{-}Cys)_2$, **P5** As(III)-γ-$(Glu\text{-}Cys)_2$, **P6** GS-As(III)-PC_2, **P7** GS-As(III)-γ-$(Glu\text{-}Cys)_2$-Ala, **P8** As(III)-PC_3/ MMA(III)-PC_2, **P9** MMA(III)-PC_2, **P10** As(III)-PC_3/ As(III)-$(PC_2)_2$, **P11** As(III)-$(PC_2)_2$/ As(III)-γ-$(Glu\text{-}Cys)_3$-Ala/ As(III)-γ-$((Glu\text{-}Cys)_2)_2$-Ala/ MMA(III)-γ-$(Glu\text{-}Cys)_2$-Ala, **P12** As(III)-PC_4 and **P13** As(III)-PC_4.

Table 4. 11 ANOVA General Linear Model (GLM) for univariate analysis of variance, analysis of covariance, and regression, for each response variable (Tukey-Kramer). For concentration of As-GS/PC complexes in *C. vulgaris* cells exposed to different concentrations of As(III) for 48 h analysed by HPLC-ICP-MS, n = 3.

P4

	10	20	50	100
20	NS			
50	NS	NS		
100	NS	NS	NS	
200	0.0045	0.0046	NS	0.0082

P8

	10	20	50	100
20	NS			
50	NS	NS		
100	NS	NS	NS	
200	0.0086	0.0085	0.0242	0.0463

P6

	10	20	50	100
20	NS			
50	NS	NS		
100	NS	NS	NS	
200	0.0165	0.0167	0.0193	0.0244

P9

	10	20	50	100
20	NS			
50	NS	NS		
100	NS	NS	NS	
200	0.0008	0.0018	0.0022	0.0037

NS: Not significant, $p > 0.05$

c) DMA

The results for the quantification of sulphur in experiments with cells exposed to 50 mg L^{-1} of DMA for different periods of time (4, 24, 48 and 72 h) can be seen in Fig 4.47A. The results for cells exposed for 48 h to DMA at different concentrations (10, 50, 100 and 200 mg L^{-1}) can be seen in Fig 4.47B.

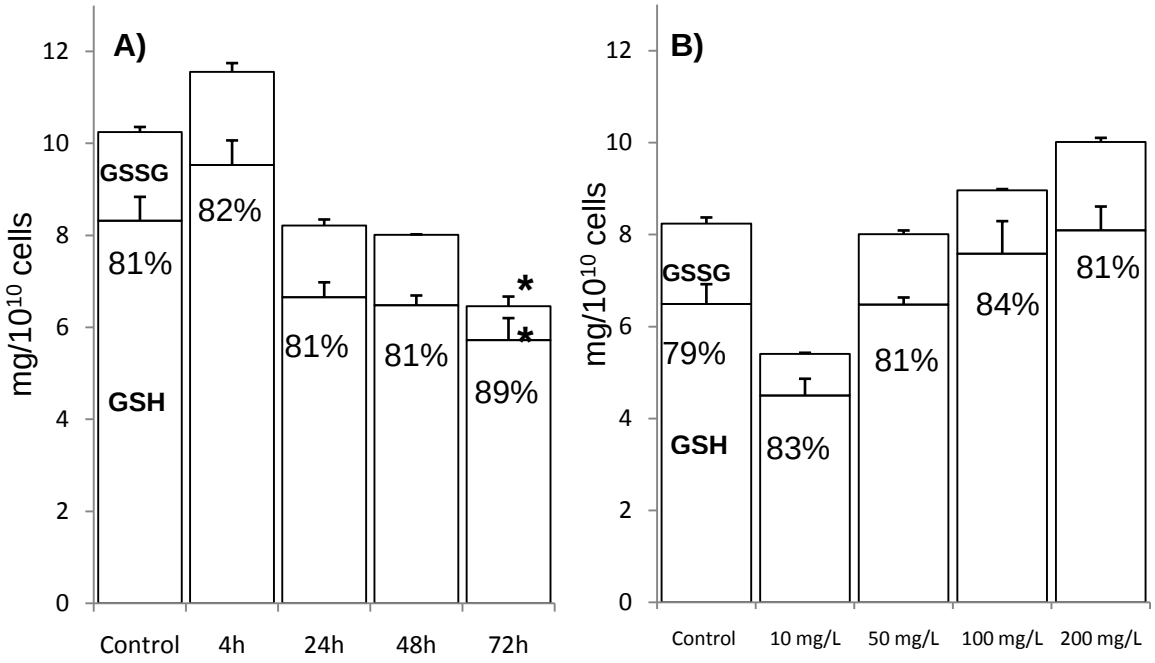

Fig 4. 47 Concentration of GSH (bottom bars) and GSSG (top bars) for *C. vulgaris* exposed to A) 50 mg L^{-1} of DMA at different exposure times and B) different concentrations for 48 h. Analysed by HPLC-ICP-MS (O_2, CCT) m/z 48. * denotes statistical difference using ANOVA-GLM ($p <= 0.05$). Percentages indicate the ratio of GSH/(GSH+GSG). Vertical bars denote + 1 standard error, n = 3

Insufficient evidence for a statistical difference was found in the level of GSH, GSSG or the GSH/(GSH+GSG) ratio at any of the exposure concentrations or exposure periods with exemption of treatment for 72 h compared to the control experiments as shown in Fig 4.47 and Table 4.12.

Table 4. 12 ANOVA General Linear Model (GLM) for univariate analysis of variance, analysis of covariance, and regression, for each response variable (Tukey-Kramer). For concentration of As-GS/PC complexes in *C. vulgaris* cells exposed to 50 mg L^{-1} of DMA at different exposure times analysed by HPLC-ICP-MS, n = 3

GSH

	control	4h	24h	48h
4h	NS			
24h	NS	0.0044		
48h	NS	0.0029	NS	
72h	0.0089	0.0005	NS	NS

Ratio GSH/(GSH+GSG)

	control	4h	24h	48h
4h	NS			
24h	NS	NS		
48h	NS	NS	NS	
72h	NS	NS	0.036	NS

GSSG

	control	4h	24h	48h
4h	NS			
24h	NS	NS		
48h	NS	0.0309	NS	
72h	0.0048	0.0015	NS	NS

NS: Not significant, p > 0.05

Cells exposed to DMA shown to form only one complex of arsenic bound to GSH (Section 4.3.2.2). Results for these experiments are shown in Fig 4.48 and 4.49 along with the total amount of intracellular arsenic in the cells.

Total amount of As-GS/PC complexes formed upon exposure of As(III) and DMA was compared with the total amount of arsenic inside *C. vulgaris* cells. Total arsenic and total As-GS/PC complex formation were calculated in independent experiments. The effect of exposure time is shown in Fig 4.48. Cells exposed to As(III) were able to complex up to 73 % of the arsenic inside the cells. In contrast cells exposed to DMA were only able to form As-GS complexes after 48h and only accounted for up to 3.1% of the total arsenic inside the cells.

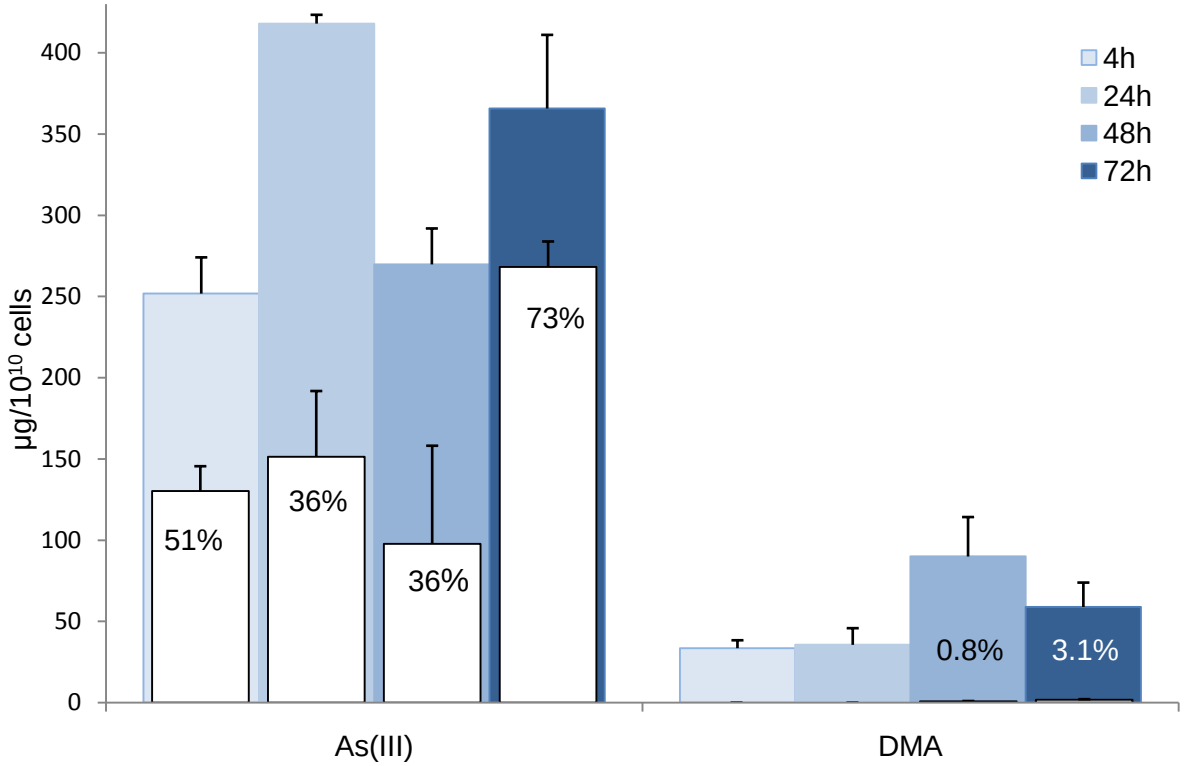

Fig 4. 48 Kinetic studies for the formation of As-GS/PC complexes in *C. vulgaris* cells exposed to 50 mg L^{-1} As(III) and DMA for different periods of time; coloured bars denote total amount of arsenic, white bars denote the amount of As-GS/PC complexes inside the cells, the amount of As-GS/PC is expressed in percentage of the total arsenic inside cells. Vertical bars denote + 1 standard error, n = 3

Results for cells exposed for 48 h to different concentrations of As(III) and DMA can be seen in Fig 4.49. Cells exposed to As(III) were able to form complexes of more than 50% of the arsenic inside the cells when exposed to 200 mg L^{-1}. Total accumulation of arsenic (absorbed) increased with an increase in concentration of arsenic in the media.

The formation As-GS by cells exposed to DMA was observed only after exposure to 50 mg L^{-1} and continued without change on exposure to 100 and 200 mg L^{-1}. The As-GS complex accounted for up to 0.8% of the total arsenic inside the cells. Accumulation of total arsenic inside the cells (absorbed) also was found to increase when the concentration of the metalloid in the media was increased.

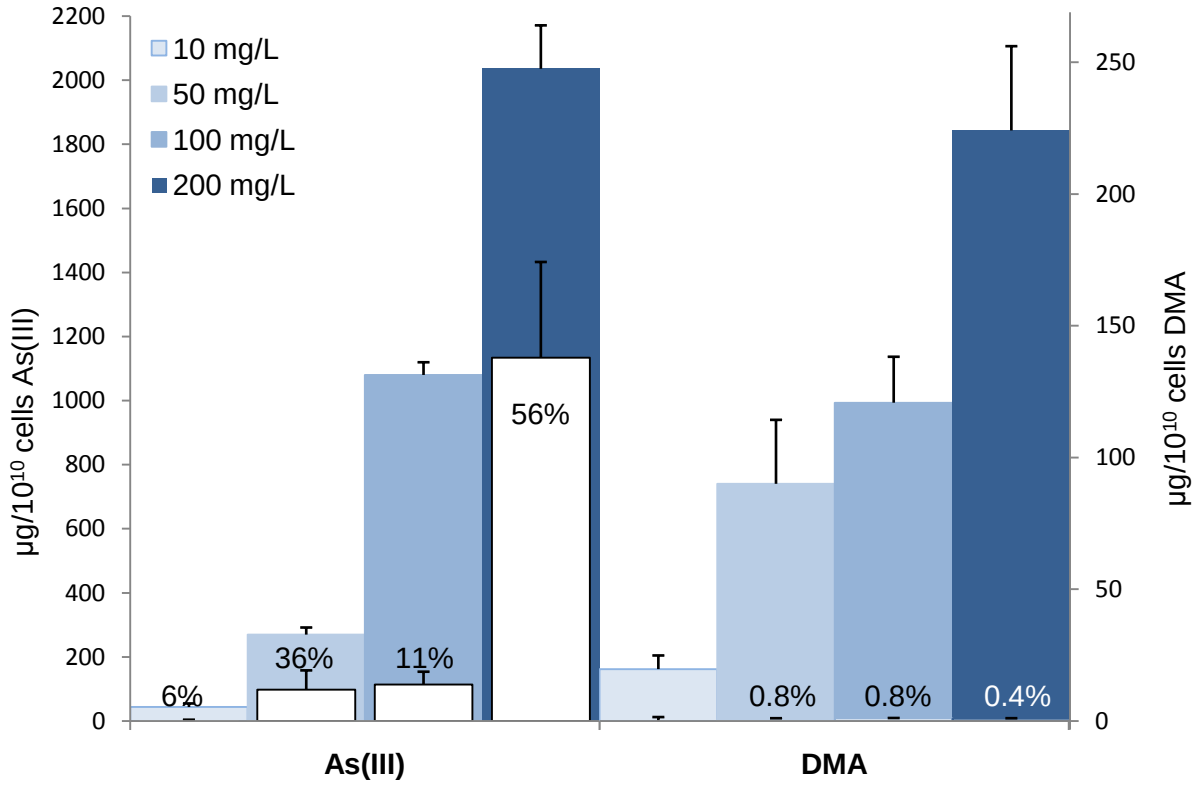

Fig 4. 49 Concentration effect for *C. vulgaris* cells exposed for 48 h to different concentrations of As(III), As(V) and DMA; coloured bars denote total amount of arsenic, white bars denote the amount of As-GS/PC complexes inside the cells; the amount of As-GS/PC is express in percentage of the total arsenic inside cells. Vertical bars denote +1 standard error, n = 3

4.3.2.5. Vacuole compartmentalisation

For the investigation of As-GS/PC vacuole transport mediated by ABCC/MRP proteins, probenecid, sodium taurocholate and MK571 were used as they are specific inhibitors of such transport. Toxicity experiments were performed in the presence / absence of As(III) and with / without inhibitors. The results for this experiment can be seen in Fig 4.50.

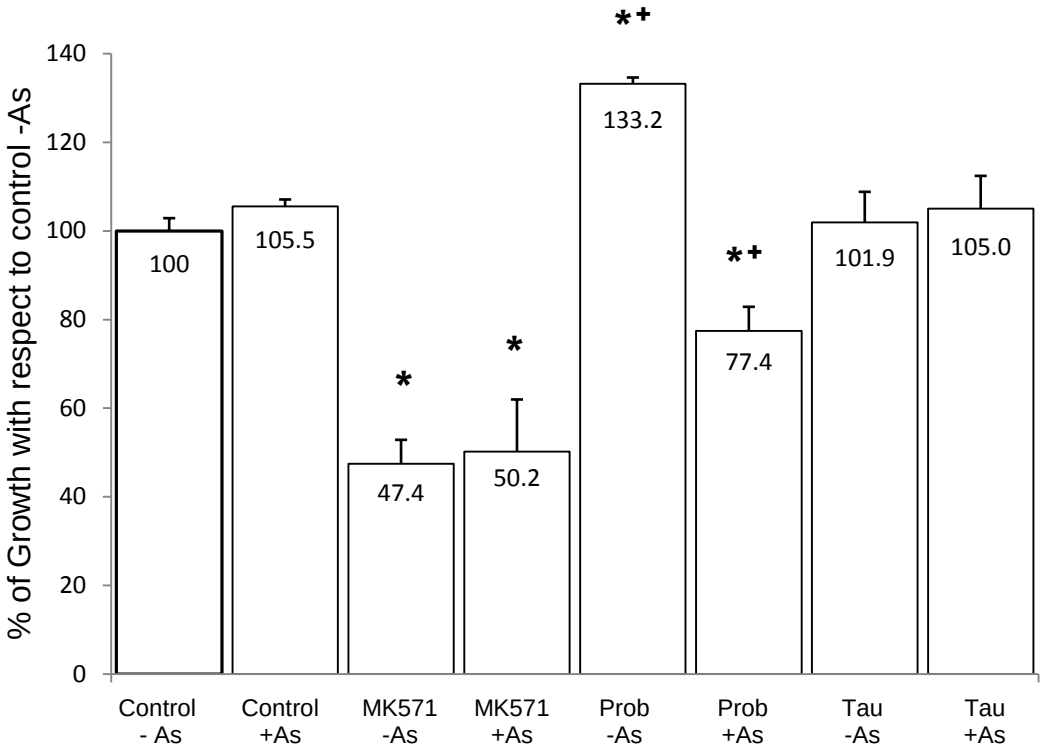

Fig 4. 50 Toxicity to As(III) (50mg L^{-1}, 72 h test, n = 3) in the presence / absence of the ABCC1/2 inhibitors: MK571 (25 μM), probenecid (500 μM) and sodium taurocholate (50 μM). * denotes statistical difference (p <= 0.05) using two-sample t-test with respect to the control. + denotes statistical difference with respect to the absence/presence of arsenic for the same inhibitor. Vertical bars denote + 1 standard error

Growth of cells was not affected by the addition of 50 mg L^{-1} of As(III) at the conditions of maximal algae growth (high concentration of phosphate and 0.05% w/v glucose). The inhibitor MK571 reduced growth to 47% (two-sample t-test, p <= 0.001, n = 3) with respect to control cells in the absence of arsenic and to 50% (p = 0.015) in arsenic's presence. However, insufficient evidence for a difference in growth was found between the treatments (absence/presence of arsenic) (p > 0.05). The inhibitor probenecid alone increased cell growth to 33% (p <= 0.001) and in the presence of arsenic decreased growth significantly to 77% (p = 0.021) of the control. Interestingly, there was a significant difference (p <= 0.001) between the treatments (absence/presence of arsenic) which may be considered as a result of the inhibition of As-GS/PC transport to vacuoles and therefore increasing arsenic toxicity to cells. Finally the drug sodium taurocholate did not have any significant effect (p > 0.05) in cell growth either in the presence or absence of arsenic.

The effects of the inhibitor probenecid alone were further investigated. Toxicity of *C. vulgaris* cells at different concentrations of probenecid (50, 150, 300, 450 and 600 µM) was investigated. Results for this experiment can be observed in Fig 4.51.

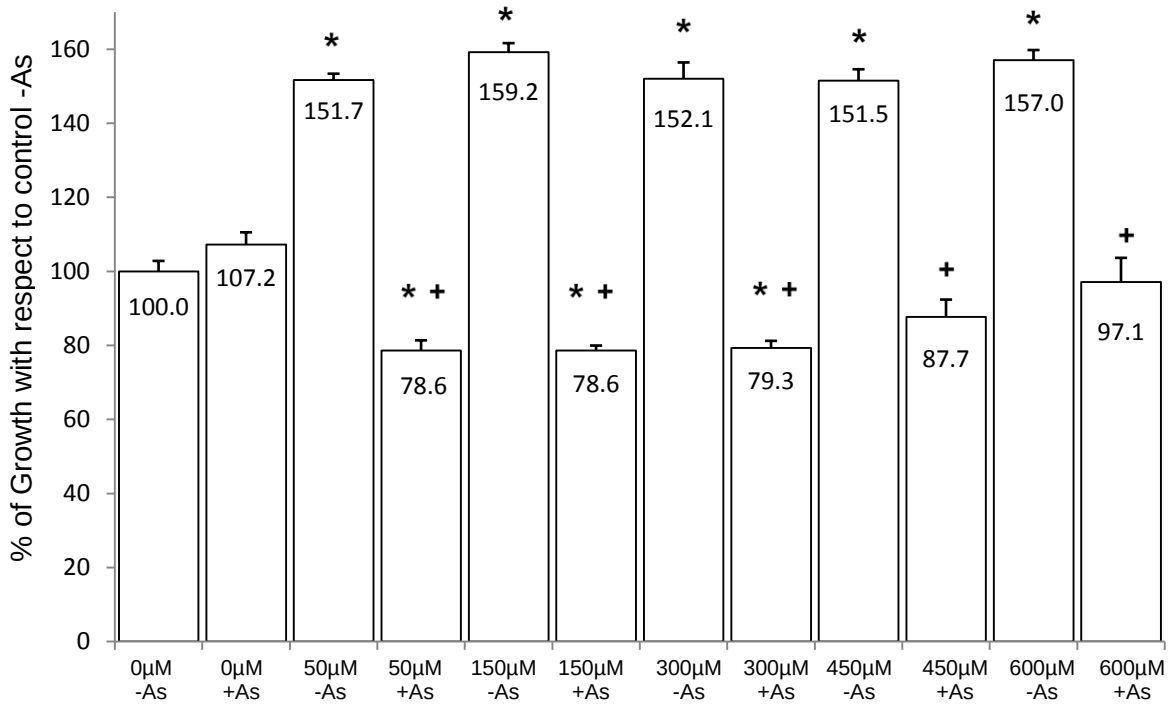

Fig 4. 51 Toxicity to As(III) (50 mg L^{-1}, 72 h test, n = 3) in the presence and absence of the ABCC1 / 2 inhibitor probenecid (50, 150, 300, 450 and 600 µM) * denotes statistical difference ($p <= 0.05$) using two-sample t-test with respect to the control. + denotes statistical difference with respect to the absence / presence of arsenic in the same test. Vertical bars denote + 1 standard error

Again, it was found that cells grew slightly more in the presence of 50 mg L^{-1} As(III) than control cells but the difference was not significant ($p > 0.05$). Cells grew significantly more (52-59%) in presence of the inhibitor alone [no As(III)] ($p <= 0.002$). In contrast cells growing in the presence of both the inhibitor and As(III) show a significant decrease in growth with respect to the control for treatments with 50, 150 and 300 µM probenecid ($p <= 0.001$) (no probenecid and no As(III)) and with respect to the inhibitor without As(III) for all treatments ($p <= 0.01$). This decrease in growth ranged between 60 to 81% with respect to the control (no arsenic with inhibitor). There was no evidence that inhibition of growth in the presence of As(III) was dependent on the concentration of probenecid at the chosen range (50 - 600 µM).

ABCC/MRP vacuole transport was further investigated by using fluorescent substrates, measured using flow cytometry. All fluorescent signals were excited with 488 nm laser. Chlorophyll fluorescence was measured at emission 670 nm (FL3) and was used to gate healthy viable cells, the same gated population was then used to measure changes in fluorescence at excitation 530 ± 15 nm (FL1) and 585 ± 20 nm (FL2). This is shown in Fig 4.52; Fig 4.52A shows dot plot diagrams for the population R-1 corresponding to high chlorophyll fluorescence (FL3 red dots) and BCECF stained cells (FL1 and FL2, Fig 4.52B and 4.52C), Fig 4.52D-E show dot plot diagrams for the same populations for CMDFA stained cells.

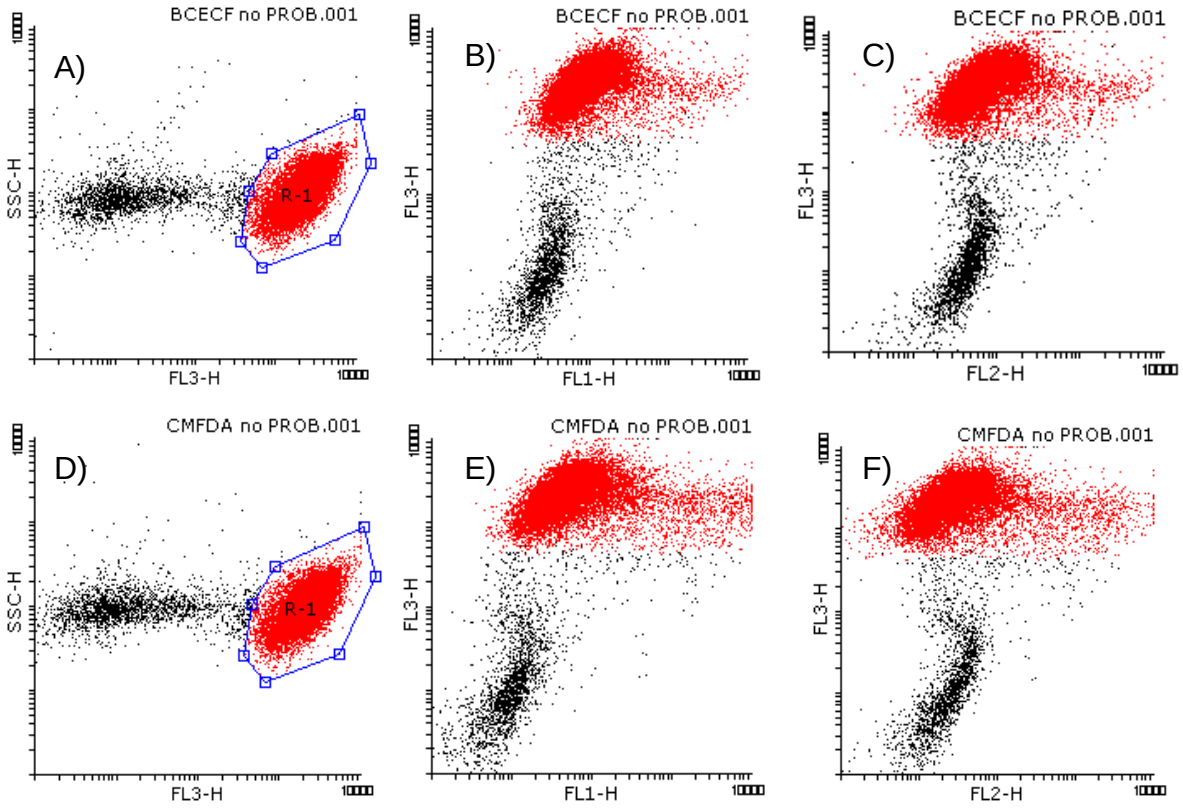

Fig 4. 52 Flow cytometry dot plots showing *C. vulgaris* cells stained with ABCC/MRP fluorescent substrates. Positive control cells (no inhibitor): A) BCECF, FL3, B) BCECF, FL1, C) BCECF, FL2, D) CMFDA, FL3, E) CMFDA, FL1, F) CMFDA, FL2; chlorophyll (FL3 488 nm excitation, 670 nm emission) was used to gate healthy viable cells (R-1), which was then used in FL1 (488 nm excitation, 530 ±15 nm emission) and FL2 (488 nm excitation, 585 ± 20 nm emission) fluorescent levels. Treatment time 60 min, n = 20,000.

a) Flow cytometry, probenecid effect

As mentioned in section 4.1.2, D-values are the focus of interpretation of distribution differences. Therefore D-values obtained from Kolmogorov-Smirnov statistics, were categorised in the following way: Strong (D > 0.30), moderate (0.20 < D <= 0.30), weak (0.15 < D <= 0.20) and negligible (D <= 0.15) difference (Lebedeva, Pande and Patton, 2011). Kolmogorov-Smirnov statistics obtained in this way are shown in Table 4.13. Sample size n = 20,000 was used for all the experiments.

When negative control cells (heat-killed) were stained with BCECF, the fluorescent intensity was higher than that of probenecid treated cells and non-treated cells for the two different channels FL1 (D = 0.20) and FL2, (D = 0.38) (Fig 4.53A and 4.53B). When negative control cells were stained with CMFDA, the fluorescent intensity was lower than that of probenecid treated cells and non-treated cells (D = 0.74) (Fig 4.53E).

Cells treated with probenecid showed weaker fluorescence intensity than non-treated cells when stained with BCECF for the two different channels FL1 (D = 0.18) and FL2 (D = 0.16) (Fig 4.53A and 4.53B). In contrast, a negligible difference was found when cells were treated with CMFDA (D = 0.08) (Fig 4.53E).

Because BCECF shows a pH dependent spectral shift, greater fluorescence intensity may indicate that cells with probenecid have a higher internal pH than non-treated cells. Another possibility, one that has been consistently reported e.g. Barley aleurone vacuoles and *A. thaliana* (Jiang et al., 2011; Forestier et al., 2003), is that the dye was effectively transported by non-treated cells via ABCC/MRP transport. In such case, the effect could be effectively reversed by treatment with probenecid which is reflected in an increase of fluorescence intensity. However, ABCC/MRP transport would not explain the increase in fluorescent signal for negative control cells (heat killed) that have no active transport systems (Fig 4.53A and 4.53B).

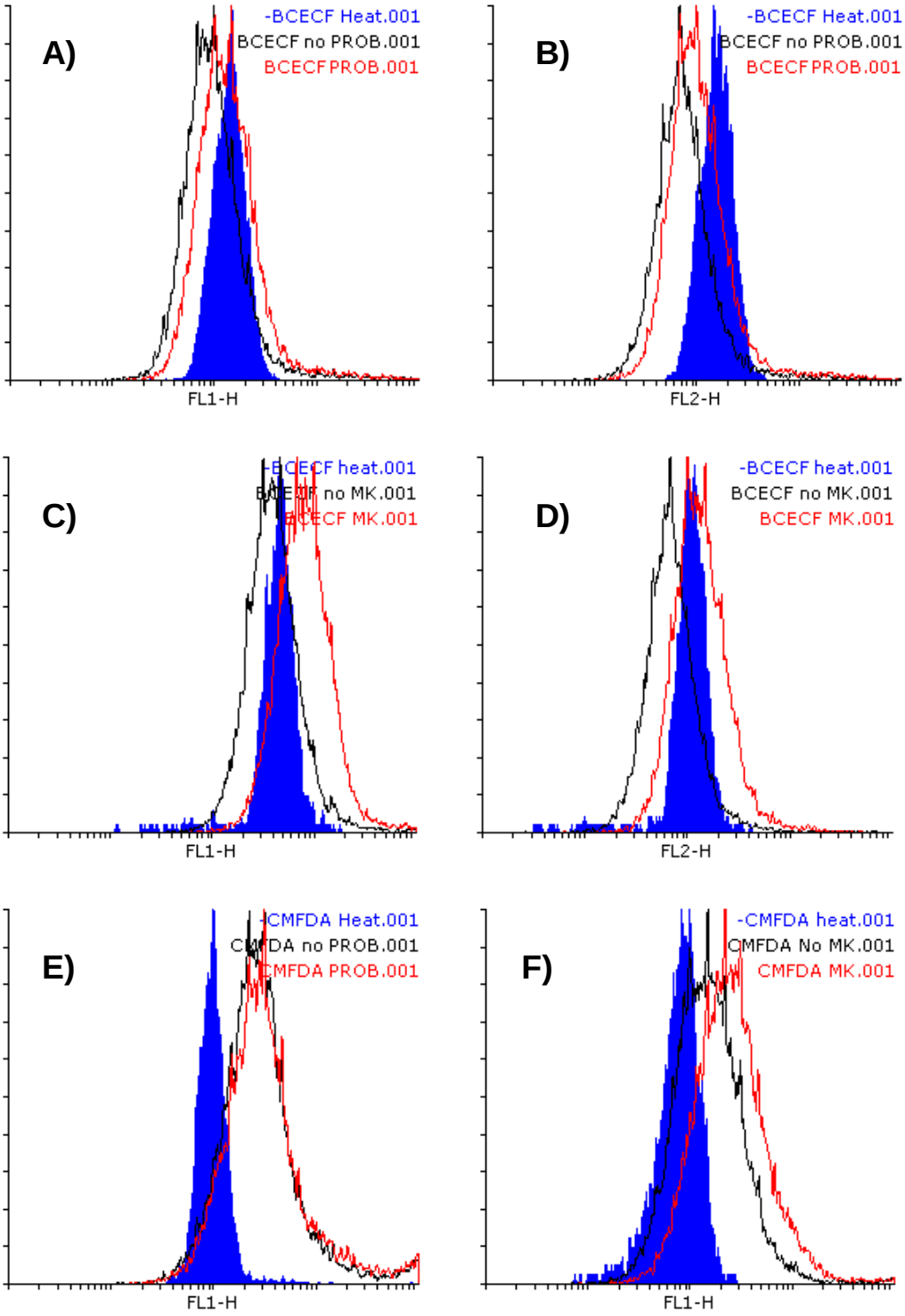

Fig 4. 53 Flow cytometry histogram distributions of negative control cells (heat-killed, blue), probenecid (50 µM) and MK571 (25 µM) (specific ABCC/MRP inhibitors) treated (red) and non-treated (black) cells. Stained used, inhibitor, Channel: A) BCECF, probenecid, FL1; B) BCECF, probenecid, FL2; C) BCECF, MK571, FL1; D) BCECF, MK571, FL2; E) CMFDA, probenecid, FL1; F) CMFDA, MK571, FL1. Measured at 530 ± 15 nm (FL1) and 585 ± 20 nm (FL2). Treatment time 60 min, n = 20,000.

Table 4. 13 Kolmogorov-Smirnov statistics calculated using BD CellQuest software for negative control cells (heat-killed, -C), probenecid (+P) (50 µM) and Mk571 (+MK) (25 µM) (specific ABCC/MRP inhibitors) treated and non-treated cells (-P, -MK), stained with BCECF and CMFDA measured at 530 ± 15nm (FL1) and 585 ± 20nm (FL2). * significant p <= 0.001. Treatment time 60 min, n = 20,000

BCECF FL1			
D-value	-P1	-P2	-P3
-C1	0.14*	0.12*	0.14*
-C2	0.31*	0.30*	0.16*
-C3	0.15*	0.14*	0.32*
+P1	0.22*	0.21*	0.23*
+P2	0.18*	0.17*	0.19*
+P3	0.13*	0.12*	0.14*

BCECF FL2			
D-value	-P1	-P2	-P3
-C1	0.32*	0.31*	0.33*
-C2	0.47*	0.46*	0.48*
-C3	0.34*	0.33*	0.35*
+P1	0.20*	0.19*	0.21*
+P2	0.16*	0.15*	0.17*
+P3	0.11*	0.10*	0.12*

CMFDA FL1			
D-value	-P1	-P2	-P3
-C1	0.77*	0.76*	0.75*
-C2	0.73*	0.72*	0.72*
-C3	0.74*	0.73*	0.72*
+P1	0.06*	0.06*	0.09*
+P2	0.07*	0.08*	0.11*
+P3	0.07*	0.08*	0.11*

BCECF FL1			
D-value	-MK1	-MK2	-MK3
-C1	0.21*	0.20*	0.08*
-C2	0.33*	0.32*	0.13*
-C3	0.39*	0.38*	0.19*
+MK-1	0.47*	0.48*	0.62*
+MK-2	0.39*	0.40*	0.55*
+MK-3	0.27*	0.28*	0.44*

BCECF FL2			
D-value	-MK1	-MK2	-MK3
-C1	0.14*	0.15*	0.35*
-C2	0.08*	0.07*	0.21*
-C3	0.14*	0.13*	0.19*
+MK-1	0.46*	0.48*	0.61*
+MK-2	0.38*	0.39*	0.54*
+MK-3	0.26*	0.26*	0.44*

CMFDA FL1			
D-value	-MK1	-MK2	-MK3
-C1	0.57*	0.56*	0.54*
-C2	0.64*	0.64*	0.62*
-C3	0.67*	0.66*	0.64*
+MK-1	0.26*	0.27*	0.30*
+MK-2	0.30*	0.31*	0.33*
+MK-3	0.25*	0.26*	0.28*

Strong (D > 0.30)
Moderate (0.20 < D <= 0.30)
Weak (0.15 < D < =0.20)
Negligible (D <= 0.15)

b) Flow cytometry, MK571 effect

When negative control cells were stained with BCECF, the fluorescent intensity was moderately higher than that of non-treated cells (MK571) (D = 0.25) but lower than MK571 treated cells (Fig 4.53C and 4.53D). When negative control cells were stained with CMFDA, the fluorescent intensity was strongly lower than that of non-treated cells (MK571) (D = 0.62) and MK571 treated cells (Fig 4.53F).

Cells treated with MK571 (stained with BCECF) exhibited greater fluorescence intensity than non-treated cells and even higher intensity than negative control cells for the two different channels FL1 (D = 0.43) and FL2 (D = 0.42) (Fig 4.53C and 4.53D) (which was not the case for probenecid treated cells, Fig 4.53A and 4.53B). This behaviour may indicate that cells treated with MK571 have a higher internal pH than non-treated cells. The other possibility is that the dye was effectively transported by non-treated cells.

Cells treated with MK571 (stained with CMFDA) exhibited greater fluorescence intensity than non-treated cells (D = 0.28) and negative control cells (Fig 4.53F). In contrast to BCECF, CMFDA contains a chloromethyl or bromomethyl group that reacts with thiols, and does not show a pH dependent spectral shift. Also once inside the cell, CMFDA is transformed into cell-impermeant reaction molecules. Therefore a greater intensity strongly indicates that the dye is effectively transported by non-treated cells. This strongly suggests that ABCC/MRP transport was in fact reversed by treatment with MK571.

It can be observed from Table 4.13 that the fluorescence intensity of the two dyes was strongly changed by treatment with MK571, whereas only BCECF fluorescence was moderately changed by treatment with probenecid and with negligible results for CMFDA fluorescence by treatment with probenecid.

Overall, given the large sample sizes, it should be noted that all the differences (shown in Table 4.13) were statistically significant including the small differences between with/without probenecid for CMFDA via channel FL1. For more insightful inference of these differences, the magnitude of the D statistic is the more meaningful statistic and clear instances of strong differences, where D > 0.30 can clearly be seen throughout these analyses.

4.3.2.6. Arsenic efflux

The fate of arsenic inside cells of *C. vulgaris* cells after exposure to 150 mg L^{-1} of As(III) for 24 h, using the two ABCC/MRP inhibitors probenecid (50 µM) and MK571 (25 µM) was investigated. Cells were harvested, counted and extracted as described in 3.5.1.1.a.

Insufficient evidence was found to establish a difference in the amount of arsenic inside treated (probenecid) and control (non-treated) cells (two-sample t-test, $p > 0.05$, $n = 12$). There was, however, strong evidence for a difference in the amount of arsenic inside treated (MK571) and control (non-treated) cells ($p = 0.005$, $n = 10$). This can be observed in Fig 4.54.

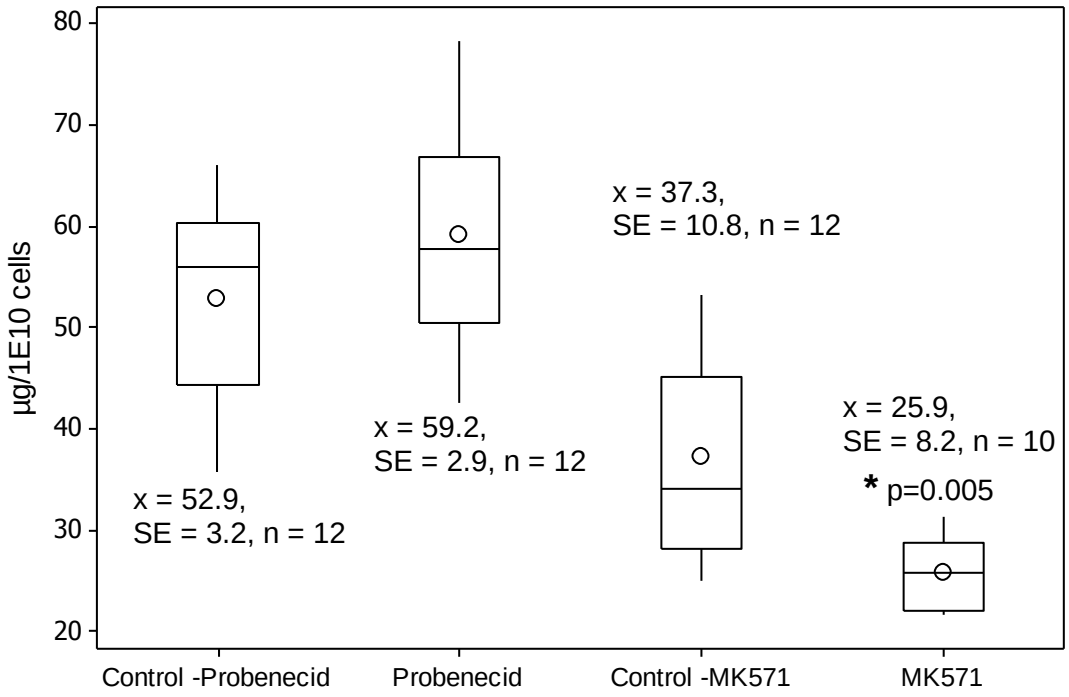

Fig 4. 54 Box plot of intracellular concentration of arsenic in *C. vulgaris* cells exposed to 150 mg L^{-1} of As(III) for 24 h with and without the specific ABCC/MRP inhibitors probenecid (50 µM) and MK571 (25 µM). Circles denote mean values (o).

4.3.2.7. Protein phosphatase inhibition experiments

Cantharidin, tautomycin and okadaic acid were used for protein phosphatase inhibition experiments. The results for cells exposed to 50 mg L^{-1} of As(III) for 48 h and exposed to no inhibitors (control), 100 nM cantharidin, 0.3 nM tautomycin and 1 nM okadaic acid, can be seen in Fig 4.55 and 4.56.

Fig 4.55 shows the concentrations of GSH, GSSG and their ratio of GSH/(GSH+GSG). Controls treated with phosphatase inhibitor with arsenic present and absent can be seen in Fig 4.55B.

Insufficient evidence was found for a difference in the level of reduced glutathione, GSSG and the ratio of GSH/(GSH+GSG) (two-sample t-test, $p > 0.05$, $n = 3$) when compared to the control (with no inhibitor) except for cantharidin ($p = 0.0272$).

Insufficient evidence was found for a difference in the levels of reduced GSH in the controls for absence and present of arsenic (with inhibitor, Fig 4.55B) ($p > 0.05$).

However, some evidence was found for a difference in the level of GSSG for treatments with tautomycin (p = 0.025), cantharidin (p = 0.011) and okadaic acid (p = 0.017) and the ratios of GSH/(GSH+GSG) for treatments with cantharidin (p = 0.016) and okadaic acid (p = 0.029) (Fig 4.55B).

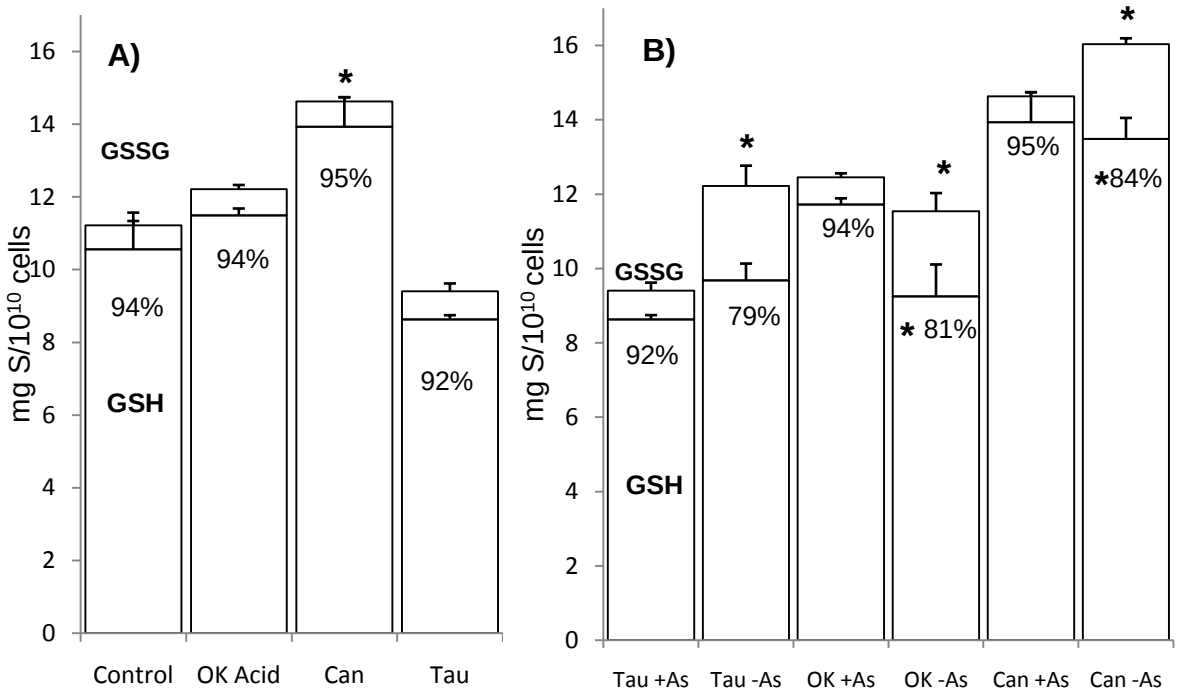

Fig 4. 55 Concentration of GSH (bottom bars) and GSSG (top bars) for *C. vulgaris* cells exposed to A) 50 mg L^{-1} of As(III) for 48 h and non-treated (control) or treated with 100 nM cantharidin, 0.3 nM tautomycin or 1 nM okadaic acid and B) treated with inhibitor with arsenic present and absent; analysed by HPLC-ICP-MS (O_2, CCT) m/z 48. Percentages indicate the ratio of GSH/(GSH+GSG). * denotes statistical difference using two-sample t-test (p <= 0.05). Vertical bars denote + 1 standard error

Fig 4.56 shows the concentrations of bound As-GS/PC complexes. Some statistical evidence was found for an increase in the amount of As-GS/PC complexes due to the effect of the inhibition of protein phosphatase, more specifically cantharidin in peaks U2 (p = 0.0281), P8 (p = 0.0263) and P11(p = 0.0113).

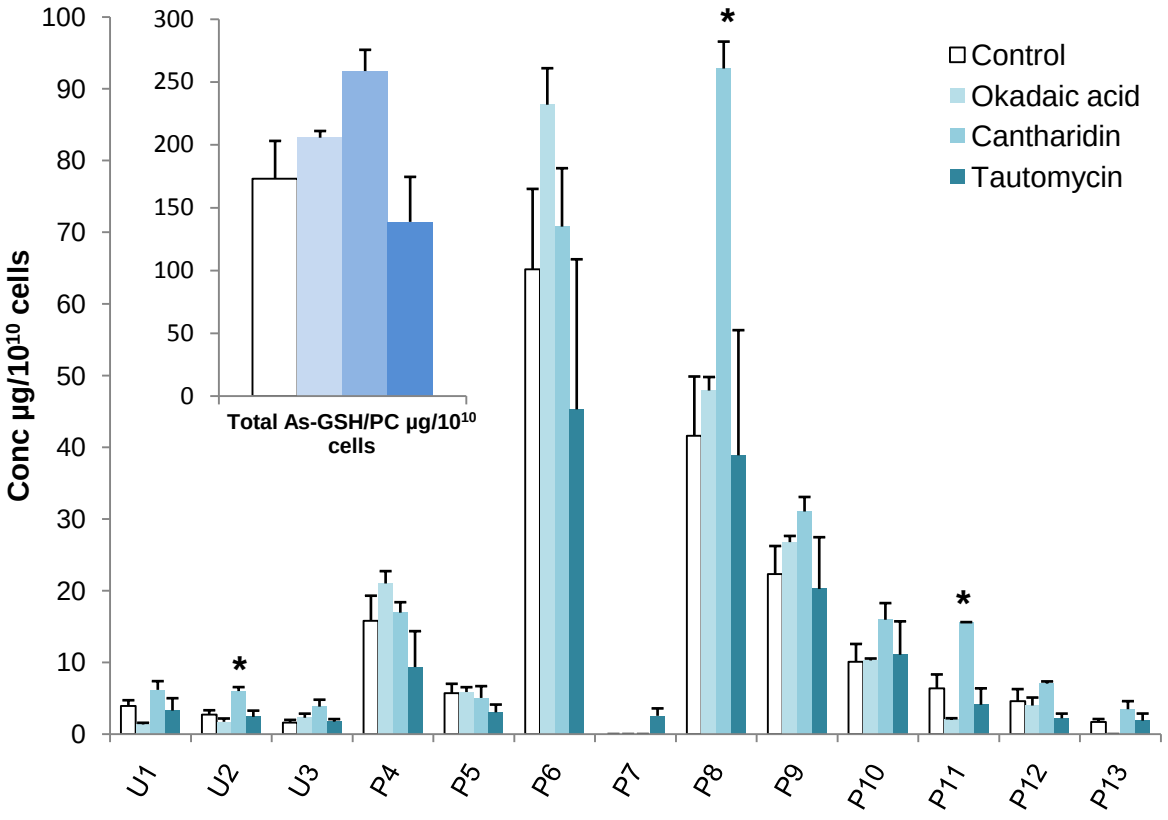

Fig 4. 56 Concentration of As-GS/PC complexes for *C. vulgaris* cells exposed to 50 mg L^{-1} of As(III) for 48 h and non-treated (control) or treated with 100 nM cantharidin or 0.3 nM tautomycin or 1 nM okadaic acid, (inset, total As-GS/PC concentration), analysed by HPLC-ICP-MS (O_2, CCT) m/z 91. * denotes statistical difference using two-sample t-test (p <= 0.05). Vertical bars denote +1 standard error. Peak identification: **U1-3** Unknowns, **P4** GS-As(III)-PC_2/GS-As(III)-γ-(Glu-Cys)$_2$, **P5** As(III)-γ-(Glu-Cys)$_2$, **P6** GS-As(III)-PC_2, **P7** GS-As(III)-γ-(Glu-Cys)$_2$-Ala, **P8** As(III)-PC_3/ MMA(III)-PC_2, **P9** MMA(III)-PC_2, **P10** As(III)-PC_3/ As(III)-$(PC_2)_2$, **P11** As(III)-$(PC_2)_2$/ As(III)-γ-(Glu-Cys)$_3$-Ala/ As(III)-γ-((Glu-Cys)$_2$)$_2$-Ala/ MMA(III)-γ-(Glu-Cys)$_2$-Ala, **P12** As(III)-PC_4 and **P13** As(III)-PC_4.

4.3.2.8. GSH transport stimulation experiments

Stimulation of ABCC mediated transport was investigated by using the flavonoid apigenin and the calcium channel blocker verapamil. The results of this experiment are shown in Fig 4.57 and 4.58. Fig 4.57A shows the concentrations of reduced GSH, GSSG and the ratio of GSH/(GSH+GSG) for cells exposed to 50 mg L^{-1} of As(III) for 48 h without treatment (control) and treated with 30 µM verapamil or 15 µM apigenin. Controls treated with the stimulators with arsenic present and absent can be seen in Fig 4.57B.

Insufficient evidence for a difference was found for all the treatments for reduced GSH, GSSG and their ratios (two-sample t-test, $p > 0.05$, $n = 3$). However there was some statistical evidence for an increase in the level of GSSG for verapamil ($p = 0.03$) and apigenin ($p = 0.004$) as well as a decrease in the ratio of GSH/(GSH+GSG) for verapamil ($p = 0.048$) compared to cells only treated with stimulator (without arsenic), as shown in Fig 4.57B.

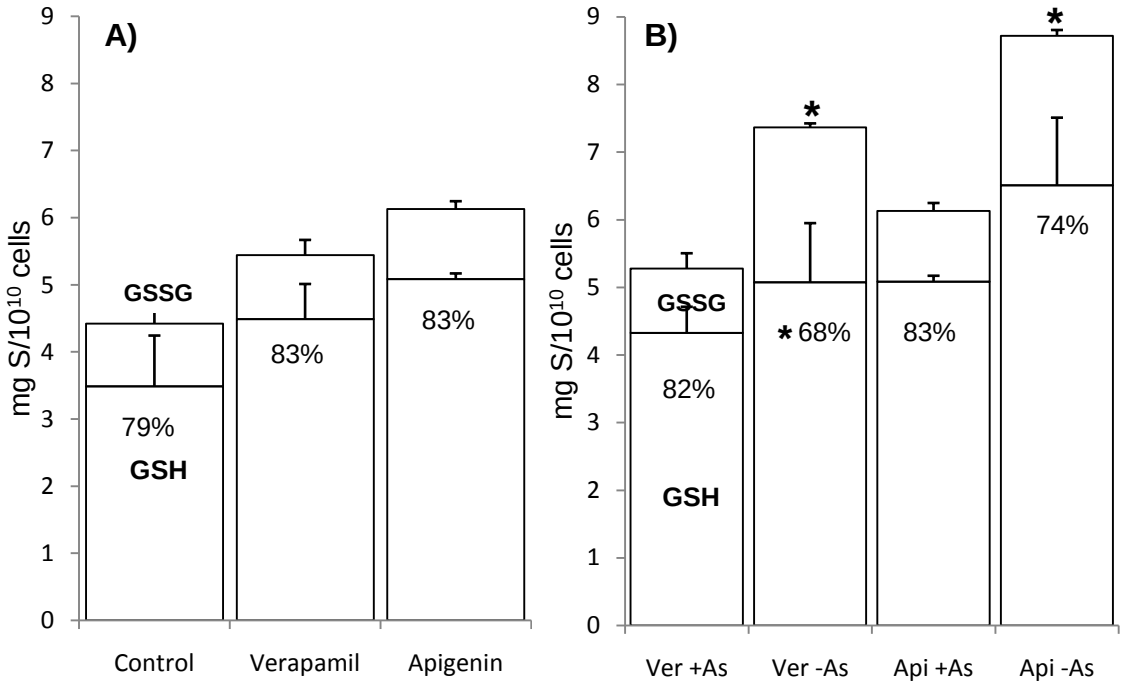

Fig 4. 57 Concentration of GSH (bottom bars) and GSSG (top bars) for *C. vulgaris* exposed to A) 50 mg L^{-1} of As(III) for 48 h and non treated (control) or treated with 30 µM verapamil or 15 µM apigenin and B) Treated with inhibitor with arsenic present and absent, analysed by HPLC-ICP-MS (O_2, CCT) m/z 48. Percentages indicate the ratio of GSH/(GSH+GSG). * denotes statistical difference using two-sample t-test ($p <= 0.05$). Vertical bars denote + 1 standard error

Fig 4.58 shows the concentrations of bound As-GS/PC complexes for cells exposed to 50 mg L^{-1} of As(III) for 48 h and exposed to no treatment (control), an treated with 30 µM verapamil or 15 µM apigenin.

Strong statistical evidence was found for a difference in the level of total As-GS/PC complexes for cells treated with verapamil ($p = 0.0049$) as well as some evidence for a difference in the level of the individual peaks U1 ($p = 0.0125$), P4 ($p = 0.0072$), P5 ($p = 0.0217$), P6 ($p = 0.0177$), P8 ($p = 0.0076$), P9 ($p = 0.0014$) and P10 ($p = 0.0029$). There was insufficient evidence for a difference in the levels of total As-

GS/PC complexes for cells treated with apigenin ($p > 0.05$); however, some evidence was found for a difference in the level of individual peaks P8 ($p <= 0.0001$) and P9 ($p = 0.0186$).

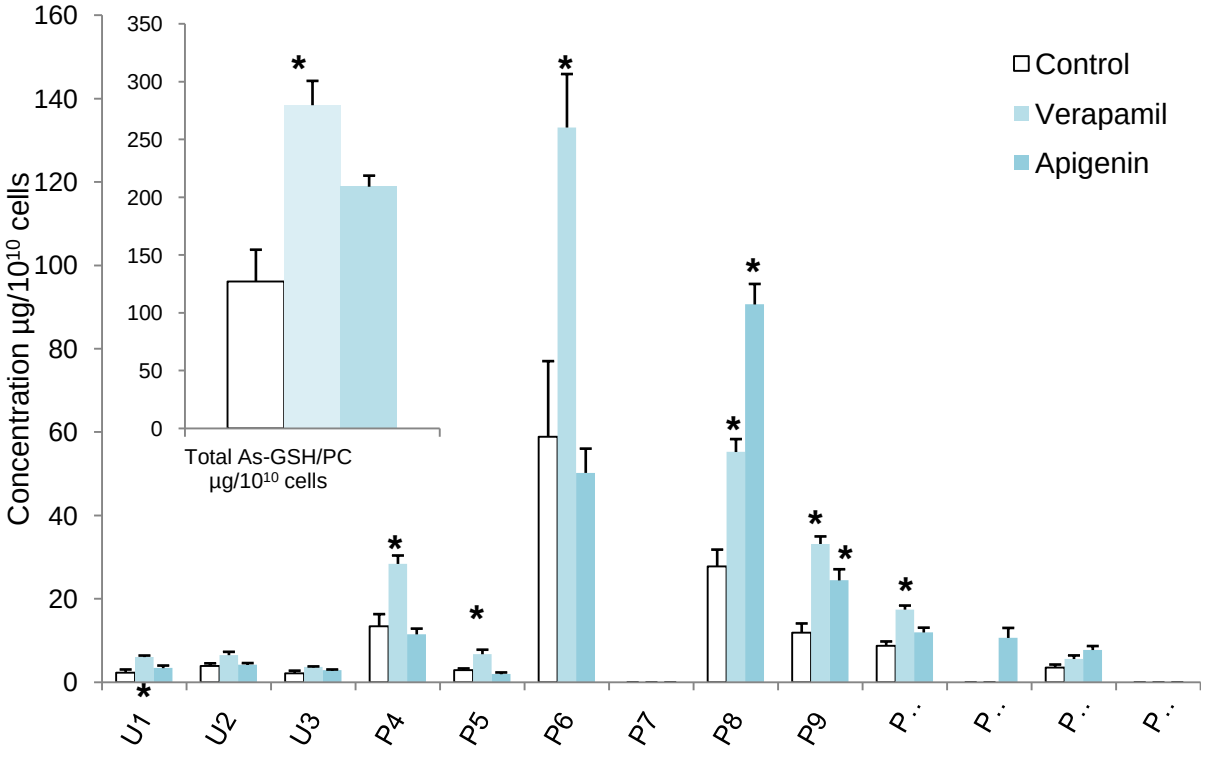

Fig 4. 58 Concentration of As-GS/PC complexes for *C. vulgaris* cells exposed to 50 mg L^{-1} of As(III) for 48 h; non-treated (control) or treated with 30 µM verapamil or 15 µM apigenin (inset, total As-GS/PC concentration), analysed by HPLC-ICP-MS (O_2, CCT) m/z 91. * denotes statistical difference using two-sample t-test ($p <= 0.05$). Vertical bars denote +1 standard error. Peak identification: **U1-3** Unknowns, **P4** GS-As(III)-PC_2/GS-As(III)-γ-(Glu-Cys)$_2$, **P5** As(III)-γ-(Glu-Cys)$_2$, **P6** GS-As(III)-PC_2, **P7** GS-As(III)-γ-(Glu-Cys)$_2$-Ala, **P8** As(III)-PC_3/ MMA(III)-PC_2, **P9** MMA(III)-PC_2, **P10** As(III)-PC_3/ As(III)-$(PC_2)_2$, **P11** As(III)-$(PC_2)_2$/ As(III)-γ-(Glu-Cys)$_3$-Ala/ As(III)-γ-((Glu-Cys)$_2$)$_2$-Ala/ MMA(III)-γ-(Glu-Cys)$_2$-Ala, **P12** As(III)-PC_4 and **P13** As(III)-PC_4.

4.4. Genetic markers for arsenic resistance in *C. vulgaris*

The full set of results is shown in Appendix 5 (Table 1A5). Four genes in *C. vulgaris* C-169 were found to share similarity with *Arabidopsis thaliana* genes related to arsenic resistance. These genes correspond to the ATP binding cassette ABCC1/2 (COCSUDRAFT_46284), ABCD1 (COCSUDRAFT_65142) and ABCD2 (COCSUDRAFT_16703) as well as the phytochelatin synthase PCS1 (COCSUDRAFT_19902). One gene in *C. vulgaris* was found to share similarity with

the gene in *Medicago truncatula* related to homoglutathione synthesis (gshs2) (COCSUDRAFT_52209). Finally, one gene in *C. vulgaris* was found to share similarity with the gene in *Saccharomyces cerevisiae* related to As(III) reduction (ACR1) (COCSUDRAFT_66432).

The genes from *C. vulgaris* C-169 mentioned above were subsequently used as a template to find similarities among all other species in the Uniprot database (426,778 species).

In summary, 127 species were found that shared 34-50% identity with ABCC1/2 (COCSUDRAFT_46284), 151 species shared 33-73% identity with PCS1 (COCSUDRAFT_19902), 156 species shared 30-53% identity with ABCD1 (COCSUDRAFT_65142), 176 species shared 35-63% identity with gshs2 (COCSUDRAFT_52209), 177 species shared 34-65% identity with ABCD2 (COCSUDRAFT_16703) and 193 species shared 24-48% identity with ACR1 (COCSUDRAFT_66432),

However, only 22 species may show to express simultaneously the three genes known to be required to confer arsenic resistance via PC's chelation (ABCC1/2 and PCS1). From those 22 species, 20 species showed to express simultaneously four genes (ABCC1/2, PCS1 and gshs2 for Ala-GSH synthesis). These results are shown in Table 4.14.

Table 4. 14 *C. vulgaris* C-169 sequence similarity search BLASTP using the Uniprot (BLASTP 2.2.28+ software) database (Uniprot, 2009); hPC production refers to phytochelatins where Gly is substituted by Ala, Ser, Gln or Glu or is absent. Species are listed in order of identity to ABCC1/2

	ABCC 1/2	**PCS 1**	**Ala GSH**	**ABCD 1**	**ABCD 2**	**As reductase**
COCSUDRAFT_(number)	**(46284)**	**(19902)**	**(52209)**	**(65142)**	**(16703)**	**(66432)**
Species / Gene name	**Identity**	**Identity**	**Identity**	**Identity**	**Identity**	**Identity**
Hordeum vulgare var. distichum (Two-rowed barley)	50%	57%	*49%	52%	65%	NF
Musa acuminata subsp. malaccensis (Wild banana)	46%	60%	45%	48%	52%	NF
*Selaginella moellendorffii (*Spikemoss)	44%	60%	47%	50%	52%	45%
Populus trichocarpa (Populus balsamifera subsp. trichocarpa)	44%	59%	NF	49%	53%	33%
Vitis vinifera (Grape)	44%	57%	45%	51%	51%	34%
Prunus persica (Peach) (Amygdalus persica)	44%	56%	48%	49%	52%	35%
Glycine max (Soybean) (Glycine hispida)	44%	62%	*47%	52%	49%	38%
Capsella rubella (Plant)	44%	56%	45%	48%	51%	36%
Ricinus communis (Castor bean)	44%	57%	46%	48%	51%	37%
Brassica rapa subsp. pekinensis (Chinese cabbage)	44%	58%	46%	49%	53%	36%
Solanum lycopersicum (Tomato) (Lycopersicon esculentum)	43%	57%	*49%	51%	48%	38%
Setaria italica (Foxtail millet) (Panicum italicum)	43%	56%	49%	49%	50%	NF
Sorghum bicolor (Sorghum) (Sorghum vulgare)	43%	56%	43%	50%	49%	NF
Brachypodium distachyon (Purple false brome)	43%	57%	47%	50%	50%	NF
Arabidopsis lyrata (Lyre-leaved rock-cress)	43%	56%	47%	50%	51%	36%
Arabidopsis thaliana (Mouse-ear cress)	42%	56%	46%	50%	52%	36%
Oryza brachyantha (Rice)	42%	56%	*47%	49%	49%	NF
Oryza glaberrima (African rice)	42%	56%	*45%	50%	51%	NF
Oryza sativa subsp. japonica (Rice)	42%	55%	*46%	48%	50%	NF
Triticum urartu (Red wild einkorn) (Crithodium urartu)	43%	50%	40%	47%	NF	NF
Ciona savignyi (Pacific transparent sea squirt)	39%	49%	38%	NF	NF	NF
Nematostella vectensis (Starlet sea anemone)	39%	47%	NF	32%	NF	NF

Note: * denotes that the species have been reported in the literature to produce hPC's

5. Discussion

5.1. Overview

This study aimed to examine the interactions of arsenic with the microalgae *C. vulgaris* and its potential to bio-remediate arsenic from water. The present chapter is a critical evaluation of the outcomes from the experimental approach. The chapter is intended to state the author's interpretations and opinions, to explain the implications of the new findings, to explain the limitations of the present research and to make suggestions for future research.

This chapter is organised following the same structure taken in materials and methods, chapter 3, section 3.1, Fig 3.2. Thus the chapter is divided in four main experimental sections: Arsenic toxicity to *C. vulgaris*, surface adsorption, arsenic biotransformations inside *C. vulgaris* cells and genetic markers for arsenic resistance.

A summary of the discussion is provided at the end of the chapter (section 5.6) in which the independent outcomes from the experimental section are combined to explain the mechanisms for the interaction of arsenic with the microalgae *C. vulgaris.* This summary is also represented in a graphical way (section 5.6, Fig 5.4) and the theoretical mechanisms (section 2.4.2, Fig 2.2) are contrasted with the new findings.

An emphasis was made on arsenic biotransformations inside *C. vulgaris* cells, more specifically the complexation of arsenic with rich free thiol (SH) molecules (GSH/PC). The reason for this was the success in developing a new extraction protocol that enabled the identification and characterisation of several novel molecules never observed in *C. vulgaris* cells (Pantoja et al., 2014). These new findings also enabled the study of a more detailed implication of GSH/PC complex formation and in the detoxification mechanism of arsenic employed by *C. vulgaris* cells.

5.2. Toxicity tests

The use of the whole water technique (section 3.3.2) to extract chlorophyll a, b and other related pigments demonstrated to be reliable, accurate and time efficient, allowing measurement of cell populations as low as 1000 cells mL^{-1} with a narrow deviation and high correlation (simple linear least squares, R^2 = 0.995-0.999, n = 3) (section 4.1, Fig 4.1 and 4.2). This is important because it enables toxicity tests to be carried out using low initial concentration of algae or other photosynthetic microorganisms and reflects more precisely the conditions in natural environments. High concentration of cells can also decrease the concentration of arsenic in the media due to bioadsorption/bioabsorption and therefore decrease the toxic load of the arsenic concentration tested. The decrease in toxic load can be minimised by using low initial concentrations of cells and thus better estimations of toxic effects can be assessed.

This method is particularly well suited for studies on arsenic toxicity to green microalgae because arsenic does not interfere with the photosynthetic apparatus of the organisms and therefore the correlation of chlorophyll a and other pigments content with cell numbers is constant throughout the experiments (Stolz et al., 2006; Maeda et al., 1985).

5.2.1. Arsenic toxicity to *C. vulgaris*

Different concentrations of phosphate were used to investigate the toxic effects of As(III) and As(V). Controls growing at low concentration of phosphate (0.15 mg L^{-1} of PO_4^{-3}) only attained a specific growth rate of 0.92 day^{-1} which is on the borderline of acceptability of the test (0.90 day^{-1}) (ASTM, 2004). In contrast, cells growing in 13 mg L^{-1} phosphate reached a specific growth rate of 1.17 day^{-1}. This was probably one of the reasons for the poor results for cells tested under low phosphate concentrations.

The fifty percent, As(III) inhibition concentration (72 h, IC_{50}) at 13 mg L^{-1} phosphate was 55.33 mg L^{-1} (95% CI, 48.95-61.42). Toxicity of *C. vulgaris* to As(III) is not likely to be affected by the presence of phosphate. This was true for this type of algae (section 4.1.1.a, Fig 4.5 and 4.11). However, similar studies performed with the freshwater algae *Chlorella sp.* found a 72 h IC_{50} of 25.2 mg L^{-1} and complete growth

inhibition above 50 mg L^{-1} of As(III) (Levy et al., 2005). Therefore the IC_{50} concentration found in the present study is surprisingly high even for an arsenic tolerant organism. In contrast, the IC_{50} for As(V) was found to be 1.07 mg L^{-1}, at low concentration of phosphate, this was obtained by extrapolation.

No difference in the lag phase period was observed for the cells treated with As(III) and control cells (with no arsenic added). In contrast cells treated with As(V) remained in lag phase for one more day than control cells (section 4.1.1, Fig 4.3 and 4.13). This indicates that any possible tolerance mechanism for As(III) may be constitutively expressed (this is a gene that is transcribed continually with no need for a external stressor) by this type of algae whereas tolerance for As(V) is triggered and then the algae express the defence mechanisms (e.g. enzyme / protein production) that help in arsenic detoxification.

It was found that As(V) is at least 50 times more toxic than As(III) to *C. vulgaris* cells under the same conditions of low level of phosphate (corresponding to that found in surface waters). High levels of phosphate (> 13 mg L^{-1} of phosphate) reduced the toxicity of As(V) and remarkably together, high levels of phosphate and As(V) improved significantly algae growth (ANOVA-GLM, $p = 0.0125$, $n = 3$, section 4.1.1.b, Fig 4.12). Even when As(V) can replace phosphate in energy molecules such as arsenylated ATP, ADP and AMP these molecules are more easily hydrolysed and have lower energy levels than their phosphate analogues (2 - 3 kcal mol^{-1} lower energy) therefore rendering algae less likely to survive when present (Xu, Ma and Nussinov, 2012). Another disadvantage for cells living in low phosphate and high As(V) environments is that when As(V) is bound to ADP, AMP, glucose, ribose and adenine (this happens spontaneously), many enzymes have been found to reduce As(V) in the presence of glutathione. This reduction does not happen with phosphate, thus being more stable and useful at storing energy than the As(V) analogues (Nemeti, Anderson and Greus, 2012; Gregus et al., 2009; Nemeti et al., 2010). However, the reason for an increase in growth with respect to the controls in cells living at high As(V) and phosphate concentrations is not fully understood (section 4.1.1.b, Fig 4.12).

Phosphate is more important to plants than human cells and that may be the reason for the higher toxic effects that As(V) exerts in plant cells compared to As(III). This is

the opposite of human cells in which toxicity to As(III) is considerably higher than As(V) (Frankenberg, 2002). However not enough studies involving plants have taken into consideration the fact that phosphate reduces As(V) toxicity, by using high levels of phosphate in toxicity tests, thus underestimating arsenic toxicity (Murray et al., 2003; Maeda et al., 1992).

The toxic effects of As(III) and DMA were assessed at different concentrations of sulphur. This is because cells are capable of forming complexes of arsenic with sulphur-containing peptides such as GSH and PC's upon exposure to As(III) and DMA only.

No toxic effects were found in *C. vulgaris* cells upon DMA exposure. Also no difference was found in growth for cells treated with DMA and As(III) compared to controls (without arsenic) at low concentrations of sulphur in the media (0.1 g L^{-1}). This is an indication that the amount of sulphur available for uptake does not play an important role in arsenic resistance. The amount of sulphur does influence growth for normal metabolic processes inside the cells such as amino acid and protein formation, normal glutathione production and redox control among others but under low sulphur conditions these normal metabolic processes become limited before the toxicity of arsenic can be properly assessed.

The above discussion regarding the toxic effects of DMA only gives a partial explanation into toxicity of *C. vulgaris* cells to DMA. This is because a loss in buoyancy was observed that led to strong sedimentation (sinking) of the cells, potentially masking the toxicity of DMA. The reason for this is not fully understood, nor has a method been developed to measure sedimentation as a toxic response to green microalgae. In some species of algae a reduction in the sinking rate is obtained by increasing their lipid content (Barsanti and Gualtieri, 2006). If this is the case, perhaps the measurement of the lipid content can give an indication of the capacity of the cells to keep afloat and therefore an indication of toxicity. Nevertheless, detailed methodologies describing the measurement of toxicity to microalgae cells by means of loss of buoyancy or rate of sedimentation would be of interest when the toxicity of DMA is investigated.

Continuous (5 min intervals) monitoring of dissolved oxygen, pH, temperature and redox potential revealed that the conditions for the experiments were stable. Only an increase in the redox potential from -160 to -60 mV for treatments with As(III) was observed. However this increase is not likely to change arsenic speciation in the media by itself as reducing conditions remained throughout the course of the experiments.

5.2.2. Oxidative stress, GSH and pH measurements by flow cytometry

Flow cytometry was used to test the involvement of intracellular pH, GSH and oxidative stress upon exposure to As(V) and As(III) at IC_{50} concentrations: As(III) (50 mg L^{-1} of As at 153.3 mg L^{-1} of PO_4^{-3}) and As(V) (1 mg L^{-1} of As at 0.3 mg L^{-1} of PO_4^{-3}).

Treatment with As(III) had negligible effect on intracellular pH (Kolmogorov-Smirnov, D = 0.06, n = 20,000) as well as in the concentration of free thiols (GSH) (D = 0.03). It was also found that As(III) had a negligible effect on the induction of oxidative stress, measured by the formation H_2O_2 free radical (D = 0.02) and O_2^- super oxide radical (D = 0.03) (section 4.1.2.1, Fig 4.19-4.22 and Table 4.1-4.4).

Two possibilities exist to explain these results. Firstly, it can be implied that there is no toxic response or effects to *C. vulgaris* cells upon exposure to As(III).

Secondly, immediately after As(III) gets inside the cells, GSH binds/chelates with As(III) and triggers the formation of PC's that will chelate As(III) in a stronger way because of the multiple cysteine residues compared to one cysteine in GSH. Inside the cells, reduced PCn and oxidised PCn may act as redox buffer systems in the same way GSH/GSSG act, thus the redox pair NADP/NADPH and glutaredoxin may also act as cofactors and reducing enzymes respectively preventing Reactive Oxygen Species (ROS) formation and oxidative damage inside the cells (Hirata, Tsuji and Miyamoto, 2005). Moreover, phytochelatins have been found to be more effective at preventing oxidative stress than GSH (Tsuji et al., 2002). This is followed by As-GS/PC complex compartmentalisation to vacuoles. Once arsenic is inside the vacuoles, GSH and PC's may be recycled (Zenk, 1996). The pool of GSH is then rapidly restored and thus no significant increase in the levels of free GSH and redox

status is observed. The formation of reactive oxygen species is not observed as well as a negligible change in the intracellular pH (Kolmogorov-Smirnov, D = 0.06, n = 20,000) because As(III) is not able to bind to any other molecules or enzymes in the cytosol.

In contrast, treatment with As(V) had a moderate decrease in intracellular pH (Kolmogorov-Smirnov, D = 0.30, n = 20,000) and a strong increase in the concentration of free thiols (GSH) (D = 0.56). However it had a negligible effect on the induction of oxidative stress, measured by the formation of H_2O_2 free radical (D = 0.07) and O_2^- super oxide radical (D = 0.10).

It would appear that after As(V) gets inside the cells, it is capable of binding with several molecules and replace phosphate, this induces stress which is reflected by an increase of free thiols (GSH) and oxidative stress (H_2O_2 free radical and O_2^- super oxide radical among others). Because the affinity of GSH to hard As(V) is much lower than that of As(III), no chelation or binding is observed (section 4.3.2.4.a, Fig 4.41 and 4.42). This in turn, allows GSH to scavenge the free radicals immediately formed. Even when this strategy alleviates the damaging oxidative stress inside cells, reactive As(V) is still able to exert its toxicity (replacement of phosphate in metabolic pathways, interference in enzymatic activity, ATP and energy processes and DNA methylation among others) (Xu, Ma and Nussinov, 2012; Nemeti et al., 2010) .

The reason for a change on the intracellular pH upon exposure to As(V) is not fully understood. However, this along with a higher redox capacity given by the increased level of free GSH will certainly have major effects on cell functioning since most of the cytoplasmic processes are sensitive to the concentration of H^+ ions, mostly involving chemical (ATP) and electrical (NADPH) energy process, since the two are pH and redox potential dependent respectively (Nobel, 2009).

The reasons mentioned above can explain the lower toxicity observed in *C. vulgaris* cells on exposure to As(III) than As(V) at the same low concentration of phosphate.

5.3. Surface adsorption

When surface adsorption was investigated using dry *C. vulgaris* cells, pseudo-equilibrium was observed after 4 h for As(III) and As(V) as shown in section 4.2.1, Fig 4.23A and 4.24A. However the release of phosphorus (most likely in the form of soluble phosphate) reached constant values after 3 and 2 h for As(III) and As(V) respectively (section 4.2.1, Fig 4.23B and 4.24B).

For As(III), the amount of phosphate released at the two pH tested, was not related to the amount of arsenic adsorbed because when no As(III) was added, the release of phosphate was not significantly different from the experiments with As(III) addition (two-sample t-test, p = 0.5, n=9).

In the case of As(V) because no adsorption was observed at all (section 4.2.1, Fig 4.24A), the release of phosphate cannot be considered to be related to the adsorption of As(V). This release of phosphate appeared to be pH dependent as many desorption processes are, being more pronounced at pH 7 than at pH 4.

The poor adsorption observed on kinetic experiments was corroborated by isotherm studies, in which the adsorption of As(III) was tested. Strong correlation coefficients were found for Langmuir (simple least squares; pH 4, R^2 =0.89; pH 7, R^2 = 0.96; n = 3) and Freundlich (simple least squares; pH 4, R^2 =0.97; pH 7, R^2 = 0.99; n = 3) isotherms. However the values for adsorption capacities were negative (pH 4, Q_0 = -0.01; pH 7, Q_0 = -0.01), which indicates poor adsorption behaviour (section 4.2.2, Fig 4.25 and Table 4.5).

In order to test if adsorption of arsenic (As(III), As(V) and DMA) was an active process, experiments involving living cells were performed.

The adsorption of As(V) and DMA showed a normal saturation curve after 48 h of exposure with the corresponding form of arsenic. In contrast, As(III) adsorption did not show saturation at any of the exposure periods tested. Importantly, this may indicate that As(III) adsorption takes place by an active mechanism. Moreover, 15 times more As(III) was adsorbed than As(V) and DMA when cells were exposed to 50 mg L^{-1} of the corresponding arsenic form at different exposure times (section 4.2.3, Fig 4.26).

Adsorption of the three forms of arsenic was concentration dependent. Adsorption of As(V) and DMA was found to be linearly correlated (simple linear least squares; As(V), R^2 = 0.793; DMA, R^2 = 0.780, n = 3), whereas As(III) adsorption followed a second order polynomial curve (simple polynomial least squares, R^2 = 0.988 n = 3). Adsorption of As(III) was 17 times higher than that of As(V) and DMA when cells were exposed to different concentrations of the corresponding arsenic form for 48 h (section 4.2.3 Fig 4.27 and 4.28).

Because the cell surface of the algae is a strong electron donor and weak electron acceptor and also because the iso-electric point of the cell wall is 2.9 (Hadjoudja, Deluchat and Baudu, 2010), cells will attract only positively charged molecules efficiently at a wide range of pH (2.9 to 14), therefore explaining the weak adsorption of negatively charged As(V) shown in this study.

Both As(III) and DMA are predominantly present as uncharged molecules and are not likely to be affected by electrostatic interactions. DMA is not likely to be chelated inside cells, so no more active interactions are envisaged. However the high affinity of As(III) for thiol groups in small peptides and proteins can make the process an active coordination/complexation mechanism for this form of arsenic and thus could also dynamically promote an increase in surface adsorption.

5.4. Arsenic biotransformation experiments

5.4.1. Reduction/oxidation, methylation/demethylation and arsenosugar formation

Total arsenic inside the cells (absorbed) was calculated for cells exposed to As(III), As(V) and DMA. For the three species, the total amount of arsenic inside the cells did not increase with an increase in the exposure time (simple least squares; As(III), R^2 = 0.00; As(V), R^2 = 0.660 ; DMA, R^2 = 0.130; n = 3). This indicates that, if there is an absorption mechanism, this mechanism is likely to be very rapid and efficient. For As(V) phosphate channels are involved, aquaporin channels have been described for As(III) and passive diffusion is involved for DMA absorption, all efficient and rapid processes (Sun, 2011). However, 8 times more As(III) than As(V) or DMA was found inside the cells (section 4.3.1.1 Fig 4.29).

The amount of arsenic inside the cells depended on the concentration of arsenic in the media for the three forms of arsenic tested. This behaviour was linearly correlated for all forms with some difference in the slopes and correlation coefficients (simple least squares; As(III), R^2 = 0.98; As(V), R^2 = 0.91; DMA, R^2 = 0.98; n = 3). The poorest absorption was observed for cells exposed to As(V), being 6 times lower than DMA absorption and 55 times less efficient than As(III) absorption. DMA absorption was 9 times lower than that of As(III) (section 4.3.1.1 Fig 4.30 and 4.31).

Toxicity of As(V) was reduced by an increase in the amount of phosphate present in the culture media. It would appear that phosphate is able to release the toxicity of As(V) in two ways: firstly, because As(V) is poorly adsorbed in the presence of phosphate and thus being less available for intracellular uptake; and secondly, because the phosphate transport channel is much more efficient at pumping phosphate inside the cells than As(V) when the two are present in the media at similar concentrations [1.62 mM of PO_4^{-3} and from 0.013 - 2.67 mM of As(V)]. In general, studies have reported slightly better affinity for phosphate than As(V) (Meharg, Nylor and Macnair, 1994); however, this does not appear to be the case for *C. vulgaris* cells. This will require a more detailed investigation into the low and high affinity phosphate channels (by means of genetic manipulation of the phosphate transport genes or by using isotopically labelled As(V) and phosphate), which is out of the scope of the present investigation.

Toxicity of As(III) was found to be 50 times lower than As(V) (section 4.1.1 Fig 4.5 and 4.14) and surprisingly cells are capable of absorbing 55 times more As(III) than As(V) in the same conditions of high phosphate (section 4.3.1.1 , Fig 4.29 and 4.30).

Upon exposure to DMA, in short term experiments (up to 72 h) most of the arsenic was still in DMA form, nonetheless, cells were able to transform up to 7% of DMA to As(V) but no As(III) was observed.

It was observed that upon exposure of As(V) to *C. vulgaris* cells, 41% remained in this form followed by 30% methylation to DMA, and 29% reduction to As(III). Interestingly no free MMA was detected under the conditions used in this study (short term exposure, up to 72 h and high concentration of phosphate, 153.3 mg L^{-1}).

Upon exposure to As(III), on average 90% of the arsenic was still in As(III) form, and only 5% was oxidised or methylated to DMA with the exemption for treatments with 50 mg L^{-1} for 48 h. Again no free MMA was detected. Speciation of As-GS/PC complexes using a strong anion exchange column has revealed to break the As-S bonds giving only As(III) signals (Raab et al., 2004). Therefore the signal for As(III) in this set of results could come either from As-GS/PC complexes or As(III). For this reason the speciation of cells exposed to As(III) was explored further in experiments described in section 4.3.2.3.

5.4.2. GS/PC complexation

5.4.2.1. Focused sonication extraction for GS/PC complexes validation (Pantoja et al., 2014)

Extraction efficiency using focused sonication in *C. vulgaris* cells was lower than that of Kelp powder. This can be explained by the fact that *C. vulgaris* cells produce more lipids (up to 26% by weight) and these can combine with arsenic to form lipid-soluble arsenic compounds (Widjaja, Chien and Ju, 2009).

Previous studies found extraction efficiencies in *C. vulgaris* cells in the range of 11-27% (Murray et al., 2003). Focused sonication has been used to extract arsenic from environmental samples but without giving specific information of the conditions (Pedersen and Francesconi, 2000; Geiszinger et al., 2001). However, in this study, a considerable improved extraction efficiency of 71.1% was achieved. It appears that focused sonication funnels more energy, enabling more targeted intermolecular force disruption and thus mobilising more arsenic into aqueous solution. The method therefore achieves representativeness of water soluble arsenic species in *C. vulgaris* without compromising species integrity through the minimisation of the treatment time (30 s).

When the extraction method using focused sonication was validated, it was shown (section 4.3.2.3, Fig 4.39 and 4.40) that there is no indication of any of the peaks suffering disintegration caused by the high energy sonication.

5.4.2.2. Qualitative analysis using on-line HPLC-ESI-MS and HPLC-ICP-MS

The presence of As(V) in the culture media resulted only in signals for GSH, GSSG and oxidised PC_2. No arsenic bound to GS/PC was detected.

At first the most likely explanation was that As(V) is hardly reduced by this alga, since previous studies (Murray et al., 2003) have reported only 1-6% reduced As(V) following 7 days exposure experiments and methanol/water (1:1) extraction. Furthermore, the affinity of sulphur for As(III) is much stronger than for As(V). Therefore As(V), would not be expected to bind to sulphur and as such will not result in the formation of any As-GS/PC complexes.

However, our findings indicate that As(V), in the presence of high phosphate concentrations, is somehow excluded from surface adsorption and intracellular absorption being 17 and 55 fold lower respectively when compared to As(III) (section 4.2.3 Fig 4.26-4.28, section 4.3.1 Fig 4.29-4.31). It was also found in this study that only 29% of As(V) was reduced to As(III). Furthermore, it has recently been reported that the reduction of As(V) mediated by phosphorolitic-arsenolitic enzymes is also inhibited by increasing concentrations of phosphate, ATP and glycine. These enzymes are characterised for the formation of the intermediates, Ribose-1-As(V), Glucose-1-As(V), Glycerate-3-phosphate-1-As(V), Acetyl-As(V), Adenoside-monophosphate-As(V) and Adenosine-diphosphate-As(V) (Gregus et al., 2009; Nemeti, Anderson and Greus, 2012; Nemeti et al., 2010).

For the reasons mentioned above, it is highly unlikely for cells to take up high amounts of As(V), to reduce it to As(III) so it can form complexes with GS/PC efficiently enough to be detected by the method used in this study (HPLC-ICP-MS).

These findings corroborate the interpretation of the results found in section 4.1.2 for intracellular oxidative stress, GSH and pH using flow cytometry in which, following As(V) cellular entry, this it is capable of binding with several molecules and replace phosphate, inducing stress reflected by an increase of free thiols (GSH). Free thiols are not capable of binding to As(V) and no chelation is observed; however, thiols are able to reduce oxidative stress very quickly and therefore no H_2O_2 free radical and O_2^- super oxide radical among others are observed.

The interpretation of the results mentioned above does not explain the presence of arsenosugars found in other studies in which *C. vulgaris* cells were also challenged with As(V) (Murray et al., 2003), because according to the methylation pathway (Cullen, McBride and Reglinski, 1984), arsenosugars are the final products of the reiterative reduction/oxidative methylation sequence where As(V) has to be reduced in the presence of glutathione in the initial step.

When cells were exposed to DMA, the formation of one As-GS complex was observed ($DMAS^{V}$-GS) in addition to GSH, reduced PC_2 and oxidised PC_2.

Strong evidence for the existence of $DMAS^{V}$-GS is provided in the present study. The evidence is given in the form of molecular information: high resolution mass calculations, expressed as the difference between the theoretical mass and the experimental mass (section 4.3.2.2, Table 4.6), as well as MS/MS information (Appendix 4 Fig 7A4) along with elemental information: high resolution peak signals for arsenic and sulphur (section 4.3.2.2, Fig 4.34).

The formation of $DMAS^{V}$-GS has been regarded as the breakdown of a heavier complex molecule, rather than one synthesised via a specific mechanism (Bettencourt et al., 2011). One possible pathway for the formation of $DMAS^{V}$-GS is proposed here and is illustrated in Fig 5.1. When DMA is present in the cytosol, it is then complexed with GSH and cysteine rich protein. If the complex is not stable after extraction in proton rich conditions (1% formic acid), the protein will precipitate releasing soluble $DMAS^{V}$-GS.

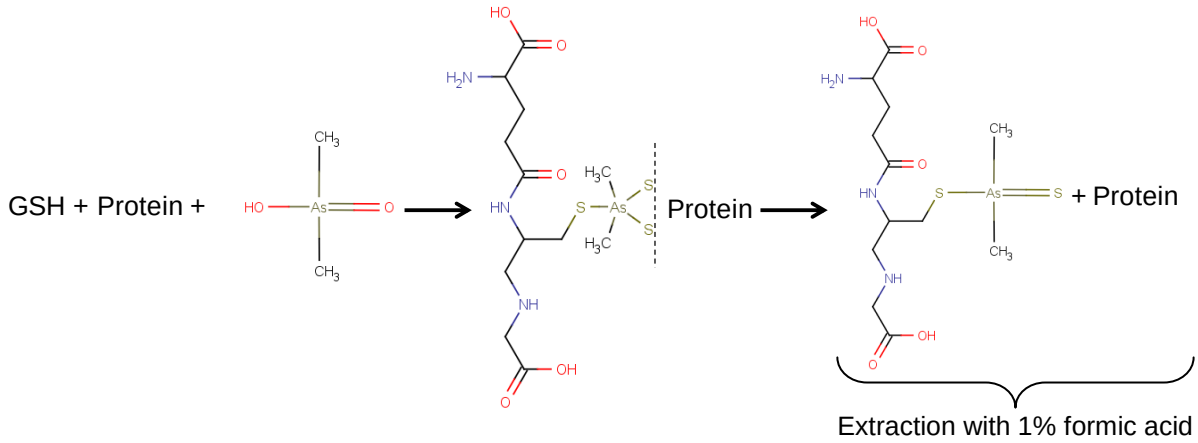

Fig 5. 1 Synthesis of $DMAS^{V}$-GS (m/z 444 $[M+H^{+}]$) from DMA, GSH and cysteine rich protein

Under the conditions used in this study (C_{18} column and a gradient elution with 0.1% formic acid (eluent A) and 99.9% HPLC grade methanol (eluent B)), reduced PC_2 co-eluted with $DMAS^V$-GS (section 4.3.2.2, Fig 4.34), signals for S and As were observed at the same elution time; even though the signal for arsenic can only come from $DMAS^V$-GS, the signal for PC_2 may have hampered the identification of $DMAS^V$-GS in other studies, since its presence has only been reported once *in vivo* (Raab et al., 2007).

In contrast, arsenic was complexed with GS/PC's and hGS/PC's when *C. vulgaris* cells were exposed to As(III).

Signals of eleven unbound peptides were observed and fully characterised, including GSH, desGly-GSH (GSH where Gly is absent), Ala-GSH (GSH where Gly is substituted by Ala) as well as free PC's, desGly-PC's and Ala-PC's along with some oxidised forms (GSSG, oxidised PC_2 and oxidised PC_3) (section 4.3.2.2, Fig 4.35).

Signals of free GSH/PC's and hGSH/PC's are more difficult to quantify and analyse at low concentrations. From the elemental point of view, sulphur is the only element in these molecules that can be quantified using ICP-MS, it has a poor ionisation in the ICP flame and therefore has high quantification limits: 4.9 $\mu g.L^{-1}$ for high resolution ICP-MS and 100 mg L^{-1} for quadrupole based ICP-MS (due to spectral interference, ^{32}S and $^{16}O_2+$, section 2.5.1.1, Table 2.4). From the molecular point of view, although free GSH/PC's and hGSH/PC's are easy to identify, the strong matrix effects make it very challenging to quantify using ESI-MS alone without the use of commercial standards (in order to perform standard addition as quantification method).

Another factor that makes quantification of free GSH/PC's and hGSH/PC's difficult is the fact that under the conditions used in this study several molecules co-eluted: oxidised PC_3 / GS-As(III)-PC_2, γ-(Glu-Cys)$_3$-Ala / As(III)-PC_3 / MMA(III)-PC_2 and γ-(Glu-Cys)$_2$ / reduced PC_2 (section 4.3.2.2 Fig 4.35 and 4.36).

Twelve signals of bound As-GS/PC were observed and fully characterised (section 4.3.2.2, Fig 4.36). Peaks for GS-As(III)-PC_2 (9.31 / 10.07 min), As(III)-$(PC_2)_2$ (13.23 / 14.12 min), As(III)-PC_4 (15.18 / 16.22 min), MMA(III)-PC_2 (11.42 / 12.17 min) and GS-As(III)-(Glu-Cys)$_2$ (8.14 / 8.89 min) showed two isomers. The presence of two

isomers (with the same m/z but eluting at different time) is mainly due to the presence of two separate peptide chains in the same molecule and has already been previously reported (Simmons and Emery, 2011). Their presence makes quantification and interpretation of the results also a more difficult task. A simplification of the structures of such molecules is shown in Fig 5.2.

Because the following complexes eluted at very similar retention times, the individual quantification of those complexes was not possible: GS-As(III)-PC_2 / GS-As(III)-(Glu-Cys)$_2$ (8.31 / 8.14 min), As(III)-PC_3 / MMA(III)-PC_2 (11.42 / 11.42 min), As(III)-PC_3 / As(III)-$(PC_2)_2$ (13.23 / 13.23 min) and As(III)-$(PC_2)_2$ / As(III)-(Glu-Cys)$_3$-Ala / As(III)-((Glu-Cys)$_2$)$_2$-Ala / MMA(III)-(Glu-Cys)$_2$-Ala (14.12 / 14.35 / 14.39 / 14.78 min).

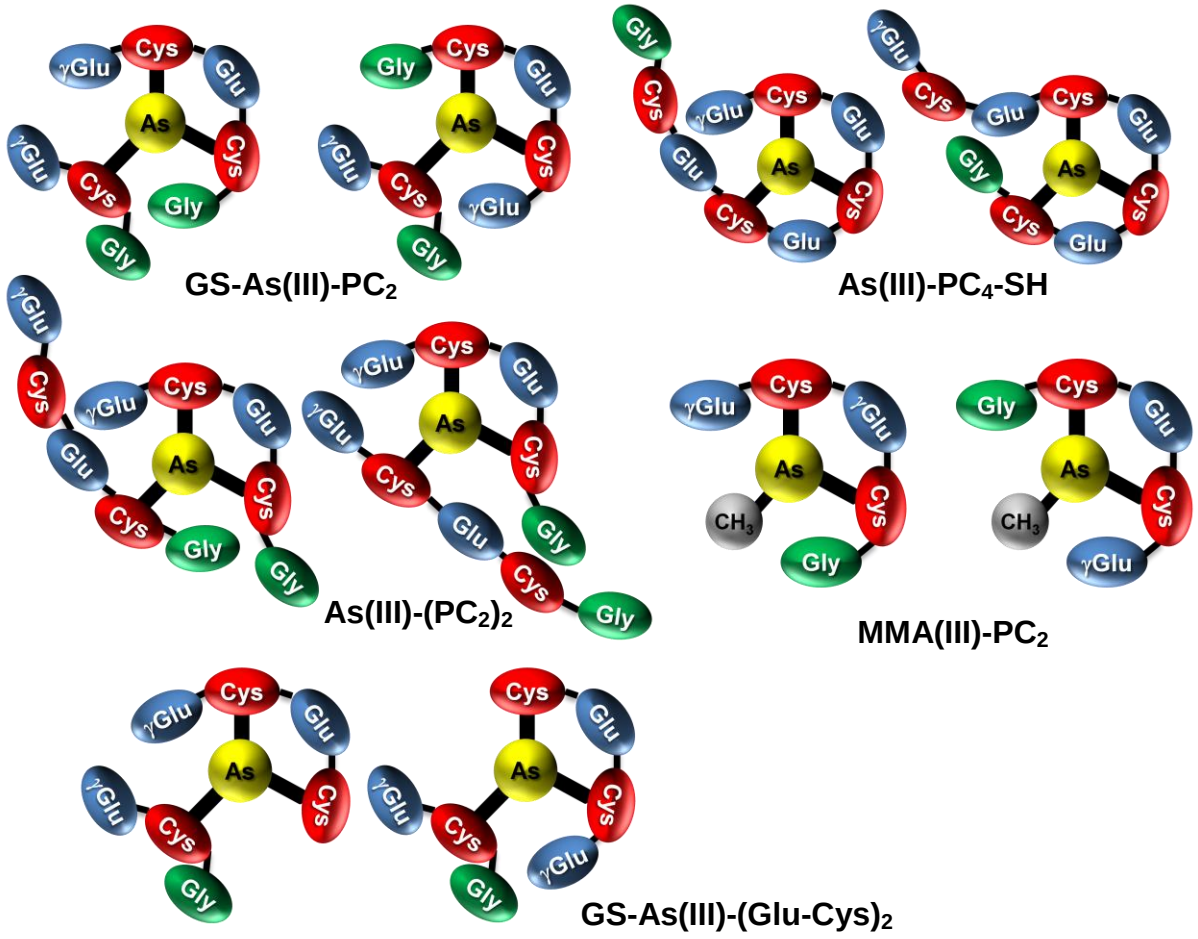

Fig 5. 2 Simplification of the structure in isomer forms observed for *C. vulgaris* cells exposed to 50 mg L^{-1} of As(III) for 48 h, extracted in 1% formic acid 30 s focused sonication.

The difference between the monoisotopic theoretical mass and the experimental mass did not exceed 2.04 ppm for any of the As-GS/PC complexes and 2.20 for As-

hGS/PC (section 4.3.2.2 Table 4.7). Although the difference in masses presented here does not comply with the requirements for unambiguous determination for the exact formulae (i.e. 0.018 ppm for m/z 740 for the range $C_{0\text{-}100,}$ $H_{3\text{-}74}$, $O_{0\text{-}4}$ and $N_{0\text{-}4}$) (Webb et al., 2004), it is mitigated by the fact that the results presented here include arsenic and sulphur in the formulae which makes the unambiguous requirement less rigorous. The data presented here also provided elemental information (ICP-MS signals for S and As) for each of the complexes. Moreover, the signals for GS-As(III)-PC_2, MMA(III)-PC_2, As(III)-PC_3, As(III)-$(PC_2)_2$, As(III)-PC_4, $DMAS^V$-GS, γ-(Glu-Cys)$_2$Ala, As(III)-(Glu-Cys)$_3$-Ala, As(III)-((Glu-Cys)$_2$)$_2$-Ala, MMA(III)-(Glu-Cys)$_2$-Ala (m/z 642), γ-(Glu-Cys)$_2$ and GS-As(III)-(Glu-Cys)$_2$ were strong enough to isolate and perform MS/MS analysis (Appendix 4, Fig 1A4-13A4).

The dissociation fragments for the molecules mentioned above are summarised in Table 1A4 (Appendix 4). Very similar fragments have been previously reported (Iglesia-Turiño et al., 2006; Wood et al., 2011; Liu et al., 2010; Chassaigne et al., 2001; Raab, Feldmann and Meharg, 2004). However, dissociation fragments have not been previously reported for the following complexes: As(III)-(Glu-Cys)$_3$-Ala, As(III)-((Glu-Cys)$_2$)$_2$-Ala, MMA(III)-(Glu-Cys)$_2$-Ala and GS-As(III)-(Glu-Cys)$_2$.

The results presented above provide extremely strong evidence for the existence of all these complexes.

When extraction using focused sonication was compared to extraction using the conventional method of grinding with liquid nitrogen, comparable results were obtained. Apart from the unequivocal reduction in time (1 h to 30 s) employed in the method proposed here, several peaks showed weaker signals for the conventional method, thus presenting another advantage that is closely linked with the enhanced stability of the complexes over time using the focused sonication technique.

a) Peak identification

The results found in the peak identification analysis were used to perform quantification; however some results gave only partial or incomplete information which precluded unequivocal identification of some peak signals from the quadrupole based ICP-MS method. Firstly, three arsenic peaks U1-U3 (section 4.3.2.2.b Fig

4.37) did not give enough information to match with their corresponding masses from the molecular analysis. This was because of their low intensity signal and early elution; in these conditions free GSH/PC's were eluting at the same time and thus hampered the analysis and correct identification of the arsenic signals for peaks U1-U3.

Secondly, arsenic signals for the following complexes could not be used for individual peak quantification because of their co-elution: P4 GS-As(III)-PC_2 / GS-As(III)-γ-$(Glu\text{-}Cys)_2$, P8 As(III)-PC_3 / MMA(III)-PC_2, P10 As(III)-PC_3 / As(III)-$(PC_2)_2$ and P11 As(III)-$(PC_2)_2$ / As(III)-γ-$(Glu\text{-}Cys)_3$-Ala / As(III)-γ-$((Glu\text{-}Cys)_2)_2$-Ala / MMA(III)-γ-$(Glu\text{-}Cys)_2$-Ala.

Nevertheless, the signals for the following individual complexes could be used for individual peak quantification, P5 As(III)-γ-$(Glu\text{-}Cys)_2$, P6 GS-As(III)-PC_2, P7 GS-As(III)-γ-$(Glu\text{-}Cys)_2$-Ala, P9 MMA(III)-PC_2, P12 As(III)-PC_4 and P13 As(III)-PC_4.

The results showed that all the peaks for arsenic signals eluting after 10 min correspond to As-GS/PC related complexes and therefore total formation of As-GS/PC complexes can be quantified by adding up all the individual signals, even though, the individual contribution of some peaks that co-eluted could not be quantified .

In the present study, the occurrence of oxidised PC_2, reduced PC_2, oxidised PC_3 and reduced PC_3 in *C. vulgaris* cells challenged with arsenic is reported for the first time. These peptides have only been reported in *C. vulgaris* in experiments using oxygen-free extraction with cells challenged with cadmium and selenate (Simmons and Emery, 2011; Simmons et al., 2009). It has also been reported that 90% of these peptides can be lost by freeze-drying alone; hence their presence in this study denotes stability of the extraction. The results presented in this study indicate that one of the most important factors in PC's and related molecules analysis is the stability of the complexes over time, rather than using oxygen-free conditions which is inherently more difficult to achieve. For this same reason some reported studies

on PC formation may have underestimated its presence, formation and role in metal(loid) detoxification.

Arsenic was complexed with GS/PC and hGS/PC only when exposed to As(III) inside *C. vulgaris* cells. We report the presence of GS-As(III)-PC_2, As(III)-$(PC_2)_2$, MMA(III)-PC_2, As(III)-PC_3 and As(III)-PC_4 in *C. vulgaris* cells which have not been previously documented. Its presence has been previously reported only in *Holcus lanatus*, *Pteris cretica* and *Helianthus annuus* (Raab, Feldmann and Meharg, 2004; Raab et al., 2007; Huang et al., 2008).

We also report for the first time the presence of $DMAS^V$-GS in *C. vulgaris* cells. The production of this complex *in vivo* has only been reported once in *Brassica oleracea* plants.

Inorganic pentavalent arsenic is predicted and never has been found to bind to soft sulphur in a bio-molecule (peptide). This assumption was made according to the Pearson's hard/soft acid-base (HSAB) concept (Raab et al., 2007). The presence of $DMAS^V$-GS then corroborates the view that the two methyl groups in DMA render hard inorganic pentavalent arsenic softer and therefore is an exemption for the HSAB concept.

To our knowledge, the presence of intact arsenic bound to hGS/PC has not been reported before. Thus we report for the first time As bound to hGS/PC in the following molecules: As(III)-γ-$(Glu\text{-}Cys)_3$-Ala, GS-As(III)-γ-$(Glu\text{-}Cys)_2$-Ala, As(III)-γ-$((Glu\text{-}Cys)_2)_2$-Ala, MMA(III)-γ-$(Glu\text{-}Cys)_2$-Ala, As(III)-γ-$(Glu\text{-}Cys)_2$ and GS-As(III)-γ-$(Glu\text{-}Cys)_2$.

It has been demonstrated in other studies that desGly-PCs are not generated as immediate by-products of PC synthase action when PC's are formed (Vatamaniuk et al., 2004). Moreover, it has also been demonstrated that the presence of desGly-GSH or Ala-GSH alone is sufficient for the formation of hPC's. Thus, PC synthase can catalyse the synthesis of hPC's without the need for a specific enzyme (Loscos et al., 2006). Therefore, the sole presence and production of desGly-GSH and Ala-GSH in C. vulgaris cells before production of hPCs is very important in the first instance. In this study unbound GSH/PCs were not quantified due to the high detection limits of sulphur using single quadrupole ICP-MS. However, the fact that

there is no reported production of As-hGS/PC complexes in the literature and the fact that these complexes can form without the need for a specific enzyme gives further evidence that the method used in the present study for extraction of As-GS/PC complexes promotes complex stability, otherwise other studies would have already reported the formation of As-hGS/PC that form parallel to As-GS/PC.

The effects on the substitution of the terminal amino acid Gly by Ala or its absence (desGly) in polypeptides have been studied mostly in helical regions of proteins. In such molecules, changes in the functional, conformational and stability properties of the protein have been observed (Margarit et al., 1992). The ability of arsenite to prevent metal interactions with the synthetic phytochelatin molecule $(Glu\text{-}Cys)_3$-Gly-Arg (PC_3R) and thus preventing aggregation of the metal-PC_3R complex has also been reported recently (Xia et al., 2012). However there are no studies related to changes in the properties of hGSH/PC when such substitutions take place *in vivo* or to changes in the properties of As-hGS/PC complexes.

The findings described above suggests that *C. vulgaris* possesses not only the mechanism for GS/PC complexation but also the specific transport system to store this complexes in the vacuole (with conditions suitable for stability such as acidic pH). This agrees with previously reported research in which PC production alone does not confer resistance to arsenic in *Arabidopsis thaliana* cells but a transport mechanism is needed too (Song et al., 2010).

There was no evidence for irreversible retention of arsenic or sulphur in the C_{18} column with recoveries of 94.27 and 98.24% for arsenic and sulphur respectively. This is a good indication that the interaction of the column with arsenic complexes is mild and favours complex integrity as described by Raab et al., (2004). Even when this group described the integrity of the complexes in a very specific column, it would appear that other C_{18} columns are suitable for separation of these complexes.

The maximum amount of methanol added to the ICP-MS for arsenic quantification was 3.6% (20% of 0.2 mL min^{-1}, in a 1.1 mL min^{-1} total flow rate). This amount of methanol led to a two fold increase on the arsenic signal. A correction factor for signal molecules eluting from 10 and until 32 min was calculated. The correction factors range from 0.5 to 0.95. Although the method is easy to use and suitable for a long elution profile (40 min), the base signal which is directly correlated to the MQL is

also affected by the methanol effect. This was not discussed by the authors in the original method (Amayo et al., 2011), but in general terms would lead to an increase of the MQL in the same order of magnitude as the correction factor for the methanol effect.

5.4.2.3. Quantitative analysis, kinetics and concentration effect experiments

MQL for arsenic at m/z 91 and sulphur at m/z 48 using different instruments and different collision cell parameters with the same collision gas (O_2) have been reported at 0.9 and 86 µg L^{-1} respectively. In this study, MQL were: 0.55 µg L^{-1} (SE = 0.067, n = 10) for arsenic at m/z 91 (O_2, CCT) and 20.20 µg L^{-1} (SE = 2.28, n=13) for sulphur at m/z 48 (O_2, CCT).

The quantification limits reported in the present study rank well among ICP-MS quadrupole based methods but are still short when compared with high resolution ICP-MS instruments (0.38 and 4.9 µg.L^{-1} for As and S), using derivatisation with p-hydroxymercuri-benzoic acid (0.48 pg L^{-1} for S) or with desolvation ICP-MS (7.7 and 5 µg L^{-1} for As and S). However this is a great improvement of normal ICP-MS without collision cells in which quantification limits are reported to be 3 µg L^{-1} for arsenic and 100 mg L^{-1} for sulphur. There are different advantages and disadvantages for the use of different techniques mentioned above and these are discussed in more detail elsewhere (Bluemlein et al., 2008; Wood and Feldmann, 2012) but choosing ICP-MS with O_2 as collision cell fulfilled the needs for quantification of arsenic at the levels observed in the present experiments using *C. vulgaris* cells and gave some insight on the levels of sulphur in the molecules complexed with arsenic as well as GSH and GSSG.

a) As(V)

It has been previously reported (using HPLC) that As(V) induces the production of GSH in *C. vulgaris* cells in 7 day exposure experiments (Jiang et al., 2011). However in the present study (using HPLC) there was insufficient evidence (ANOVA-GLM, $p > 0.05$, n = 3) to establish a difference in the levels of GSH in *C. vulgaris* cells exposed to 50 mg L^{-1} of As(V) at different exposure times and to different concentrations of

As(V) for 48 h (section 4.3.2.4.a, Fig 4.43). However, a moderate positive correlation was found for an increase in the level of total GSH (GSH+GSSG) with respect to treatment time (simple linear least squares, R^2 = 0.562, n = 3) and a weak positive correlation with respect to the concentration of arsenic in the media (simple linear least squares, R^2 = 0.144, n = 3).

Results in this study (using flow cytometry) have also shown a strong increase (Kolmogorov-Smirnov, D = 0.56, n = 20,000) in intracellular free thiols, where GSH is the most abundant, measured as CMFDA fluorescence after a 2 h exposure to As(V).

At first these results may seem contradictory; however this study has also found that *C. vulgaris* cells are not only able to synthesise GSH but also hGSH, which may have accounted for the difference found in CMFDA fluorescence (which measures all free thiols, not just GSH). There is also one difference regarding the level of phosphate in the two experiments, high phosphate (153.3 mg L^{-1} PO_4^{-3}) for the HPLC based method and low phosphate (0.3 mg L^{-1} PO_4^{-3}) for the flow cytometry based method. The justification for the difference in phosphate levels was because the method for HPLC quantification requires much more sample (200 mL per sample) and higher cell concentrations than the flow cytometry based method (where fluorescence is measured in individual cells and thus less than 1 mL of sample is needed). The compromise between toxic load and high biomass production at the selected exposure times (4 to 48h) for the HPLC method justifies this decision but makes the interpretation of the results more delicate.

As demonstrated in the toxicity experiments (section 4.1.1), at different concentrations of phosphate (153.3 mg L^{-1} PO_4^{-3} for the HPLC based method and 0.3 mg L^{-1} PO_4^{-3} for the flow cytometry method), the toxicity of As(V) is different, therefore the results for the two experiments are not comparative but complementary since the HPLC method gives quantitative information at conditions of low toxicity of As(V) and the flow cytometry method gives only qualitative information at conditions of high toxicity of As(V).

b) As(III)

Even when insufficient evidence (ANOVA-GLM, $p > 0.05$, $n = 3$) was found for a difference in the levels of reduced GSH due to exposure to 50 mg L^{-1} of As(III) over time, strong statistical evidence was found ($p <= 0.01$) for a reduction in the level of oxidised glutathione over time compared to the controls (without arsenic) as well as in the ratio of GSH/(GSH+GSG) (section 4.3.2.4.b, Fig 4.44A and Table 4.9). This indicates that even when the levels of GSH remained unchanged, the redox status was altered significantly. The results presented in this section are in accordance with results found in section 4.1.2.2 where negligible effect in CMFDA fluorescence was observed also indicating negligible change in intracellular GSH (Fig 4.20, Table 4.2, Kolmogorov-Smirnov, $D = 0.03$, $n = 20,000$).

One of the drawbacks of the analysis of free thiols using flow cytometry with CMDFA is that it only accounts for reduced thiols without giving information on the redox status, based on the concentration of total GSH (GSH+GSSG) and the concentration of oxidised GSSG. The information provided *in vitro* using the HPLC method agrees with and complements the observations found *in vivo* using flow cytometry.

Insufficient evidence (ANOVA-GLM, $p > 0.05$, $n = 3$) was found for a difference in the concentration of reduced GSH with an increase of As(III) concentration in the media. There was however some evidence ($p = 0.0319$) for a difference in the concentration of GSH and GSSG in the treatments for cells exposed to 100 mg L^{-1} compared to treatments with 200 mg L^{-1} As(III) (section 4.3.2.3.b, Fig 4.44B). This difference appeared to have been caused by errors in the handling of the samples in which cells need to be kept under logarithmic growth which is sometimes difficult to achieve.

Some statistical evidence (ANOVA-GLM, $p = 0.0191$, $n = 3$) was found (section 4.3.2.4.b, Fig 4.45 and Table 4.10) for an increase in the amount of As-GS/PC complexes with time. It would appear that cells are able to form As-GS/PC very rapidly upon exposure to As(III) with some of the peaks (U2, GS-As(III)-PC_2/GS-As(III)-γ-$(Glu\text{-}Cys)_2$, As(III)-γ-$(Glu\text{-}Cys)_2$, GS-As(III)-PC_2 and MMA(III)-PC_2) showing a significant increase after 72 h of exposure time. This agrees with information found in the toxicological experiments (section 4.1.1.a) where no difference in the lag phase period was observed between cells treated with As(III) and control cells (with no

arsenic added) indicating that the tolerance mechanism for As(III) may be constitutively expressed in *C. vulgaris* cells

In contrast, strong evidence was found for an increase in the production of bound As-GS/PC complexes with an increase in the concentration of As(III) in the media (section 4.3.2.4.b, Fig 4.46 and Table 4.11). Results for total arsenic bio-accumulated inside *C. vulgaris* cells (section 4.3.1.1, Fig 4.29 and 4.30) also showed that accumulation of arsenic was concentration rather than time dependent.

Often methods to measure GSH and related thiols rely on indirect determination with a derivatisation reaction or in conditions where bound As-GS/PC's are not stable and are even converted to free thiols by addition of reducing agents. This analytical methodology would account for the bound fraction of thiols into the unbound fraction. Also it has been found that other compounds such as coumarins may give false positive signals thus overestimating the amount of PC's and related molecules (Berlich et al., 2002). This also can explain the increased level of GSH over time found in other studies using derivatisation methods (Jiang et al., 2011) and not observed in the present investigation.

It would appear that immediately after cells are in contact with As(III), arsenic starts binding with GSH, which is the first step in PC formation and activation, GSH with S blocked groups (Vatamaniuk et al., 2000). Then the production of GSH is triggered or this is immediately recycled by reducing available GSSG leading to a reduction in GSSG levels and an imbalance in redox status.

Cells exposed to 50 mg L^{-1} of As(III) over different periods of time were able to complex/chelate up to 73 % of arsenic inside the cells to As-GS/PC's. When cells were exposed to different concentrations of As(III) for 48 h, they were able to complex more than 50% of the arsenic inside the cells and total accumulation of arsenic increased with an increase in concentration of As(III) in the media (section 4.3.2.4, Fig 4.48 and 4.49). This gave a strong indication that chelation of As(III) with GS/PC and to a lesser extent hGS/PC is a major detoxification mechanism employed by *C. vulgaris* cells when they are exposed to As(III).

c) DMA

Strong statistical evidence was found for a difference in the level of GSH and GSSG for treatments with 50 mg L^{-1} of DMA over 72 h compared to control experiments (section 4.3.2.4.c, Fig 4.47 and Table 4.12). However insufficient evidence (ANOVA-GLM, $p > 0.05$, $n = 3$) was found for a difference in the levels of GSH, GSSG and the ratio of GSH/(GSH+GSG) at any of the other exposure concentrations or exposure periods.

Only the formation of one complex was observed upon exposure to DMA: $DMAS^{V}$-GS. However only up to 3.1% of the total arsenic inside the cells exposed to different concentrations of DMA and over different exposure times was in $DMAS^{V}$-GS form. Even though the cells bio-accumulated increasing amounts of arsenic upon exposure to increasing amounts of DMA, the formation of $DMAS^{V}$-GS did not seem to be related to this fact. As mentioned in section 5.4.2.2, it would appeared that the formation of $DMAS^{V}$-GS is not part of a major detoxification mechanism but rather a by-product of another detoxification mechanism, perhaps the binding of DMA with rich cysteine proteins. In order to further investigate this assumption, an arsenic lipid-soluble fraction speciation analysis is needed which is out of the scope of the present investigation.

5.4.2.4. Vacuole compartmentalisation

Experiments involving transport inhibitors have commonly targeted cells expressing ABCC/MRP proteins in the plasma membrane (to export toxins) whereas in experiments involving vacuole sequestration in plant/algae cells, the inhibitors in addition of passing through the cell membrane have to be directed across the cytosol and then bind to the vacuole membrane to be effective.

Results found in this study have shown that MK571 (25 µM) was toxic (72 h tests) to the cells and in addition did not cause any further effect in the presence of arsenic (two-sample t-test, $p = 0.841$, $n = 3$) (section 4.3.2.5, Fig 4.50). The increase in toxicity when cells were exposed to MK571 is not rare as ABCC/MRP transporters are ubiquitously expressed in cells and are implicated in many natural processes, such as chlorophyll catabolite excretion and folate homologues storage into vacuoles (Kang et al., 2011).

Contrary to this, sodium taurocholate (50 µM) was not toxic to the cells nor was there a difference in toxicity observed when As(III) was added (two-sample t-test, p = 0.773, n = 3). Remarkably, probenecid (500 µM) had a significant stimulating effect on cell growth (p <= 0.001) that was reduced by the presence of 50 mg L^{-1} of As(III) to levels below those observed by control experiments (p = 0.021). It would appear that probenecid is permeable enough to cross the cell membrane, remain stable in the cytosol and then bind to the vacuole membrane, where it is capable of inhibiting ABCC transport. In this case it had both a reduction in cell growth with respect to the control (without arsenic) from 100 to 77% and with respect to the drug alone, from 133 to 77% (p <= 0.001) (section 4.3.2.5, Fig 4.50).

In other studies, 5 to 50 µM of MK571 and 0.1 to 2.0 mM of probenecid have been shown to reduce ABCC/MRP transport in ZF4 zebrafish cells by means of accumulation of Calcein-AM and rhodamine 123 (both substrates of ABCC/MRP proteins) in a concentration dependent manner with very similar inhibition. The two inhibitors showed an increase in toxicity of cells exposed to Cd, Hg and As(III) (with cells not being able to excrete the heavy metal(loids). In contrast, the inhibitors did not change the toxicity towards As(V) (Long et al., 2011).

When the effects of probenecid were investigated further, it was found that cells grew slightly more in the presence of 50 mg L^{-1} As(III) than control cells but the difference was not significant (two-sample t-test, p = 0.203, n =3) (section 4.3.2.5, Fig 4.51). Cells grew significantly more (51-59%) in presence of the inhibitor alone (no As(III), p <= 0.002). In contrast cells growing in the presence of both the inhibitor and As(III) showed a significant decrease in growth with respect to the control for treatments with 50, 150 and 300 µM probenecid (no probenecid and no As(III), p <= 0.001) and with respect to the inhibitor without As(III) for all treatments (p <= 0.01). However, there was no evidence that inhibition of growth in the presence of As(III) was dependent on the concentration of probenecid in the media.

Probenecid has been found to inhibit transport of several organic anions including prostaglandins, leukotrienes, glutathione, bilirubin, lactate and several fluorescent dyes. Moreover, the sequestration of the fluorescent dye Lucifer Yellow to vacuoles was possible to assess in J774 mouse peritoneal macrophages that express both transporters in the cellular and vacuolar membrane. The macrophage transporter

present within the plasma membrane was inhibited by 5 mM probenecid and this transport appeared to be faster than vacuolar sequestration, interestingly the inhibition was reversible after incubation in medium without probenecid (Steinberg et al., 1987; Steinberg, Swanson and Silverstein, 1988).

The closest investigation on ABCC transport inhibition in eukaryotic algae was carried out in the marine diatom *Thalassiosira rotula*. Verapamil, probenecid and MK571 were used as inhibitors of multidrug resistance P-glycoprotein (MDR1), organic anion transport and multidrug resistance-associated protein (MRP/ABCC) respectively, using the fluorescent dye Fura 2 acetoxymethylester (AM) as model substrate. Dye loading into the cells was only observed in the presence of MK571 at concentrations higher than 50 µM and not with the other inhibitors. The authors concluded that a MRP rather than MDR1 or organic anion transport was implicated (Scherer, Wiltshire and Bickmeyer, 2008).

ABCC vacuole transport was further investigated in the present study by using fluorescent substrates and flow cytometry. The two fluorescent substrates used BCECF (Kolmogorov-Smirnov, D = 0.43, n = 20,000) and CMFDA (D = 0.28) showed a moderate to strong shift in fluorescent signal intensity when cells were treated with MK571 (section 4.3.2.5.a / b, Fig 4.53C, D and F, and Table 4.13). BCECF only, showed a moderate shift in fluorescent signal intensity when cells were treated with probenecid (D = 0.18), section 4.3.2.5.a /b, Fig 4.53A, B and E, and Table 4.13.

Because the correct interpretation of the results needed more information, the fate of arsenic inside cells of *C. vulgaris* after exposure to 150 mg L^{-1} As(III) for 24 h, using the two inhibitors probenecid (50 µM) and MK571 (25 µM) was investigated (section 4.3.2.6).

Insufficient evidence to establish a difference in the amount of arsenic inside treated (probenecid) and control (non-treated) cells was found (two-sample t-test, $p > 0.05$, $n = 12$). There was however, strong evidence for a difference in the amount of arsenic inside treated (MK571) and control (non-treated) cells ($p = 0.005$, $n = 10$, Fig 5.54).

When ABCC/MRP transport is investigated using fluorescent substrates and the levels are measured *in vivo* (e.g. using flow cytometry), five scenarios are possible, as represented in Fig 5.3. When ABCC/MRP transport is expressed in the plasma

membrane in cells having no vacuoles, cells show less fluorescence than cells treated with a specific inhibitor of such transport. This is illustrated in Fig 5.3A. Fluorescent intensity with/without inhibitors will depend on the presence/absence of vacuole like organelles which can/cannot express ABCC/MRP transport. Fluorescent intensity will also depend on the size of the vacuole like organelles (Fig 5.3C and 5.3D). When the ABCC/MRP inhibitor is present, the fluorescence intensity would be expected to increase for cases illustrated in Fig 5.3A, 5.3B and 5.3C2. In contrast, lower fluorescence intensity would be expected for cases illustrated in Fig 5.3C1 and 5.3D.

When cells having vacuoles express ABCC/MRP transport in the plasma membrane but not in the vacuole membrane, the expected behaviour is the same as with cells having no vacuoles (Fig 5.3B) (Cordula, Karen and Ulf, 2008; Lebedeva, Pande and Patton, 2011; Long et al., 2011).

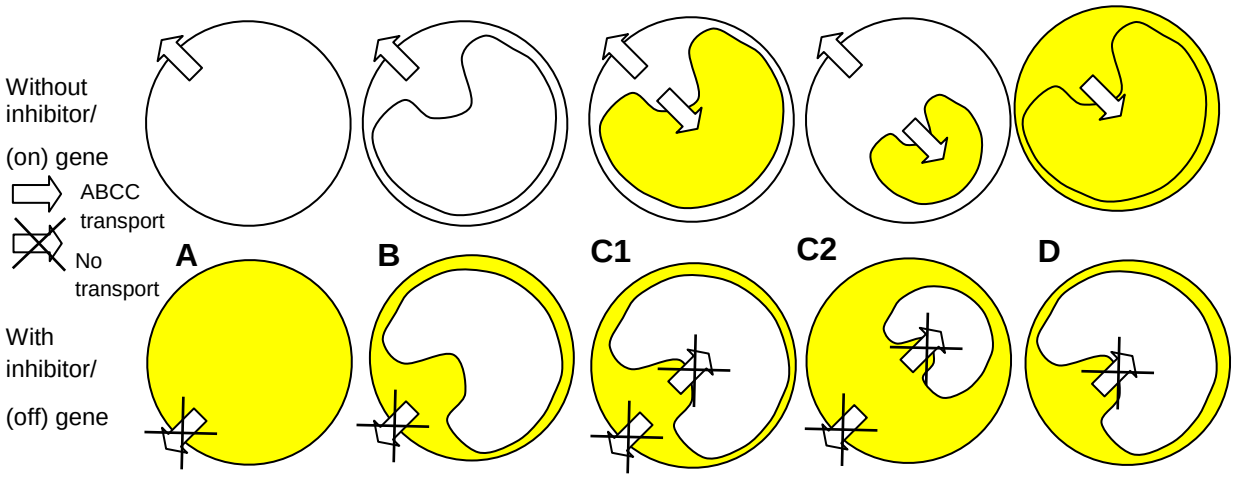

Fig 5. 3 ABCC/MRP activity assay in cells after exposure to fluorescent substrates (e.g. Calcein-AM, Fura2, Lucifer Yellow, BCECF, CMFDA) (fluorescence intensity indicated in yellow colour) with/without specific ABCC/MRP inhibitors (e.g. probenecid, MK571, taurocholate) or on/off gene silenced cells. ABCC/MRP expression in plasma membrane is observed in cases A, B, C. The presence of vacuole-like organelles is observed in cases B, C, D. ABCC/MRP expression in vacuoles and thus cells are able to incorporate fluorescent substrates inside vacuoles is observed in cases C, D only.

In contrast if cells express ABCC/MRP activity in the plasma and vacuole membranes, the interpretation of the results depends on microscopic observations or efflux measurements, because the difference in fluorescence intensity inside the cells alone depends on the size of the vacuoles themselves, as shown in Fig 5.3C(1)

and 5.3C(2). In Fig 5.3C(1) a higher intensity is expected in non-treated cells than in treated cells (ABCC/MRP inhibited) when vacuoles occupy a high volume of the cell. However, the behaviour is reversed when the vacuoles occupy a low volume of the cell, where a high fluorescence is expected in treated cells (ABCC/MRP inhibited) than non-treated cells [Fig 5.3C(2)] (Gayet et al., 2006; Forestier et al., 2003; Swanson, Bethke and Jones, 1998).

ABCC/MRP expression in plasma membranes in plants or cells having internal vesicles has rarely been reported. This is because the internal vesicles (vacuoles) also express ABCC/MRP transport which makes the interpretation of the results a more difficult task. Some evidence suggests that such transport is not active in plasma membranes of plants, but is triggered by high concentrations of xenobiotics inside the cells such in the case of the plant *Nicotiana plumbaginifolia* that is able to excrete the antifungal sclareolide using ABC transport only after relatively high concentration of the chemical is inside the cells (Jasinski et al., 2001).

Contradictory results were found in this study, where increased fluorescence was observed by treatment with the two inhibitors (60 min treatment time, section 4.3.2.5, Fig 4.53). This contrasted with the results for arsenic efflux experiments (24 h treatment) where a decrease in the amount of arsenic inside cells treated with MK571 compared with non-treated cells was observed (section 4.3.2.6, Fig 4.54).

In order to correctly interpret these results, further reference to the scenarios represented in Fig 5.3 should be undertaken. Firstly, the scenario described by Fig 5.3A is clearly not possible because plant cells do have acidic vacuoles. Secondly, the case scenario described by Fig 5.3B is not likely to be observed as it would not be beneficial for non-motile plant cells to only express transport proteins to extrude toxic substances in media where the substance can re-enter the cells. Finally, cases described in Fig 5.3C and 5.3D, although dependent on the toxic load/concentration of the chemical, are the most probable scenarios. Summarising, Fig 5.3C(2) scenario would explain the increase in fluorescent observed in treated cells, whereas Fig 5.3C(1) and 5.3D would both explain the decrease in concentration of arsenic inside treated cells. Nevertheless, in either case, strong statistical evidence has been found in this study for a difference in the behaviour of toxicity and accumulation of specific ABCC/MRP substrates (As-GS/PC, BCECF and CMFDA) upon exposure to the specific inhibitors probenecid and MK571(Fig 4.50, 4.51, 4.53, 4.54 and Table 4.13).

When the vacuolar arsenic-PC transporter (atABCC1/2) was reported for the first time, vacuoles from model organisms were isolated to subsequently measure transport. Then, two *in vitro* strategies were used: vacuoles were inhibited by milimolar concentrations of vanadate and vacuoles taken from ABCC knockout plants. It was found that atABCC1 and atABCC2 were needed to mediate transport of PC conjugated with arsenic in addition for cells to be able to produce PC's (Song et al., 2010). However this strategy allows the analysis of only a handful of As-PC complexes due to their labile nature *in vitro*. Also the authors made the assumption that ABCC transport was not expressed in the plasma membrane of model organisms without further testing this assumption. More recently it has been found that these two transporters are also needed for cadmium and mercury PC conjugate transport using the same strategy (Park et al., 2012).

In order to unequivocally verify the results presented in this section, two strategies can be undertaken; Firstly, the isolation of vacuoles and the use of ABCC knockout cells as described by Song et al., (2010) can be performed to further test the ABCC transport in the same way as described in the present study. Secondly, the incorporation of Green Fluorescent Protein (GFP) into the ABCC transport genes as described by Geisler et al., (2004), to subsequently undertake microscopic observations to determine the exact site of ABCC expression after exposure to As(III).

The importance of the findings produced in the present study resides in two parts: firstly, it allows the experimentation of As-GS/PC complexes in living plant/algae cells without the disturbance and inconvenience of isolating organelles (vacuoles) for subsequent experimentation and secondly it permits the study of the As-GS/PC complex interaction with two inhibitors of ABCC1 and ABCC2 proteins that are needed for such transport, because As-GS/PC are difficult to synthesise and maintain due to their labile nature.

5.4.2.5. Protein phosphatase inhibition experiments

In this study, it was found a significant difference (two-sample t-test, $p = 0.0272$, $n = 3$) in the level of GSH for treatments with 50 mg L^{-1} of As(III) for 48 h and cantharidin whereas no evidence for a difference was found for the other inhibitors: tautomycin

and okadaic acid ($p > 0.05$). However there was some evidence for an increase in the level of GSSG for treatment with tautomycin ($p = 0.025$), okadaic acid ($p = 0.017$) and cantharidin ($p = 0.011$) (without arsenic) compared with control experiments (with arsenic) as well as a decrease in the ratio of GSH/(GSH+GSG) for treatment with okadaic acid ($p = 0.029$) and cantharidin ($p = 0.016$) (section 4.3.2.7, Fig 4.55).

Treatment with the inhibitors in the absence of arsenic, was enough to trigger an increase in the level of GSSG, reflected by a decrease in the ratio of GSH/(GSH+GSG). However, the presence of arsenic appeared to reverse the increase in GSSG levels and the decrease in the ratios of GSH/(GSH+GSG) to those observed in control experiments (with arsenic and no inhibitors) with the exemption of cantharidin that showed a significant increase in the level of reduced GSH as well as GSSG (section 4.3.2.7, Fig 4.55A). In addition, a significant increase in the levels of bound As-GS/PC complexes was found for cells treated with cantharidin for peaks: P8 (As(III)-PC_3 / MMA(III)-PC_2) and P11 (As(III)-$(PC_2)_2$ / As(III)-γ-$(Glu\text{-}Cys)_3$-Ala / As(III)-γ-$((Glu\text{-}Cys)_2)_2$-Ala / MMA(III)-γ-$(Glu\text{-}Cys)_2$-Ala), (section 4.3.2.7 Fig 4.56).

The fact that cantharidin appeared to have induced an increase in the levels of GSH and As-GS/PC complexes whereas tautomycin did not, suggests that protein phosphatase PP2A and PP4 rather than PP1 (section 2.4.2.3.c, Table 2.2) may be implicated in PC's regulation pathway and therefore activation and synthesis of PC's. It should be noted that treatment with okadaic acid at the concentration used in this experiment (1nM) should have triggered the same results as cantharidin. However results for levels of GSH and As-GS/PC's were not statistically different from the control treatments and therefore the role of protein phosphatases in the regulation of PC production needs to be further investigated, perhaps with different combinations of inhibitors and different ranges of concentration of these inhibitors as well as the measurement of unbound PC's.

5.4.2.6. GSH transport stimulation experiments

Insufficient evidence was found to establish a difference in the levels of reduced GSH for cells treated with the flavonoid apigenin and the calcium channel blocker verapamil (two-sample t-test, $p > 0.05$, $n = 3$) (section 4.3.2.8, Fig 4.57).

However, strong evidence was found for an increase in the level of total As-GS/PC complexes for cells treated with verapamil (two-sample t-test, p = 0.0049, n = 3) as well as some evidence for a difference in the level of peaks U1 (p = 0.0125), P4 (p = 0.0072), P5 (p = 0.0217), P6 (p = 0.0177), P8 (p = 0.0076), P9 (p = 0.0014) and P10 (p = 0.0029) (section 4.3.2.8 Fig 4.57).

It is to be noted, that experiments using the two stimulators have targeted GSH conjugates and not PC conjugates (Leslie, Deeley and Cole, 2003; Trompier et al., 2004). This can explain the reason for the apparent lack of stimulation in the level of total As-GS/PC complexes for treatment with apigenin. There are two roles of GSH in ABCC/MRP mediated transport; one in which GSH is the substrate of transport and the other by catalysing the transport of non-conjugated molecules. Flavonoids stimulate ABCC/MRP mediated GSH transport by increasing the affinity of the transporter for GSH and there is no evidence that a co-transport mechanism is enhanced (transport of the stimulator itself). In contrast the mode of action of verapamil is not fully understood (Laberge et al., 2007).

In this study none of the single GSH conjugates with arsenic were found to be formed, namely ATG, MADG and DMAG. Only the formation of $DMAS^{V}$-GS was observed when cells were exposed to DMA. Unfortunately GSH stimulation transport experiments were not performed upon exposure to DMA because a low production of $DMAS^{V}$-GS was observed. In order to perform these experiments, a correct assessment of lipid-soluble extraction efficiencies and lipid-soluble fraction arsenic speciation analysis are needed such as the one performed by Raab et al., (2013).

The formation of GS-As(III)-PC_2 was observed when the cells were exposed to As(III). This molecule is both conjugated with GSH and PC and for which no transport mechanism has been described so far.

Apigenin was found to stimulate the production of two complexes: As(III)-PC_3/ MMA(III)-PC_2 and MMA(III)-PC_2, none of them having single GS conjugates (section 4.3.2.8, Fig 4.58). In contrast verapamil was found to stimulate the production of total As-GS/PC as well as the following individual complexes: U1, GS-As(III)-PC_2 / GS-As(III)-γ-$(Glu\text{-}Cys)_2$, As(III)-γ-$(Glu\text{-}Cys)_2$, GS-As(III)-PC_2, As(III)-PC_3 / MMA(III)-PC_2, MMA(III)-PC_2 and As(III)-PC_3 / As(III)-$(PC_2)_2$. In this case there was a mixture of

single and multiple GSH conjugates that were stimulated by the calcium channel blocker verapamil. It would appear that stimulation is not exclusive to single GSH conjugates and that PC's and hPC's can also be subject to transport stimulation as well as the two ABCC1 and ABCC2 transport systems. However, in order to correctly investigate such effect, further investigations into optimisation of the concentration range of the stimulants would be of interest.

5.5. Genetic markers of arsenic resistance in *C. vulgaris*

In order to provide a deeper interpretation of the findings, a comparison was made at the genetic level with other organisms in order to evaluate their ability to produce PC's, hGSH, hPC and relate this to arsenic resistance. Such speculations can provide a predictive framework for such processes in other organisms.

The following genes were found to share similarity with genes implicated in arsenic resistance in *C. vulgaris* C-169 and model organisms: The ATP binding cassette ABCC1/2 (COCSUDRAFT_46284), ABCD1 (COCSUDRAFT_65142), ABCD2 (COCSUDRAFT_16703), the phytochelatin synthase (COCSUDRAFT_19902), homoglutathione syntethase (COCSUDRAFT_52209) and As(III) reductase (COCSUDRAFT_66432) (section 4.4, Table 4.14).

The results showed that 127-193 species shared similarity with genes related to arsenic resistance. However, only 22 species showed to express simultaneously the three genes known to be required to confer arsenic resistance via PC's chelation (ABCC1/2 and PCS1). From those 22 species, 20 species showed to express simultaneously four genes (ABCC1/2, PCS1 and gshs2 for Ala-GSH synthesis) (section 4.4, Table 4.14).

Interestingly from those 20 species, 6 have been reported to produce hPC's in addition to PC's as shown in Table 4.14 (Klapheck, Schlunz and Bergmann, 1995; Oven et al., 2002; Mounicou et al., 2001; Carrasco-Gil et al., 2011; Leopold, Gunther and Neumann, 1998). The analysis presented in this study can predict the occurrence of hGSH/PC's in the rest of the 14 species that share identity with the genes for phytochelatin synthase, ABCC transport system to the vacuoles as well as hGSH/PC production.

Several attempts have been made to enhance arsenic resistance and accumulation in organisms via overexpression of genes implicated in either PC production (PCS phytochelatin synthase) or As-PC compartmentalisation to vacuoles (ABCC transport proteins). However, contradictory results have been achieved in which overexpression of PC synthase has led to hypersensitive mutants (Lee et al., 2003; Li et al., 2004; Wojas et al., 2008) and ABCC knock-out mutants that continue to exhibit PC accumulation into vacuoles (Prévéral et al., 2009; Sooksa-nguan et al., 2009). These attempts did not considered or were done before the discovery that the two independent ABCC1 and ABCC2 proteins were required for As-PC transport (Song et al., 2010). Moreover, arsenic tolerance/resistance is mediated not only by PC production (PC synthase) or PC compartmentalisation by a single ABCC transport system but the two transport molecules are needed for complex transport to the vacuole (Mendoza-Cozatl et al., 2011).

In the present study, it was found that in addition to PC production, *C. vulgaris* are able to synthesise hPC, for which no transport system has been reported so far. It was also found that inhibitors of ABCC transport led to an increase in arsenic toxicity to *C. vulgaris* cells. However, there was some residual arsenic resistance (77.4-79.3%, Section 4.3.2.5 Fig 4.50 and 4.51) that can be explained by the formation and compartmentalisation of As-hPC complexes by other transport system, perhaps ABCD1 and ABCD2. Even though, the role of ABCD1 and ABCD2 has been reported as the importation of acetyl coenzyme A to perixosomes for beta oxidation of fatty acids (Kang et al., 2011), the species found in the present analysis appeared to share high identity with genes implicated in arsenic resistance and are perhaps involved in hGSH/PC transport. This is very important because so far arsenic resistance based on formation and compartmentalisation of As-hPC has not been described so far. The study of arsenic resistance and PC production in the 20 species reported in section 4.4, Table 4.14 can help to give evidence to support the hypothesis that As-hPC production and compartmentalisation play a key role in arsenic resistance in other organisms.

The results presented in this section can also help to improve arsenic resistance and accumulation in organisms via overexpression of the following genes from *C. vulgaris*: ATP binding cassette ABCC1/2 (COCSUDRAFT_46284), ABCD1

(COCSUDRAFT_65142), ABCD2 (COCSUDRAFT_16703), phytochelatin synthase (COCSUDRAFT_19902) and homoglutathione syntethase (COCSUDRAFT_52209). This constructive strategy for gene cloning is intended to avoid the pitfalls made in the past by other researchers (Lee et al., 2003; Li et al., 2004; Wojas et al., 2008) and also to maximise arsenic resistance and bioaccumulation.

5.6. Discussion Summary

This study aimed to examine the interactions of arsenic with the green microalgae *C. vulgaris* and the potential to bio-remediate arsenic from water. This has provided information about the factors affecting tolerance and toxicity of the interaction of arsenic with *C. vulgaris*.

Firstly, an improvement of arsenic extraction from *C. vulgaris* customized for GS/PC complex speciation analysis was achieved with 71.1% extraction efficiency. This made the analysis of GS/PC complex representative of the real conditions inside *C. vulgaris* cells.

Secondly, experiments regarding surface adsorption, arsenic efflux and speciation, more specifically arsenic reduction and oxidation, arsenic methylation and demethylation as well as the involvement of glutathione and phytochelatins, have given valuable information regarding the mechanisms underpinning such interactions. This study also points out to future experiments with very restricted conditions in order to further test the interaction of arsenic with *C. vulgaris*.

The mechanism and pathways found in the present investigation are illustrated and summarised in Fig 5.4.

Passive surface adsorption was found to be negligible for dry cells exposed to DMA and As(V). However, adsorption of As(III) was found to be an active process in the surface of *C. vulgaris* cells. It can be said that adsorption of As(III) was active because such adsorption did not show saturation as well as the fact that it followed a second order polynomial curve, being 17-18 times higher than that of As(V) and DMA under the same conditions respectively. This is shown in Fig 5.4(1).

Intracellular uptake, toxicity and the detoxification mechanisms to *C. vulgaris* cells differed significantly depending on the form of arsenic that the cells were exposed to.

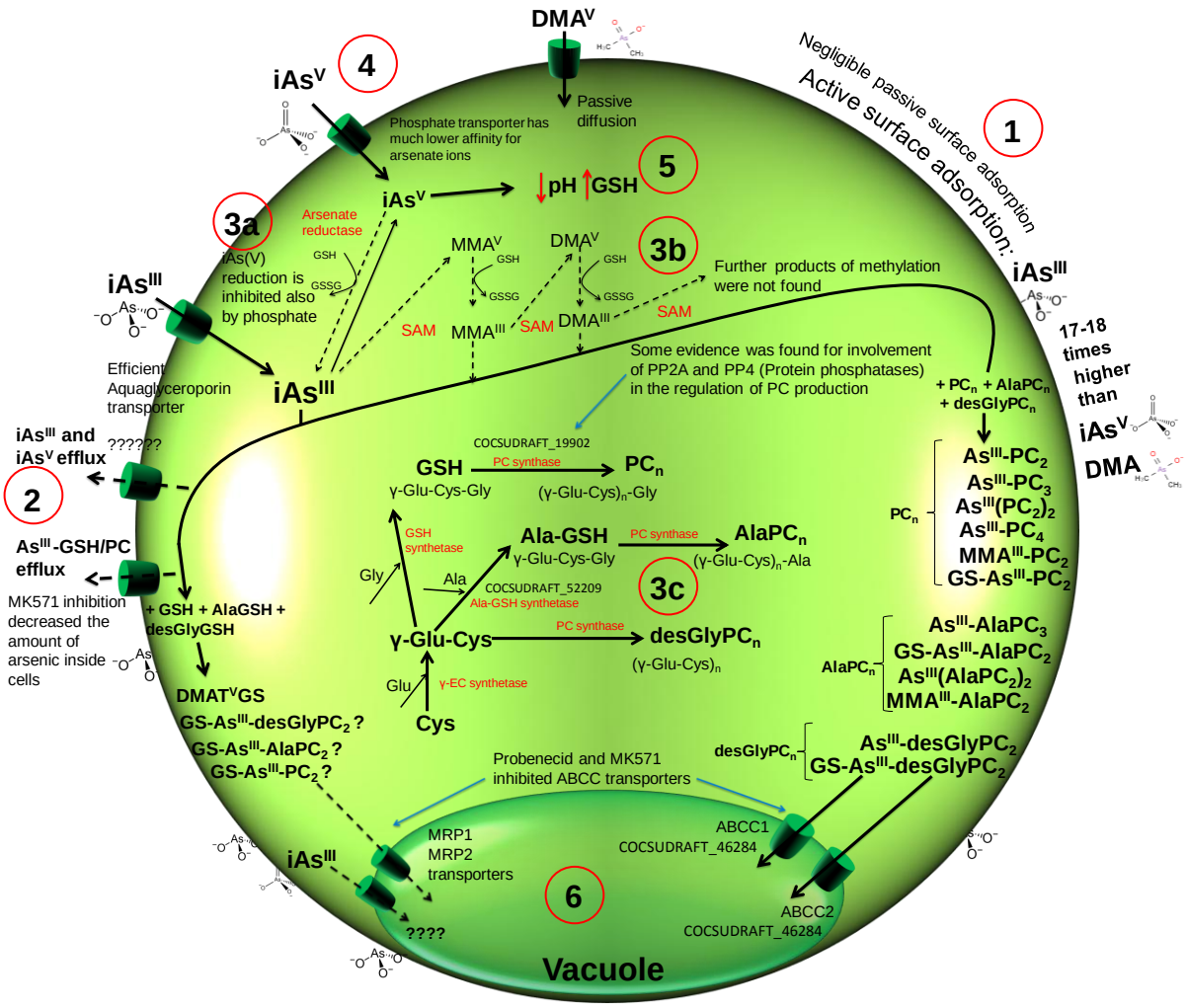

Fig 5. 4 Representation of the experimental proposed arsenic tolerance/toxicity mechanisms in *C. vulgaris* cells (1: surface adsorption, 2: efflux, 3a: reduction/oxidation, 3b methylation/demethylation, 3c: GS/PC complexation, 4: Phosphate channels, 5: As(V) toxic effects, 6: Vacuole compartmentalisation)

Uptake of As(V) was found to be 55 times lower than that of As(III) under the same conditions of high phosphate (1.62 mM of PO_4^{-3}) in the culture media. At this same condition, no toxic effects were observed for exposure to As(V) whereas a significant decrease in growth of 50% of the cells was observed at more than 50 mg L^{-1} of As(III). However, when the concentration of phosphate was lowered (to that observed in natural environments,3.2 µM of PO_4^{-3}), As(V) was 50 times more toxic

than As(III) to *C. vulgaris* cells whereas the toxicity of As(III) did not change with regard to the concentration of phosphate in the media.

The effects upon exposure to As(V) can be explained in the following way depending on the concentration of phosphate in the media:

At high concentration of phosphate (1.62 mM of PO_4^{-3}), poor adsorption of As(V) leads to low arsenic availability for intracellular uptake [Fig 5.4(1)]. Phosphate channels [Fig 5.4(4)] are much more efficient at transporting phosphate in the presence of As(V) than previously thought, at constant concentrations of 1.62 mM of PO_4^{-3} and over a range of As(V) concentrations from 0.013 - 2.67 mM. Intracellular uptake of As(V) was observed to be very poor whereas growth and therefore uptake of PO_4^{-3} was not affected. In addition to this, reduction of As(V) [Fig 5.4(3a)] mediated by phosphorolitic-arsenolitic enzymes is also inhibited by high concentrations of phosphate, which may be the reason for the absence of production/chelation of arsenic with GS/PC and related molecules [Fig 5.4(3c)]. The inhibitory effects on reducing enzymes are also likely to affect methylation and further formation of arsenosugars and other less toxic products [Fig 5.4(b)].

At low concentration of phosphate (3.2 µM of PO_4^{-3}), even though the production of GS/PC's was not explored in this study (due to low growth), strong evidence was found for an increase in the level of free thiols (where GSH is the most abundant) upon exposure to 13 µM of As at 3.2 µM of PO_4^{-3} for 120 min. A moderate decrease in intracellular pH was also observed as well as insufficient evidence for signals of oxidative stress in cells exposed under the same conditions [Fig 5.4(5)]. ATP is essential for reduction of As(V), GSH and PC formation as well as for vacuole compartmentalisation of GS/PC complexes (Zhao et al., 2009; Grill, Tausz and De Kok, 2002). However, immediately after As(V) enters the cells under a low phosphate environment, As(V) is capable of binding and disrupting chemical energy processes such as ATP utilisation (pH dependent) due to changes on intracellular pH. Moreover, a change in redox potential (given by an increase in the level of free thiols) also affects electrical NADPH energy processes (redox potential dependent). Therefore cells depleted of most of their energy (already under low phosphate concentration) are not likely to form GS/PC's, methylated arsenic products and arsenosugars upon exposure to As(V). Also high toxicity to As(V) is observed.

C. vulgaris cells formed $DMAS^{V}$-GS upon exposure to DMA. Toxicity of *C. vulgaris* to DMA was not affected by a change in the concentration of sulphur in the growth media. However, our observations indicate that a more suitable toxicity test should be used when investigating effects of DMA to *C. vulgaris* because strong sedimentation of the cells was observed whereas chlorophyll a and other pigments remained unchanged and therefore the effects of DMA were not correctly assessed with the methodology employed in this study. Also the formation of $DMAS^{V}$-GS was found not to be related to the concentration of arsenic in the media nor to the exposure time. This fact could mean that the formation of $DMAS^{V}$-GS is part of another detoxification mechanism and the complex is perhaps a fragment of a bigger molecule. If so, this molecule is likely to be lipid-soluble and therefore another analytical strategy is needed to perform extraction, separation and quantification of arsenic lipid-soluble fractions.

Uptake and toxicity of As(III) to *C. vulgaris* was found to be unrelated to the concentration of phosphate or sulphate in the growth media. Moreover, there was insufficient evidence for a difference of signals of oxidative stress, pH changes or the increase of free GSH. Instead of an increase of free GSH, GSH production was found to be related to the production of PC's, complexation of As(III) with GS/PC's and final compartmentalisation of the complexes to the vacuoles. It was also found that As(III) triggers the formation of hGSH/PC's, complexes of As(III) with hGS/PC's and compartmentalisation to the vacuoles as well.

C. vulgaris cells were resistant to surprisingly high concentrations of As(III) (IC_{50} of 55.33 mg L^{-1}). This resistance can be explained in the following way:

C. vulgaris cells are able to chelate As(III) in three ways, as pointed out in the genetic analysis and illustrated in Fig 5.4(3c). Cells are able to produce γ-EC synthetase, the enzyme responsible of producing γ-Glu-Cys. This is the first step in the production of GSH in which cysteine is the limiting substrate and is also feedback inhibited by the concentration of GSH (1.5 mM) itself (Grill, Tausz and De Kok, 2002). After this step, three alternatives exist: Firstly, the commonly described formation of GSH via the catalytic action of GSH synthetase, followed by the formation of PC's by the action of PC synthase (COCSUDRAFT_19902) upon exposure to As(III). Secondly, we found that cells are able to produce Ala-GSH via the catalytic action of

the enzyme Ala-GSH synthetase (COCSUDRAFT_52209); this is followed by the production of Ala-PC's, catalysed also by the action of the enzyme PC synthase (COCSUDRAFT_19902). This is because it has been demonstrated that there is no need for a specific enzyme for the production of hPC's (Loscos et al., 2006). Finally, the same PC synthase enzyme can catalyse the formation of desGly-PC's from desGly-GSH before GSH is formed as it has been demonstrated in the present study.

The three strategies mentioned above are followed by compartmentalisation to vacuoles. Vacuole compartmentalisation was tested by using specific ABCC/MRP inhibitors and fluorescent substrates [Fig 5.4(6)]. Some evidence was also found for ABCC/MRP related efflux into the media also mediated by ABCC/MRP1/2 transport [Fig 5.4(2)]. However, the latter needs to be further investigated perhaps with the use of isotopically labelled arsenic.

Some evidence was also found for the involvement of protein phosphatase PP2A and PP4 in the regulation of PC's synthesis. As well as some evidence for As-GS/PC transport stimulation by the flavonoid apigenin and the calcium channel blocker verapamil.

To recapitulate, the novel academic contributions that this study provides are:

- Toxicity experiments of arsenic to *C. vulgaris* under different conditions of phosphorus and sulphur.
- Enhanced arsenic extraction method customized for GSH/PC complex speciation analysis, this method facilitated to report for the first time:
    - The presence of oxidised PC_2, reduced PC_2, oxidised PC_3 and reduced PC_3 along with their arsenic bound complexes in *C. vulgaris* cells challenged with arsenic.
    - The presence of $DMAS^{V}$-GS in any algae.
    - The presence of intact arsenic bound to hGS/PC has not been previously reported in any organism: As(III)-γ-$(Glu\text{-}Cys)_3$-Ala, GS-As(III)-γ-$(Glu\text{-}Cys)_2$-Ala, As(III)-γ-$((Glu\text{-}Cys)_2)_2$-Ala, MMA(III)-γ-$(Glu\text{-}Cys)_2$-Ala, As(III)-γ-$(Glu\text{-}Cys)_2$ and GS-As(III)-γ-$(Glu\text{-}Cys)_2$.
- Vacuole compartmentalisation experiments using fluorescent substrates, specific ABCC inhibitors and flow cytometry techniques in green microalgae.
- Efflux experiments using specific ABCC inhibitors in green microalgae cells.

- Protein phosphatase inhibition experiments to investigate the role of PC production in *C. vulgaris* cells.
- GSH transport stimulation experiments using *C. vulgaris* cells.

Further studies are suggested regarding:

- Detailed methodologies describing toxicity indicators to microalgae taking into account the loss of buoyancy or rate of sedimentation when the toxicity of DMA is investigated.
- The investigation into the relationship between the low and high affinity phosphate channels and the transport of As(V) (by manipulation of the genes involved or by using isotopically labelled As(V) and phosphate
- The study of changes in the properties of hGSH/PC when such changes take place *in vivo* or changes in the properties of As-hGS/PC complexes
- The isolation of vacuoles and the use of ABCC knockout cells as described by Song et al., (2010), can be performed to further test ABCC transport in the same way as described in the present study.
- The incorporation of Green Fluorescent Protein (GFP) into the ABCC transport genes as described by Geisler et al., (2004) to subsequently undertake microscopic observations to determine the exact site of ABCC expression in *C. vulgaris* cells
- Optimization of the dose-response behaviour of protein phosphatase inhibitors to investigate the role of regulation of PC production as well as the use of different combinations of inhibitors
- Optimization of the dose-response behaviour of GS/PC transport stimulators
- The involvement of hGSH/PC production, detoxification and transport of heavy metal(loids) in the 14 species described in section 5.4, Table 4.14.

When the potential to bio-remediate arsenic from water is analysed, considerations for the full life cycle or the remediation strategy from start to finish in the context of all the possible implications or outcomes that might be generated have to be taken into account.

In this study, most of the variables that are of importance in the interaction of arsenic with *C. vulgaris* were investigated at short time exposure intervals (maximum 72 h).

The most important implications in terms of the potential to bio-remediate arsenic from water are:

- Under conditions of low phosphorus (3.2 µM of PO_4^{-3}) and in the presence of As(V), *C. vulgaris* are not likely to grow and be efficient at bio-remediating arsenic from water.
- Under conditions of high phosphorus (1.62 mM of PO_4^{-3}) and in the presence of As(V), *C. vulgaris* are highly likely to grow but are not likely to be efficient at bio-remediating arsenic from water. However the potential to transform As(V) into more toxic (for human life) As(III) is very low.
- Under any condition of phosphorus and in the presence of As(III), *C. vulgaris* have a high potential to bio-remediate arsenic from water, by storing As(III) into the cell biomass while having significantly high growth rates.

This makes the potential of *C. vulgaris* cells highly selective to bio-remediate the more dangerous As(III) without the potential hazard to reduce As(V) to As(III).

6. CONCLUSIONS

The results described in this study represent an important contribution to the development of a deeper understanding of the processes taking place when algal cells are challenged with arsenic. *Chlorella vulgaris* has an established potential as an organism for detoxification of arsenic contaminated drinking water. Given that arsenic contamination of drinking water remains a major global public health concern, continuing efforts, including the use of phytoremediation to optimise detoxification of contaminated water is warranted and, to this end, this study has enhanced the understanding of detoxification mechanisms of arsenic in *C. vulgaris* and contributed to potential future improved/optimised arsenic remediation techniques.

Because the main difficulty in the investigation of the mechanisms of arsenic interactions is extraction from *C. vulgaris* cells, a method was developed to enhance arsenic extraction customized for GSH/PC complex speciation analysis. In this way 71.1% extraction efficiency was achieved. This allowed the characterisation and quantification of intact complexes of As with glutathione and phytochelatins that have never been observed in *C. vulgaris* cells and made the analysis of GS/PC complexes representative of the real conditions inside *C. vulgaris* cells (Pantoja et al., 2014).

Surface adsorption was found to be negligible for *C. vulgaris* cells exposed to DMA and As(V). However, adsorption of As(III) was found to be an active process in the surface of *C. vulgaris* cells perhaps enhanced by internal chelation with rich small thiol molecules (GS/PC).

The results found in this study indicate that intracellular uptake, toxicity and the detoxification mechanisms of *C. vulgaris* cells respond in a different way depending on the form of arsenic that the cells were exposed to.

The effects on *C. vulgaris* after exposure to As(V) can be explained in a number of ways depending on the concentration of phosphate in the media: At high concentration of phosphate (1.62 mM of PO_4^{-3}); poor adsorption of As(V) leads to low arsenic availability for intracellular uptake. At low concentrations of phosphate (3.2 µM of PO_4^{-3}); strong evidence was found for an increase in the level of free thiols (where GSH is the most abundant). A moderate decrease in intracellular pH was also observed and there was insufficient evidence for signals of oxidative stress.

Chlorella vulgaris cells did not produce any GS/PC complexes when exposed to As(V).

Strong sedimentation of *C. vulgaris* cells exposed to DMA was observed that hampered the investigation of the toxic effects of this form of arsenic. It is therefore recommended a more suitable toxicity test when investigating effects of DMA on *C. vulgaris* cells. The formation of $DMAS^{V}$-GS was observed when *C. vulgaris* cells were exposed to DMA. The formation of $DMAS^{V}$-GS was found not to be related to the concentration of arsenic in the media nor to exposure time. This fact could mean that the formation of $DMAS^{V}$-GS is part of another detoxification mechanism and the complex is perhaps a fragment of a bigger molecule.

It was found that As(III) triggers the formation of hGSH/PC's, complexes of As(III) with hGS/PC's and compartmentalisation to the vacuoles. *Chlorella vulgaris* cells are able to chelate As(III) in three ways: cells are able to produce As-γ-Glu-Cys, As-Ala-GS and As-GS/PC complexes.

The findings suggest that there is ABCC/MRP related efflux into the media also mediated by ABCC/MRP1/2 transport. However, the latter needs to be further investigated perhaps with the use of isotopically labelled arsenic.

In addition, there is indication for the involvement of protein phosphatase PP2A and PP4 in the regulation of PC's synthesis as well as some evidence for As-GS/PC transport stimulation by the flavonoid apigenin and the calcium channel blocker verapamil.

The following empirical observations point to clear future directions in the design of more complete remediation strategies using *C. vulgaris* cells: *Chlorella vulgaris* cells have different potential to bioremediate arsenic depending on the arsenic form. Cells are not likely to grow or be efficient to bioremediate As(V) from water under a wide range of low phosphorus concentrations (3.2 µM to 1.62 mM of PO_4^{-3}). Moreover, the potential to transform As(V) into more toxic (for human life) As(III) is very low. Cells are highly likely grow and be efficient to bioremediate As(III) under any condition of phosphorus, by storing As(III) into the cell biomass while having significantly high growth rates.

All the above gives strong indication that the potential of *C. vulgaris* cells is highly selective and effective in the bio-remediation of the more dangerous As(III) (to human health) without the potential hazard to reduce As(V) to As(III).

Resistance to arsenic by *C. vulgaris* cells at the genetic level can help in the design of improved bioremediation strategies by cloning genes found to confer arsenic resistance to *C. vulgaris* in other organisms. These genes are ATP binding cassette ABCC1/2, ABCD1, ABCD2, phytochelatin synthase and homoglutathione syntethase. This strategy for gene cloning is intended to maximise arsenic resistance and bioaccumulation by producing and storing arsenic complexes with homophytochelatins as well as phytochelatins.

REFERENCES

Abedin, M.J., Feldmann, J. and Meharg, A.A. (2002) 'Uptake Kinetics of Arsenic Species in Rice Plants', *Plant Physiology*, vol. 128, pp. 1120-1128.

Afkar, E., Ababna, H. and Fathi, A.A. (2010) 'Toxicological Response of the Green Alga Chlorella vulgaris to some heavy metals', *Am J Environ Sci*, vol. 6, pp. 230-237.

Ahmed, K.M., Bhattacharya, P., Hasan, M.A., Akhter, S.H., Alam, S.M.M., Bhuyian, M.A.H., Imam, M.B., Khana, A.A. and Sracek, O. (2004) 'Arsenic enrichment in groundwater of the alluvial aquifers in Bangladesh: an overview', *Applied Geochemistry*, vol. 19, pp. 181–200.

Ahuja, S. (2008) *Arsenic Contamination of Groundwater*, Ne Jersey: John Wiley & Sons.

Altschul, S.F., Madden, T.L., Schäffer, A.A., Zhang, J., Zhang, Z., Miller, W. and Lipman, D.J. (1997) 'Gapped BLAST and PSI-BLAST: a new generation of protein database search programs', *Nucl. Acids Res*, vol. 25, no. 17, pp. 3389-3402.

Amayo, K.O., Petursdottir, A., Newcombe, C., Gunnlaugsdottir, H., Raab, A., Krupp, E.M. and Feldmann, J. (2011) 'Identification and Quantification of Arsenolipids Using Reversed-Phase HPLC Coupled Simultaneously to High-Resolution ICPMS and High-Resolution Electrospray MS without Species-Specific Standards', *Analytical Chemistry*, vol. 83, pp. 3589-3595.

Andersen, R.A. (2005) *Algal culturing techniques*, Burlington: Elsevier.

Anderson, C.L., Williams, J. and Hille, R. (1992) 'The purification and characterization of arsenite oxidase from Alcaligenes faecalis, a molybdenum-containing hydroxylase', *Journal of Biological Chemistry*, vol. 267, pp. 23674-23682.

Aragon, A. and Thompson, B. (2005) 'Rapid Small-Scale Column Testing for arsenic Adsorption Media', *Arsenic Water Technology Partnership's*.

Asano, T., Burton, F.L., Leverenz, H.L., Tsuchihashi, R. and Tchobanoglous, G. (2007) *Water Reuse: Issues, technologies, and applications.*, Metcalf & Eddie Inc.

Asku, Z. (1992) 'The biosorption of Cu (II) by C. vulgaris and Z. ramigera', *Environ Technol*, vol. 13, pp. 579-586.

ASTM (2004) *Standard Guide for Conducting Static Toxicity Tests with Microalgae*, West Conshohocken: ASTM International.

Bajguz, A. (2011) 'Suppression of Chlorella vulgaris growth by cadmium, lead, and copper stress and its restoration by endogenous brassinolide', *Arch Environ Contam Toxicol*, vol. 60, pp. 406-416.

Barhoumi, R., Bowen, J.A., Stein, L.S., Echols, J. and Burghardt, C. (1993) 'Concurrent Analysis of Intracellular Glutathione Content and Gap Junctional Intercellular Communication', *Cytometry*, vol. 14, pp. 747-756.

Barsanti, L. and Gualtieri, P. (2006) *Algae: Anatomy, Biochemistry and Biotechnology*, Florida: CRC Press.

Beceiro Gonzalez, E., Taboada de la Calzada, A., Alonso Rodriguez, E., Lopez Mahia, P., Muniategui Lorenzo, S. and Prada Rodriguez, D. (2000) 'Interaction between metallic species and biological substrates: approximation to possible interaction mechanisms between the alga Cholrella vulgaris and arsenic (III)', *Trends in Analytical Chemistry*, vol. 19, pp. 475-480.

Becker, J.S. (2007) *Inorganic Mass Spectrometry. Principles and Applications*, West Sussex: John Wiley & Sons Ltd.
Bentley, R. and Chasteen, T.G. (2002) 'Microbial Methylation of Metalloids: Arsenic, Antimony, and Bismuth', *Microbiology and Molecular Biology Reviews*, vol. 66, pp. 250–271.
Berlich, M., Menge, S., Bruns, I., Schmidt, J., Schneider, B. and Krauss, G.J. (2002) 'Coumarins give misleading absorbance with Ellman's reagent suggestive of thiol conjugates', *Analyst*, vol. 127, pp. 333-336.
Bettencourt, A.M., Filomena, M.D., Helena, M.F., Henriques, F.F., Madeira, P.A., Ines, P.M. and Filipe, L.V.B. (2011) 'Possible key intermediates in arsenic biochemistry: Synthesis and identification by liquid chromatography electrospray ionization mass spectrometry and high resolution mass spectrometry', *Microchemical Journal*, vol. 99, pp. 218-234.
Blaise, C. and Ferard, J.-F. (2005) *Small-Scale Freshwater Toxicity Investigations. Volume 1: Toxicity test methods*, Dordrecht: Springer.
Blasco, F., Gaudin, C. and Jeanjean, R. (1971) 'Absorption des ions arseniate par les Chlorelles. Reduction partielle de l'arseniate en arsenite', *Comptes Rendus de l'Académie des Sciences Serie D*, vol. 273, pp. 812-815.
Bluemlein, K., Raab, A. and Feldmann, J. (2009) 'Stability of arsenic peptides in plant extracts: off-line versus on-line parallel elemental and molecular mass spectrometric detection for liquid chromatographic separation', *Anal Bioanal Chem*, vol. 393, no. 1, pp. 358-366.
Bluemlein, K., Raab, A., Meharg, A.A., Charnock, J.M. and Feldmann, J. (2008) 'Can we trust mass spectrometry for determination of arsenic peptides in plants: comparison of LC–ICP–MS and LC–ES-MS/ICP–MS with XANES/EXAFS in analysis of Thunbergia alata', *Anal Bioanal Chem*, vol. 390, no. 7, pp. 1739-1751.
Bobrowicz, P., Wysocki, R., Owsianik, G. and Ulaszewski, S. (1997) 'Isolation of three contiguous genes, ACR1, ACR2 and ACR3, involved in resistance to arsenic compounds in the yeast Saccharomyces cerevisiae', *Yeast*, vol. 9, pp. 819-828.
Bold, H.C. (1949) 'The morphology of Chlamydomonas Chlamydogama Sp. Nov.', *Bulletin of the Torrey Botanical Club*, vol. 72, pp. 101-108.
Bosnjak, I., Uhlinger, K.R., Heim, W., Smital, T., Franekic-Kolic, J., Coale, K., Epel, D. and Hamdoun, A. (2009) 'Multidrug Efflux Transporters Limit Accumulation of Inorganic, but Not Organic, Mercury in Sea Urchin Embryos', *Environ Sci Technol*, vol. 43, pp. 8374–8380.
Boyer, M.J. and Hedley, D.W. (1994) 'Measurement of Intracellular pH', *Methods in Cell Biology*, vol. 41, pp. 135-148.
Broer, S., Ji, G., Broer, A. and Silver, S. (1993) 'Arsenic efflux governed by the arsenic resistance determinant of Staphylococcus aureus Plasmid pI258', *Journal of Bacteriology*, vol. 175, pp. 3480-3485.
Brown, T.A. (2010) *Gene Cloning and DNA analysis: An introduction*, 6th edition, John Wiley & Sons Ltd.
Carrasco-Gil, S., Alvarez-Fernandez, A., Sobrino-Plata, J., Millan, R., Carpena-Ruiz, R.O., Leduc, D.S., Andrews, J.C., Abadia, J. and Hernandez, L.E. (2011)

'Complexation of Hg with phytochelatins is important for plant Hg tolerance', *Plant cell and environment*, vol. 34, pp. 778-791.
Caussy, H. and Priest, N. (2008) 'Introduction to Arsenic Contamination and Health Risk Assessment with Special Reference to Bangladesh', *Reviews of Environmental Contamination and Toxicology*, vol. 197.
Chassaigne, H., Vaccina, V., Kutchan, T.M. and Zenk, M.H. (2001) 'Identification of phytochelatin-related peptides in maize seedlings exposed to cadmium and obtained enzymatically in vitro', *Phytochemistry*, vol. 56, pp. 657-668.
Cobbett, C. and Goldbrough, P. (2002) 'Phytochelatin and metallothioneins: Roles in heavy metal detoxification and homeostasis', *Annual Reviews on Plant Biology*, vol. 53, pp. 159-182.
Cole, L., Coleman, J., Evans, D. and Hawes, C. (1990) 'Internalisation of fluorescein isothiocyanate and fluorescein isothiocyanate-dextran by suspension-cultured plant cells', *J Cell Sci*, vol. 96, pp. 721-730.
Cole, L., Coleman, J., Kearns, A., Morgan, G. and Hawes, C. (1991) 'The organic anion trasport inhibitor, probenecid, inhibits the transport of Lucifer Yellow at the plasma membrane and the tonoplast in suspension-cultured plant cells', *J Cell Sci*, vol. 99, pp. 545-555.
Cordula, S., Karen, W. and Ulf, B. (2008) 'Inhibition of multidrug resistance transporters in the diatom Thalassiosira rotula facilitates dye staining', vol. 46, pp. 100-103.
Cornelis, R., Caruso, J., Crews, H. and Heumann, K. (2003) *Handbook of Elemental Speciation: Techniques and Methodology*, West Sussex: John Wiley & Sons Ltd.
Cossarizza, A., Ferraresi, R., Troiano, L., Roat, E., Gibellini, L., Bertoncelli, L., Nasi, M. and Pinti, M. (2009) 'Simultaneous analysis of reactive oxygen species and reduced glutathione content in living cells by polychromatic flow cytometry', *Nature Protocols*, vol. 4, no. 12, pp. 1790-1797.
Cullen, W.R., McBride, B.C. and Picke, A.W. (1990) 'The uptake of arsenicals by Candida humicola', *Applied Organometallic Chemistry*, vol. 4, pp. 119-125.
Cullen, W.R., McBride, B.C. and Reglinski, J. (1984) 'The reduction of trimethylarsineoxide to trimethylarsine by thiols: a mechanistic model for the biological reduction of arsenicals', *Journal of Inorganic Biochemistry*, vol. 21, pp. 45-60.
Daemen, E.A.M.J. (1986) 'Comparison of methods for the determination of Chlorophyll in estuarine sediments', *Netherlands Journal of Sea Research*, vol. 20, pp. 21-28.
Dean, J.R. (2005) *Practical Inductively Coupled Plasma Spectroscopy*, West Sussex: John Wiley & Sons Ltd.
Deneke, S.M. (2001) 'Thiol-Based Antioxidants', *Current Topics in Cellular Regulation*, vol. 36, pp. 151-180.
Dereeper, A., Audic, S., Claverie, J.M. and Blanc, G. (2010) 'BLAST-EXPLORER helps you building datasets for phylogenetic analysis', *BMC Evol Biol*, vol. 10, pp. 1-6.

Dogan, A.L., Legrand, O., Faussat, A.-M., Perrot, J.-Y. and Marie, J.-P. (2004) 'Evaluation and comparison of MRP1 activity with three fluorescent dyes and three modulators in leukemic cell lines', *Leukemia Res*, vol. 28, pp. 619-622.
Donmez, G.C., Aksu, Z., Ozturk, A. and Kutsal, T. (1999) 'Comparative study on heavy metal biosorption characteristics of some algae', *Process Biochemistry*, vol. 34, pp. 885-892.
Draper, M.P., Martell, R.L. and Levy, S.B. (1997) 'Active efflux of the free acid form of the fluorescent dye 2',7'-bis(2-carboxyethyl)-5(6)-carboxyfluorescein in multidrug-resistance-protein-overexpressing murine and human leukemia cells', *Eur J Biochem*, vol. 243, pp. 219-224.
Duncan, E., Foster, S. and Maher, W. (2010) 'Uptake and metabolism of arsenate, methylarsonate and arsonobetaine by axenic cultures of the phytoplankton Dunaliella tertiolecta', *Botanica Marina*, vol. 53, pp. 377-386.
Edmonds, J.S. and Francesconi, K.A. (1981) 'Arseno-sugars from brown kelp (Ecklonia radiata) as intermediates in cycling of arsenic in a marine ecosystem', *Nature*, vol. 289, pp. 602-604.
Everett, A.J. (1998) *Adsorption of metals by geomedia*, Academic press.
Feldmann, J. (2005) 'What can the different current detection methods offer for element speciation?', *Trends in Analytical Chemistry*, vol. 24, pp. 228-242.
Feldmann, J. (2008) 'Elemental and molecular mass spectrometry for speciation analysis', *Analytical Bioanalytical Chemistry*, vol. 390, pp. 1683–1684.
Feldmann, J. and Krupp, E.M. (2011) 'Critical review or scientific opinion paper: Arsenosugars—a class of benign arsenic species or justification for developing partly speciated arsenic fractionation in foodstuffs?', *Analytical and Bioanalytical Chemistry*, vol. 399, pp. 1735-741.
Forestier, C., Frangne, N., Eggmann, T. and Klein, M. (2003) 'Differential sensitivity of plant and yeast MRP (ABCC)-mediated organic anion transport process towards sulfonylureas', *Febbs Let*, vol. 554, pp. 23-29.
Francesconi, K.A. (2003) 'Working methods: Complete extraction of arsenic species: a worthwhile goal?', *Applied Organometallic Chemistry*, vol. 17, pp. 682-683.
Francesconi, K.A. and Kuehnelt, D. (2004) 'Determination of Arsenic species: a critical review and applications 2000-2003', *Analyst*, pp. 373-395.
Frankenberg, W.T. (2002) *Environmental Chemistry of Arsenic*, New york: Marcel Dekker, Inc.
Franklin, N.M., Stauber, J.L., Apte, S.C. and Lim, R.P. (2002) 'Effect of initial cell density on the bioavailability and toxicity of copper in microalgal bioassays', *Environmental Toxicology and Chemistry*, vol. 21, pp. 742-751.
Frendo, P., Harrison, J., Norman, C., Hernandez-Jimenez, M.J., Van-de-Sype, G., Gilabert, A. and Puppo, A. (2005) 'Glutathione and homoglutathione play a critical role in the nodulation process of Medicago truncatula', *Mol Plant Microbe Interact*, vol. 18, no. 3, pp. 254-259.
Friedl, T. and O'Kelly, C. (2002) 'Phylogenetic relationships of green algae assigned to the genus Planophila (Chlorophyta): evidence from 18S rDNA sequence data and ultrastructure', *European Journal of Phycology*, vol. 37, p. 373±384.

Garcia, S.S., Quijano, N.M. and Bonilla, S.M.M. (2006) 'Optimisation of sample treatment for arsenic speciation in alga samples by focused sonication and ultrafiltration', *Talanta*, vol. 68, pp. 522-1527.
Garelick, H., Jones, H., Dybowska, A. and Valsami-Jones, E. (2008) 'Arsenic pollution sources', *Reviews of Environmental Contamination*, vol. 197, pp. 17-60.
Gayet, L., Picault, N., Cazale, A.-C., Beyly, A., Lucas, P., Jacquet, H., Suso, H.-P., Vavasseur, A., Peltier, G. and Forestier, C. (2006) 'Transport of antimony salts by Arabidopsis thaliana protoplasts over-expressing the human multidrug resistance-associated protein 1 (MRP1/ABCC1)', *Febs Lett*, vol. 580, pp. 6891-6897.
Geisler, M., Girin, M., Brandt, S., Vincenzetti, V., Plaza, S., Paris, N., Kobae, Y., Maeshima, M., Billion, K., Kolukisaoglu, U.H., Schulz, B. and Martinoia, E. (2004) 'Arabidopsis Immunophilin-like TWD1 Functionally Interacts with Vacuolar ABC Transporters', *Molecular Biology of the Cell*, vol. 15, pp. 3393-3405.
Geiszinger, A., Goessler, W., Pedersen, S.N. and Francesconi, K.A. (2001) 'Arsenic biotransformation by the brown macroalga Fucus serratus', *Environmental Toxicology and Chemistry*, vol. 20, pp. 2255-2262.
Golubev, I.A. (2011) *Handbook of Bioremediation*, New York: Nova Science Publishers, Inc.
Gregus, Z., Roos, G., Geerlings, P. and Nemeti, B. (2009) 'Mechanism of Thiol-Supported arsenate reduction mediated by phosphorolytic-arsenolytic enzymes', *Toxicological Sciences*, vol. 110, pp. 282-292.
Grill, D., Tausz, M. and De Kok, L.J. (2002) *Significance of Glutathione to plant adaptation to the Environment*, Kluwer Academic Publishers.
Gulnaz, O. and Dincer, S. (2009) 'Biodegradation of Bisphenol a by Chlorella vulgaris and Aeromonas', *J Applied Biological Sciences*, vol. 3, pp. 79-84.
Guoa, J., Xua, W. and Ma, M. (2012) 'The assembly of metals chelation by thiols and vacuolar compartmentalization conferred increased tolerance to and accumulation of cadmium and arsenic in transgenic Arabidopsis thaliana', *Journal of Hazardous Materials*, vol. 199-200, pp. 309– 313.
Guo, H., Stuben, D. and Berner, Z. (2007) 'Adsorption of arsenic (III) and arsenic (V) from groundwater using natural siderite as the adsorbent', *Journal of Colloid Interface Science*, vol. 315, pp. 47-53.
Gusmao-Lima, A.I., Da-Cruz-eSilva, E. and Almeida-Figueira, E.M.P. (2012) 'Cd-induced signaling pathways in plants: Possible regulation of PC synthase by protein phosphatase 1', *Environmental and Experimental Botany*, vol. 79, pp. 31-36.
Hadjoudja, S., Deluchat, V. and Baudu, M. (2010) 'Cell surface characterisation of Mycrocystis aeruginosa and Chlorella vulgaris', *Journal of Colloid Interface Science*, vol. 342, pp. 293-299.
Harris, P.O. and Ramelow, G.J. (1990) 'Binding of metal ions by particulate biomass from Chlorella vulgaris and Scenedesmus quadricauda', *Environ Sci Technol*, vol. 24, pp. 220-228.
Hedley, D.W. and Chow, S. (1994) 'Evaluation of Methods for Measuring Cellular Glutathione Content Using Flow Cytometry', *Cytometry*, no. 15, pp. 349-358.

Henke, K.R. (2009) *Arsenic. Environmental Chemistry, Health Threats and Waste Treatment*, West Sussex: John Wiley and Sons.
Higashiva, T. and Yamada, T. (1991) 'Electrophoretic karyotyping and chromosomal gene mapping of Chlorella', *Nucleic Acids Res*, vol. 19, pp. 6191-6195.
Hill, S.J. (2007) *Inductively Coupled Plasma Spectrometry and its Applications*, Oxford: Blackwell Publishing Ltd.
Hirata, K., Tsuji, N. and Miyamoto, K. (2005) 'Biosynthetic Regulation of Phytochelatins, Heavy Metal-Binding Peptides', *J Biosci Bioeng*, vol. 100, no. 6, pp. 593-599.
Hoffmann, E. and Stroobant, V. (2007) *Mass Spectrometry. Principles and Applications*, West Sussex: John Wiley & Sons Ltd.
Holm-Hansen, O. and Booth, C.R. (1996) 'The Measurement of Adenosine Triphosphate in the Ocean and its Ecological Significance', *Limnology and Oceanography*, vol. 11, pp. 510-519.
Holm-Hansen, O., Sutcliffe, W.H. and Sharp, J. (1968) 'Measurement of Deoxyribonucleic Acid in the Ocean and its Ecological Significance', *Limnology and Oceanography*, vol. 13, pp. 507-514.
Huang, Z.C., Chen, T.B., Lei, M., Liu, Y. and Hu, T.D. (2008) 'Difference of Toxicity and Accumulation of Methylated and Inorganic Arsenic in Arsenic-Hyperaccumulating and -Hypertolerant Plants', *Environ. Sci. Technol*, vol. 42, pp. 5106–5111.
Iglesia-Turiño, S., Febrero, A., Jauregui, O., Caldelas, C., Araus, J.L. and Bort, J. (2006) 'Detection and Quantification of Unbound Phytochelatin 2 in Plant Extracts of Brassica napus Grown with Different Levels of Mercury', *Plant Physiology*, vol. 142, pp. 742–749.
Inthorn, D., Sidititoon, N. and Silapanuntakul, S. (2011) 'Sorption of mercury, cadmium and lead by microalgae', *Research Article Science Asia*, vol. 28, pp. 253-261.
Jang, M., Min, S.H., H, K.T. and K., P.J. (2006) 'Removal of Arsenite and Arsenate using Hydrous Ferric Oxide incorporated into naturally occurring porous diatomite', *Environmental Science and Technology*, vol. 40, pp. 1636-1643.
Janssen, C.R. and Heijerick, D.G. (2003) 'Algal toxicity tests for environmental risk assessment of metals', *Reviews of environmental Contamination and Toxicology*, vol. 178, pp. 23-52.
Jasinski, M., Stukkens, Y., Degand, H., Purnelle, B., Marchand-Brynaert, J. and Boutry, M. (2001) 'A Plant Plasma Membrane ATP Binding Cassette-Type Transporter Is Involved in Antifungal Terpenoid Secretion', *The plant cell*, vol. 13, pp. 1095–1107.
Jeanjean, R. and Blasco, F. (1970) 'Influence des ions arseniate sur l'absorption des ions phosphate par les chlorelles', *Comptes Rendus de l'Académie des Sciences Serie D*, vol. 270, pp. 1897-1900.
Jeanjean, R., Blasco, F. and Gaudin, C. (1971) 'L'absorption des ions arseniate par les chlorelles', *Comptes Rendus de l'Académie des Sciences Serie D*, vol. 272, pp. 64-67.

Jiang, Y., Purchase, D., Jones, H. and Garelick, H. (2011) 'Effects of arsenate on growth and production of glutathione and phytochelatins (PCs) in chlorella vulgaris.', *Int. J. Phytorem*, pp. 834-44.
Jones, H., Visoottiviseth, P., Bux, M.K., Foldenyi, R., Kovats, N., Borbely, G. and Galbacs, Z. (2008) *Case Reports: Arsenic Pollution in Thailand, Bangladesh and Hungary. In: Reviews of Environmental Contamination and Toxicology. Arsenic Pollution and Remediation: An International Perspective*, New York: Springer.
Kadar, A., Noel, L., Chekri, R., Vastel, C., Millour, S. and Guerin, T. (2011) 'Optimisation of ICP-MS collision/reaction cell conditions for the determination of elements likely to be interfered (V, Cr, Fe, Co, Ni, As and Se) in foodstuffs', *Talanta*, vol. 85, pp. 2605-2613.
Kala, S.V., Neely, M.W., Kala, G., Prater, C.I., Atwood, D.W., Rice, J.S. and Lieberman, M.W. (2000) 'The MRp2/cMoat transporter and arsenic-glutathione complex fromation are required for biliary excretion of arsenic', *The journal of Biological Chemistry*, vol. 275, pp. 33404-33408.
Kanaki, K. and Pergantis, S. (2008) 'Development of mass spectrometric methods for detecting Arsenic-Glutathione complexes', *Am Soc Mass Spectrom*, pp. 1559-1567.
Kang, J., Park, J., Choi, H., Burla, B., Kretzschmar, T., Lee, Y. and Martinoia, E. (2011) 'Plant ABC transporters', vol. 9, pp. 1-25.
Karajova, I.B., Slaveykova, V.I. and Tsalev, D.L. (2008) 'The biouptake and toxicity of arsenic species on the green microalga Chlorella salina in seawater', *Aquatic Toxicology*, vol. 87, pp. 264-271.
Karp, G. (2010) *Cell and Molecular Biology: Concepts and Experiments*, 6th edition, John Wiley & Sons, Inc.
Kawakami, S.K., Gledhill, M. and Achterberg, E.P. (2006) 'Determination of phytochelatins and glutathione in phytopalnkton from natural waters using HPLC with fluorescence detection', *Trends in Analytical Chemistry*, pp. 133-142.
Kirk, J.T.O. (1994) *Light and photosynthesis in aquatic ecosystems*, Cambridge: Cambridge Universtity Press.
Klapheck, S. (1988) 'Homoglutathione: isolation, quantification and occurrence in legumes', *Physiologia Plantarum*, pp. 727-732.
Klapheck, S., Schlunz, S. and Bergmann, L. (1995) 'Synthesis of Phytochelatins and Homo-Phytochelatins in Pisum sativum 1', *Plant Physiol*, vol. 107, pp. 515-521.
Knauer, K., Behra, R. and Hemond, H. (1999) 'Toxicity of inorganic and methylated arsenic to algal communities from lakes along an arsenic contamination gradient', *Aquatic Toxicology*, vol. 46, pp. 221-230.
Koch, I., Wang, L., Ollson, C.A., Cullen, W.R. and Reimer, K.J. (2000) 'The Predominance of Inorganic Arsenic Species in Plants from Yellowknife, Northwest Territories, Canada', *Environ. Sci. Technol.*, vol. 34, pp. 22-26.
Kohlmeyer, U., Kuballa, J. and Jantzen, E. (2002) 'Simultaneous separation of 17 inorganic and organic arsenic compounds in marine biota by means of high performance liquid chromatography/inductively coupled plasma mass spectrometry', *Rapid communications in mass spectrometry*, vol. 16, pp. 965-974.

Kong, Q., Zhu, L. and Shen, X. (2010) 'The toxicity of naphthalene to marine Chlorella vulgaris under different nutrient conditions', *J. Hazardous Mat*, vol. 178, pp. 282-286.
Krauthammer, M., Rzhetsky, A., Morozov, P. and Friedman, C. (2000) 'Using BLAST for identifying gene and protein names in journal articles', *Gene*, vol. 259, pp. 245–252.
Laberge, R.-M., Karwatsky, J., Lincoln, M.C., Leimanis, M.L. and Georges, E. (2007) 'Modulation fo GSH levels in ABCC1 expresing tumor cells triggers apoptosis through oxidative stress', *Biochemical Pharmacology*, vol. 73, pp. 1727-1737.
Lai, V.W.M., Cullen, W.R., Harrington, C.F. and Reimer, K.J. (1997) 'The characterization of arsenosugars in commercially available algal products including a Nostoc species of terrestrial origin', *Applied Organometallic Chemistry*, vol. 11, pp. 797-803.
Langsrud, S. and Sundheim, G. (1996) 'Flow cytometry for rapid assessment of viability after exposure to a quaternary ammonium compound', *Journal of Applied Bacteriology*, vol. 81, no. 4, pp. 411-418.
Lau, P.S., Tam, N.F.Y. and Wong, Y.S. (1996) 'Wastewater Nutrients Removal by Chlorella Vulgaris: Optimization Through Acclimation', *Environ Tech*, vol. 17, pp. 183-189.
Lebedeva, I.V., Pande, P. and Patton, W.F. (2011) 'Sensitive and Specific Fluorescent Probes for Functional Analysis of the Three Major Types of Mammalian ABC Transporters', *Plos One*, vol. 6, no. 7, pp. 1-12.
Lee, R.E. (2008) *Phycology*, Cambridge: Cambridge University Press.
Lee, S., Moon, J.S., Ko, T.S., Petros, D., Goldsbrough, P.B. and Korban, S.S. (2003) 'Overexpression of Arabidopsis phytochelatin synthase paradoxically leads to hypersensitivity to cadmium stress', *Plant Physiol*, vol. 131, pp. 656-63.
Leopold, I., Gunther, D. and Neumann, D. (1998) 'Application of high performance liquid chromatography - inductively coupled plasma mass spectrometry to the investigation of phytochelatin complexes and their role in heavy metal detoxification in plants', *Analusis*, vol. 26, no. 6.
Leslie, E.M. (2012) 'Arsenic–glutathione conjugate transport by the human multidrug resistance proteins (MRPs/ABCCs)', *Journal of Inorganic Biochemistry*, vol. 108, pp. 141–149.
Leslie, E.M., Deeley, R.G. and Cole, S.P. (2003) 'Bioflavonoid stimulation of glutathione transport by the 190-kDa multidrug resistance protein 1 (MRP1)', *Drug Metabolism and Disposition*, vol. 31, pp. 11-15.
Levy, J.L., Stauber, J.L., Adams, M.S., Maher, W.A., Kirby, J.K. and Jolley, D.F. (2005) 'Toxicity, Biotransformation and mode of action of arsenic in two freshwater microalgae (Chlorella sp. ans Monoraphidium Arcuatum)', *Environmental Toxicology and Chemistry*, vol. 24, pp. 2630-2639.
Liang, Y., Sarkany, N. and Cui, Y. (2009) 'Biomass and lipid productivities of Chlorella vulgaris under autotrophic, heterotrophic and mixotrophic growth conditions', *Biotechnology Letters*, vol. 31, pp. 1043-1049.

Li, Y., Dhankher, O.P., Carreira, L., Lee, D., Chen, A., Schroeder, J.I., Balish, R.S. and Meagher, R.B. (2004) 'Overexpression of Phytochelatin Synthase in Arabidopsis Leads to Enhanced Arsenic Tolerance and Cadmium Hypersensitivity', *Plant Cell Physiol*, vol. 45, pp. 1787-1797.
Lim, S.L., Chu, W.L. and Phang, S.M. (2010) 'Use of Chlorella vulgaris for bioremediation of textile wastewater', *Bioresour Technol*, vol. 19, pp. 7314-7322.
Liu, Z., Carbrey, J.M., Agre, P. and Rosen, B.P. (2004) 'Arsenic trioxide uptake by human and rat aquaglycerolporins', *Biochemical and Biophysical Research Communications*, vol. 316, pp. 1178-1185.
Liu, W.J., Wood, B.A., Raab, A., McGrath, S.P., Zhao, F.-J. and Feldmann, J. (2010) 'Complexation of arsenite with phytochelatins reduces arsenite efflux and translocation from roots to shoots in arabidopsis', *Plant Physiology*, pp. 2211-2221.
Lombi, E. and Holm, P.E. (2010) 'Metalloids, Soil Chemistry and the Environment', in Thomas, P.J. and Gerd, P.B. *MIPs and Their Role in the Exchange of Metalloids*, New York: Springer.
Long, Y., Li, Q., Wang, Y. and Cui, Z. (2011) 'MRP proteins as potential mediators of heavy metal resistance in zebrafish cells', *Comparative Biochemistry and Physiology, part C*, vol. 153, pp. 310-317.
Loscos, J., Naya, L., Ramos, J., Clemente, M.R., Matamoros, M.A. and Becana, M. (2006) 'A Reassessment of Substrate Specificity and Activation of Phytochelatin Synthases from Model Plants by Physiologically Relevant Metals', *Plant Physiology*, vol. 140, pp. 1213–1221.
Luan, T.G., Jin, J., Chan, M.S.N., Wong, Y.S. and Tam, N.F.Y. (2006) 'Biosorption and biodegradation of tributyltin (TBT) by alginate immobilized Chlorella vulgaris beads in several treatment cycles', *Process Biochemistry*, vol. 41, pp. 1560-1565.
Lui, G., Fernandez, A. and Cai, Y. (2011) 'Complexation of Arsenite with Humic Acid in the Presence of Ferric Iron', *Environmental Science and Technology*, vol. 45, pp. 3210–3216.
Lu, Y.-P., Li, Z.-S., Drozdowicz, Y.M., Hortensteiner, S., Martinoia, E. and Rea, P.A. (1998) 'AtMRP2, an arabidopsis ATP binding cassette transporter able to transport glutathione S-conjugates and chlorophyll catabolites: Functional comparisons with AtMRP1', *The Plant Cell*, vol. 10, pp. 267-282.
Lunde, G. (1977) 'Occurrence and Transformation of Arsenic in the Marine Environment', *Environmental Health Perspectives*, vol. 19, pp. 47-52.
Maeda, S., Arima, H., Ohki, A. and Naka, K. (1992) 'The association mode of arsenic accumulated in the freshwater alga Chlorella vulgaris', *Applied Organometallic Chemistry*, vol. 6, pp. 393-397.
Maeda, S., Kumamoto, T., Yonemoto, M., Nakajima, S. and Takeshita, T. (1983) 'Bioaccumulation of arsenic by freshwater algae and the application to the removal of inorganic arsenic from an aqueous phase. Part 1. Screening of freshwater algae having high resistance to inorganic arsenic', *Separation science and technology*, vol. 18, pp. 375-385.

Maeda, S., Kusadome, K., Arima, H., Ohki, A. and Naka, K. (1992) 'Biomethylation of arsenic and its excretion by the algae Chlorella Vulgaris', *Applied Organometallic Chemistry*, vol. 6, pp. 407-413.
Maeda, S., Kusadome, K., H., A., Ohki, A. and Naka, K. (1992) 'Uptake and excretion of total inorganic arsenic by the freshwater alga Chlorella vulgaris', *Applied Organometallic Chemistry*, vol. 6, pp. 399-405.
Maeda, S., Mizoguchi, M., Ohki, A. and Takeshida, T. (1990) 'Bioaccumulation of Zinc and Cadmium in freshwater alga. Part 1, toxicity and accumulation', *Chemosphere*, vol. 21, pp. 953-963.
Maeda, S., Nakashima, S., Takeshida, T. and Shiro, H. (1985) 'Bioaccumulation of arsenic by freshwater algae and the application to the removal of inorganic arsenic from an aqueous phase. Part II. By Chlorella vulgaris isolated from arsenic-polluted environment', *Separation Science and Technology*, vol. 20, pp. 153-161.
Maeda, S., Ohki, A., Tokuda, T. and Ohmine, M. (1990) 'Transformation of arsenic compounds in a freshwater food chain', *Applied Organometallic Chemistry*, vol. 4, pp. 251-254.
Maloney, T.E., Donovan Jr., E.J. and Robinson, E.L. (1962) 'Determination of Numbers and Sizes of Algal Cells with an Electronic Particle Counter', *Phycologia*, vol. 2, pp. 1-8.
Margarit, I., Camagnoli, S., Frigerio, F., Grandi, G., De-Filippis, V. and Fontana, A. (1992) 'Cumulative stabilizing effects of glycine to alanine substitutions in Bacillus subtilis neutral proteas', *Protein Eng*, vol. 5, no. 6.
Masella, R. and Mazza, G. (2009) *Glutathione and sulfur aminoacids in human health and disease*, John Wiley & Sons, Inc.
Mayer, P., Cuhel, R. and Nyholm, N. (1997) 'A simple in vitro fluorescence method for biomass measurements in algal growth inhibition tests', *Water Research*, vol. 31, pp. 2525-2531.
Mcmaster, M.C. (2005) *LC/MS A Practical User's Guide*, New Jersey: John Wiley & Sons, Inc.
McSheehy, S., Szpunar, J., Morabito, R. and Quevauviller, P. (2003) 'The speciation of arsenic in biological tissues and the certification of reference materials for quality control', *Trends in Analytical Chemistry*, vol. 22, pp. 191-209.
Meharg, A.A. (2005) *Venomous Earth: How Arsenic Caused The World's Worst Mass Poisoning*, Hampshire: Mcmillan.
Meharg, A., Nylor, J. and Macnair, M. (1994) 'Phosphorus Nutrition of Arsenate-Tolerant and Non-tolerant Phenotypes of Velvetgrass', *Journal of Environmental Quality*, vol. 23, pp. 234-238.
Meier, J., Kienzl, N., Goessler, W. and Francesconi, K.A. (2005) 'The Occurrence of Thio-Arsenosugars in Some Samples of Marine Algae', *Environmental Chemistry*, vol. 2, pp. 304-307.
Mendoza-Cozatl, D.G., Jobe, T.O., Hauser, F. and Schroeder, J.I. (2011) 'Long-distance transport, vacuolar sequestration, tolerance, and transcriptional responses induced by cadmium and arsenic', *Current Opinion in Plant Biology*, vol. 14, pp. 554–562.

Meng, Y.-L., Liu, Z. and Rosen, B.P. (2004) 'As(III) and Sb(III) Uptake by GlpF and Efflux by ArsB in Escherichia coli', *Journal of Biological Chemistry*, vol. 279.
Miguens-Rodriguez, M., Pickford, R. and Thomas-Oates, J.E. (2002) 'Arsenosugar identification in seaweed extracts using high-performance liquid chromatography/electrospray ion trap mass spectrometry', *Rapid Commun Mass Spectrom.*, vol. 16, pp. 323-331.
Mohan, D. and Pittman, C.U. (2007) 'Arsenic removal from water/wastewater using adsorbents. A critical review', *Journal of Hazardous Materials*, vol. 142, pp. 1–53.
Moorhead, G. (2007) *Protein Phosphatase Protocols*, Totowa: Humana Press.
Mounicou, S., Vacchina, V., Szpunar, J., Potin-Gautier, M. and Lobonski, R. (2001) 'Determination of phytochelatins by capillary zone electrophoresis with electrospray tandem mass spectrometry detection (CZE-ES MS/MS)', *Analyst*, vol. 126, pp. 624-632.
Munoz, R. and Guieysse, B. (2006) 'Algal-bacterial processes for the treatment of hazardous contaminants: A review', *Water Research*, vol. 40, pp. 2799-2815.
Murray, L.A., Raab, A., Marr, L.L. and Feldmann, J. (2003) 'Biotransformation of arsenate to arsenosugars by Chlorella vulgaris', *Applied Organometallic Chemsitry*, vol. 17, pp. 669-674.
Nelms, S.M. (2005) *ICP Mass Spectrometry Handbook*, Oxford: Blackwell Publishing Ltd.
Nemeti, B., Anderson, M. and Greus, Z. (2012) 'Glutathione synthase promotes the reduction of arsenate via arsenolysis of glutathione', vol. 94, pp. 1327-1333.
Nemeti, B., Regonesi, M.E., Tortora, P. and Greus, Z. (2010) 'Polynucleotide phosphorylase and mitochondrial ATP synthase mediate reduction of arsenate to the more toxic arsenite by forming arsenylated analogues of ADP and ATP', *Toxicological Sciences*, vol. 117, pp. 270-281.
Nobel, P.S. (2009) *Physicochemical and environmental plant physiology*, 4th edition, Oxford: Elsevier.
Nriagu, J.O. and Pacyna, J.M. (1988) 'Quantitative assessment of worldwide contamination of air, water and soils by trace metals', *Nature*, vol. 333, pp. 134-139.
Oparka, K.J., Murant, K.M., Wright, D.A. and Prior, D.A.M. (1991) 'The drug probenecid inhibits the vacuolar accumulation of fluorescent anions in onion epidermal cells', *J Cell Sci*, vol. 99, pp. 557-563.
Ortiz, D.F., Ruscitti, T., McCue, K.F. and Ow, D.W. (1995) 'Transport of metal-binding peptides by HTM1, a fission yeast ABC-type vacuolar membrane protein', *The Journal of Biological Chemistry*, vol. 270, no. 9, pp. 4721-4728.
Oven, M., Page, J.E., Zenk, M.H. and Kutchan, T.M. (2002) 'Molecular Characterization of the Homo-phytochelatin Synthase of Soybean Glycine max', *J Biol Chem*, vol. 277, no. 7, pp. 4747-4754.
Pandey, P.K., Yadav, S., Nair, S. and Bhui, A. (2002) 'Arsenic contamination of the environment A new perspective from central-east India', *Environment International*, vol. 28, pp. 235– 245.
Pantoja, L., Purchase, D., Jones, H., Feldmann, J. and Garelick, H. (2014) 'Enhanced determination of As-phytochelatin complexes in Chlorella vulgaris using

focused sonication for extraction of water-soluble species', *Anal Methods*, vol. 6, pp. 791-797.
Park, J., Song, W.Y., Ko, D., Eom, Y., Hansen, T.H., Schiller, M., Lee, T.G., Martinoia, E. and Lee, Y. (2012) 'The phytochealtin transporters AtABCC1 and AtABCC2 mediate tolerance to cadmium and mercury', *Plant Journal*, vol. 69, pp. 278-88.
Pawlik-Skowronska, B., Pirszel, J., Kalinowska, R. and Skowronski, T. (2004) 'Arsenic availability, toxicity and direct role of GSH and phytochelatins in As detoxification in the green alga Stichococcus bacillaris', *Aquatic Toxicology*, vol. 70, pp. 201-212.
Pedersen, S.N. and Francesconi, K.A. (2000) 'Liquid chromatography electrospray mass spectrometry with variable fragmentor voltages gives simultaneous elemental and molecular detection of arsenic compounds', *Rapid Communications in Mass Spectrometry*, vol. 14, pp. 641-645.
Peperzak, L. and Brussaard, C.P.D. (2010) 'Phytoplankton Viability Assay for Oil Compounds in Water', in Timmis, K.N. *Handbook of Hydrocarbon and Lipid Microbiology*, Springer Berlin Heidelberg.
Peperzak, L. and Brussaard, C.P.D. (2011) 'Flow cytometric applicability of fluorescent vitality probes on phytoplankton', *J Phycol*, vol. 47, pp. 692-702.
Perales-Vela, H.Y., Pena-Castro, J.M. and Canizares Villanueva, R.O. (2006) 'Heavy metal detoxification in eukaryotic microalgae', *Chemosphere*, vol. 64, pp. 1-10.
Perales-Vela, H.V., Pena-Castro, J.M. and Canizares-Villanueva, R.O. (2006) 'Heavy metal detoxification in eukaryotic microalgae', *Chemosphere*, vol. 64, pp. 1-10.
Phillips, D.J.H. (1990) 'Arsenic in aquatic organisms: a review emphasizing chemical speciation', *Aquatic Toxicology*, vol. 16, pp. 151-186.
Phinney, D.A. and Yentsch, C.S. (1985) 'A novel phytoplankton chlorophyll technique: toward automated analysis', *Journal of Plankton Research*, vol. 7, pp. 633-642.
Pickering, I.J., Prince, R.C., George, M.J., Smith, R.D., George, G.N. and Salt, D.E. (2000) 'Reduction and Coordination of Arsenic in Indian Mustard', *Plant Physiology*, vol. 122, pp. 1171–1177.
Prévéral, S., Gayet, L., Moldes, C., Hoffmann, J., Mounicou, S., Gruet, A., Reynaud, F., Lobinski, R., Verbatz, J.-M., Vavasseur, A. and Forestier, C. (2009) 'A common highly conserved cadmium detoxification mechanism from bacteria to humans: Heavy metal tolerance conferred by the ATP-binding cassette (ABC) transporter SpHMT1 requires glutathione but not metal-chelating phytochelatin peptides', *J Biol Chem*, vol. 284, pp. 4936–4943.
Price, C.A. (1957) 'A new thiol in legumes', *Nature*, vol. 180, pp. 148-149.
Raab, A., Feldmann, J. and Meharg, A.A. (2004) 'The Nature of Arsenic-Phytochelatin Complexes in Holcus lanatus and Pteris cretica', *Plant Physiol*, vol. 134, pp. 1113-1122.
Raab, A., Ferreira, K., Meharg, A.A. and Feldmann, J. (2007) 'Can Arsenic-phytochelatin complex formation be used as an indicator for toxicity in Helianthus annuus?', *Journal of Experimental Botany*, vol. 58, pp. 1333-1338.

Raab, A., Meharg, A.A., Jaspars, M., Genney, D.R. and Feldmann, J. (2004) 'Arsenic-Glutathione complexes- their stability in solution and during separation by different HPLC modes', *J. Anal. At. Spectrom.*, vol. 19, pp. 183-190.
Raab, A., Newcombe, C., Pitton, D., Ebel, R. and Feldmann, J. (2013) 'Comprehensive analysis of lipophilic arsenic species in a brown Alga (Saccharina latissima)', *Anal. Chem.*, no. 85, pp. 2817-2824.
Raab, A., Schat, H., Meharg, A.A. and Feldmann, J. (2005) 'Uptake, translocation and transformation of arsenate and arsenite in sunflower (Helianthus annus): formation of arsenic-phytochelatin complexes during exposure to high arsenic concentrations', *New phytologist*, vol. 168, pp. 551-558.
Raab, A., Wright, S.H., Japars, M., Meharg, M.A. and Feldmann, J. (2007) 'Pentavalent arsenic can bind to biomolecules', *Angew Chem Int Edit*, pp. 2594-2597.
Regaldo, L., Gagneten, A.M. and Troiani, H. (2009) 'Accumulation of chromium and interaction with other elements in Chlorella vulgaris', *J Environ Biol*, vol. 30, pp. 213-216.
Regmi, R., Milne, B.F. and Feldmann, J. (2007) 'Hydride generation activity of arsenosugars and thioarsenicals', *Analytical and Bioanalytical Chemistry*, vol. 388, pp. 775-782.
Rink, T.J., Tsien, R.Y. and Pozzan, T. (1982) 'Cytoplasmic pH and Free Mg 2+ in Lymphocytes', *Journal of Cellular Biology*, vol. 95, pp. 189-196.
Rosemberg, H., Gerdes, R. and Chegwidden, K. (1977) 'Two systems for the uptake of phosphate in Escherichia Coli', *Journal of Bacteriology*, vol. 131, pp. 505-511.
Rubio, R., Ruiz Chancho, M.J. and Lopez Sanchez, J.F. (2010) 'Sample pre-treatment and extraction methods that are crucial to arsenic speciation in algae and aquatic plants', *Trends in analytical Chemistry*, vol. 29, pp. 53-69.
Sandau, E., Pulz, P. and Zimmermann, O. (1996) 'Heavy metal sorption by Marine Algae and algal by-products', *Acta Biotechnology*, vol. 16, pp. 103-119.
Sayed, O.H. and El-Shahed, A.M. (2000) 'Growth, photosynthesis and circadian patterns in Chlorella vulgaris (Chlorophyta) in response to growth temperature', *Cryptogamie Algologie*, vol. 21, pp. 283–290.
Scherer, C., Wiltshire, K. and Bickmeyer, U. (2008) 'Inhibition of multidrug resistance transporters in the diatom Thalassiosira rotula facilitates dye staining', *Plant Physiol Biochem*, vol. 46, pp. 100-103.
Schmeisser, E., Goessler, W. and Kienzl, N. (2005) 'Direct measurement of lipid-soluble arsenic species in biological samples with HPLC-ICPMS', *Analyst*, vol. 130, pp. 948-955.
Schmidt, A.C., Koppelt, J., Neustadt, M. and Otto, M. (2007) 'Mass spectrometric evidence for different complexes of peptides and proteins with arsenic(III), arsenic(V), copper(II), and zinc(II) species', *Rapid Communications in Mass Spectrometry*, vol. 21, pp. 153-163.
Simmons, D.B.D. and Emery, R.J.N. (2011) 'Phytochelatin induction by selenate in Chlorella vulgaris, and regulation of effect by sulfate levels', *Environmental Toxicology and Chemistry*, vol. 30, pp. 469-476.

Simmons, D.B.D., Hayward, A.R., Hutchison, T.C. and Emery, R.J.N. (2009) 'Identification and quantification of glutathione and phytochelatins from Chlorella vulgaris by RP-HPLC ESI-MS/MS and Oxygen-free extraction', *Anal. Bioanal. Chem.*, vol. 395, pp. 809-817.
Smith, R.D. and Walker, J.C. (1996) 'Plant Protein Phosphatases', *Annual Review of Plant Physiology and Plant Molecular Biology*, vol. 47, pp. 101-125.
Song, W.Y., Park, J., Mendoza-Cozatl, D., Suter-Grotemeyer, M., Shim, D., Hortensteiner, S., Geisler, M., Weder, B., Rea, P.A., Rentsh, D., Schroeder, J.I., Lee, Y. and Martinoia, E. (2010) 'Arsenic tolerance in Arabidopsis is mediated by two ABCC-type phytochelatin transporters', *PNAS*, vol. 107, pp. 21187-21192.
Sooksa-nguan, T., Yakubov, B., Kozlovskyy, V.I., Barkume, C.M., Howe, K.J., Thannhauser, T.W., Rutzke, M.A., Hart, J.J., Kochian, L.V., Rea, P.A. and Vatamaniuk, O.K. (2009) 'Drosophila ABC Transporter, DmHMT-1, Confers Tolerance to Cadmium: DmHMT-1 AND ITS YEAST HOMOLOG, SpHMT-1, are not essential for vacuolar phytochelatin sequestration', *J Biol Chem*, vol. 284, pp. 354-362.
Steeman-Neilson, E. (1952) 'The Use of Radioactive Carbon (C-14) for Measuring Organic Production in the Sea', *Journal du Conseil International pour Exploration de la Mer*, vol. 18, pp. 117-140.
Steinberg, T.H., Newman, A.S., Swanson, J.A. and Silverstein, S.C. (1987) 'Macrophages possess probenecid-inhibitable organic anion transporters that remove fluorescent dyes from the cytoplasmic matrix', *Journal of Cell Biology*, vol. 105, pp. 2695-2702.
Steinberg, T., Swanson, J. and Silverstein (1988) 'A prelysosomal compartment sequesters membrane-impermeant fluorescent dyes from the cytoplasmic matrix of J774 macrophages', *Journal of Cell Biology*, vol. 107, pp. 887-896.
Stevenson, R.J., Bothwell, M.L. and Lowe, R.L. (1996) *Algal Ecology, Freshwater bentic ecosystems*, San Diego: Academic Press.
Stolz, J.F., Basu, P., Santini, J.M. and Oremland, R.S. (2006) 'Arsenic and Selenium in Microbial Metabolism', *Annual Reviews of Microbiology*, vol. 60, pp. 107-130.
Suggett, D.J., Borowitzka, M.A. and Prásil, O. (2010) *Chlorophyll a Fluorescence in Aquatic Sciences: Methods and Applications*, Dordrecht: Springer Netherlands.
Suhendrayatna, Ohki, A., Kuroiwa, T. and Maeda, S. (1999) 'Arsenic compounds in the freshwater green microalgae Cholrella vulgaris after exposure to arsenite', *Applied Organometallic Chemistry*, vol. 13, pp. 127-133.
Sun, H. (2011) *Biological Chemistry of Arsenic, Antimony and Bismuth*, West Sussex: Wiley.
Swanson, S.J., Bethke, P.C. and Jones, R.L. (1998) 'Barley aleurone cells contain two types of vacuoles: Characterization of lytic organelles by use of fluorescent probes', *The plant cell*, vol. 10, pp. 685-698.
Taboada de la Calzada, A., Villa Lojo, M.C., Becerio Gonzalez, E., Alonso Rodriguez, E. and Prada Rodriguez, D. (1999) 'Accumulation of Arsenic (III) by chlorella vulgaris', *Applied Organometallic Chemistry*, vol. 13, pp. 159-162.

Templeton, D.M., Ariese, F., Cornelis, R., Danielsson, L.-G., Muntau, H., Van Leeuwen, H.P. and Lobinski, R. (2000) 'Guidelines for terms related to chemical speciation and fractionation of elements', *Pure and Applied Chemistry*, vol. 72, pp. 1453-1470.
Thomas, J.P. and Gerd, B.P. (2010) *MIPs and Their Role in the Exchange of Metalloids*, New York: Springer.
Trompier, D., Chang, X.B., Barattin, R., Hardemare, A.D.M., Pietro, A.D. and Baubichon-Cortay, H. (2004) 'Verapamil and its derivative trigger apoptosis through glutathione extrusion by multidrug resistance protein MRP1', *Cancer Research*, vol. 64, pp. 4950-4956.
Tsuji, N., Hirayanagi, N., Okada, M., Miyasaka, H., Hirata, K., Zenk, M.H. and Miyamoto, K. (2002) 'Enhancement of tolerance to heavy metals and oxidative stress in Dunaliella tertiolecta by Zn-induced phytochelatin synthesis', *Biochem Biophys Res Comm*, vol. 293, pp. 653-659.
Tuan, L.Q., Huong, T.T.T., Hong, P.T.A., Kawakami, T., Shimanouchi, T., Umakoshi, H. and Kuboi, R. (2008) 'Arsenic (V) induces fluidization of algal cell and liposome membranes', *Toxicology in vitro*, vol. 22, pp. 1632-1638.
UNACCSWR (2012) *United Nations Synthesis Report on Arsenic in Drinking Water*, [Online], Available: http://www.who.int/water_sanitation_health/dwq/arsenic3/en/ [19 September 2012].
Uniprot, C. (2009) *UniProt*, [Online], Available: www.uniprot.org [16 July 2013].
Vatamaniuk, O.K., Mari, S., Lang, A., Chalasani, S., Demkiv, L.O. and Rea, P.A. (2004) 'Phytochelatin Synthase, a Dipeptidyltransferase That Undergoes Multisite Acylation with g-Glutamylcysteine during Catalysis', *The Journal of Biological Chemistry*, vol. 279, no. 21, pp. 224490-22460.
Vatamaniuk, O., Mari, S., Lu, Y. and Rea, P. (1999) 'AtPCS1, a phytochelatin synthase from Arabidopsis: isolation and in vitro reconstitution', *PNAS*, vol. 96, no. 12, pp. 7110-7115.
Vatamaniuk, O.K., Mari, S., Lu, Y.-P. and Rea, P.A. (2000) 'Mechanism of Heavy Metal Ion Activation of Phytochelatin (PC) Synthase', *The Journal of Biological Chemistry*, vol. 275, pp. 31451-31459.
Vatamanuik, O.K., Bucher, E.A., Ward, J.T. and Rea, P.A. (2001) 'A new pathway for heavy metal detoxification in animals: phytochelatin synthase is required for cadmium tolerance in Caenorhabditis elegans', *J. Biol. Chem*, vol. 276, pp. 20817-20820.
Wang, M., Feng, W., Lu, W., Li, B., Wang, B., Zhu, M., Wang, Y., Yuan, H., Zhao, Y. and Chai, Z. (2007) 'Quantitative analysis of proteins via sulfur determination by HPLC coupled to isotope dilution ICPMS with hexapole collision cell', *Analytical Chemistry*, vol. 79, pp. 9128-9134.
Wang, S. and Mulligan, C.N. (2006) 'Occurrence of arsenic contamination in Canada: Sources,behavior and distribution', *Science of the Total Environment*, vol. 366, pp. 701-721.

Wang, H.-C., Wu, J.-S., Chia, J.-C., Yang, C.-C., Wu, y.-J. and Juang, R.-H. (2009) 'Phytochelatin Synthase is regulated by protein phsophorylation at a threonine near its catalytic site', *Journal of Agricultural and Food Chemistry*, vol. 57, pp. 7348-7355.
Webb, K., Bristow, T., Sargent, M. and Stein, B. (2004) *Methodology for accurate mass measurement of small molecules*, Teddington: LGC Limited.
Weber, C.I. (1973) *Bioassay Techniques and Environmental Chemistry*, Ann Arbor: Science Publication, Inc.
Weiss, J., Theile, D., Ketabi-Kiyanvash, N., Lindenmaier, H. and Haefeli, W.E. (2007) 'Inhibition of MRP1/ABCC1, MRP2/ABCC2, and MRP3/ABCC3 by Nucleoside, Nucleotide, and Non-Nucleoside Reverse Transcriptase Inhibitors', *Drug metab Dispos*, vol. 35, pp. 340-344.
Widjaja, A., Chien, C.C. and Ju, Y.H. (2009) 'Study of increasing lipid production from fresh water microalgae Chlorella vulgaris', *Journal of the Taiwan Institute of Chemical Engineers*, vol. 40, pp. 13-20.
Willey, N. (2007) *Phytoremediation. Methods ans Reviews*, Totowa, New Jersey: Humana Press.
Wojas, S., Clemens, S., Hennig, J., Sklodowska, A., Kopera, E., Schat, H., Bal, W. and Antosiewicz, D.M. (2008) 'Overexpression of phytochelatin synthase in tobacco: distinctive effects of AtPCS1 and CePCS genes on plant response to cadmium', *J Exp Bot*, vol. 59, pp. 2205–2219.
Wong, W.S.F., Zhu, H. and Liao, W. (2007) 'Cysteinyl leukotriene receptor antagonist MK-571 alters bronchoalveolar lavage fluid proteome in a mouse asthma model', *European Journal of Pharmacology*, vol. 575, pp. 134-141.
Wood, B.A. and Feldmann, J. (2012) 'Quantification of phytochelatin and their metal(loid) complexes: critical assesment of currect analytical methodology', *Analytical and Bioanalytical Chemistry*, vol. 402, pp. 3299-3309.
Wood, B.A., Miyashita, S., Kaise, T., Raab, A., Meharg, A.A. and Feldmann, J. (2011) 'Arsenic is not stored as arsenite-phytochelatin in complexes in the seaweeds Fucus spiralis ans Hizikia fusiforme', *Environmental Chemistry*, vol. 8, pp. 30-43.
Xia, N., Shi, Y., Zhang, R., Zhao, F., Liu, F. and Liu, L. (2012) 'Simple, rapid and label-free colorimetric assay for arsenic based on unmodified gold nanoparticles and a phytochelatin-like peptide', *Analytical methods*, vol. 4, pp. 3937-3941.
Xu, Y., Ma, B. and Nussinov, R. (2012) 'Structural and functional consequences of phsophate-arsenate substitutions in selected nucleotides: DNA, RNA and ATP', *Physical Chemistry*, vol. 116, pp. 4801-4811.
Xu, X.Y., McGrath, S.P. and Zhao, F.J. (2007) 'Rapid reduction of arsente in the medium mediated by plant roots', *New Phytologist*, vol. 176, pp. 590-599.
Yan, C., Zhao, Y., Zheng, Z. and Luo, X. (2013) 'Effects of various LED light wavelengths and light intensity supply strategies on synthetic high-strength wastewater purification by Chlorella vulgaris', *Biodegradation*, vol. 24, pp. 721-732.
Yin, X., Wang, L., Duan, G. and Sun, G. (2011) 'Characterization of arsenate transformation and identification of arsenate reductase in a green alga Chlamydomonas reinhardtii', *Journal of Environmental Sciences*, vol. 23, pp. 1186-93.

Zenk, M.H. (1996) 'Heavy metal detoxification in higher plants - a review', *Gene*, vol. 179, pp. 21-30.
Zhang, D. and Surapaneni, S. (2012) *ADME-Enabling Technologies in Drug Design and Development*, New Jersey: John Wiley & Sons Ltd.
Zhao, E.J., Ma, J.F., Meharg, A.A. and McGrath, S.P. (2009) 'Arsenic uptake and metabolism in plants', *New phytologist*, vol. 181, pp. 777-794.
Zhu, C.J. and Lee, Y.K. (1997) 'Determination of biomass dry weight of marine microalgae', *Journal of Applied Phycology*, vol. 9, pp. 189-194.
Zhu, H., Liu, Z., Tang, L., Liu, J., Zhou, M., Xie, F., Wang, Z., Wang, Y., Shen, S., Hu, L. and Yu, L. (2012) 'Reversal of P-gp and MRP1-mediated multidrug resistance by H6, a gypenoside aglycon from Gynostemma pentaphylum, in viscristine-resistant human oral cancer (KB/VCR) cells', *Eur J Pharmacol*, vol. 696, pp. 43-53.
Zouboulis, A.I. and Katsoyiannis, I.A. (2005) 'Recent advances in the bioremediation of arsenic-contaminated groundwaters', *Environment International*, vol. 31, pp. 213-219.

Appendix 1 Population growth or biomass production indicator parameters with advantages and disadvantages

Table 1A1 Population growth or biomass production indicator parameters with advantages and disadvantages

Surrogate	Determination method	Advantage	Disadvantage	Reference
Dry weight	Heat or freeze dried cells in analytical balance	Closest parameter to biomass production	Time consuming, low accuracy, requires high amount of cells	(Zhu and Lee, 1997; Afkar, Ababna and Fathi, 2010)
Cell counts	Counting chamber Microscope	Good precision (400 or more cells per treatment)	Time consuming, can take 6-8 h	(Andersen, 2005)
	Flow cytometer	Good precision, it can measure more than one parameter in a single run (e.g. GSH, viability, ROS)	High cost	(Peperzak and Brussaard, 2010; Blaise and Ferard, 2005; Cossarizza et al., 2009)
	Electronic particle counter	Good precision	High cost	(Maloney, Donovan Jr. and Robinson, 1962)
Carbon 14 assimilation	Measure the assimilation of radio-labeled inorganic carbon	Good precision	High cost of isotopes, some considerations for cultures in dark conditions	(Steeman-Neilson, 1952)
Optical density	Spectrophotometer	Low-medium precision	Extraction step required, low precision at low cell densities , only suitable to $1X10^5$ cells.mL^{-1}	(Weber, 1973)
Chlorophyll a, b	In-vivo fluorometer	High precision, no extraction required	High noise, interferences	(Kirk, 1994)
	In-vitro spectrophotometer	High precision	Extraction step required, time	(Daemen, 1986)

			consuming	
	In vitro fluorometer	High precision	Extraction step required, high cost	(Mayer, Cuhel and Nyholm, 1997)
	Flow cytometer	High precision, no extraction required	High cost	(Suggett, Borowitzka and Prásil, 2010)
ATP	Bioluminescence assay based on luciferin-luciferase reaction	High precision	Arsenate strongly inhibits reaction	(Holm-Hansen and Booth, 1996)
DNA	Formation of fluorescent complex with several dyes	High precision	One possible mechanism of arsenic toxicity is DNA alteration	(Holm-Hansen, Sutcliffe and Sharp, 1968)

Appendix 2 Theoretical and experimental information for related GS/PC molecules and arsenosugars

Table 1A2 Theoretical and experimental information for related GSH/PC molecules and arsenosugars

Short	Name	Monoisotopic mass	Formula	Protonated formation	m/z	Molecular structure and protonation followed by induced dissociation	Experimental mass spectrum obtained from the complex
GSH	Glutathione	307.08381	$C_{10}H_{17}N_3O_6S$	**$[M+H]^+$**	**308.084**	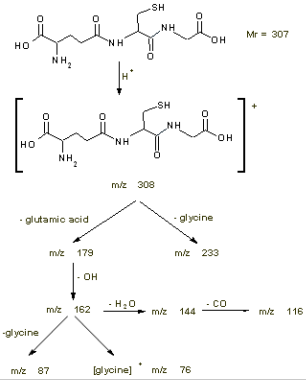	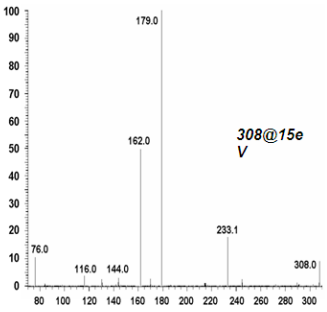
				Fragment	162		
				Fragment	179		
				Fragment	233		
				$[2M+H]^+$	**615**		
				$[3M+H]^+$	**922**		
				$[CSSC+H]^+$	241		
				$[M-H]^-$	**306**		
			Adducts	**$[M+Na]^+$**	**330**		
				$[M+2H]^{2+}$	154.5		
GSSG	Glutathione oxidised	612.151962	$C_{20}H_{32}N_6O_{12}S_2$	**$[M+H]^+$**	**613.152**	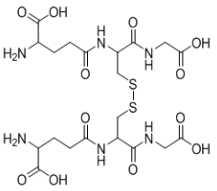	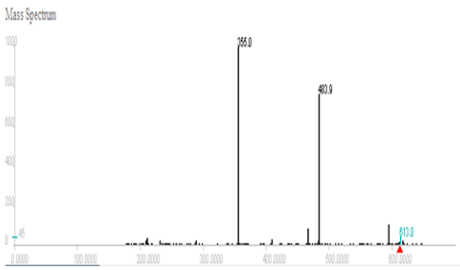
				Fragment	484.117		
				Fragment	355.075		
				$[M+2H]^{2+}$	**307**		
				$[2M+H]^+$	1225		
				$[M-H]^-$	**611**		
			Adducts	**$[M+Na]^+$**	**635**		
DMA	Dimethyl arsenate	137.966201	$C_2H_7AsO_2$	**$[M+H]^+$**	**138.966**	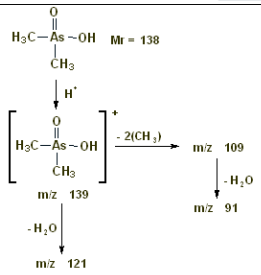	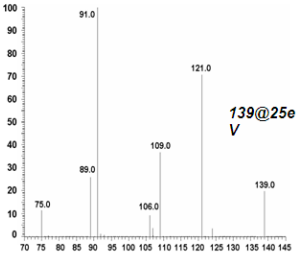
				Fragment	121		
				Fragment	109		
				Fragment	91		
				$[2M-H_2O+H]^+$	**259**		
				$[2M+H]^+$	**277**		
				$[3M-2H_2O+H]^+$	**397**		
				$[M-H]^-$	**137**		
			Adducts	**$[M+Na]^+$**	**161**		
				$[2M+Na]^+$	**299**		
MMA	Mono methyl arsenate	139.945465	$CH_3OAs(OH)_2$	**$[M+H]^+$**	**140.945**	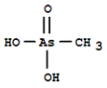	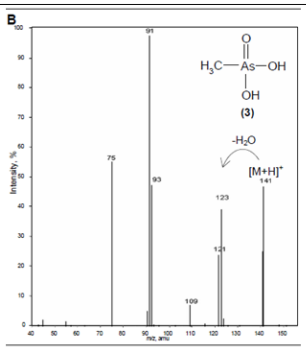
				Fragment	123		
				Fragment	109		
				Fragment	93		
				Fragment	91		
				$[2M+H]^+$	**281**		
				$[3M+H]^+$	**421**		
				$[4M+H]^+$	**561**		
				$[M-H]^-$	**139**		
			Adducts	**$[M+Na]^+$**	**163**		
				$[M+2Na]^+$	**185**		
				$[M+3Na]^+$	**207**		
				$[2M-H_2O+H]^+$	**263**		
				$[3M-2H_2O+H]^+$	**385**		
				$[M+H]^+ + H2($	**159**		
TMA	Tetramethyl arsonium ion	135.015497	$C_4H_{12}As+$	**$[M+H]^+$**	**136.016**	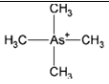	
				Fragment	120		
				Fragment	105		
				$[2M+H]^+$	271		
AsB	Arsenobetaine	177.997501	$C_5H_{11}AsO_2$	**$[M+H]^+$**	**178.998**	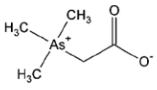	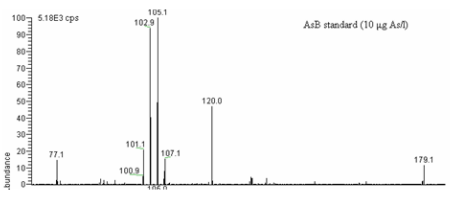
				Fragment	120		
				Fragment	105		
				$[2M+H]^+$	**357**		
				$[3M+H]^+$	535		
				$[4M+H]^+$	713		
				$[5M+H]+$	891		
				$[6M+H]+$	1069		
				$[M+H]^+$	275		

Short	Name	Monoisotopic mass	Formula	Protonated formation	m/z	Molecular structure and protonation followed by induced dissociation	Experimental mass spectrum obtained from the complex
TMAO	Trimethylarsine oxide	135.986936	C_3H_9AsO	**$[M+H]^+$**	**136.987**	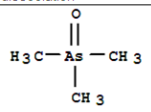	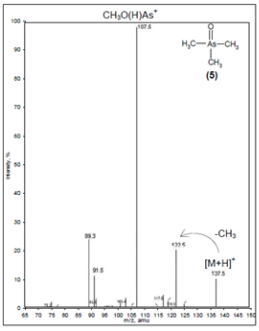
				Fragment	122		
				Fragment	107		
				$[2M+H]^+$	273		
					272.96		
DMAG	GSH+DMA	411.04453	$C_{12}H_{22}N_3O_6SAs$	**$[M+H]^+$**	**412.045**	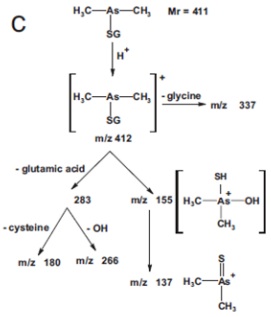	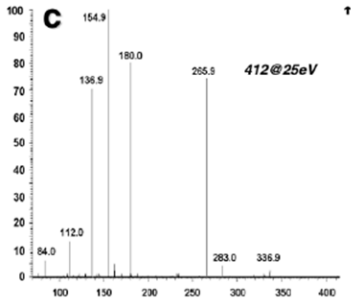
				Fragment	337		
				Fragment	283		
				Fragment	155		
				Fragment	266		
				Fragment	180		
				Fragment	137		
				$[2M+H]^+$	**823**		
				$[M+2H]^{2+}$	**206.5**		
				$[M-H]^-$	410		
			Adducts	**$[GSH+DMA]^+$**	**446**		
				$[M+Na]^+$	**434**		
				Positive mode		Negative mode	
						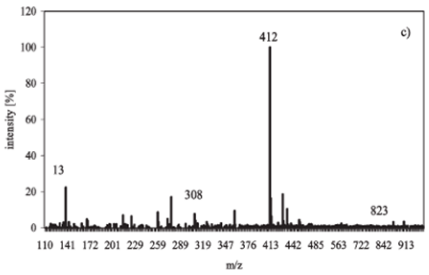	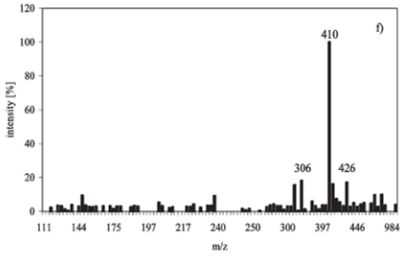
DMATV-GSH	DMATV+GSH	443.0166	$C_{12}H_{22}N_3O_6S_2A$	**$[M+H]^+$**	**444.017**	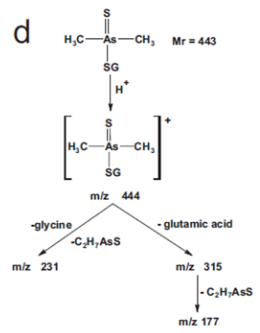	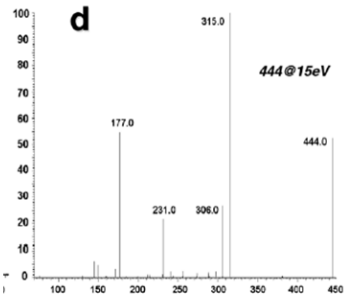
				Fragment	315		
				Fragment	231		
				Fragment	177		
				$[2M+H]^+$	887		
				$[M+2H]^{2+}$	222.5		
			Adduct	**$[GSH+DMA]^+$**	**446**		
						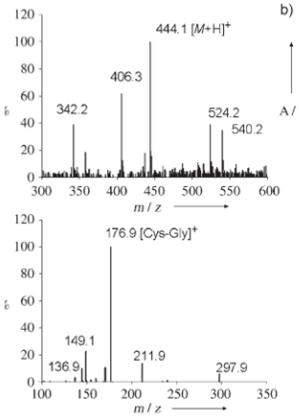	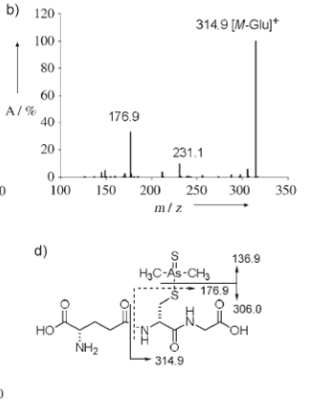

Short	Name	Monoisotopic mass	Formula	Protonated formation	m/z	Molecular structure and protonation followed by induced dissociation	Experimental mass spectrum obtained from the complex
MADG	MMA+GSH	702.09703	$C_{21}H_{35}N_5O_{12}S_2As$	**$[M+H]^+$**	**703.097**	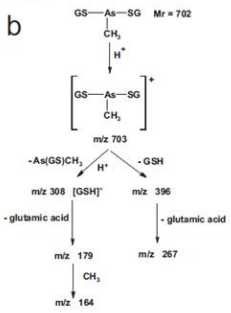	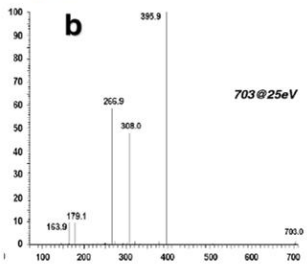
				Fragment	396		
				Fragment	308		
				Fragment	267		
				Fragment	179		
				Fragment	164		
				Fragment	306		
				Fragment	394		
				$[M+2H]^{2+}$	**352.021**		
				$[2M+H]^+$	1405		
				$[M-H]^-$	701		
				Positive mode		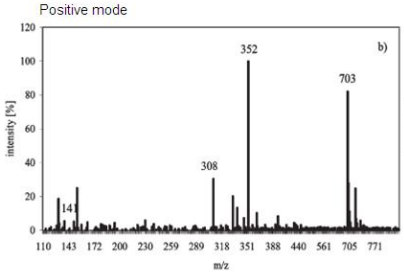	Negative mode 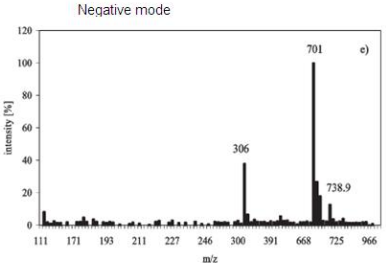
ATG	As(III)+GSH	993.14954	$C_{30}H_{48}N_9O_{18}S_3As$	**$[M+H]^+$**	**994.15**	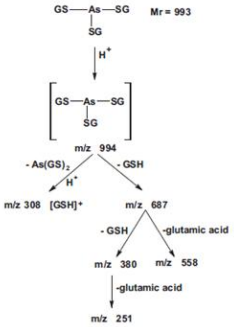	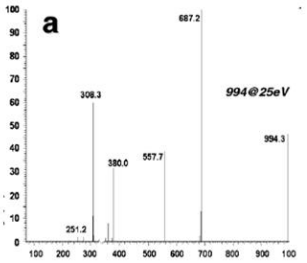
					687		
					308		
					558		
					380		
					251		
				$[M+2H]^{2+}$	**497.5**		
				$[M-H]^-$	992		
					306		
					611		
				$[M-2H]^{2+}$	495.5		
				Positive mode		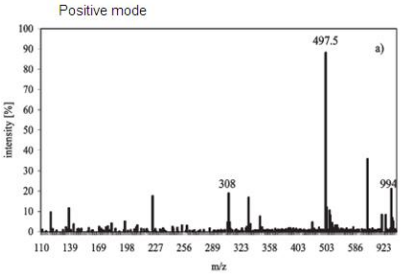	Negative mode 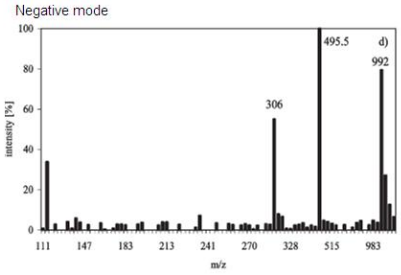
$DMTA^V$		154.95118	C_2H_5AsSO	**$[M+H]^+$**	**155.951**	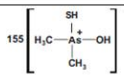	
					137		
					109		
				$[2M+H]^+$	309		

Short	Name	Monoisotopic mass	Formula	Protonated formation	m/z	Molecular structure and protonation followed by induced dissociation	Experimental mass spectrum obtained from the complex
Reduced PC_2	Red-PC_2	539.1355836	$C_{18}H_{29}N_5O_{10}S_2$	**$[M+H]^+$**	**540.1356**	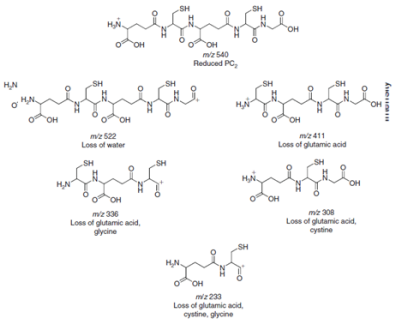	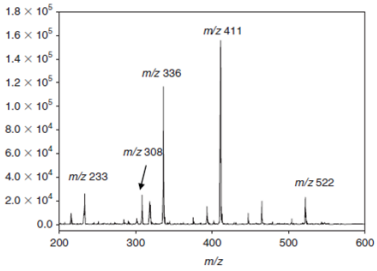
				Fragment	522		
				Fragment	411		
				Fragment	336		
				Fragment	308		
				Fragment	**233**		
				$[2M+H]^+$	**1079**		
				$[M+2H]^{2+}$	**270.5**		
				$[M-H]^-$	538		
			Adducts	**$[M+Na]^+$**	**562**		
				$[M+H+2Na]^+$	**584**		
				$[M+H+Na+K]^+$	**594**		
				$[M+H+2K]^+$	**616**		
	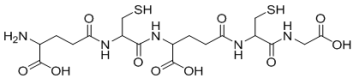						
Oxidised PC_2	Ox-PC_2	537.1199335	$C_{18}H_{27}N_5O_{10}S_2$	**$[M+H]^+$**	**538.1199**	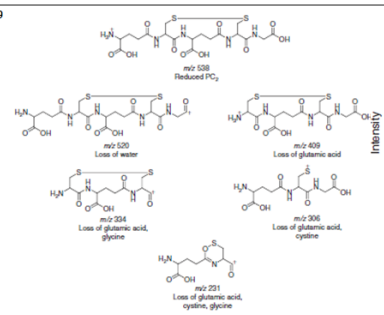	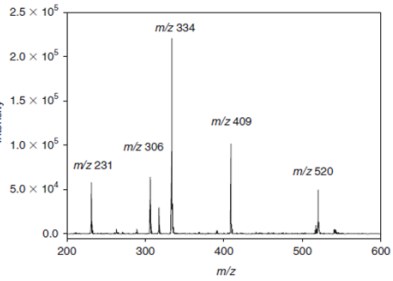
				Fragment	520		
				Fragment	409		
				Fragment	334		
				Fragment	306		
				Fragment	231		
				$[2M+H]^+$	**1075**		
				$[M+2H]^{2+}$	269.5		
				$[M-H]^-$	536		
			Adducts	**$[M+K]^+$**	**576**		
	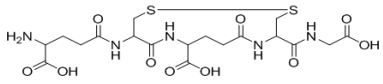						
Oxidised PC_3	Ox-PC_3	769.1717111	$C_{26}H_{39}N_7O_{14}S_3$	**$[M+H]^+$**	**770.1717**	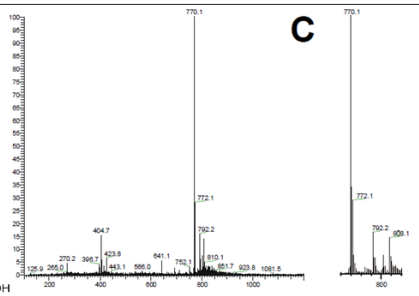	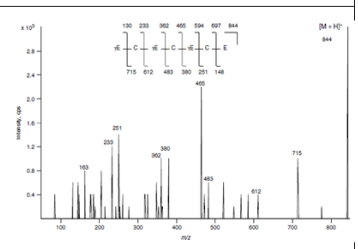
				Fragment	715		
				Fragment	612		
				Fragment	483		
				Fragment	380		
				Fragment	251		
				Fragment	148		
				$[M+2H]^{2+}$	385.5		
				$[2M+H]^+$	**1539**		
				$[M-H]^-$	768		
	iso-PC_3(Glu)	843.2084905	$C29H45N7O16S3$	**$[M+H]^+$**	844.2085		
	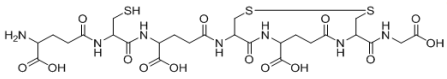						
Reduced PC_3	Red-PC_3	771.1873611	$C_{26}H_{41}N_7O_{14}S_3$	**$[M+H]^+$**	**772.1874**	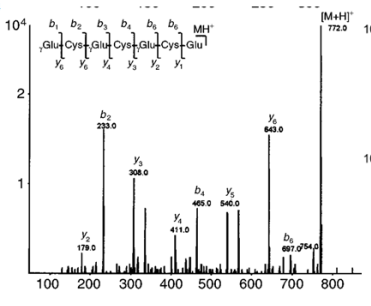	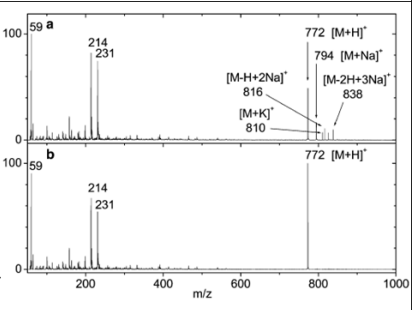
				Fragment	643		
				Fragment	540		
				Fragment	485		
				Fragment	411		
				Fragment	308		
				$[M+2H]^{2+}$	**386.6**		
				$[M-H]^-$	770		
				$[M+Na]^+$	**794**		
				$[M+H+2Na]^+$	**816**		
				$[M+K]^+$	**810**		
				$[M+2H+3Na]^+$	**838**		
	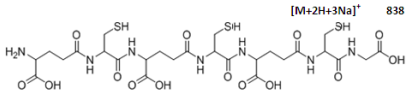						
Ox-PC_4	OxidisedPC$_4$	999.2078386	$C_{34}H_{49}N_9O_{18}S_4$	**$[M+H]^+$**	**1000.208**	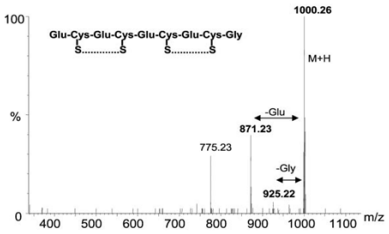	
				Fragment	925		
					871		
					775		
				$[M+2H]^{2+}$	500.5		
				$[M-H]^-$	998		
				$[M+K]^+$	**1038**		
	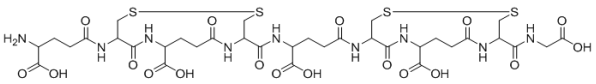						
Red-PC_4	Reduced PC$_4$	1003.239139	$C_{34}H_{53}N_9O_{18}S_4$	**$[M+H]^+$**	**1004.239**	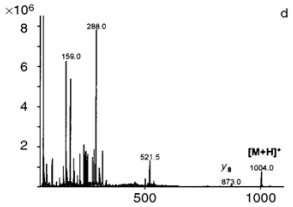	
				$[M+2H]^{2+}$	502.5		
				$[M-H]^-$	1002		

Short	Name	Monoisotopic mass	Formula	Protonated formation	m/z	Molecular structure and protonation followed by induced dissociation	Experimental mass spectrum obtained from the complex
As(III)-PC$_3$	As(III)-PC$_3$	843.0854825	$C_{26}H_{38}N_7O_{14}S_3As$	**[M+H]$^+$**	**844.0855**	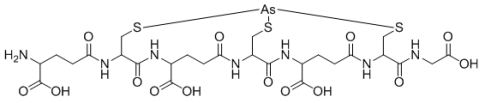	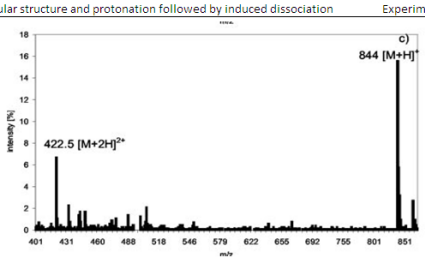
				Fragment	433		
				Fragment	506		
				[M+2H]$^{2+}$	**422.5**		
				[M-H]$^-$	842		
GS-As(III)-PC$_2$		918.1175109	$C_{28}H_{43}N_8O_{16}S_3As$	**[M+H]$^+$**	**919.1175**		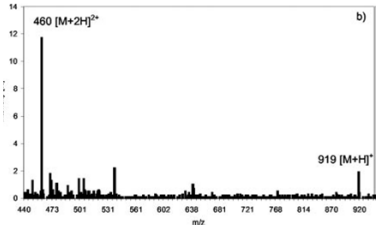
				[M+2H]$^{2+}$	**460**		
				Fragment	540		
				Fragment	640		
				Fragment	471		
				Fragment	501		
				Fragment	504		
				[M-H]$^-$	917		
PC$_2$-GS		844.2037395	$C_{28}H_{44}N_8O_{16}S_3$	**[M+H]$^+$**	**845.2037**		
				[M+2H]$^{2+}$	**423**		
				[M-H]$^-$	843		
PC$_3$-GS		1076.255517	$C_{36}H_{52}N_{10}O_{20}S_4$	**[M+H]$^+$**	**1077.256**		
				[M+2H]$^{2+}$	**539**		
				[M-H]$^-$	1075		
As(III)-PC$_2$		629.0442696	$C_{18}H_{28}N_5O_{11}S_2As$	**[M+H]$^+$**	**630.0443**		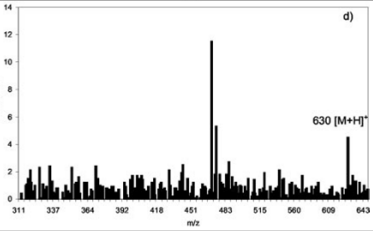
				[M+2H]$^{2+}$	**315.5**		
				[M-H]$^-$	628		
As(III)-(PC$_2$)$_2$		1150.169288	$C_{36}H_{53}N_{10}O_{20}S_4As$	**[M+2H]$^{2+}$**	**576.5847**	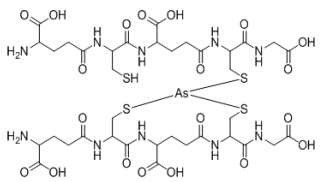	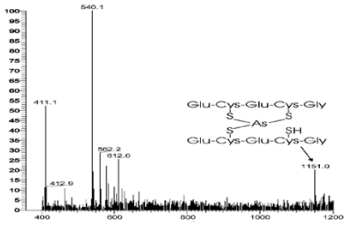
				[M+H]$^+$	**1151.169**		
				Fragment	540.1		
				Fragment	612		
				Fragment	562.2		
				Fragment	412.9		
				Fragment	411.1		
				[M-H]$^-$	1149		
As(III)-PC$_4$	As(III)-PC$_4$-SH	1075.13726	$C_{34}H_{50}N_9O_{19}S_4As$	**[M+H]$^+$**	**1076.137**	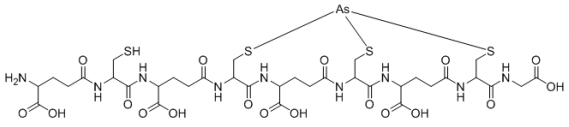	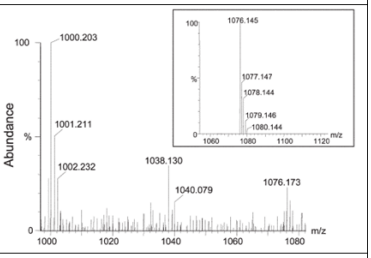
				[M-H]$^-$	1074		
				[M+2H]$^{2+}$	538.5		
MMA(III)-PC$_2$		627.065005	$C_{19}H_{30}N_5O_{10}S_2As$	**[M+H]$^+$**	**628.0651**	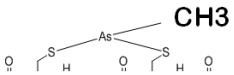	
				[M+2H]$^{2+}$	314.5		
				[2M+H]$^+$	1255		
				[M-H]$^-$	626		

Short	Name	Monoisotopic mass	Formula	Protonated formation	m/z	Molecular structure and protonation followed by induced dissociation	Experimental mass spectrum obtained from the complex
Arsenosugar H		238.0186304	$C_7H_{15}O_4As$	$[M+H]^+$	239.0186	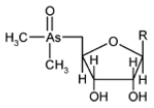	
				$[2M+H]^+$	477		
				$[M+2H]^{2+}$	120		
				$[M-H]^-$	237		
Arsenosugar OH DMAsSugarGlycol		328.0503244	$C_{10}H_{21}O_7As$	$[M+H]^+$	329.0503	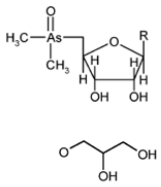	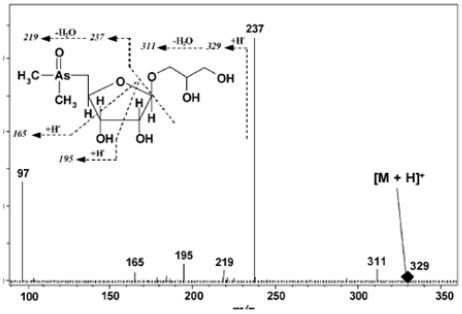
				Fragment	311		
				Fragment	237		
				Fragment	219		
				Fragment	195		
				Fragment	165		
				$[2M+H]^+$	657		
				$[M+2H]^{2+}$	165		
				$[M-H]^-$	327		
Arsenosugar SO_3 DMAsSugarSulfonate		392.0122244	$C_{10}H_{21}O_8SAs$	$[M+H]^+$	393.0122	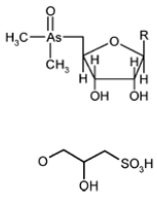	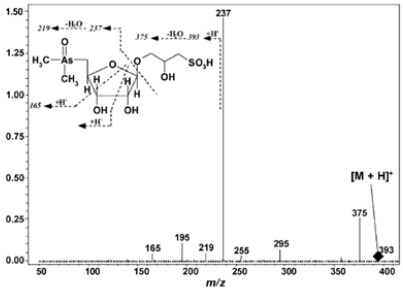
				Fragment	375		
				Fragment	295		
				Fragment	255		
				Fragment	237		
				Fragment	219		
				Fragment	195		
				Fragment	165		
				$[2M+H]^+$	785		
				$[M+2H]^{2+}$	197		
				$[M-H]^-$	391		
Arsenosugar SO_4 DMThioAsSugarSulfonate		408.007139	$C_{10}H_{21}O_{10}SAs$	$[M+H]^+$	409.0071	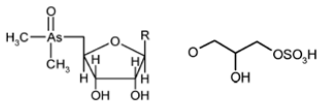	
				$[2M+H]^+$	817		
				$[M+2H]^{2+}$	205		
				$[M-H]^-$	407		
Arsenosugar PO_4 DMAsSugarPhosphate		482.0534343	$C_{13}H_{28}O_{12}PAs$	$[M+H]^+$	483.0534	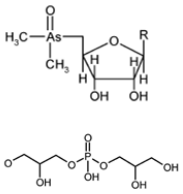	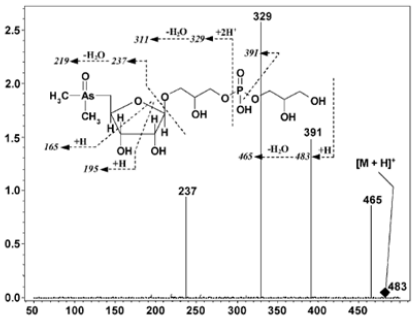
				Fragment	465		
				Fragment	391		
				Fragment	329		
				Fragment	237		
				$[2M+H]^+$	965		
				$[M+2H]^{2+}$	242		
				$[M-H]^-$	481		
DMAsSugarAminoSulfo		391.0282088	$C_{10}H_{22}NO_8SAs$	$[M+H]^+$	392	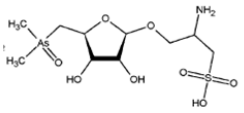	
					295		
				97	237		
					195		
					150		
					149		
				$[2M+H]^+$	783		
				$[M+2H]^{2+}$	196.5		
				$[M-H]^-$	390		

Appendix 3 Synthetic standards analysis by HPLC-ITToF

Synthetic standards were prepared and injected in the HPLC-ESI-ITToF using conditions set in section 3.5.2.2.a, to identify their elution profiles. The instrument was used in scan mode to identify all the possible molecules within 100 to 1000 m/z ratio. The results for the ATG, MADG, DMAG and DMAS^{V}-GS synthetic standard are shown in Figure 1.

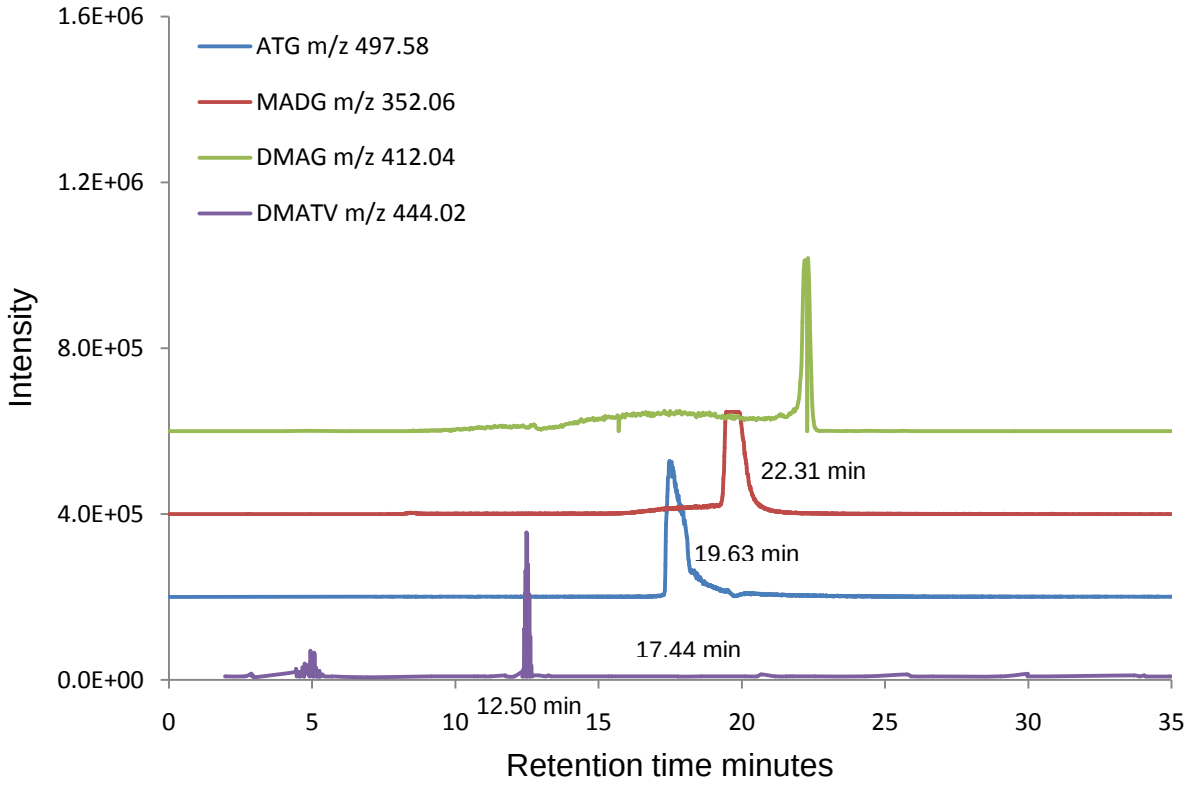

Fig 1A3 HPLC-ESI-ITTOF elution profile for the ATG (m/z 497.52) MADG (m/z 352.06), DMAG (m/z 412.04) and DMAS^{V}-GS (m/z 444.02) synthetic standards

The peak eluting at 17.44 min (Fig 1) has a m/z 497.58 which indicates the following protonated mass $[M+2H]^{2+}$. Peaks for subsequent dissociations of this molecule were found at m/z: 687.98, 558.03, 379.98, 308.09 and 250.94. This can be observed in Fig 2.

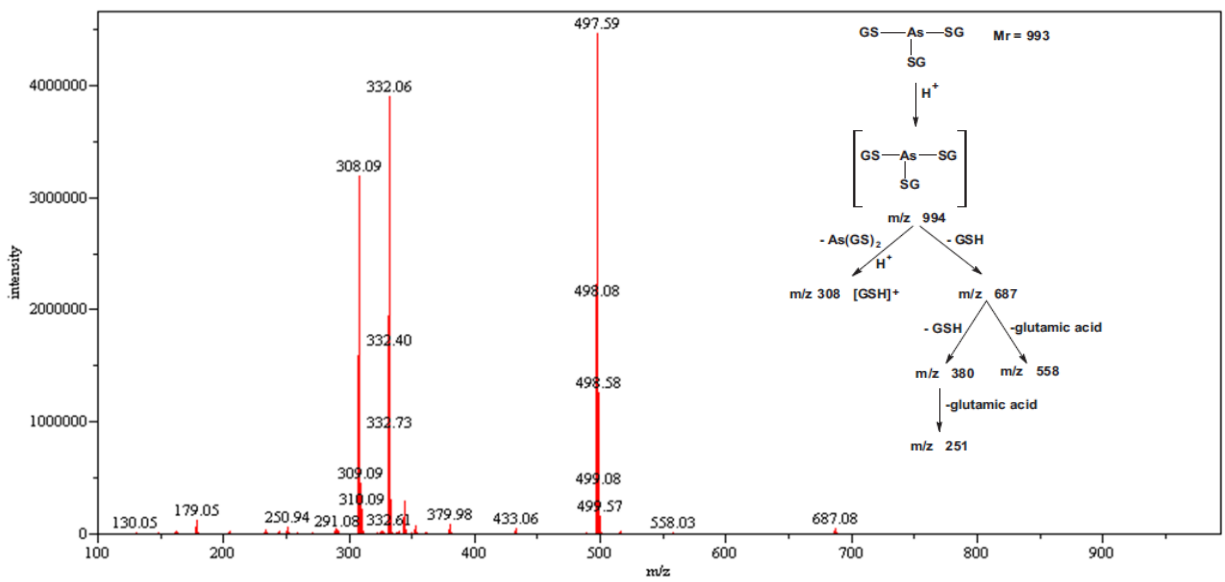

Fig 2A3 HPLC-ESI-ITTOF mass spectra in positive mode for the peak eluting at 17.44 min for the ATG synthetic standard and protonation pathway

When the MADG synthetic standard was injected, a strong signal was recorded at 19.63 min (Fig 1). The peak in positive mode had a weak signal indicating the following protonated mass $[M+H]^{+}$ at m/z: 703.09 as expected and subsequent dissociations at m/z: 396.02, 308.09, 266.97 and 179.05. There was also a strong signal for the protonated mass $[M+2H]^{+2}$ at m/z 352.06 (Fig 3).

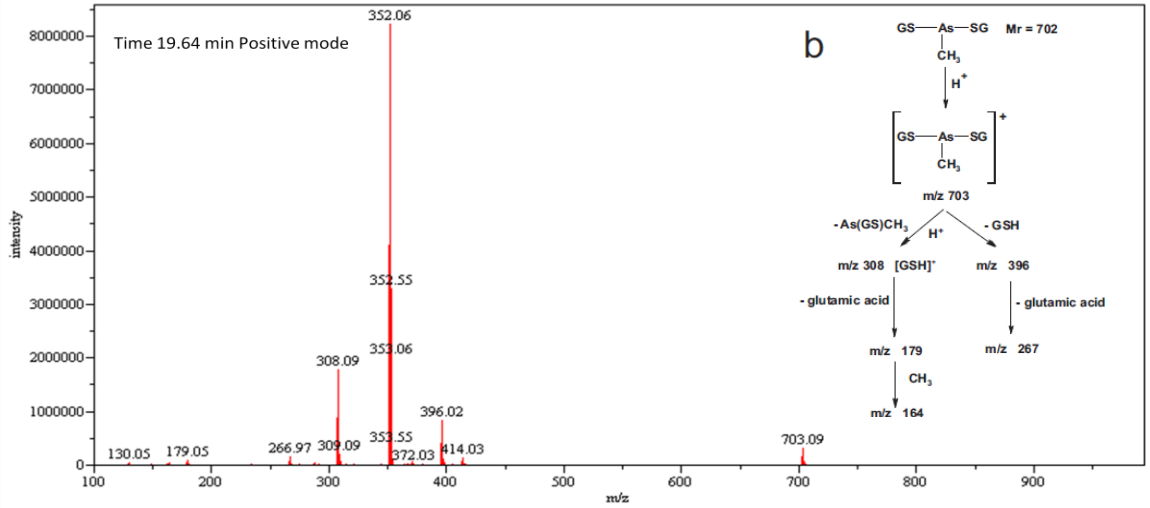

Fig 3A3 HPLC-ESI-ITTOF mass spectra in positive mode for the peak eluting at 19.63 min for the MADG synthetic standard and protonation pathway

Moreover, in negative mode there was also a strong signal recorded at the same time 19.63 min with the following protonated mass $[M-H]^-$ at m/z: 701.07 and subsequent dissociations at m/z: 394.00 and 306.07 (Fig 4)

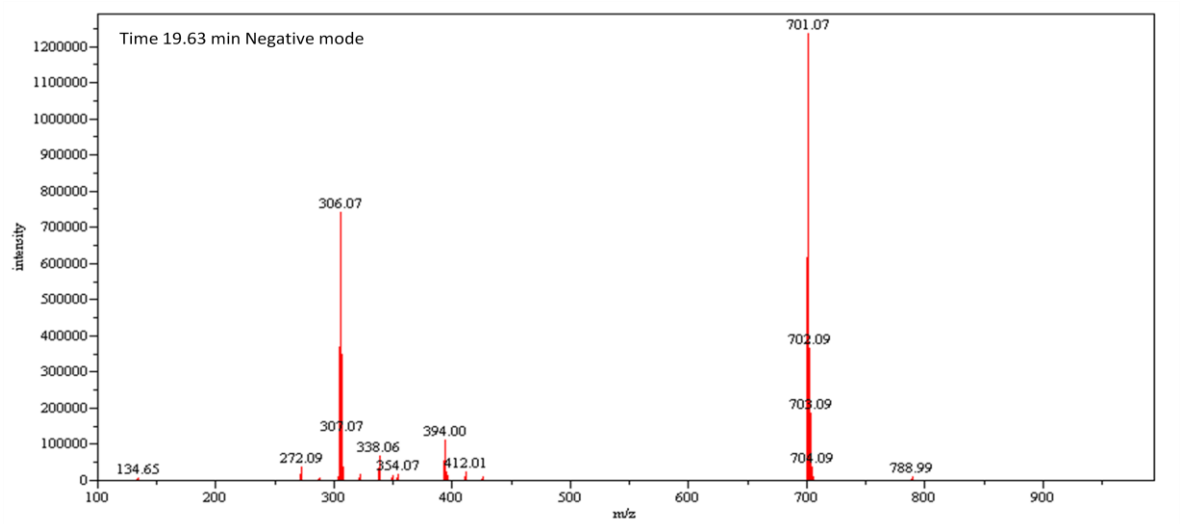

Fig 4A3 HPLC-ESI-ITTOF mass spectra in negative mode for the peak eluting at 19.63 min for the MADG synthetic standard

The results for the injection of the DMAG synthetic standard showed a strong signal recorded at 22.31 min (Fig 1). The ion trap was used to focus the precursor ion at m/z 412.04 to produce MS/MS dissociation. Dissociation products at m/z: 265.99, 283.01 and 337.02 were found (Fig 5). There was also a strong signal for the protonated mass $[M+2H]^{+2}$ at m/z 352.06.

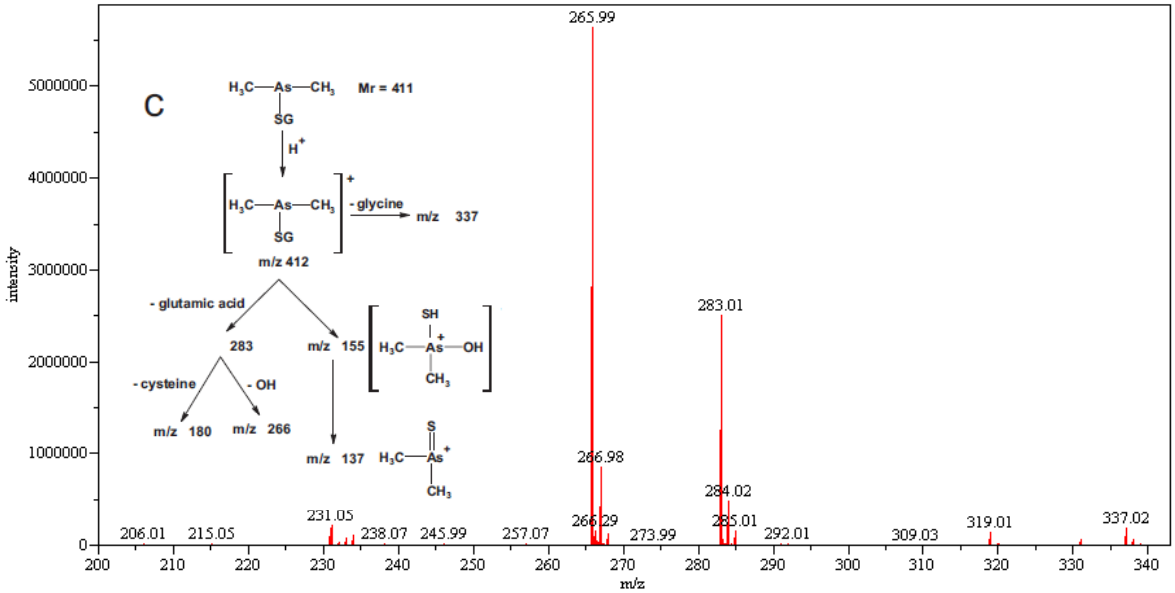

Fig 5A3 HPLC-ESI-ITTOF MS/MS spectra in positive mode for the peak eluting at 22.31 min for the DMAG synthetic standard at m/z 412.05.

When the DMAS^{V}-GS synthetic standard was injected, a signal was recorded at 12.50 min (Fig 1). Dissociations at m/z: 314.97 and 231.05 were observed (Fig 6).

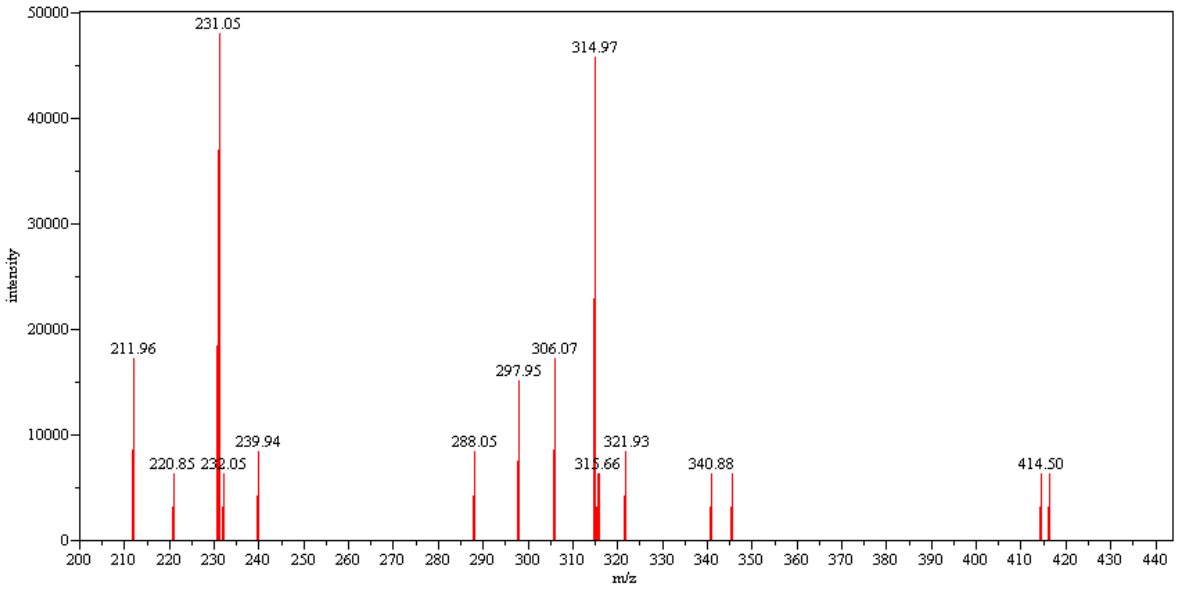

Fig 6A3 HPLC-ESI-ITTOF MS/MS spectra in positive mode for the peak eluting at 12.50 min for the DMAS^{V}-GS synthetic standard at m/z 444.02

Appendix 4 MS/MS analysis of As-GS/PC molecules

GS/PC molecules:

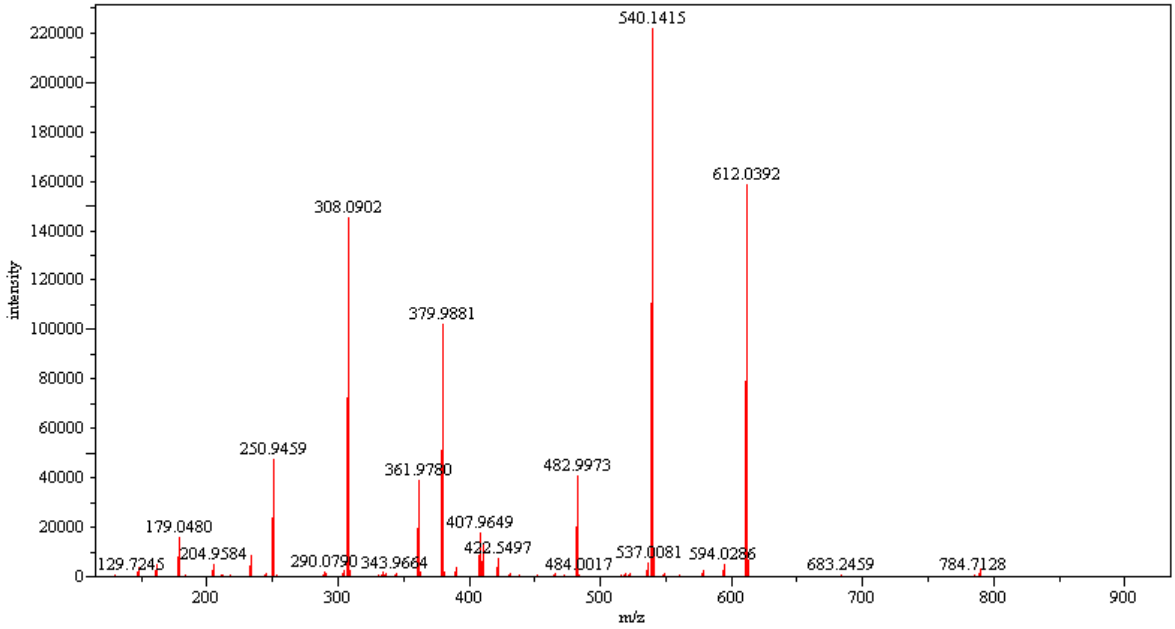

Fig 1A4 MS/MS spectra for GS-As(III)-PC_2 m/z 460.0663 RT:9.88 min, *C. vulgaris* cells exposed to 50 mg L^{-1} As(III), analysed using ESI-MS/MS (Orbitrap Discovery LTQ-XL)

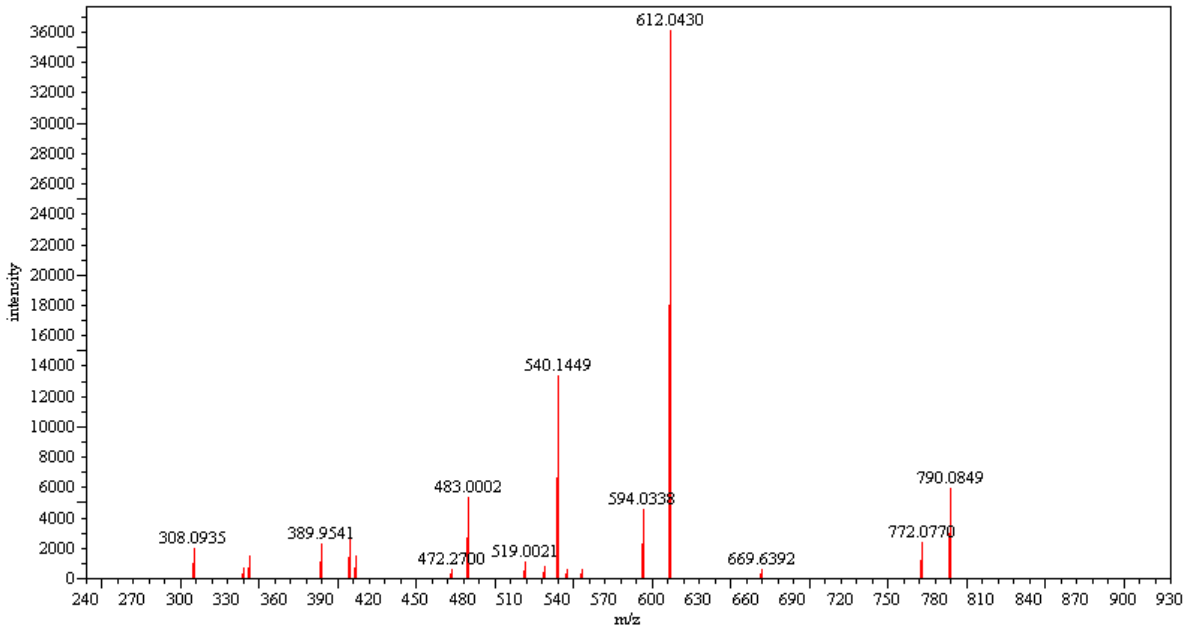

Fig 2A4 MS/MS spectra for GS-As(III)-PC_2 m/z 919.1247 RT:9.92 min, *C. vulgaris* cells exposed to 50 mg L^{-1} As(III), analysed using ESI-MS/MS (Orbitrap Discovery LTQ-XL)

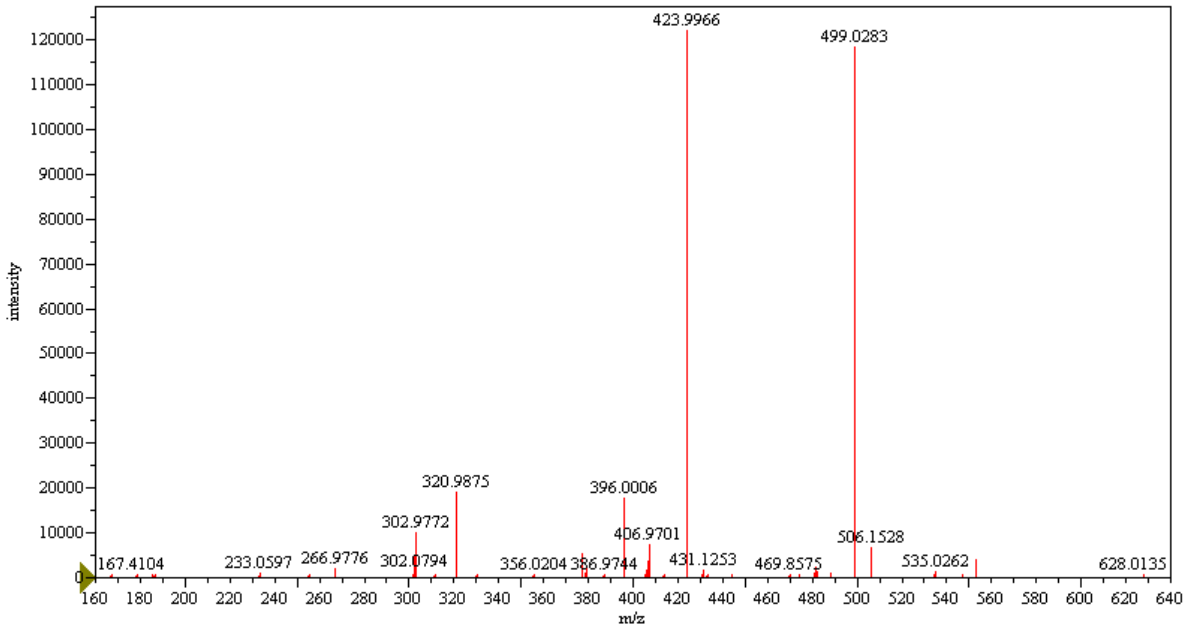

Fig 3A4 MS/MS spectra for MMA(III)-PC_2 m/z 628.0729 RT:11.31 min, *C. vulgaris* cells exposed to 50 mg L^{-1} As(III), analysed using ESI-MS/MS (Orbitrap Discovery LTQ-XL)

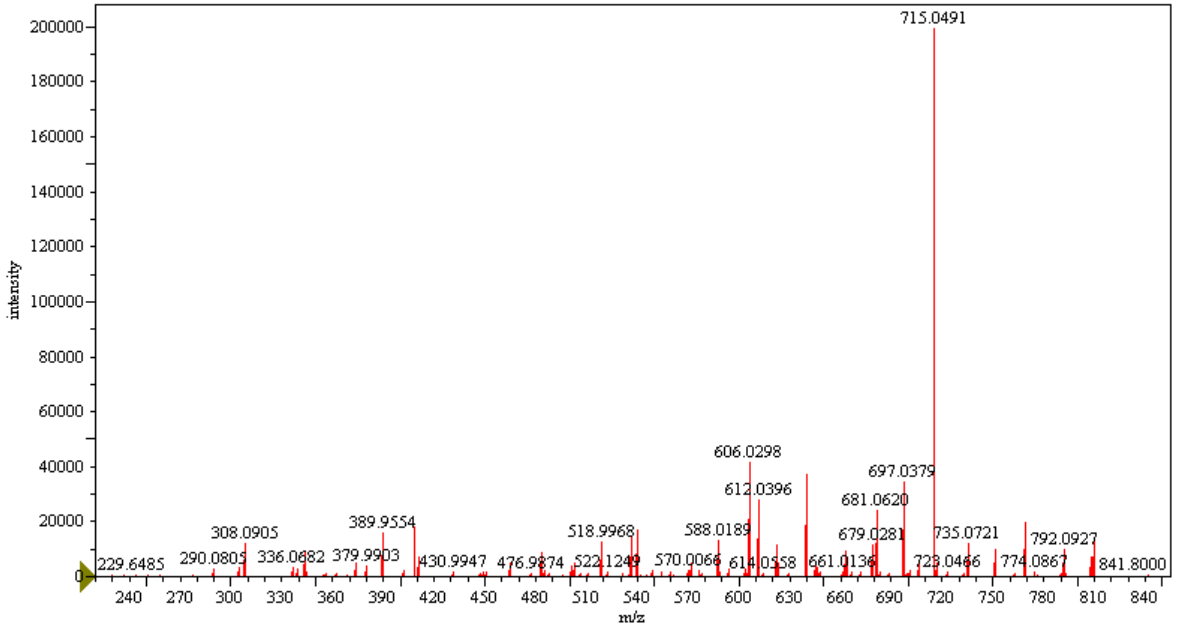

Fig 4A4 MS/MS spectra for As(III)-PC_3 m/z 844.0931 RT:11.49 min, *C. vulgaris* cells exposed to 50 mg L^{-1} As(III), analysed using ESI-MS/MS (Orbitrap Discovery LTQ-XL)

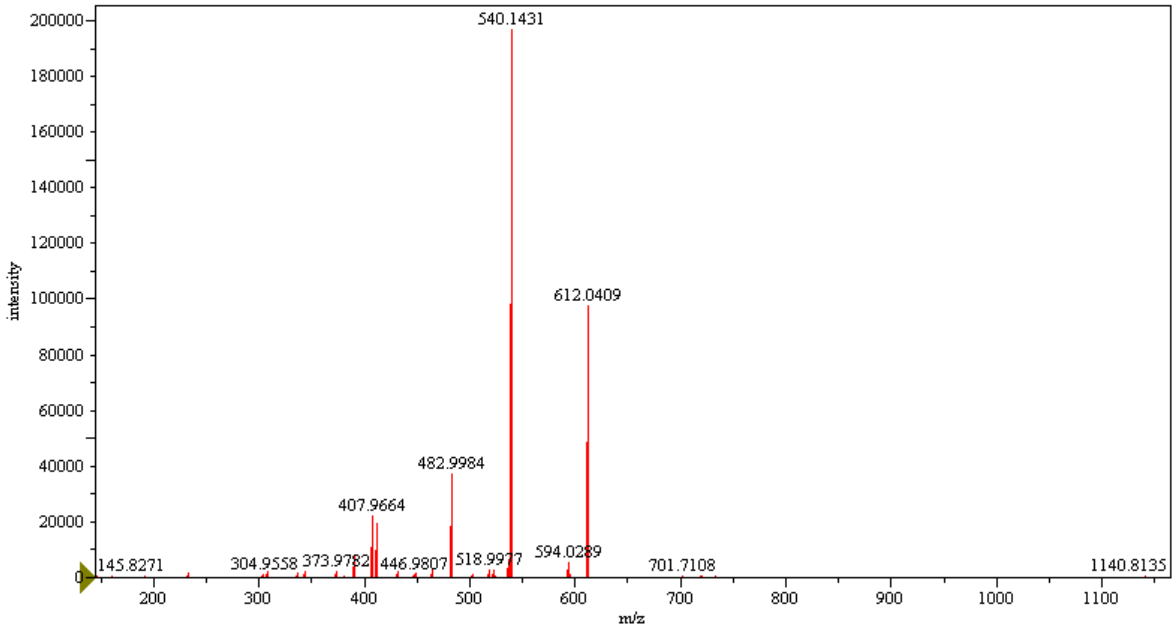

Fig 5A4 MS/MS spectra for As(III)-$(PC_2)_2$ m/z 576.0923 RT:13.07 min, *C. vulgaris* cells exposed to 50 mg L^{-1} As(III), analysed using ESI-MS/MS (Orbitrap Discovery LTQ-XL)

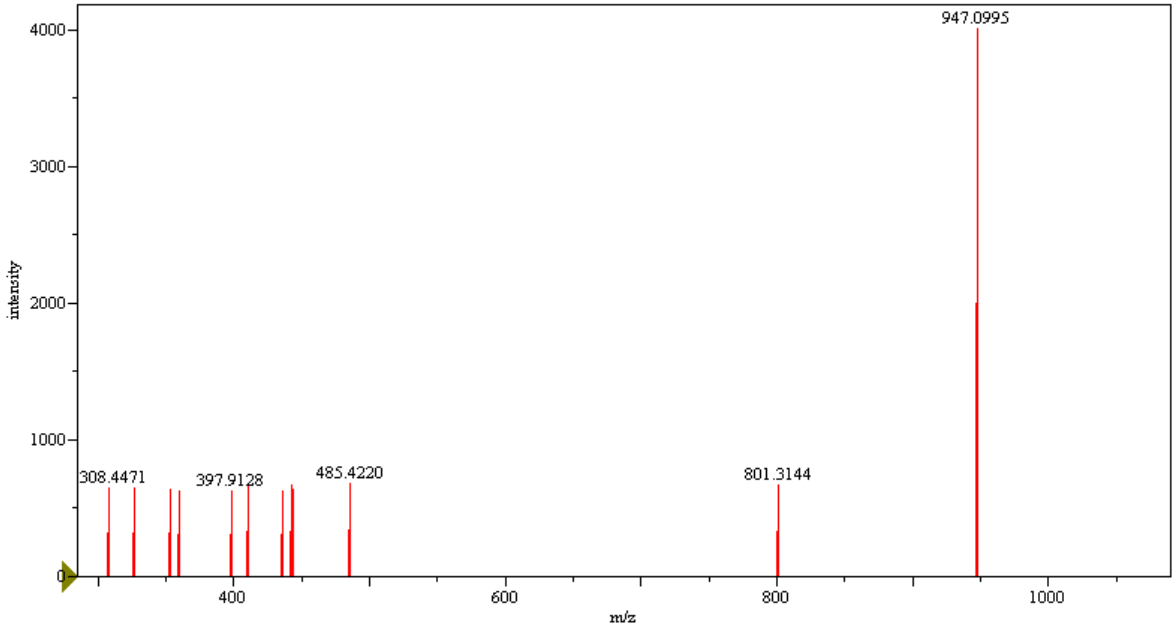

Fig 6A4 MS/MS spectra for As(III)-PC_4 m/z 1076.1455 RT:15.02 min, *C. vulgaris* cells exposed to 50 mg L^{-1} As(III), analysed using ESI-MS/MS (Orbitrap Discovery LTQ-XL)

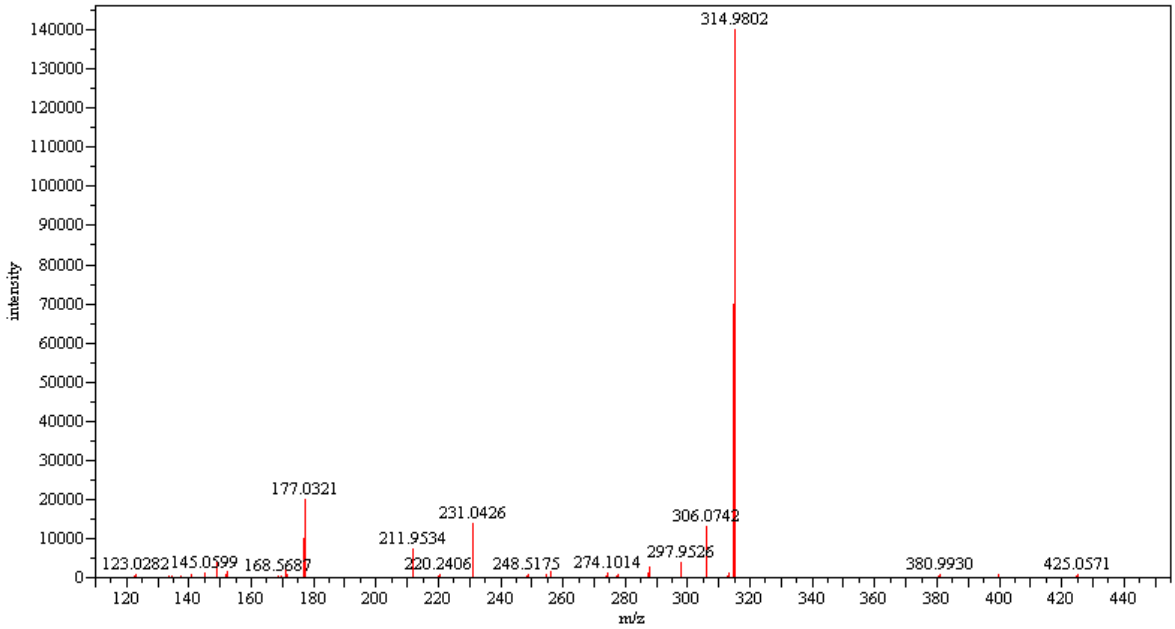

Fig 7A4 MS/MS spectra for DMAS^{V}-GS m/z 444.0247 RT:4.37 min, *C. vulgaris* cells exposed to 50 mg L^{-1} As(III), analysed using ESI-MS/MS (Orbitrap Discovery LTQ-XL)

hGSH/PC molecules:

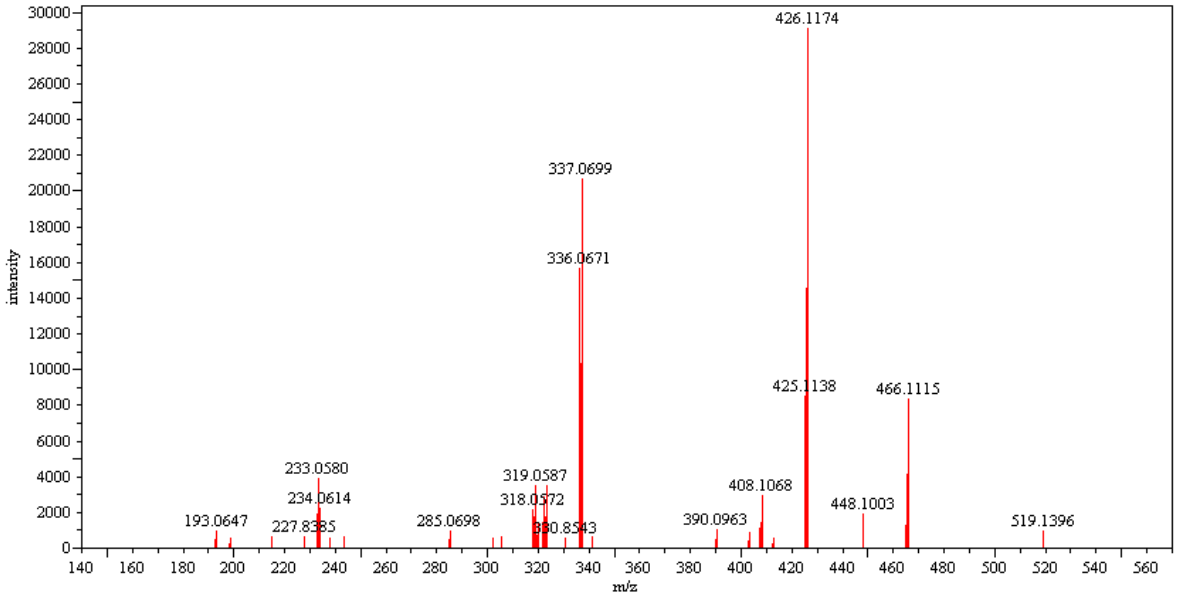

Fig 8A4 MS/MS spectra for γ-(Glu-Cys)$_2$-Ala m/z 554 RT 6.2845 min *C. vulgaris* cells exposed to 50 mg L^{-1} As(III), analysed using ESI-MS/MS (Orbitrap Discovery LTQ-XL)

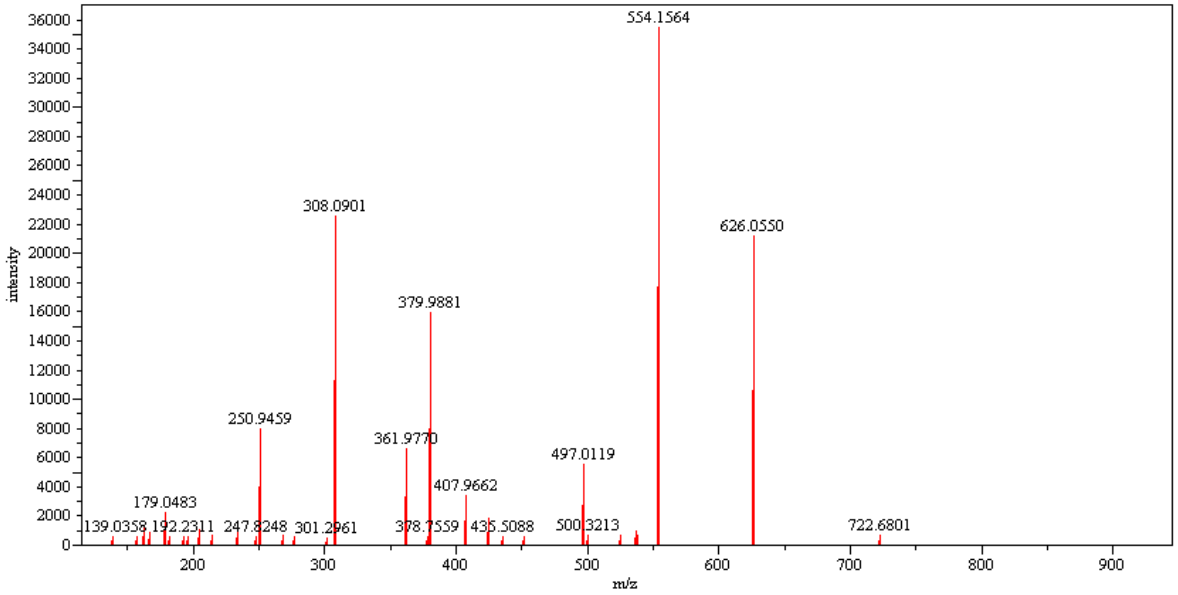

Fig 9A4 MS/MS spectra for As(III)- γ-(Glu-Cys)$_3$-Ala m/z 858 RT 10.9082 min *C. vulgaris* cells exposed to 50 mg L^{-1} As(III), analysed using ESI-MS/MS (Orbitrap Discovery LTQ-XL)

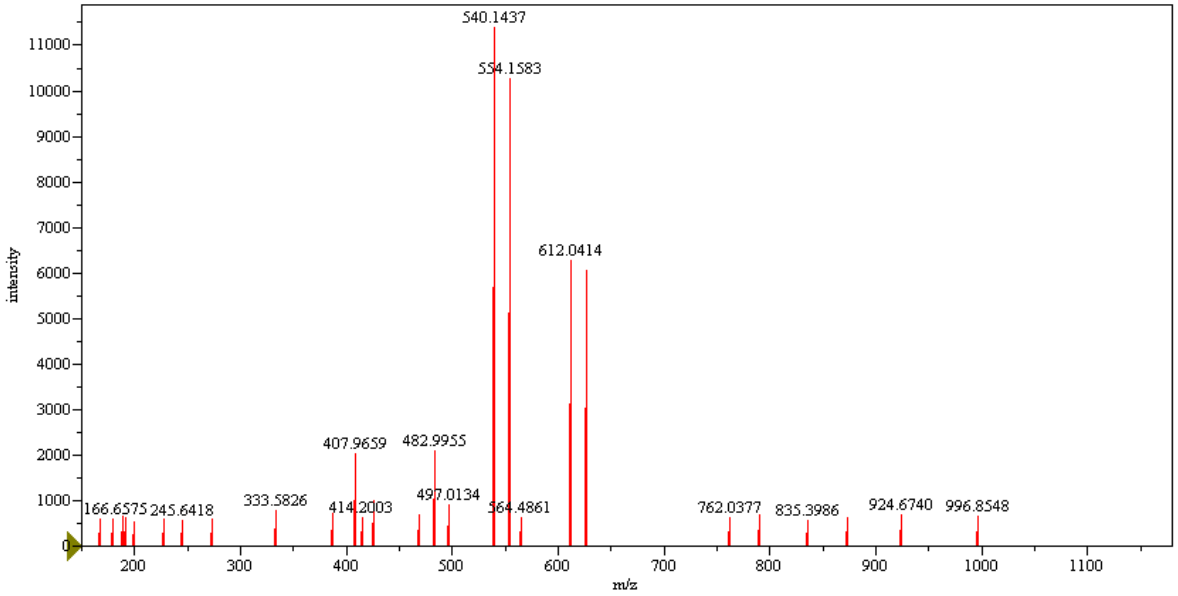

Fig 10A4 MS/MS spectra for As(III)- γ-((Glu-Cys)$_2$)$_2$-Ala m/z 583 RT 14.6667 min *C. vulgaris* cells exposed to 50 mg L^{-1} As(III), analysed using ESI-MS/MS (Orbitrap Discovery LTQ-XL)

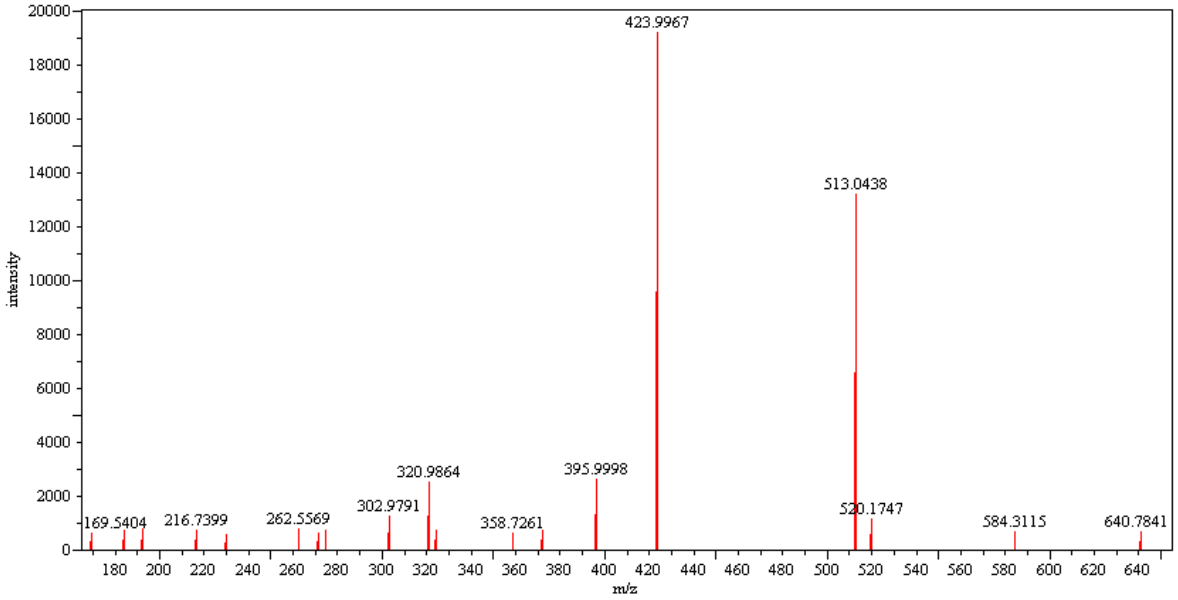

Fig 11A4 MS/MS spectra for MMA(III)-γ-(Glu-Cys)$_2$-Ala m/z 642 RT 14.8483 min *C. vulgaris* cells exposed to 50 mg L^{-1} As(III), analysed using ESI-MS/MS (Orbitrap Discovery LTQ-XL)

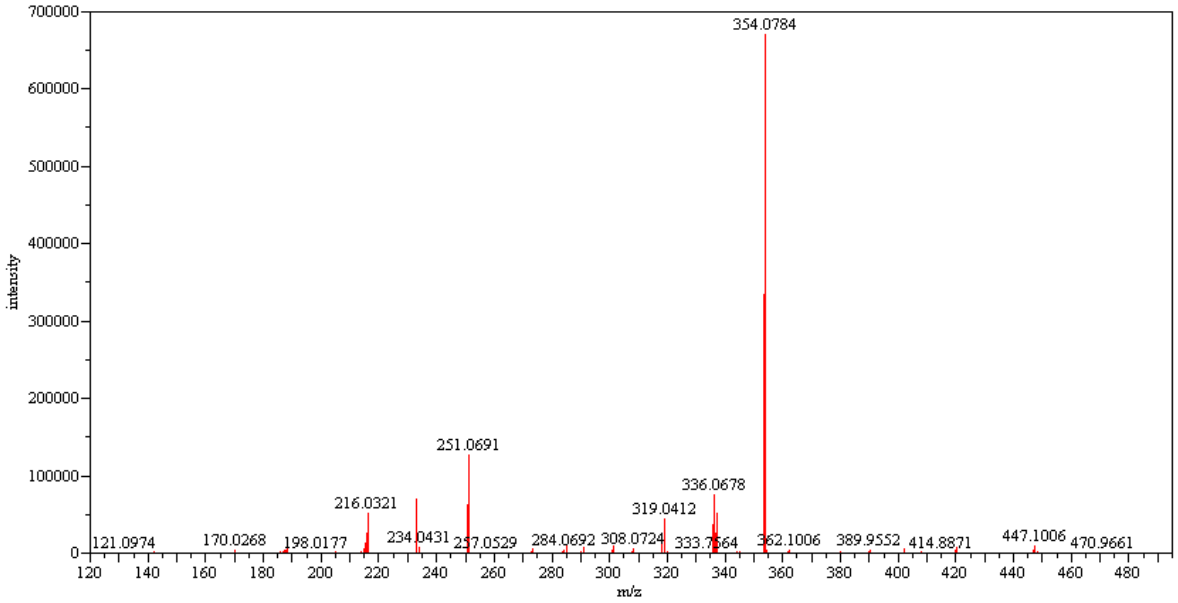

Fig 12A4 MS/MS spectra for γ-(Glu-Cys)$_2$ m/z 483 RT 4.6997 min *C. vulgaris* cells exposed to 50 mg L^{-1} As(III), analysed using ESI-MS/MS (Orbitrap Discovery LTQ-XL)

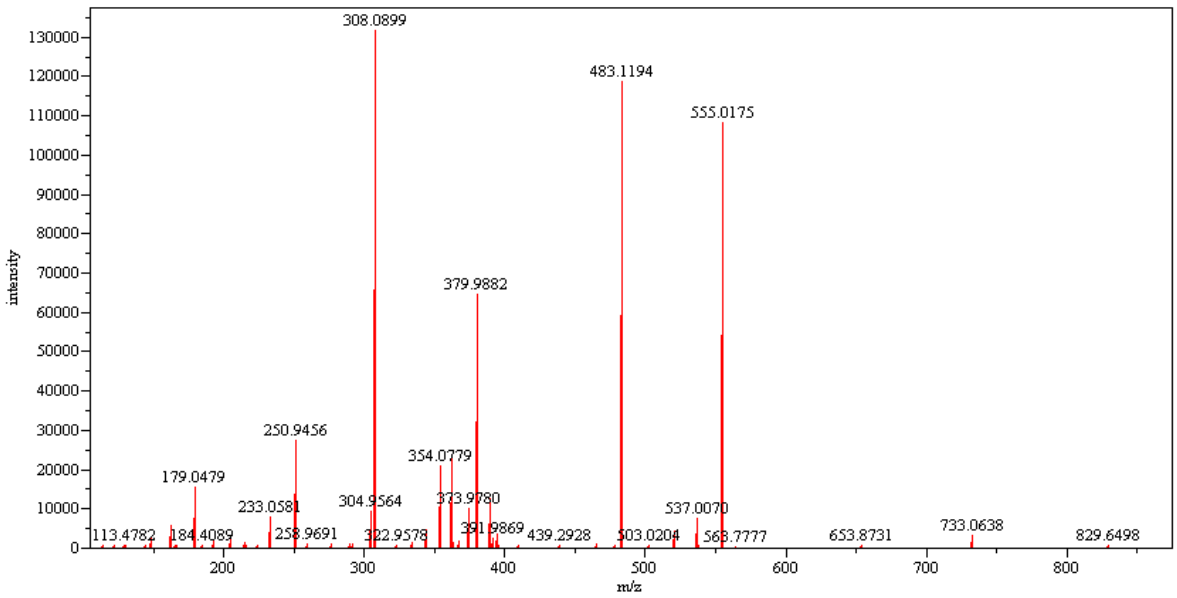

Fig 13A4 MS/MS spectra for min GS-As(III)-γ-(Glu-Cys)$_2$ m/z 431 RT 8.0730 *C. vulgaris* cells exposed to 50 mg L^{-1} As(III), analysed using ESI-MS/MS (Orbitrap Discovery LTQ-XL)

Table 1A4 Summary of fragments found in MS/MS analysis *C. vulgaris* cells exposed to 50 mg L^{-1} As(III), analysed using ESI-MS/MS (Orbitrap Discovery LTQ-XL) (n.o. not observed)

Molecule	m/z		b1	y8	b2	y7	b3	y6	b4	y5	b5	y4	b6	y3	b7	y2	b8	y1
Phytochelatins																		
PC_2	540	T	130.1	------	233.1	------	362.1	------	465.1	------	------	411.1	------	308.1	------	179.1	------	76.0
		F	130.1	------	233.1	------	362.1	------	465.1	------	------	411.1	------	308.1	------	179.1	------	76.0
PC_3	772	T	130.1	------	233.1	------	362.1	643.2	465.1	540.1	594.2	411.1	697.2	308.1	------	179.1	------	76.0
		F	130.1	------	233.1	------	362.1	643.2	465.1	540.1	n.o.	411.1	697.2	309.1	------	n.o.	------	76.0
As(III)-PC_3	844	T	130.1	------	233.1	------	362.1	643.2	465.1	540.1	594.2	411.1	697.2	308.1	------	179.1	------	76.0
		F	n.o.	------	n.o.	------	362.0	n.o.	465.1	540.1	594.0	411.1	697.0	308.1	------	n.o.	------	n.o.
GS-As(III)-PC_2	460	T	130.1	------	233.1	------	362.1	------	465.1	540.1	------	411.1	------	308.1	------	179.1	------	76.0
		F	129.7	------	233.1	------	362.0	------	n.o.	540.1	------	422.1	------	308.1	------	179.0	------	n.o.
As(III)-$(PC_2)_2$	576	T	130.1	------	233.1	------	362.1	------	465.1	540.1	594.2	411.1	------	308.1	------	179.1	------	76.0
		F	n.o.	------	233.1	------	n.o.	------	465.1	540.1	594.0	411.1	------	308.1	------	n.o.	------	n.o.
As(III)-PC_4	1076	T	130.1	875.1	233.1	772.2	362.1	643.2	465.1	540.1	594.2	411.1	697.2	308.1	826.2	179.1	929.2	76.0
		F	n.o.	n.o.	n.o.	n.o.	n.o.	n.o.	n.o.	n.o.	n.o.	411.1	n.o.	308.4	n.o.	n.o.	n.o.	n.o.
MMA(III)-PC_2	628	T	130.1	------	233.1	------	362.1	------	465.1	------	------	411.1	------	308.1	------	179.1	------	76.0
		F	n.o.	------	233.1	------	n.o.	------	n.o.	------	------	n.o.	------	n.o.	------	178.8	------	n.o.
$DMAS^V$-GS	444	T	136.9	------	231.1	------	------	------	------	------	------	------	------	------	------	176.9	------	------
		F	136.9	------	231.1	------	------	------	------	------	------	------	------	------	------	176.9	------	------
Ala GSH/PC																		
γ-$(Glu\text{-}Cys)_2Ala$	554	T	130.1	------	233.1	------	362.1	------	465.1	------	------	425.1	------	322.1	------	193.1	------	90.1
		F	130.1	------	233.1	------	362.1	------	465.1	------	------	425.1	------	322.1	------	193.1	------	90.1
GS-As(III)-γ-$(Glu\text{-}Cys)_2$-Ala	467	T	130.1	------	233.1	------	362.1	------	465.1	554.2	------	425.1	------	322.1	------	193.1	------	90.1
		F	n.o.	------	233.1	------	362.0	------	n.o.	554.2	------	425.1	------	n.o.	------	192.2	------	n.o.
As(III)-γ-$((Glu\text{-}Cys)_2)_2$-Ala	583	T	130.1	------	233.1	------	362.1	------	465.1	554.2	------	425.1	------	322.1	------	193.1	------	90.1
		F	n.o.	------	n.o.	------	n.o.	------	n.o.	554.2	------	425.1	------	n.o.	------	n.o.	------	n.o.
DesGLY GSH/PC																		
γ-$(Glu\text{-}Cys)_2$	483	T	130.1	------	233.1	------	362.1	------	------	------	------	------	------	354.1	------	251.1	------	122.0
		F	n.o.	------	233.1	------	362.1	------	------	------	------	------	------	354.1	------	251.1	------	121.2
GS-As(III)-γ-$(Glu\text{-}Cys)_2$	431	T	130.1	------	233.1	------	362.1	------	380.0	483.1	------	------	------	354.1	------	251.1	------	122.0
			n.o.	------	233.1	------	362.0	------	380.0	483.1	------	------	------	354.1	------	250.9	------	122.1

Appendix 5 Genetic analysis on *C. vulgaris* C-169

Table 1A5 *C. vulgaris* C-169 sequence similarity search BLASTP using the Uniprot (BLASTP 2.2.28+ software) database (Uniprot, 2009), phytochelatin synthase (PCS), alanine phytochelatin synthase (Ala PCS), amino acids (aa)

	ABCC 1/2		**ABCD 1**		**ABCD 2**		**PCS 1**		**As reductase**		**Ala PCS**	
Species / Gene name COCSUDRAFT(NUMBER)	**46284**		**65142**		**16703**		**19902**		**66432**		**52209**	
	Length (aa)	Identity	Length (aa)	Identity	Length (aa)	Identity	Length (aa)	Identity	Length (aa)	Identity	Length (aa)	Identity
Coccomyxa subellipsoidea C-169 (*Chlorella vulgaris*)	**1730**	**100%**	**1325**	**100%**	**586**	**100%**	**207**	**100%**	**130**	**100%**	**486**	**100%**
Hordeum vulgare var. distichum (Two-rowed barley)	845	50%	1131	52%	326	65%	500	57%	----	----	364	49%
Hordeum vulgare var. distichum (Two-rowed barley)	964	49%	769	51%	325	65%	----	----	----	----	475	46%
Hordeum vulgare var. distichum (Two-rowed barley)	965	49%	1322	49%	755	51%	----	----	----	----	539	43%
Hordeum vulgare var. distichum (Two-rowed barley)	----	----	1319	0.49	----	----	----	----	----	----	515	42%
Hordeum vulgare var. distichum (Two-rowed barley)	----	----	716	0.49	----	----	----	----	----	----		
Musa acuminata subsp. malaccensis (Wild banana) (Musa malaccensis)	1276	46%	1346	48%	613	52%	500	60%	----	----	504	45%
Musa acuminata subsp. malaccensis (Wild banana) (Musa malaccensis)			1374	47%			498	59%	----	----		
Selaginella moellendorffii (Spikemoss)	1601	44%	1306	50%	616	52%	472	60%	138	45%	488	47%
Selaginella moellendorffii (Spikemoss)	1599	44%	1369	49%	615	52%	472	60%	139	43%	488	46%
Selaginella moellendorffii (Spikemoss)	----	----	----	----	648	0.49	----	----	----	----	----	----

Selaginella moellendorffii (Spikemoss)	----	----	----	----	649	0.49	----	----	----	----	----	----
Selaginella moellendorffii (Spikemoss)	----	----	----	----	648	0.49	----	----	----	----	----	----
Selaginella moellendorffii (Spikemoss)	----	----	----	----	607	0.48	----	----	----	----	----	----
Selaginella moellendorffii (Spikemoss)	----	----	----	----	608	0.47	----	----	----	----	----	----
Selaginella moellendorffii (Spikemoss)	----	----	----	----	476	0.47	----	----	----	----	----	----
Selaginella moellendorffii (Spikemoss)	----	----	----	----	669	0.45	----	----	----	----	----	----
Populus trichocarpa (Populus balsamifera subsp. trichocarpa)	1617	44%	1309	49%	651	53%	503	59%	130	33%	----	----
Populus trichocarpa (Populus balsamifera subsp. trichocarpa)	1607	41%	----	----	----	----	496	58%	----	----	----	----
Populus trichocarpa (Populus balsamifera subsp. trichocarpa)	1488	41%	----	----	----	----	----	----	----	----	----	----
Vitis vinifera (Grape)	1623	44%	892	51%	765	51%	466	57%	130	34%	477	45%
Vitis vinifera (Grape)	1624	42%			1504	50%			130	34%	----	----
Prunus persica (Peach) (Amygdalus persica)	1631	44%	1335	49%	637	52%	501	56%	132	35%	557	48%
Prunus persica (Peach) (Amygdalus persica)	1600	42%	----	----	----	----	483	53%	----	----	----	----
Glycine max (Soybean) (Glycine hispida)	1620	44%	485	52%	770	49%	499	62%	159	38%	478	47%
Glycine max (Soybean) (Glycine hispida)	1620	44%	1336	49%	----	----	498	55%	131	37%	545	46%
Glycine max (Soybean) (Glycine hispida)	1615	42%	1338	49%	----	----	497	55%	----	----	547	43%
Glycine max (Soybean) (Glycine hispida)	----	----	1338	49%	----	----	----	----	----	----	499	42%
Glycine max (Soybean) (Glycine hispida)	----	----	1327	49%	----	----	----	----	----	----	547	42%
Glycine max (Soybean) (Glycine hispida)	----	----	1316	47%	----	----	----	----	----	----	449	41%
Capsella rubella (Plant)	1619	44%	1267	48%	701	51%	485	56%	146	36%	539	45%

Capsella rubella (Plant)	1623	43%	----	----	----	----	----	----	----	----	----	----
Capsella rubella (Plant)	1494	42%	----	----	----	----	----	----	----	----	----	----
Ricinus communis (Castor bean)	1569	44%	1339	48%	742	51%	502	57%	131	37%	492	46%
Ricinus communis (Castor bean)	1626	42%	----	----	----	----	----	----	----	----		
Brassica rapa subsp. pekinensis (Chinese cabbage)	1444	44%	1433	49%	693	53%	474	58%	144	36%	463	45%
Brassica rapa subsp. pekinensis (Chinese cabbage)	1590	43%	----	----	----	----	449	56%	----	----	458	43%
Brassica rapa subsp. pekinensis (Chinese cabbage)	1626	43%	----	----	----	----	481	55%	----	----	----	----
Brassica rapa subsp. pekinensis (Chinese cabbage)	1623	42%	----	----	----	----	452	54%	----	----	----	----
Brassica rapa subsp. pekinensis (Chinese cabbage)	1512	42%	----	----	----	----	492	52%	----	----	----	----
Solanum lycopersicum (Tomato) (Lycopersicon esculentum)	1626	43%	1344	51%	705	48%	545	57%	132	38%	546	49%
Setaria italica (Foxtail millet) (Panicum italicum)	1629	43%	1324	49%	753	50%	508	56%	----	----	268	53%
Setaria italica (Foxtail millet) (Panicum italicum)	----	----	1322	49%	----	----	425	55%	----	----	345	49%
Setaria italica (Foxtail millet) (Panicum italicum)	----	----	----	----	----	----	478	55%	----	----	508	46%
Sorghum bicolor (Sorghum) (Sorghum vulgare)	1627	43%	1264	50%	760	49%	507	56%	----	----	439	43%
Sorghum bicolor (Sorghum) (Sorghum vulgare)	----	----	1324	48%	----	----	463	55%	----	----	498	41%
Brachypodium distachyon (Purple false brome) (Trachynia distachya)	1629	43%	1245	50%	754	50%	502	57%	----	----	478	47%
Brachypodium distachyon (Purple false brome) (Trachynia distachya)	----	----	1325	49%	----	----	----	----	----	----	533	47%
Arabidopsis lyrata subsp. lyrata (Lyre-leaved rock-cress)	1623	43%	1337	50%	722	51%	485	56%	132	36%	538	47%
Arabidopsis lyrata subsp. lyrata (Lyre-leaved rock-cress)	1622	42%	----	----	----	----	415	55%	----	----	----	----
Arabidopsis lyrata subsp. lyrata (Lyre-leaved rock-cress)	1495	42%	----	----	----	----	----	----	----	----	----	----

Arabidopsis lyrata subsp. lyrata (Lyre-leaved rock-cress)	1490	42%	----	----	----	----	----	----	----	----	----	----
Arabidopsis thaliana (Mouse-ear cress)	1623	42%	1337	50%	706	52%	485	56%	146	36%	528	46%
Arabidopsis thaliana (Mouse-ear cress)	1622	42%	1338	50%	----	----	485	56%	----	----	539	46%
Arabidopsis thaliana (Mouse-ear cress)	1495	42%	1352	49%	----	----	452	54%	----	----	----	----
Arabidopsis thaliana (Mouse-ear cress)	1495	42%	----	----	----	----			----	----	----	----
Oryza brachyantha (Rice)	1628	43%	1325	49%	565	49%	505	56%	----	----	481	47%
Oryza brachyantha (Rice)	1648	42%	1376	48%			467	52%	----	----	501	46%
Oryza glaberrima (African rice)	1628	42%	1266	50%	771	51%	518	56%	----	----	561	45%
Oryza glaberrima (African rice)			1325	49%			246	55%	----	----	483	45%
Oryza sativa subsp. japonica (Rice)	1628	42%	1321	48%	785	50%	473	55%	----	----	540	46%
Oryza sativa subsp. japonica (Rice)	1650	41%	1431	47%	771	51%	498	56%	----	----	488	45%
Oryza sativa subsp. japonica (Rice)	1627	42%	1272	47%	1585	50%	415	50%	----	----	562	45%
Oryza sativa subsp. japonica (Rice)	1628	42%	310	53%	----	----	260	56%	----	----	884	45%
Oryza sativa subsp. japonica (Rice)	----	----	1150	50%	----	----	246	56%	----	----	446	44%
Oryza sativa subsp. japonica (Rice)	----	----	768	50%	----	----	519	56%	----	----	417	44%
Oryza sativa subsp. japonica (Rice)	----	----	1338	48%	----	----	502	55%	----	----	540	43%
Oryza sativa subsp. japonica (Rice)	----	----	1321	48%	----	----	543	53%	----	----	485	41%
Oryza sativa subsp. japonica (Rice)	----	----	1272	47%	----	----	----	----	----	----	491	41%
Oryza sativa subsp. japonica (Rice)	----	----	1244	45%	----	----	----	----	----	----	504	40%
Triticum urartu (Red wild einkorn) (Crithodium urartu)	1630	43%	1315	47%	----	----	414	50%	----	----	445	40%
Triticum urartu (Red wild einkorn) (Crithodium urartu)	----	----	----	----	----	----	393	50%	----	----	----	----
Ciona savignyi (Pacific transparent sea squirt)	1424	39%	----	----	----	----	333	49%	----	----	432	38%

Nematostella vectensis (Starlet sea anemone)	1222	39%	727	32%	----	----	225	47%	----	----	----	----
Nematostella vectensis (Starlet sea anemone)	----	----	----	----	----	----	193	43%	----	----	----	----
Nematostella vectensis (Starlet sea anemone)	----	----	----	----	----	----	244	42%	----	----	----	----
Nematostella vectensis (Starlet sea anemone)	----	----	----	----	----	----	250	38%	----	----	----	----

Appendix 6 Publications